ACADEMY OF SCIENCES USSR

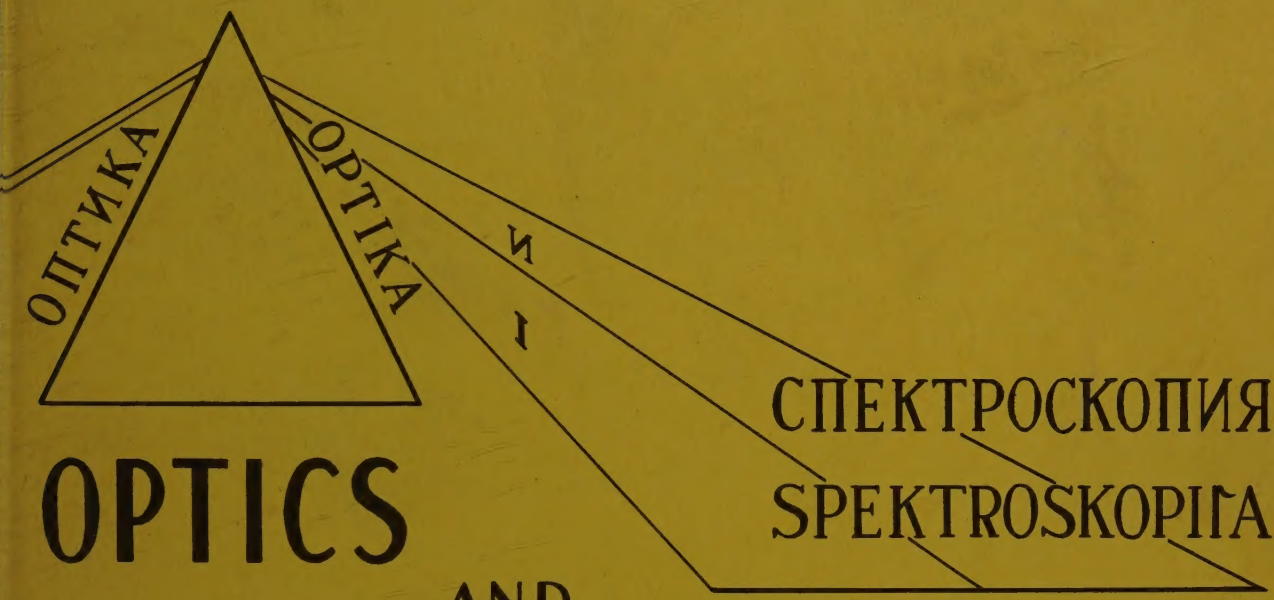

OPTICS AND SPECTROSCOPY

JULY 1959 · VOL. VII · NO. 1

Translated on the Initiative of
THE OPTICAL SOCIETY OF AMERICA, INC.
With a Grant-in-Aid from
THE NATIONAL SCIENCE FOUNDATION
by MORRIS D. FRIEDMAN, INC.

RUSSIAN EDITORIAL STAFF

Editor: S. E. FRISH

Assistant Editor: P. P. FEOFILOV

Corresponding Secretary: L. S. SAZONOV

Associate Editors:

M. M. GUREVICH M. A. EL'IASHEVICH A. A. LEBEDEV V. P. LINNIK
S. L. MANDEL'SHTAM I. V. OBREIMOV V. K. PROKOF'EV
N. N. SOBOLEV A. N. TERENIN A. I. TUDOROVSKII

Translation Editorial Staff

MORRIS D. FRIEDMAN

DR. JAMES R. ARONSON, *Arthur D. Little, Inc.*
FRED W. BEHNKE, *Perkin-Elmer Corp.*
DR. RICHARD DALVEN, *Raytheon Company, Research Division,*
DR. SUMNER P. DAVIS, *University of California*
CYRUS FELDMAN, *Oak Ridge National Laboratory*
DR. CARL GARLAND, *Massachusetts Institute of Technology*
DR. D. W. MAYO, *Massachusetts Institute of Technology*
DR. CONRAD J. RAUCH, *Massachusetts Institute of Technology — Lincoln Laboratory*
DR. JOHN S. WAUGH, *Massachusetts Institute of Technology*

Published monthly by the Optical Society of America, Inc. Executive office: 1155 Sixteenth Street, N.W., Washington, D.C. Subscriptions for one year to members of the Society: Associates $13.00; Regular members and Fellows $17.00. Subscriptions for non-members of the Society: One year U. S. and Possessions, $25.00; Foreign $28.00. Back numbers: $3.00 per copy. Second-class postage paid at Ann Arbor, Michigan.

Printed in the U.S.A. by Edwards Brothers, Inc., Ann Arbor, Michigan.

ОМ VII, Vyp 1 OPTIKA I SPEKTROSKOPIIA Iiul', 1959
DL. VII, No. 1 OPTICS AND SPECTROSCOPY July, 1959

Effective Excitation Cross-Sections of n^1P Levels of He by Slow Electrons

L. A. VAINSHTEIN AND G. G. DOLGOV

Abstract: By means of a numerical solution of radial differential equations, without exchange, but taking nto account strong coupling, we have calculated effective excitation cross sections of n^1P-levels of He n = 2 – 4). The effects of individual partial waves with various l are investigated, and it is shown that ven near the threshold the basic role is played by transitions of the exciting electron with a scattered wave ngular momentum $l \geq 1$.

INTRODUCTION

The values of effective cross sections of tomic excitation by slow electrons with an energy p to 100 eV are necessary for computation of many rocesses studied in the physics of gas discharges, strophysics, etc. The simplest theory of perturba- ions (Born's method) is not applicable at such nergies. When set up more accurately, the problem ets very complicated, since it leads to a set of ifferential or integro-differential equations hich must be solved numerically.

Up until now, the calculations were carried out or excitation of low s-states of hydrogen and elium. Only in the recent work of Khashaba and assey [1] was the excitation of the p-state of ydrogen examined. In the majority of cases the equations were solved by a variational method, and hus the results depended heavily on a successful hoice of trial functions.

The use of electronic computers permitted olving the problem by direct numerical integration f the equations and getting results for a broad lass of cases. In the first work of this kind, arried out by Ochkur, the excitation cross sections f a number of s-, p-, and d-levels of hydrogen ere computed [2].

At low energies the essential role in the exci- tation is played by exchange interaction. However, accounting for the exchange is tied in with computa- tional difficulties, and in particular, requires a large memory and considerable expenditure of computer time. At the same time a number of cross section properties may be obtained with approxima- tions without exchange. In particular, up to now, the role of individual partial waves of the exciting electron was practically uninvestigated. The scat- tered waves with $l > 0$ are taken into account only in [1], but their relative contribution to the total cross section is not given there.

In this work the computation of excitation cross sections of n^1P-levels of He is carried out without accounting for exchange. Let us note here too, that such computations are necessary as an initial approximation when accounting for exchange interaction. The cross sections obtained were used for calculating the polarization of radia- tion from the 3^1P-level.

BASIC EQUATIONS

Radial wave equations and the expression for cross sections are conveniently written in a repre- sentation of total angular momentum. The general formulae for the excitation of a hydrogen atom are given by Percival and Seaton [3]. In the case of atoms with two and more electrons these formulas get very complicated. However, in computing the excitation cross section without accounting for ex- change the role of the inner electron is limited to contributing to the stationary potential, and, con- sequently, the results of the work [3] are applicable (in this article, a somewhat different nomenclature is used).

The complete wave function of the system may be represented in the form

$$\Psi = \sum_{\Gamma} \frac{F_{\Gamma}^{\Gamma_0}(r)}{r} \Psi_{\Gamma}(\vec{r}_i, \theta, \varphi); \quad \Gamma = \alpha l L M, \tag{1}$$

where $\alpha = n_i l_i L^a$ is a set of quantum numbers of the atom, l is the orbital angular momentum of the exciting electron, L is the total orbital angular momentum of the system, Ψ_{Γ} is the eigenfunction of the corresponding angular moments. The zero subscript corresponds to the ground state of the atom. The radial functions $F_{\Gamma}^{\Gamma_0}(r)$ satisfy a set of equations of the form

$$\left[\frac{d^2}{dr^2} - \frac{l(l+1)}{r^2} + k_{\alpha}^2\right] F_{\Gamma}^{\Gamma_0}(r) = 2 \sum_{\Gamma'} V_{\Gamma\Gamma'}(r) F_{\Gamma'}^{\Gamma_0}(r) \tag{2}$$

with the boundary conditions

$$F_{\Gamma}^{\Gamma_0}(0) = 0; \tag{3}$$

$$F_{\Gamma}^{\Gamma_0}(r) \sim \delta_{\Gamma\Gamma_0} \sin\left(k_0 r - \frac{l_0\pi}{2}\right) + T_{\Gamma_0\Gamma} \exp\left[i k_{\alpha} r - i \frac{l\pi}{2}\right],$$

where k_0 and k_{α} are the wave numbers of the incident and scattered electrons; $T_{\Gamma_0\Gamma}$ is proportional to $\delta_{L_0L}\delta_{M_0M}$ and does not depend on M. The total cross section equals the sum of partial cross sections and is represented by the expression

$$\sigma^{\alpha} = \sum_{Ll_0l} \sigma^{\alpha}_{\Gamma_0\Gamma} = \frac{4\pi k_{\alpha}}{k_0^3} \sum_{Ll_0l} \frac{2L+1}{2L_0^a+1} |T_{\Gamma_0\Gamma}|^2, \tag{4}$$

where L_0^a is the orbital angular momentum of the initial state of the atom.

Further, we will restrict ourselves, as is usually done, to an approximation of two states, neglecting the effect of intermediate states. Then,

in the right-hand side of (2) only the terms with $\Gamma' = \Gamma_o$ and $\Gamma' = \Gamma$ remain, and the system is split into pairs of related equations. In case of transitions such as $s^2{}^1S - sp^1P$ in a He atom (or in the other elements of group II of the periodic table), these equations may be written in the form (atomic units are used)

$$(5)\quad \left[\frac{d^2}{dr^2} - \frac{l_o(l_o+1)}{r^2} - \frac{2\zeta_o(r)}{r} + k_o^2\right] F_o = b_{ol}\frac{\zeta_{ol}^1(r)}{r} F_1;$$

$$\left[\frac{d^2}{dr^2} - \frac{l_1(l_1+1)}{r^2} - \frac{2\zeta_1(r)}{r} - b_{11}\frac{\zeta_{11}^2(r)}{r} + k_1^2\right] F_1 = b_{ol}\frac{\zeta_{ol}^1(r)}{r} F_o,$$

where

$$(5a)\quad \zeta_\alpha(r) = -Z + \int_o^\infty K_o(r, r')\,\rho_\alpha(r')dr';$$

$$\zeta_{ij}^q(r) = \int_o^\infty K_q(r, r')\,P_i(r')P_j(r')dr';$$

$$K_q(r,r') = \begin{cases} \left(\frac{r'}{r}\right)^q & \text{for } r' < r; \\ \left(\frac{r}{r'}\right)^{q+1} & \text{for } r' > r. \end{cases}$$

Here $P_i(r)$ are the radial wave functions of the atomic electrons, $\rho_\alpha(r)$ is the electron density in the state α. The coefficients b_{11} and b_{01} are expressed as Racah coefficients [4]. The subscripts 0 and 1 correspond to initial and final states respectively; the following notation is customary $F_{\Gamma_o}^{\Gamma_o} = F_o$; $F_{\Gamma}^{\Gamma_o} = F_1$.

In the case under examination $L_o^a = 0$, $L = l_o$ and its each transition is sufficient to describe by the angular moments of incident and scattered electrons l_o, l_1. The total cross section is $\sigma = \Sigma\sigma_{l_o l_1}$.

On excitation of P-states of an atom, it follows from the conservation of total angular momentum and parity that $l_o = l_1 \pm 1$. In Born's approximation the p — s- transition of the exciting electron plays the main role near the threshold. The question of the effect of individual partial waves was not discussed in any detail within the framework of more accurate methods. In this work the partial cross sections with l_o, $l_1 \leqslant 4$, were calculated for the transition $1^1S - 3^1P$, and cross sections with l_o, $l_1 \leqslant 2$, for the transitions $1^1S - 2^1P$, 4^1P.

The excitation cross sections $\sigma^{\alpha\mu}$ of sublevels with the projection $L_z^a\mu$, are necessary for calculati of the radiation polarization. In the gereral case the formulae for $\sigma^{\alpha\mu}$ are cumbersome. When exciting the P-levels of atoms with a helium outer shell, the cross section is is

$$(6)\quad \sigma^{\alpha\mu} = \frac{4\pi k_1}{k_o^3}\sum_{l_1} |c_\mu^+ T_{l_1+1,\, l_1}^{\,+} + c_\mu^- T_{l_1-1,\, l_1}|^2.$$

Unlike the total cross section, $\sigma^{\alpha\mu}$ can not be represented as a sum of partial cross sections. Interference of the waves with $l_o = l_1 \pm 1$ can in some cases be considerable.

The coefficients $c_\mu^\pm$, b_{11}, and b_{01} are given by equations where $l_m = \max(l_o, l_1)$ and the two signs correspond to $l_o = l_1 \pm 1$.

$$c_1^\pm = \pm\left[\frac{(l_m \mp 1)(2l_o+1)}{2(2l_1+1)}\right]^{\frac{1}{2}}; \quad c_o^\pm = \left[\frac{l_m(2l_o+1)}{2l_1+1}\right]^{\frac{1}{2}};$$

$$b_{11} = \frac{l_m \mp 1}{5(2l_o+1)}; \quad b_{01} = \pm\left[\frac{l_m}{3(2l_o+1)}\right]^{\frac{1}{2}},$$

In a direction perpendicular to the exciting beam, the polarization of radiation for spontaneous transitions from P- to S-levels equals

$$(7)\quad II = \frac{\sigma^{\alpha_o} - \sigma^{\alpha_1}}{\sigma^{\alpha_o} + \sigma^{\alpha_1}}.$$

SOLUTION OF THE PROBLEM C AN ELECTRONIC COMPUTER

The particular solution of Eq. (5) as $r \to \infty$ has the form

$$(8)\quad F_i = A_i \sin\left(k_i r - \frac{l_i\pi}{2} + \eta_i\right), \quad i = 0, 1.$$

If two linearly independent solutions have the phases η_i, ξ_i and amplitudes A_i, B_i, then from their linear combination and eq. (3) we have

$$(9)\quad |T_{\Gamma_o\Gamma}|^2 = \frac{\sin^2(\eta_1 - \xi_1)}{\left(\frac{A_o}{A_1}\right)^2 + \left(\frac{B_o}{B_1}\right)^2 - 2\frac{A_o B_o}{A_1 B_1}\cos(\eta_1 - \xi_1 + \xi_o - \eta_o)}$$

The solution of eqs. (5) assumes the asymptotic form (8) in the case $l \neq 0$ only for very large r, which makes numerical integration difficult. Outside of the atom, when all $\frac{\zeta(r)}{r} \ll \frac{l(l+1)}{r^2}$, but when the centrifugal term is not yet sufficiently small, instead of (8) the following equation is true

$$(10)\quad F_i(r) = a_i^+ j_{l_i}(k_i r) - a_i^- n_{l_i}(k_i r),$$

ere $j_l(x)$ and $n_l(x)$ are the spherical Bessel id Neumann functions multiplied by x, which are pressed through ordinary Bessel's functions of $\frac{1}{2}$ der [5]. The coefficients at determine A and

$$\text{il)} \qquad \operatorname{tn}\eta = \frac{a^-}{a^+}, \qquad A = (a^+)^2 + (a^-)^2 .$$

All calculations were performed on the electro-c computer 'Strela'. The program consisted of ree basic parts: 1) calculation of the field, .e. the functions $\zeta_\alpha(r)$ and $\zeta^q_{ij}(r)$; 2) solu-on of the differential equations; 3) determina-on of the phases, amplitudes, and cross sections. e whole computing process, beginning with intro-ction of field parameters and coefficients l, b etc, c., proceeded automatically.

The field $\frac{\zeta_\alpha}{r}$ may be broken into two parts, e due to the atom core without the outer electron, d the other due to the outer electron itself. The irst part was computed using Slater's nodeless alytic wave functions. The program is useful for n atom core with any number of electrons. The ntribution of the outer electron to ζ_α, and also e functions ζ^q_{iq} were determined using numerical mi-empirical radial functions, obtained on the mputer by using the method given in [6].

In the numerical integration of (5) it was nvenient to introduce new variables $x = r^{\frac{1}{2}}$, $= r^{-\frac{1}{4}}F$, which allowed one to keep a constant ncrement in all of the interval $0 < x < 10$. The nterpolation method of integration with second ifferences with one corrective iteration (method I in [7]) was used. With $k_1 \leq 1$ the increment f integration (in x) was equal to 0.02. For arger k_1 it is necessary to take smaller incre-ents.

On reaching the point $r = 100$, the coefficients a_i^+ and a_i^- were determined at two points according o the values of $F_i(r)$, and then A_i and η_i ccording to eqs. (10) and (11). Further, the equations were again integrated with a different value of $\left.\frac{F_o(r)}{r^{l+1}}\right|_{r=0}$ and B_i and ζ_i were deter-ined analogously. Then the cross section $\sigma_{l_o l_1}$ as computed according to (4) and (9).

To check the accuracy of the mathematical method f solving the equations and the correctness of the rogramming, sample calculations were performed for xcitation of the 2s-level of hydrogen by electrons ith $l_o = l_1 = 0$ at $k_1 = 0.3 - 1.8$. The results btained were compared with cross sections computed n [8] with similar physical assumptions.

RESULTS OF CALCULATIONS

Partial ($\sigma_{l_o l_1}$) and total (σ) excitation ross sections of the 3^1P-level of He for energies p to 13.6 eV from threshold are given in Table 1 and Figure 1. The following two facts stand out. First, the cross sections σ_{sp} and σ_{dp} very rapidly reach a maximum value (at an energy of about 1 eV from threshold), and second, σ_{ps} does not have a maximum at all and decreases monotonically

At energies greater than 1 eV from threshold, excitation is almost completely the result of electrons with the angular momentum $l \geq 1$.

Table 1.

Effective excitation cross sections $1^1S - 3^1P$ He (in units of $10^{-2}\pi a_o^2$); $\epsilon_{\text{threshold}} = 23.308$ eV.

k_1 (in at. units)	ϵ_o (in eV)	σ_{ps}	σ_{sp}	σ_{dp}	σ_{pd}	σ_{fd}	σ_{df}	σ
0.05	23.342	0.446	0.0^320	0.172	0.0^515	0.0^446	—	0.649
0.10	23.444	0.245	0.0^243	1.52	0.0^535	0.0^256	0.0^537	1.808
0.20	23.852	0.166	0.210	3.52	0.0^212	0.606	0.0^412	4.503
0.40	25.484	0.132	0.430	2.72	0.0^226	0.745	0.0^212	4.031
0.60	27.204	0.102	0.366	2.12	0.0^232	1.135	0.0^247	3.731
0.80	32.012	0.074	0.298	1.52	0.0^228	1.286	0.0^2978	3.191
1.0	36.908	0.0503	0.233	1.02	0.0^217	1.220	0.0139	2.539

Consequently, the statement about the overwhelming role played by partial waves with a minimum angular momentum, generally speaking, is not correct even near the threshold. In order to clarify the function of partial waves with large angular momenta, the cross sections for fg- and gf-transitions were computed for three values of k_1. The results given in Figure 1 indicate that beginning with an energy of 10 eV the contribution by σ_{gf} becomes quite substantial.

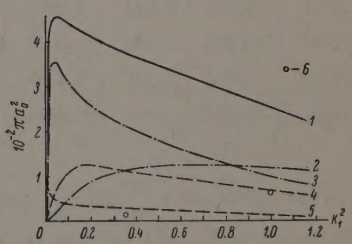

Figure 1. Partial and total excitation cross sections of the 3^1P-level of He as a function of energy of the scattered electron.
$1 - \sigma$, $2 - \sigma_{fd}$, $3 - \sigma_{dp}$, $4 - \sigma_{sp}$, $5 - \sigma_{ps}$, $6 - \sigma_{gf}$. Ordinates of curves 4 and 5 scaled up three times. The curves of σ_{pd}, σ_{df}, and σ_{fg}, coincide with the abscissa in the given scaling.

Analogous results were obtained for excitation cross sections of 2^1P and 4^1P levels of He, as shown in Tables 2 and 3. Also, the calculations performed for excitation of the 2s-level of hydrogen show that at $k_1 > 0.15$, $\sigma_{pp} > \sigma_{ss}$.

The noted properties of partial cross sections are, apparently, due to the same cause.

Monotonically changing curves of partial cross sections were obtained previously for exciting the 2s-[8], 2p, 3p [2] levels of hydrogen. We will not consider these questions in detail here, intending to return to them later. We will merely note

that the accuracy of existing experiments prohibits getting reliable information on cross sections at energies less than 1 eV from threshold.

The function of individual terms in (5) is demonstrated in Table 4 on an example of σ_{sp} and σ_{ps} for exciting the 3^1P-level.

Table 2.

Effective excitation cross sections 1^1S-2^1P He (in units of $10^{-2}\ \pi a_o^2$); $\epsilon_{threshold} = 21.211$ eV.

k_1 in (atomic units)	ϵ_o (in eV.)	σ_{ps}	σ_{sp}	σ_{dp}	σ_{pd}
0.05	21.245	1.13	0.0^343	0.036	–
0.10	21.347	0.976	0.0^213	0.291	0.0^624
0.20	21.755	0.601	0.024	3.72	0.0^568
0.60	25.107	0.274	1.28	9.16	0.0^343
1.00	34.811	0.128	0.810	4.44	0.0^420

Table 3.

Effective excitation cross sections 1^1S-4^1P HE (in units of $10^{-2}\ \pi a_o^2$); $\epsilon_{threshold} = 23.734$ eV.

k_1 (in atomic units)	(ϵ_o in eV)	σ_{ps}	σ_{sp}	σ_{dp}	σ_{pd}
0.05	23.768	0.139	0.0^325	0.250	0.0^561
0.10	23.870	0.092	0.011	1.075	0.0^310
0.20	24.278	0.075	0.541	1.210	0.0^223
0.60	27.630	0.050	0.172	0.820	0.0^227
1.00	37.334	0.026	–	0.406	0.0^217

Table 4.

Excitation cross sections σ_{sp} and σ_{ps} of the 3^1P level (in units of $10^{-2}\ \pi a_o^2$) in various approximations.

k_1 (in atom. units)	ϵ_o (in eV)	σ_{sp} s.c.	σ_{sp} d.w.	σ_{sp} $b_{11}=0$	σ_{sp} Born	σ_{ps} s.c.	σ_{ps} d.w.	σ_{ps} Born
0.1	23.444	0.0^243	0.044	0.33	0.0^316	0.245	0.233	0.213
0.6	27.204	0.366	0.346	0.369	0.017	0.102	0.096	0.706
1.0	36.908	0.233	0.186	0.235	0.030	0.050	0.040	0.500

Note: Arbitrary notations: s.c. - strong coupling, d.w. - method of distorted waves.

In columns marked s.c. the data of Table 1, corresponding to accurate solution of Eqs. (5), are repeated. In the 4th and 8th columns are given the results which were obtained supposing that there is a weak coupling between the incident and scattered waves, when the right-hand side of the first equation of (5) is set equal 0). As is seen, taking strong coupling into account does not significantly affect the cross section. The data of column five were obtained neglecting dipole interaction [$b_{11} = 0$ in Eqs. (5)]. Immediately near the threshold dipole interaction is quite considerable. Finally, cross sections with Born's approximation, which in this case is completely useless, are given in columns si and nine. It is interesting to note that Born's approximation leads to lower rather than higher val as is usually the case.

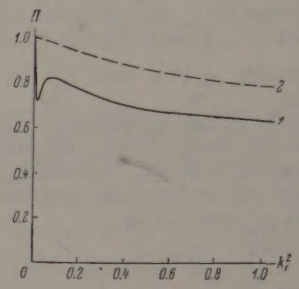

Figure 2. The curve of radiation polarizatio of the $3^1P - m^1S$ transition versus energy of the scattered electron.

1 - Computed from exact solutions, 2 - from Born's approximation.

The curve of radiation polarization versus ene of incident electrons computed from Eqs. (6) and (7 using exact solutions of Eq.(5) and also Born's app mation, are given in Figure 2. As can be seen from Figure 2, polarization in both cases slowly decreas with increasing energy of incident electrons. In t same range of energies the experiment shows a rise polarization from 0 to 0.2 (with a maximum of the order of 0.3 at 25 eV from threshold). Th unlike the cross sections, the exact solution of th radial equations (without exchange) leads to practi cally the same answer of polarization as Born's method.

The authors express deep gratitude to G. F. Drukarev and S. L. Mandel'shtam for their interest in this work and valuable suggestions.

July 21, 195

REFERENCES

1. S. KHASHABA, H. S. MASSEY: Proc. Phys. Soc., 71, 574, (1958)
2. V. I. OCHKUR: Vestn. LGU, No. 4, 53 (1958)
3. I. C. PERCIVAL, M. J. SEATON: Proc. Cambr. Phil. Soc., 53, 654 (1957)
4. G. RACAH: Phys. Rev., 62, 438, (1943)
5. L. SCHIFF: Quantum Mech. IL., M., (1957)
6. L. A. VAINSHTEIN: OiS, 3, 313, (1957)
7. V. E. MILNE: Numerical Methods in Differential Equations (IL., Moscow, 1955)
8. BRANSDEN, MC KEE: Proc. Phys. Soc., A69, 422, (1956)

TOM VII, Vyp. 1 OPTIKA I SPEKTROSKOPIIA Iiul', 1959
TOL. VII, No. 1 OPTICS AND SPECTROSCOPY July, 1959

Anomalies in the Intensities of the Components of the Hyperfine Structure of Resonance Lines in Thallium

IU. I. TURKIN

Abstract: The existence of deviations from equilibrium conditions in the population distribution over the hyperfine structure sub-levels of the ground state of thallium $6^2P_{\frac{1}{2}}$ has been demonstrated directly by the method of reversal of the spectral lines. The higher population of the upper sub-level F = 1 of the $6^2P_{\frac{1}{2}}$ term may be explained by the relatively long lifetime of the excited atom in this state.

INTRODUCTION

In an article published earlier [1] we considered the influence of the excitation conditions on the intensities of the hyperfine structure components of the resonance lines of thallium 2767.8 and 3775.7 Å. An analysis of the experimental data leads one to the supposition that along with the influence of self-absorption in a given case there occurs also a redistribution of concentrations of normal atoms over the sub-levels of the split term $6^2P_{\frac{1}{2}}$.

As is well known, under equilibrium conditions the relative populations of the levels are determined by the Boltzmann factor, which in the case of hyperfine structure corresponds practically to the ratio of the statistical weights of the sub-levels. For the state considered here $6^2P_{\frac{1}{2}}$ (cf. Fig. 1) under equilibrium conditions, the relative populations of the sub-levels with F = 1 and F = 0 is given by $\frac{N_{F=0}}{N_{F=0}} = \frac{3}{1}$. However, on the basis of the effects observed in the components of the hyperfine structure, there is a reason to suppose that the population of the upper sub-level (F = 1) is increased above the equilibrium value by the discharge process. We will later give the results of experiments to test this supposition using the method of reversal [2-4], which allows one to determine the distribution of atoms over the energy levels. As is well known, a simultaneous reversal of emission lines against the background of the spectrum of a black body corresponds to the presence of thermodynamic equilibrium in the source. The relative populations of the levels at the time of reversal is given by the relation

$$\frac{N_k}{N_i} = \frac{g_k}{g_i} \exp\left[-\frac{h\nu_{ik}}{kT}\right], \quad (1)$$

where N_k and N_i are the numbers of atoms in the respective levels, g_k and g_i are the statistical weights of the states i and k. In our case simultaneous reversal of the components a and b of the 3775.7 Å line will be indicative of the existence of equilibrium conditions for the sub-levels F = 1 and F = 0 of the ground state $6^2P_{\frac{1}{2}}$, since these components have the same upper level.

EXPERIMENTAL CONDITIONS

As a black body source in our experiments, we used a krypton lamp of very high pressure, giving an intense continuous spectrum in the ultraviolet. The high resolution apparatus was a DFS-3 four-meter diffraction spectrograph with a resolving power of 150,000 in the second order. The slit width was approximately 15μ. The thallium spectrum was excited at the anode of the discharge tube (diameter 30 mm, separation between slits 250 mm). The discharge tube was placed in an incandescent electric oven whose temperature could be varied so as to change the vapor pressure of the thallium in the discharge tube. The inert gas argon was admitted into the tube to support the discharge.

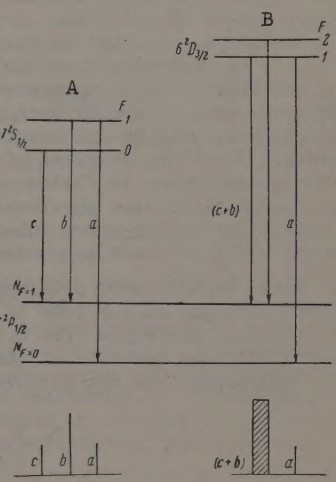

Figure 1. Level scheme for the hyperfine structure of the thallium lines 2767.8 Å (B) and 3775.7 Å (A). A – c:b: a = 1:2:1; B – (c + b): a = 3:1.

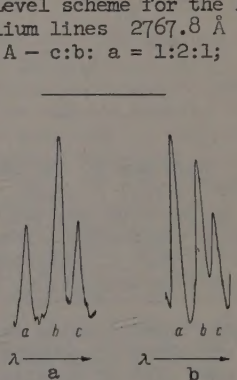

Figure 2. Microphotograms of the structure of the line at 3775.7 Å in emission at a temperature of 530° (a) and 630° (b).

A parallel light beam from the black body source was transmitted through the discharge tube containing the thallium vapor, whose emission was projected through a quartz-fluorite achromat (f = 250 mm) onto the slit of the spectrograph. Photographs were made on contrast plates (spectral type 1). Microphotograms were obtained with an MF-4 recording microphotometer.

RESULTS AND DISCUSSION

Figures 2 and 3 show microphotographs of various stages in the changing of the hyperfine structure of the thallium emission line 3775.7 Å as the vapor pressure of the thallium in the discharge tube is changed. In figure 2 are shown microphotograms of the structure of the 3775.7 Å line for temperatures of 520° ($p_T = 5 \cdot 10^{-4}$ mm Hg) and 630° ($p_T = 3 \cdot 10^{-2}$ mm Hg) in which one may see the anomalous increase in intensity of the component a relative to the other components as the vapor pressure increases. In figure 3 are shown microphotograms giving various stages in the process of reversal of the components of this line. As may be seen from the photograms, reversal does not take place simultaneously for the separate components of the line. Components b and c reverse before component a. Figure 3b is of special interest, since it shows a moment at which the a component is observed in emission, whereas simultaneously components b and c are clearly visible in absorption. Such a behavior of the components during reversal indicates, as has already been pointed out, that equilibrium conditions do not obtain among the lower sub-levels. Since the reversal of the a component takes place later, it follows that under the discharge conditions stated previously, the number of normal atoms in the lower sub-level of the ground state $6^2P_{\frac{1}{2}}$ is less than necessary for equilibrium. These results were obtained for a pressure of the inert gas in the tube of order 0.1 mm Hg. At higher pressures (of order 8 mm Hg) the non-simultaneous reversal of the hyperfine structure components was not observed.

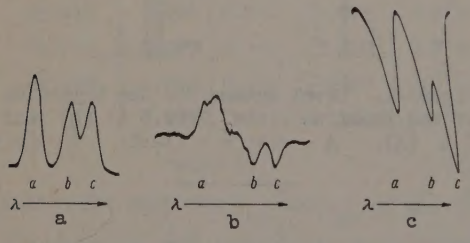

Figure 3. Reversal of the components of the structure of the 3775.7 Å line. (a) The components visible in emission against a background of a black body at a temperature close to reversal. (b) Components b and c reversed. (c) All 3 components visible in absorption.

An analogous investigation was carried out for the hyperfine structure components of another thallium resonance line of wavelength 2767.8 Å. Here as in the case of the line at 3775 Å, the reversal of the short wavelength component ending up in the sub-level with F = 0 occurred later than the reversal of the two other (not separated) components ending up in the sub-level with F = 1.

Thus direct measurements have been made to support the assertion of non-equilibrium populations in the sub-levels of the ground state $6^2P_{\frac{1}{2}}$.

Let us consider some possible reasons for the observed effect. From the level scheme of the hyperfine structure of the thallium line it follow that the upper sub-level of the term $6^2P_{\frac{1}{2}}$ with F = 1 is the final state for those transitions which make up the b and c components of the li at 3776 and 2768 Å. The lower sub-level with F = 0 is the final state only for those transitio which form the a components of these lines, and hence, in the process of emission this level will populated to a significantly lesser degree than th level with F = 1. Under conditions where there i a preferential filling up of the upper sub-level (with F = 1), the equilibrium number of atoms in these two sub-levels could obtain only if there is a large probability for a radiative transition in the radio-frequency region from the sub-levels F = 1 to the sub-level F = 0. A transition of t form F = 1 → F = 0 is forbidden by the selectio rules, and the probability of a spontaneous radio-frequency transition is proportional to ν^3, and hence must be very small. Hence one must expect a relatively longer lifetime for the sub-level F = of the $6^2P_{\frac{1}{2}}$ term, and one may regard it as meta stable.

In the present case we have an analogy with the much investigated case of the relatively long lifetime of the excited states 2^2S and 3^2S in the spectra of hydrogen and ionized helium.

Atoms may also be removed from the F = 1 le by collisions. However the cross-section for processes connected with a change in the orientation the electron spin, which occurs in this instance, very small. It is obvious that under the conditio stated, collisions do not play an important role in the distribution of atoms over the sub-levels o the term $6^2P_{\frac{1}{2}}$. From this point of view it become understandable that the magnitude of the effect depends on the pressure of the inert gas. An increase in the pressure decreases the mean free path of the atoms, increasing the number of collisions and thus leading to a decrease in the observed effect.

In conclusion I consider it my duty to thank S. E. Frish for suggesting the project and for constant interest in it, and also N.I. Kaliteevskii, G. F. Drukarev, I. P. Bogdanov, and V. I. Perel' for taking part in discussions of the results.

July 23, 195

References

1. IU. I. TURKIN: OiS, 2, 290, (1957)
2. N. KOHN: Phys. Zs., 33, 957, (1932)
3. N. P. PENKIN, A. M. SHUKHTIN: Uch. Zap, LU, (7 28, (1949)
4. S. E. FRISH: Vest. LU, (8), 129 (1953)
5. G. HERZBERG: Zs. f. Phys., 146, 3, 269, (1956)

TOM VII, Vyp. 1 OPTIKA I SPEKTROSKOPIIA Iiul', 1959
VOL. VII, No. 1 OPTICS AND SPECTROSCOPY July, 1959

On the Question of the Build-up Time for Thermodynamic Equilibrium in the Plasma of an Arc Discharge

V. K. PROKOF'EV, D. B. GUREVICH, I. M. BELOUSOVA, IU. A. SNIGIREV

Abstract: This paper presents a method for measuring the build-up time for thermodynamic equilibrium in the plasma of an arc burning in air, as well as the results of the measurements. The method consisted of momentary electrical perturbations of the arc plasma. Equilibrium was taken as established when the temperatures, as measured from the atomic and molecular spectra, were equal. The times required to establish equilibrium turned out to be of the order of 20-25 microseconds.

One of the most important questions in the field of optical pyrometry in non-stationary processes capable of flaming is that of the existence of and build-up time of thermodynamic equilibrium. Increasing attention has been given in recent years to the question of the build-up time for equilibrium in gases heated to sufficiently high temperatures by passing a current for combustion or in shock waves.

The calculations carried out by Mandel'shtam and Sukhodrev [1] for the plasma of a spark discharge gave a value of 10^{-7} sec for the time to build-up a state of equilibrium. (The temperature of the discharge was of the order of 40,000° K).

Sanger [2] theoretically considered the conditions of combustion in reaction motors, the time required for transfer of energy among various degrees of freedom, as well as the values of the temperature at different excitation levels of the corresponding degrees of freedom. According to his estimates, energy transfer in the translation modes occurs very rapidly, in a time of approximately 10^{-9} sec; in 10^{-7} sec equilibrium is reached in the rotational modes; and in a time corresponding to say 100,000 collisions, i.e. 10^{-5} sec, equilibrium is reached in the vibrational modes. These results are useful as estimates of the time to establish equilibrium. Direct measurements of the time required for the build-up of equilibrium in gases heated by shock waves were made by Griffith [3] and Blackman [4]. The latter obtained a value of about 5 μsec for air heated to 5500° K; this value refers to the establishment of vibrational equilibrium, as being the slowest of the three and therefore the one that determines arrival at complete equilibrium.

It appears that no direct measurements have as yet been made on the time for establishment of equilibrium in the plasma resulting from an electrical discharge at atmospheric pressure. Such a determination would be of interest for comparison with the values obtained for gases heated by shock waves. In the present paper we describe a method for measuring the time to establish equilibrium in an arc discharge and give the results of measurements.

In the equilibrium state the internal energy of a gas in the plasma phase is equally distributed among all degrees of freedom of a particle, and consists of: kinetic energy of translation of electrons, ions, atoms, and molecules; rotational and vibrational energy of molecules; ionization energy; dissociation energy; and energy of electron excitation. When additional energy is introduced into the plasma the excitation of each of the modes of energy or the processes of ionization or dissociation requires a finite relaxation time τ, and the establishment of complete equilibrium is determined by the longest of these relaxation times.

The essence of the method used in this investigation is that the plasma of a dc arc between carbon electrodes, in which thermodynamic equilibrium exists as is known [5], is "heated" by a short current pulse. The criterion for the establishment of equilibrium is the equality of the temperatures as measured from the molecular vibration, molecular rotation, and atomic emission spectra. The relative intensities of the atomic lines determine the so-called excitation temperature T_{exc}, which at thermodynamic equilibrium is equal to the temperature of the gas, and in the absence of equilibrium characterizes the electron energy. The vibrational temperature T_{vib}, which determines the relative densities of population of the vibrational levels or excitation of the vibrational degrees of freedom of the particles in the plasma source, is measured from the ratio of the intensities of the heads of the spectral bands. The distribution of intensity in the rotational structure of a single band determines the rotational temperature T_{rot}, which characterizes the population of rotational levels, or the excitation of the rotational degrees of freedom. The temperature defined by the vibrational and rotational molecular spectra characterizes the atomic and molecular energies, since the fundamental role in the excitation of vibrational and rotational modes is played by collisions with heavy particles.

In the equilibrium state of the plasma

$$T_{exc} = T_{vib} = T_{rot}. \tag{1}$$

In an arc perturbed from an equilibrium state, equality of these temperatures is attained at an instant corresponding to equipartition of energy among all particles and all degrees of freedom.

We therefore measured the temperatures determined from the atomic, vibrational, and rotational spectra in a dc arc, and the time-variation of these temperatures when the arc was perturbed by a pulsed current. The temperature measured with respect to atomic lines was determined by Ornshtein's usual spectroscopic method, by means of the relative intensities of atomic lines with known transition probabilities. For measurement of vibrational temperatures, Ornshtein's method was used, as developed by Smit [6] for molecular bands with unresolved rotational structure. In this connection we made use of the ratio of the areas of the intensity curves of two neighboring bands $\frac{A_{1-2}}{A_{0-1}}$ (for example, the CN bands 0-0 and 1-1 or 0-1 and 1-2). A modification of the method is the determination of the vibrational temperature by means of the ratio of the intensities of the heads of the same bands with unresolved structure. Since the modified method is much simpler experimentally, it was used in determining the vibrational temperatures. The rotational temperature was determined from the distribution of intensity in the unresolved rotational structure of a single band, that is, from the slope of the intensity curve for a single band.

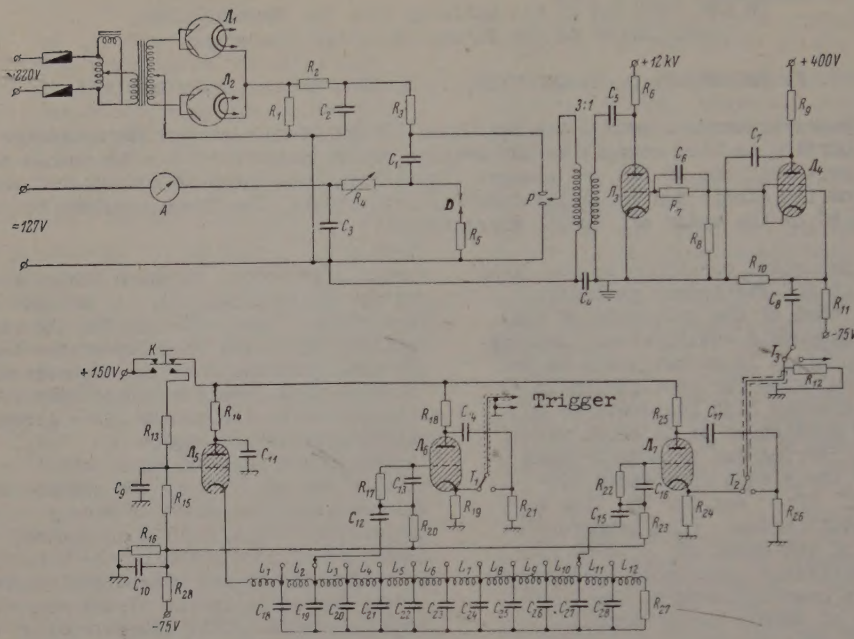

Figure 1. Generator to trigger and circuit to impose the pulse on the arc.

P – discharge gap; D – arc gap. Tubes: Л1, Л2 – 5Z3G; Л3 – TGI-1 – 400/16; Л4 – Л7 – TG1 0.1/0.3. Resis R_1, R_{14}, R_{18}, R_{25} = 1 MΩ; R_2 = 100 Ω; R_3, R_7 = 3 KΩ; R_4 – 20 Ω; R_5 = 0.02 Ω; R_6 = 2 MΩ; R_8 = 10 KΩ; R_9 R_{13} = 3 MΩ; R_{10} = 15 KΩ; R_{11}, R_{17}, R_{22}, R_{28} = 50 KΩ; R_{12} = 500 Ω; R_{15} = 500 KΩ; R_{16} = 25 KΩ; R_{19}, R_{24} = 300 Ω; R_{20}, R_{21}, R_{23} = 2 KΩ; R_{26}, R_{27} = 200 Ω. Condensers: C_1, C_2 = 5 μ F; C_3 = 30 μ F; C_4, C_5 = 0.5 μ F; C_5 = 1500 pF; C_6 = 50 pF; C_7 = 6800 pF; C_8 = 0.06 pF; C_9 = 3000 pF; C_{11}, C_{14}, C_{17} = 3000 C_{15}, C_{15}, C_{18} – C_{28} – 1000 pF; C_{13}, C_{16} = 5 pF; Inductances: L_1 – L_{12} = 150 μ H; K – button-switch; T_1 – T_3 – Tumblers.

EXPERIMENTAL SECTION

A direct current arc between carbon electrodes, with Mark 8-60 cores burning in air at atmospheric pressure was employed. The material of the cores contained a certain quantity of rare earth elements (cerium and lanthanum), sodium, calcium, and a trace of iron. The presence of the cores in the electrodes stabilized the luminous gas column in the arc. The stabilization was necessary in order that the temperatures might be measured in a single portion of the plasma. We separated out the middle portion of the inter-electrode gap, using an interval of length about 1 mm.

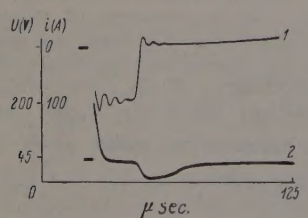

Figure 2. Current (1) and voltage (2) oscillograms for the case of current pulse superposition on an arc.

The entire gap was 4 mm in length. The radiation from this central portion was projected onto the entrance slit of a 4-channel SP-64 photoelectric spectrometer with high luminosity [7]. The exit slits of the spectrometer were set at the respectiv lines or heads of the molecular bands from which th temperatures were determined. (The background was measured in the neighborhood of these lines or band A P-5 photomultiplier was placed at the exit slit and the output signals were fed either to an accumu lator circuit, when the temperature of the arc in t steady state was being measured, or to the input of two OK-17M double-beam oscilloscopes when the temperature in the pulse-perturbed arc was being measured. The alternating current was amplified in the oscilloscope, so that the direct-current-arc emission was not recorded. The oscillograms show the time-variation of the excess illumination induc by the pulse current on the arc. The arc was pulse by a special generator shown in figure 1. The con- denser C_1 (capacitance 5 μF and potential 300V or a pulse-forming line which yielded a square wave was discharged via the auxiliary spark gap P onto the direct current arc D. The pulse-forming line consisted of 6 cells with capacitances C = 0.25 and inductances L = 10 μH. The spark gap P was fired by a TGI-1 400/16 pulse thyratron through a step-up transformer. The firing delay was of the order of a few tenths of a microsecond. A delay li was used to trigger the oscilloscope and the pheno- menon so that either could lead the other by 0.25

to 4 microseconds. The pulse width varied from 20 to 25 μsec, and the current intensity in the pulse varied from 80 to 200 A for a steady state current in the range from 5 to 15 A. Despite such a wide range of variation in the steady state and pulsed currents, we nevertheless found that the decisive role is played by the steady state arc current, since it forms the positive arc column and therefore determines the current density of the pulse. We found, for example, that the intensity of the FeI 4325.76 Å line, with the pulsed current held constant at 100 A, diminished by a factor of 1.5 when the steady state current was varied from 5 to 10 A.

The shape of the pulsed current and the voltage across the electrodes is shown in figure 2. The current pulse has a steep rise, oscillates slightly at the peak — because of imperfections in the forming line — followed by a slower decay. The electrode voltage has an interesting shape . In the stationary arc the electrode voltage is about 45 V; when the current pulse is applied the voltage increases to about 200 V, and then drops in the course of 2.5 – 3 μsec to 60 V, and varies by not more than 10 V during the rest of the pulse. The sharp voltage rise at the beginning of the pulse is connected with the need to supply significant energy to generate the sharp current rise. At the end of the current pulse the voltage falls to 5–8 V, i.e. reaches a value lower than the steady state voltage in the arc. This lowered voltage is due to the residual ionization in the plasma discharge being so high that a negligible voltage drop is sufficient to maintain the steady state current. The previous steady-state voltage (45 V) is recovered during the 100 μsec following the end of the current pulse.

For measurement of the temperature by atomic lines we used the lines FeI 5269.5 and 4325.76 Å, for which the transition probabilities were taken according to Aarts [8]. The values agree with the data obtained by King [9].

For measurement of temperature by the electron-vibration spectra we used the 0—1 and 1—2 bands of CN with heads at 4216.0 and 4197.2 Å. The superposition of the bands was taken into account, where not only the heads of the bands but also the intensity of the "tail" of the 0—1 band was measured hear the head of the 1—2 band around 4197 Å. The background was also measured in the 0—1 band. The rotational temperature was determined from the slope of the intensity curve of the 0—1 band with a head at 4216.0 Å.

Table 1

Transition Probabilities for Atomic Lines and Molecular Bands

λ(in Å)	Tran - sition	E_n (in eV)	f	
			Aarts [8]	King [9]
4325.76	a^5F_2–z^3G_3	4.47	840	760
5269.5	a^5F_5 - z^5D_4	3.21	15.6	15
λ(in Å)	Tran - sition	E (in eV)[10]	P1-2 / P0-1 [5]	—
4216.0	0–1	3.18	1.73	—
4197.2	1–2	3.56		—

Data on the values of the transition probabilities for the atomic lines and molecular bands are given in Table 1. (In Table 1, E is the total energy of the molecule state and E_n is the energy of the highest level.).

The absence of self-absorption was verified by the method of absorption with the arc and its image superimposed [11].

EXPERIMENTAL RESULTS

Tables 2 – 4 present the results of the temperature measurements in the stationary arc. It is apparent that condition (1) is well satisfied, i.e. the middle part of the arc plasma is characterized by a single temperature, independently of the method of measurement. *

Table 2

Arc temperature measured by means of atomic lines in a dc arc (i = 5A)

I_{4325}/I_{5269}	T(in °K)
1.24	4120
1.4	4250
1.4	4250
Mean Value	4200±50

Table 3

Arc temperature measured by means of vibrational spectrum of the CN molecule

I_{4197}/I_{4216}	T(in °K)
0.84	4000
0.88	4200
0.83	4100
0.9	4300
0.91	4300
Mean Value	4200±100

Table 4

Arc temperature measured by means of the rotational spectrum of the CN molecule

I_{4216}/I_{tail}	T (in °K)
4.1	3900
3.5	4500
4.2	3800
4.1	3800
3.7	4200
3.5	4500
Mean Value	4100±250

The curves of figure 3 represent the values of the temperature measured during the first 10 μsec after imposition of the pulse. It is clear that the temperatures measured with respect to the atomic lines and the vibrational spectrum increase by about 1500° K in less than 10^{-6} sec. Table 5 presents the values of the vibrational and rotational temperatures at various instants during the first 10 μsec after initiation of the pulse. The vibrational temperature is essentially constant, and equal to the temperature of the stationary arc, i.e. 4200° K

* The relatively low plasma temperature is due to the presence of Na and Ca in the cores. In the anode region the temperature as measured with respect to CN is higher and the CN bands are bright. The FeI lines, however, are very weak there.

during the first 10 μ sec. The rise in the vibrational temperature (as can be seen from the curve in Fig. 4) takes place 15 μ sec after initiation of the pulse. At some time between 20 and 25 μ sec the plasma can again be said to have reached a single temperature (see also Table 6).

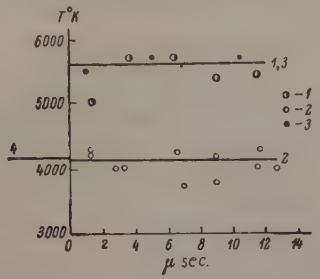

Figure 3. Time dependence of T_{exc} (1), T_{vib} (2) and T_{rot} (3) in a perturbed plasma in the 1 - 12 μ sec range. 4 - DC arc temperature up to the passage of the pulse.

Temperature (in °K): 1- 4150±400, 5600±200, 5600±100.

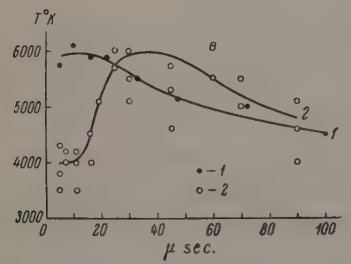

Figure 4. Time dependence of T_{exc}(1) and T_{vib}(2) in a perturbed plasma in the 1 – 100 μ sec range.

It should be noted that the error of measurement of temperature in the perturbed arc is significantly higher than the error in the stationary arc, and amounts to approximately 500° in the CN measurements; it is rather lower in the atomic line measurements (200°). It would appear that the somewhat higher values of the maximum vibrational temperature — as compared to the atomic line temperature — arise from errors of measurement.

The arc cools off rather slowly. While the pulse duration is 17 μ sec (for the curves of Fig. 4) the plasma temperature up to 100 μ sec remains higher than that of the stationary arc. Hence, we conclude that an arc burning in air at atmospheric pressure reaches equilibrium in a time of the order of 20-25 μ sec. On comparison with Blackman's results for air heated by a shock wave it is apparent that equilibrium is attained somewhat more slowly for all degrees of freedom for an arc burning in air. This discrepancy can be attributed to a different mechanism for supplying the energy. In Blackman's case the energy is immediately absorbed by atoms and molecules, and in the arc it is first absorbed by electrons.

Table 5

Results of Measuring the Temperature in the Perturbed Plasma by Means of the Molecular Spectrum of CN

Time from the start of the current pulse (in μsec)	I_{1216}/I_{tail}	T_{rot}(in °K)	I_{4216}/I_{tail}	T_{rot}(in °K)	I_{4197}/I_{4216}	T_{vib}(in °K)	I_{4197}/I_{4216}	T_{vib}(in °K)	I_{4197}/I_{4216}	$T_{...}$(in °K)
1	3.2	5100	2.6	—	0.83	4000	0.88	4200	0.9	44
4	2.8	5700	3.2	5100	0.83	4000	0.83	4000	0.83	40
6.5	2.8	5700	3.1	5200	0.88	4200	0.89	4250	0.8	38
9	3	5400	3.2	5100	0.89	4250	0.8	3800	0.87	41
11.5	3	5400	3	5300	0.91	4400	0.9	4300	0.84	40
12.5	3.2	5100	2.8	5700	0.87	4200	0.86	4000	0.84	40
mean value	—	5400± ±200	—	5500± ±400	—	4200± ±100	—	4100± ±150	—	410 ±2

Table 6

Results of Measuring the Temperature of a Plasma in a dc Arc and in a Perturbed Arc

Arc characteristic	$\frac{I_{4325}}{I_{5269}}$	T_{exc} (in °K)	$\frac{I_{4216}}{I_{tail}}$	T_{rot} (in °K)	$\frac{I_{4197}}{I_{4216}}$	T_{vib} (in °K
dc arc	1.34	4200±50	3.9	4100±250	0.87	4200±10
Pulse arc	3.4	5700±200	2.9	5600±500	0.87	4200±20
	3.7	5900±200	2.9	5600±500	1.1	6000±20

Remark: Average values for a number of measurements are presented for the temperatures in the table.

July 25, 1958

References

1. S. L. MANDEL'SHTAM, N. K. SUKHODREV: ZETF, 24, 701 (1953)
2. E. SANGER: Voprosy raketnoi tekhniki, 4, 7 (1954)
3. W. GRIFFITH, BRICKL, V. BLACKMAN: Phys. Rev., 102, 1209 (1956)
4. V. BLACKMAN: Dissertation abstracts (Princeton Univ.), 17, 651 (1957)
5. H. BRINKMANN: Dissertation, Utrecht, (1937)
6. J. SPIER, J. SMIT: Physica, 9, 422, (1942) 9, 597, (1942); J. SMIT-MIESSEN, J. SPIER: Physica, 9, 193, (1942)
7. V. K. PROKOF'EV: IAN USSR FS, 22, 437 (1958) (See CIT Bulletin)
8. J. AARTS, D. HARTING, C. J. BAKKER: Physica, 20, 1250 (1954)
9. R. B. KING, A. S. KING: Astr. J., 82, 377 (1935); 87, 24 (1938); 95, 78 (1942)
10. K. F. BARROW, A. D. CAUNT: Tables de constantes, Paris, 1951
11. I. V. PODMOSHENSKII, L. D. KONDRASHOVA: Fiz. sb. L'vov Univ., 2, No. 4(9), 204 (1958)

TOM VII, Vyp. 1
VOL. VII, No. 1

OPTIKA I SPEKTROSKOPIIA
OPTICS AND SPECTROSCOPY

Iiul', 1959
July, 1959

Theory of the Intensities of the Infrared Spectra of Methane, Ethane and Hexadeuteroethane

L. M. SVERDLOV

Abstract: A calculation was made of the intensities of the infrared bands and electro-optical parameters of the molecules methane, ethane and hexadeuteroethane in the first approximation of the valence-optical scheme.

Good agreement was obtained between calculated and observed intensities.

1. In previous work [1, 2], we showed (using ethylene and the methyl halides as examples) that it is necessary to use the first approximation of the valence-optical scheme for the calculation of intensities of infrared spectra [3]. It is of interest to consider in this approximation the very simple hydrocarbons methane and ethane in order to determine the parameters which characterize the distribution of the electron cloud and the polarity of the CH bonds.

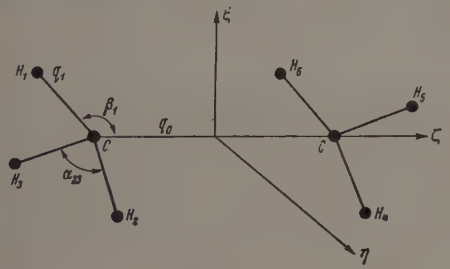

2. Measurements of the absolute integrated intensities of the infrared bands of ethane were carried out by the authors of references [4 and 5]. More trustworthy results were obtained in the latter work [5], in which the infrared spectrum of C_2D_6 was investigated at the same time. On the basis of the results obtained in the papers indicated, calculations were made of the (bond) dipole moments μ_{CH} and derivatives of the dipole moment with respect to the bond length $\frac{d\mu_{CH}}{dq}$ of ethane in the zero approximation of the valence optical scheme; for different types of symmetry A_{2u} and E_u the parameters μ_{CH} and $\frac{d\mu_{CH}}{dq}$ had different values, a fact which is devoid of physical significance.

3. For calculation of the intensities of the infrared bands of ethane we will introduce natural vibrational coordinates — changes of the length of the bonds and sizes of the angles q_i, β_i ($i = 1, 2, \ldots 6$), q_o, α_{ij} (see figure). The ethane molecule belongs to symmetry group D_{3d}. In the infrared spectrum the active vibrations are of the symmetry types A_{2u} and E_u. The symmetry coordinates S_k^K have the form

$$q^{A_{2u}} = \frac{1}{\sqrt{6}}(q_1+q_2+q_3-q_4-q_5-q_6);$$

$$\beta^{A_{2u}} = \frac{1}{\sqrt{6}}(\beta_1+\beta_2+\beta_3-\beta_4-\beta_5-\beta_6);$$

$$\alpha^{A_{2u}} = \frac{1}{\sqrt{6}}(\alpha_{12}+\alpha_{13}+\alpha_{23}-\alpha_{45}-\alpha_{46}-\alpha_{56}),$$

where

$$\alpha^{A_{2u}} + \beta^{A_{2u}} = 0;$$

$$q^{E_uII} = \frac{1}{\sqrt{3}}\left(q_1-\frac{1}{2}q_2-\frac{1}{2}q_3-q_4+\frac{1}{2}q_5+\frac{1}{2}q_6\right);$$

$$\beta^{E_uII} = \frac{1}{\sqrt{3}}\left(\beta_1-\frac{1}{2}\beta_2-\frac{1}{2}\beta_3-\beta_4+\frac{1}{2}\beta_5+\frac{1}{2}\beta_6\right);$$

$$\alpha^{E_uII} = \frac{1}{\sqrt{3}}\left(\alpha_{23}-\frac{1}{2}\alpha_{12}-\frac{1}{2}\alpha_{13}-\alpha_{56}+\frac{1}{2}\alpha_{45}+\frac{1}{2}\alpha_{46}\right).$$

Expressing these in terms of the normal coordinates Q_l, we obtain $\left(S_k^{(K)} = \sum_l L_{kl}Q_l\right)$

$$q^{A_{2u}II} = \sum_{l=5}^{6} C_{ql}Q_l; \qquad \alpha^{A_{2u}} = -\beta^{A_{2u}} = \sum_{l=5}^{6} D_{\alpha l}Q_l;$$

$$q^{A_{2u}II} = \sum_{l=7}^{9} C_{ql}Q_l; \quad \alpha^{E_uII} = \sum_{l=7}^{9} D_{\alpha l}Q_l; \quad \beta^{E_uII} = \sum_{l=7}^{9} D_{\beta l}Q_l.$$

Further, we shall introduce the valence-optical coordinates β_{ni} — changes of angles between bonds and axes. They fulfill the following 7 conditions

$$\beta_{o\zeta}^2 = \beta_{o\xi}^2 + \beta_{o\eta}^2; \quad \beta_{1\xi} - \beta_{1\zeta} = 0; \quad \beta_{2\eta} - \frac{\sqrt{7}}{3}\beta_{2\xi} - \frac{2}{3}\beta_{2\zeta} = 0;$$

$$\beta_{3\eta} + \frac{\sqrt{7}}{3}\beta_{3\xi} + \frac{2}{3}\beta_{3\zeta} = 0; \quad \beta_{4\xi} - \beta_{4\zeta} = 0; \quad \beta_{5\eta} - \frac{\sqrt{7}}{3}\beta_{5\xi} - \frac{2}{3}\beta_{5\zeta} = 0;$$

$$\beta_{6\eta} + \frac{\sqrt{7}}{3}\beta_{6\xi} + \frac{2}{3}\beta_{6\zeta} = 0.$$

We express the 14 independent coordinates β_{ni} in terms of the independent coordinates φ (changes of angles of the CH bonds with the ζ axis), ψ (rotation of the CH bonds around the ζ axis) and ω (rotations of the CC bond in the $\xi\zeta$ and $\eta\zeta$ planes.

$$\beta_{0\xi} = -\omega_\xi;\quad \beta_{0\eta} = -\omega_\eta;\quad \beta_{0\zeta} = \sqrt{\omega_\xi^2+\omega_\eta^2};\quad \beta_{1\xi} = \varphi_1;$$

$$\beta_{1\eta} = -\frac{\sqrt{8}}{3}\psi_1;\quad \beta_{1\zeta} = \varphi_1;$$

$$\beta_{2\xi} = \sqrt{\frac{6}{7}}\psi_2 - \frac{1}{2\sqrt{7}}\varphi_2;\quad \beta_{2\eta} = \sqrt{\frac{2}{3}}\psi_2 + \frac{1}{2}\varphi 2;\quad \beta_{2\zeta} = \varphi_2;$$

$$\beta_{3\xi} = -\sqrt{\frac{6}{7}}\psi_3 - \frac{1}{2\sqrt{7}}\varphi_3;\quad \beta_{3\eta} = \sqrt{\frac{2}{3}}\psi_3 - \frac{1}{2}\varphi_3;\quad \beta_{3\zeta} = \varphi_3;$$

$$\beta_{4\xi} = -\varphi_4;\quad \beta_{4\eta} = \frac{\sqrt{8}}{3}\psi_4;\quad \beta_{4\zeta} = -\varphi_4;$$

$$\beta_{5\xi} = -\sqrt{\frac{6}{7}}\psi_5 + \frac{1}{2\sqrt{7}}\varphi_5;\quad \beta_{5\eta} = -\sqrt{\frac{2}{3}}\psi_5 - \frac{1}{2}\varphi_5;\quad \beta_{5\zeta} = -\varphi_5;$$

$$\beta_{6\xi} = \sqrt{\frac{6}{7}}\psi_6 + \frac{1}{2\sqrt{7}}\varphi_6;\quad \beta_{6\eta} = -\sqrt{\frac{2}{3}}\psi_6 + \frac{1}{2}\varphi_6;\quad \beta_{6\zeta} = -\varphi_6;$$

The valence-optical symmetry coordinates have the form

$$\varphi^{A_{2u}} = \frac{1}{\sqrt{6}}(\varphi_1+\varphi_2+\varphi_3-\varphi_4-\varphi_5-\varphi_6);\quad \Big/\varphi^{E_uII} = \frac{1}{\sqrt{3}}\Big(\varphi_1 - \frac{1}{2}\varphi_2 - \frac{1}{2}\varphi_3 - \varphi_4 + \frac{1}{2}\varphi_5 + \frac{1}{2}\varphi_6\Big);\quad \Big/\psi^{E_uII} = \frac{1}{2}(\psi_2 - \psi_3 - \psi_5 + \psi_6).$$

They are expressed in terms of normal coordinates in the following way :

$$\varphi^{A_{2u}} = \sum_{l=5}^{6} E_l Q_l;\quad \varphi^{E_uII} = \sum_{l=7}^{9} E_l Q_l;\quad \psi^{E_uII} = \sum_{l=7}^{9} F_l Q_l.$$

Further we express the coefficients E_l and F_l by the coefficients D_l, which are determined from solution of the mechanical problem

$$E_l^{A_{2u}} = -D_{\alpha l}^{A_{2u}};\quad E_l^{E_uII} = D_{\beta l}^{E_uII};\quad F_l^{E_uII} = \frac{1}{3}D_{\beta l}^{E_uII} - \frac{2}{3}D_{\alpha l}^{E_uII}.$$

As a result of complicated calculations we obtain the following expressions for derivatives of the dipole moment in normal coordinates

$$\frac{\partial P_\zeta}{\partial Q_l^{A_{2u}}} = \Bigg\{\Bigg[-\sqrt{\frac{2}{3}}\Big(\frac{\partial \mu_{CH}^{(1)}}{\partial q_1} + 2\frac{\partial \mu_{CH}^{(2)}}{\partial q_1} - \frac{\partial \mu_{CH}^{(4)}}{\partial q_1} - 2\frac{\partial \mu_{CH}^{(5)}}{\partial q_1}\Big) - \frac{4}{\sqrt{3}}\mu_{CH}\Big(\frac{\partial \varphi_1}{\partial q_1} + 2\frac{\partial \varphi_2}{\partial q_1} - \frac{\partial \varphi_4}{\partial \varphi_1} - 2\frac{\partial \varphi_5}{\partial q_1}\Big)\Bigg] C_{ql} +$$

$$+\Bigg[-\frac{4}{\sqrt{3}}\cdot\frac{\mu_{CH}}{r_{CH}} - \frac{4}{\sqrt{6}}\Big(\frac{\partial \mu_{CH}^{(1)}}{\partial \varphi_1} + 2\frac{\partial \mu_{CH}^{(2)}}{\partial \varphi_1} - \frac{\partial \mu_{CH}^{(4)}}{\partial \varphi_1} - 2\frac{\partial \mu_{CH}^{(5)}}{\partial \varphi_1}\Big)\frac{1}{r_{CH}}$$

$$\frac{\partial P_\xi}{\partial Q_l^{A_{2u}}} = \frac{\partial P_\eta}{\partial Q_l^{A_{2u}}} = 0,\ (l=5,\ 6).$$

$$\frac{\partial P_\eta}{\partial Q_l^{E_uII}} = \Bigg\{\Bigg[2\sqrt{\frac{2}{3}}\Big(\frac{\partial \mu_{CH}^{(1)}}{\partial q_1} - \frac{\partial \mu_{CH}^{(2)}}{\partial q_1} - \frac{\partial \mu_{CH}^{(4)}}{\partial q_1} + \frac{\partial \mu_{CH}^{(5)}}{\partial q_1}\Big) - \frac{1}{\sqrt{3}}\mu_{CH}\Big(\frac{\partial \varphi_1}{\partial q_1} - \frac{\partial \varphi_2}{\partial q_1} - \frac{\partial \varphi_4}{\partial q_1} + \frac{\partial \varphi_5}{\partial q_1}\Big)\Bigg] C_{ql} + \Bigg[-\frac{1}{\sqrt{3}}\cdot\frac{\mu_{CH}}{r_{CH}}$$

$$+\sqrt{\frac{2}{3}}\Big(\frac{\partial \mu_{CH}^{(1)}}{\partial \varphi_1} - \frac{\partial \mu_{CH}^{(2)}}{\partial \varphi_1} - \frac{\partial \mu_{CH}^{(4)}}{\partial \varphi_1} + \frac{\partial \mu_{CH}^{(5)}}{\partial \varphi_1}\Big)\frac{1}{r_{CH}}\Bigg] E_l +$$

$$+\Big(-2\sqrt{\frac{2}{3}}\frac{\mu_{CH}}{r_{CH}}\Big)F_l\Bigg\};\quad \frac{\partial P_\xi}{\partial Q_l^{E_uII}} = \frac{\partial P_\zeta}{\partial Q_l^{E_uII}} = 0,$$

$$(l = 7,\ 8,\ 9).$$

The coefficients C_l, D_l were obtained by inverting $\left\|L^{-1}_{lk}\right\|^{A_{2u}}$ and $\left\|L^{-1}_{lk}\right\|^{E_aII}$, (which connect Q_l and S_k)* cited in reference [5]. With the help of (3) and using these coefficients we calculated the coefficients E_l, F_l (see table 1). Putting into (4) the values of $\frac{\partial P}{\partial Q_l}$ found experimentally [5] and the coefficients C_{l_1} E_{l_1} F_{l_1} and solving the resulting system of equations we obtain the derivatives of the dipole moment with respect to the symmetry coordinates $\frac{\partial P}{\partial S_k}$ of the molecules C_2H_6 and C_2D_6. In table 2 are presented the average values of $\frac{\partial P}{\partial S_k}$ for C_2H_6 and C_2D_6 which correspond to the different combinations of signs of $\frac{\partial P}{\partial Q_l}$. The designations in table 1 have the following meaning: for example, the signs + − mean that the derivatives $\frac{\partial P}{\partial Q_5}$ and $\frac{\partial P}{\partial Q_6}$ are added respectively with signs + and −. It is necessary to choose those values of $\frac{\partial P}{\partial S_k}$ for which the calculated values of $\frac{\partial P}{\partial Q_l}$ agree best with the experimental values of $\frac{dP}{dQ_l}$ simultaneously for C_2H_6 and C_2D_6.

* In [5] another coordinate, S_6, is used in place of $\alpha^{A_{2u}}$. S_6 occurs as a combination of α_{ij} and β_i, and has been transformed here into $\alpha^{A_{2u}}$

Table 1

Coefficients C_l, E_l, F_l;. C_2H_6 and C_2D_6 n units 10^{12} $g^{-\frac{1}{2}}$).

ole-cule	Coordinate	Symmetry type A_{2u}		Symmetry type E_u		
		Q_5	Q_6	Q_7	Q_8	Q_9
H_6	q	0.7604	-0.1902	0.8101	-0.0282	-0.0864
	φ	-0.1484	-0.8423	0.0578	0.2144	0.7461
	ψ	—	—	-0.0864	-0.7724	0.2623
D_6	q	0.5435	-0.1425	0.6012	-0.0293	-0.0602
	φ	-0.084	-0.6525	-0.0206	0.1202	0.5409
	ψ	—	—	-0.1281	-0.5711	0.1782

Table 2

Derivatives of the dipole moment with respect the symmetry coordinates (in units D/Å).

ri-a-ve.	Symmetry type A_{2u}		Symmetry type E_u			
	− −	+ −	+++	++ −	+ − −	+ − +
..	-1.0135	1.1151	1.0795	1.0873	1.2296	1.2219
..	0.5281	0.0554	0.5228	0.0035	-0.2492	0.2701
..	—	—	-0.3494	-0.4759	0.3152	0.4418

s follows from table 3, the best agreement is btained for the following combinations of signs of $\frac{\partial P}{\partial Q_l}$: for A_{2u} symmetry type − − or + +, for E_u ymmetry type + − + or − + − . Using the values f $\frac{\partial P}{\partial S}$ which correspond to these variants we obtain he system of electrooptical parameters of ethane see table 4). At this point we must observe that systems of parameters are obtained, which corres-ond to two possible combinations of signs of $\frac{\partial P}{\partial Q_l}$ f the symmetry types A_{2u} and E_u: + +, + − +, nd − −, + − +. The preferred system is that orresponding to the combination − −, + − +, for in the first variant the parameters $\frac{\partial \mu_{CH}^{(2)}}{\partial q_1}$ (which re discarded in the zero approximation) are too ig in comparison with $\frac{d\mu_{CH}^{(1)}}{dq_1}$.

4. Comparison of the electrical parameters of the molecules we considered (C_2H_4, C_2D_4; CH_3Cl, CD_3Cl; CH_3Br, CD_3Br; CH_3I, CD_3I; C_2H_6, C_2D_6) allows us to reach some general conclusions. First of all, the derivative of the dipole moment with respect to the length of the bond $\frac{\partial \mu_i}{\partial q_i}$ is always found in combination with other parameters ($\frac{\partial \mu_i}{\partial q_j}$, $\frac{\partial \varphi}{\partial q}$). This circumstance must always be allowed for when conclusions are drawn concerning changes of the polarity of bonds on the basis of comparison of values of $\frac{\partial \mu}{\partial q}$. In particular, conclusions concerning change of polarity of bonds made by many authors, using values of $\frac{\partial \mu}{\partial q}$ calculated by the zero approximation of the valence-optical scheme, are meaningless.

Further, in all molecules considered, the bond dipole moments μ_i and derivatives of the dipole moment with respect to the length of the bond $\frac{\partial \mu_i}{\partial q_i}$ (in some cases, $\frac{\partial \mu_i}{\partial q_j}$, $\frac{\partial \varphi}{\partial q}$) have opposite signs. This means that with increase of the length of the bonds their dipole moments decrease. The last conclusion may be used as a criterion for choice of the correct values of μ and $\frac{\partial \mu}{\partial q}$ for those molecules for which data is lacking with respect to the intensities of the infrared bands of their isotopic analogs.

5. For the calculation of methane we will introduce the natural vibrational coordinates $q_i (i = 1, 2, \ldots, 4)$, $\alpha_{ij} (i \neq j = 1, 2, \ldots, 4)$ and valence-optical coordinates $\beta_{n\xi}$, $\beta_{n\eta}$, $\beta_{n\zeta}$, $(n = 1, 2, \ldots, 4)$. The CH_4 molecule belongs to the T_d symmetry group. In the infrared spectrum, triply degenerate vibrations of the F_2 symmetry type are active. The symmetry coordinates have the form

$$q^{F_2} = \frac{1}{2}(q_1 + q_2 - q_3 - q_4); \quad \alpha^{F2} = \frac{1}{\sqrt{2}}(\alpha_{12} - \alpha_{34});$$

$$\beta^{F_2} = \frac{1}{2\sqrt{6}}(-\beta_{1\xi} - \beta_{1\eta} + 2\beta_{1\zeta} + \beta_{2\xi} + \beta_{2\eta} + 2\beta_{2\zeta} - \beta_{3\xi} + \beta_{3\eta} + 2\beta_{3\xi} + \beta_{4\xi} - \beta_{4\eta} + 2\beta_{4\zeta}).$$

Their expressions in terms of normal coordinates may be written in the following way:

$$q^{F2} = \sum_{l=3}^{4} C_l Q_l, \quad \alpha^{F2} = \sum_{l=3}^{4} D_l Q_l, \quad \beta^{F2} = \sum_{l=3}^{4} H_l Q_l,$$

Table 3

Derivatives of the dipole moment with respect to normal coordinates for C_2H_6 and C_2D_6 (in units OGSE cm $g^{\frac{1}{2}}$)

Frequency (in cm^{-1})	Symmetry	$\frac{\partial P}{\partial Q}$	Experiment	− −	+ −	Frequency (in cm^{-1})	Symmetry	$\frac{\partial P}{\partial Q}$	Experiment	+ + +	+ + −	+ − −	Error in %	+ − +	Error in %
								C_2H_6							
3061	A_{2u}	$\frac{\partial P}{\partial Q_5}$	84.57±2.5	−84.901	+83.9636	3140	E_u	$\frac{\partial P}{\partial Q_7}$	95.92±1.5	93.4876	92.2093	95.4498	0.49	96.7281	0.84
1438	A_{2u}	$\frac{\partial P}{\partial Q_6}$	24.37	−25.2099	−25.8716	1526	E_u	$\frac{\partial P}{\partial Q_8}$	31.45	35.1582	33.7741	−33.1527	5.41	−31.7685	1.01
—	—	—	—	—	—	822	E_u	$\frac{\partial P}{\partial Q_9}$	20.85±0.1	20.5162	−21.6136	−20.9486	0.47	21.1812	1.59
								C_2D_6							
2169	A_{2u}	$\frac{\partial P}{\partial Q_5}$	59.74±1.8	−59.5266	60.143	2316	E_u	$\frac{\partial P}{\partial Q_7}$	68.92±1.9	70.4548	71.4712	69.3762	0.66	68.3599	0.81
1112	A_{2u}	$\frac{\partial P}{\partial Q_6}$	20.67	−20.0182	−19.5075	1111	E_u	$\frac{\partial P}{\partial Q_8}$	25.82	23.0757	+24.0397	−24.5968	4.74	−25.5608	1.0
—	—	—	—	—	—	594	E_u	$\frac{\partial P}{\partial Q_9}$	15.36±0.5	15.5568	−14.8304	−15.2641	0.62	15.1231	1.54

Table 4

Electrooptical Parameters of Ethane and Hexaduteroethane (in units of D/Å)

Electrooptical Parameter	$A_{2u}(+\,+)$, $E_u(+\,-\,+)$	$A_{2u}(-\,-)$, $E_u(+\,-\,+)$
μ_{CH} (in units of D)	−0.2981	−0.2981
μ_{CH}/r_{CH}	−0.2705	−0.2705
$\left\{\left(\frac{\partial \mu_{CH}^{(1)}}{\partial q_1} - \frac{\partial \mu_{CH}^{(4)}}{\partial q_1}\right) + \frac{\sqrt{2}}{2}\mu_{CH}\left[\left(\frac{\partial \varphi_1}{\partial q_1} - \frac{\partial \varphi_4}{\partial q_1}\right) + 3\left(\frac{\partial \varphi_2}{\partial q_1} - \frac{\partial \varphi_5}{\partial q_1}\right)\right]\right\}$	0.085	0.9126
$\left\{\left(\frac{\partial \mu^{(2)}}{\partial q_1} - \frac{\partial \mu_{CH}^{(5)}}{\partial q_1}\right) + \frac{\sqrt{2}}{4}\mu_{CH}\left[3\left(\frac{\partial \varphi_1}{\partial q_1} - \frac{\partial \varphi_4}{\partial q_1}\right) + 5\left(\frac{\partial \varphi_2}{\partial q_1} - \frac{\partial \varphi_5}{\partial q_1}\right)\right]\right\}$	−0.6632	0.1644
$\frac{1}{r_{CH}}\left(\frac{\partial \mu_{CH}^{(1)}}{\partial \varphi_1} - \frac{\partial \mu_{CH}^{(4)}}{\partial \varphi_1}\right)$	0.2586	0.043
$\frac{1}{r_{CH}}\left(\frac{\partial \mu_{CH}^{(2)}}{\partial \varphi_1} - \frac{\partial \mu_{CH}^{(5)}}{\partial \varphi_1}\right)$	0.2237	0.0081

here:

$$H_l = \frac{\sqrt{3}}{2} D_l$$

Derivatives $\frac{\partial P}{\partial Q_l}$ in the first approximation f the valence-optical-scheme have the form:

$$\frac{\partial P_\zeta}{\partial Q_e}_{F_2} = \frac{2}{\sqrt{3}}\left(\frac{\partial \mu_{CH}^{(1)}}{\partial q_1} - \frac{\partial \mu_{CH}^{(2)}}{\partial q_1}\right) C_l - \frac{2}{\sqrt{3}} \cdot \frac{\mu_{CH}}{r_{CH}} D_l;$$

$$\frac{\partial P_\zeta}{\partial Q_l}_{F_2} = \frac{\partial P_\eta}{\partial Q_l}_{F_2} = 0 (l = 3, 4)$$

For calculation of the coefficients D_l, C_l, he mechanical problem was solved, using the zero-rder frequencies presented in reference [6]. As result of the calculation the following force onstants (in units of 10^6 cm^{-2}) were obtained*:

$$K_q = 9.2436, \quad h = 0.0036, \quad K_\alpha - 0_{\alpha\alpha} = 0.805,$$

$$a_\alpha - b_\alpha = 0.4688, \quad l_{\alpha\alpha} - Q_{\alpha\alpha} = -0.0102.$$

Table 5

ntensities and Electrooptical Parameters of Methane

	CH_4 (Experimental)			CD_4 (Calculated)	
Frequency [6] (in cm^{-1})	A_i (x 10^{10} $\frac{cycles}{sec. \cdot cm}$)	$\frac{\partial P}{\partial Q_l}$ $\left(\frac{CGSE}{cm.g^{\frac{1}{2}}}\right)$	Frequency [6] (in cm^{-1})	A_i (x 10^{10} $\frac{cycles}{sec. \cdot cm}$)	$\frac{\partial P}{\partial Q_l}$ $\left(\frac{CGSE}{cm.g^{\frac{1}{2}}}\right)$
3156.9	1075	61.6	2336.8	481	41.2
1357.6	472	40.8	1026.8	293	32.2

Electrooptical Parameter	+ +	+ −
$\left(\frac{\partial \mu_{CH}^{(1)}}{\partial q_1} - \frac{\partial \mu_{CH}^{(2)}}{\partial q_1}\right)$ (in units D/Å) ...	0.6763	0.6446
μ_{CH}/r_{CH} (in units D/Å)	−0.3382	0.2492
μ_{CH} (in units D)	−0.3696	0.2724

The coefficients C_l, D_l (in units of 10^{12} $g^{-\frac{1}{2}}$) are:

C_2H_4: C_3=0.8111, C_4= −0.0814, D_3= −0.0438, D_4= 1.2087.

C_2D_4: C_3=0.6031, C_4= −0.0467, D_3= −0.1508, D_4= 0.9181.

Absolute integrated intensities of the infrared bands of methane have been determined a number of times [4, 7-9]. The most precise results were obtained in the most recent work [8, 9]. (Unfortunately, data are lacking in the literature with respect to the intensities of the infrared bands of CD_4, which are necessary for a unique choice of the values of the electrooptical parameters).

Substituting in (5) the values of C_l, D_l and experimental values of $\frac{\partial P}{\partial Q_l}$, we calculated the parameters μ_{CH} and $\left(\frac{\partial \mu_{CH}^{(1)}}{\partial q_1} - \frac{\partial \mu_{CH}^{(2)}}{\partial q_1}\right)$ In table 5, these parameters are presented corresponding to the different combinations of signs of $\frac{\partial P}{\partial Q_l}$. To choose the true values of the parameters we may avail ourselves of the criteria formulated above. From table 5 it is evident that different signs of μ_{CH} and $\frac{\partial \mu_{CH}}{\partial q}$ are obtained only in the first variant (+ +); consequently preference is given to these parameters. With the help of these parameters the intensities of the infrared bands of CD_4 were calculated.

July 21, 1958

REFERENCES

1. L. M. SVERDLOV: OiS, 4, 697, (1958)
2. L. M. SVERDLOV: OiS, 6, 729, (1959)
3. M.V.VOL'KENSHTEIN M.A.EL'IASHEVICH AND B. I. STEPANOV: Vibrations of Molecules, 1 and 2 (GITTL, Moscow, 1949)
4. A. M. THORNDIKE: J. Chem. Phys., 15, 868, (1947)
5. I. M. NYQUIST, I. M. MILLS, W. B. PERSON AND B. CRAWFORD: J. Chem. Phys., 26, 552, (1957)
6. H. M. KAYLOR AND A. H. NIELSEN: J. Chem. Phys., 23, 2139 (1955)
7. R. ROLLEFSON AND R. HAVENS: Phys. Rev., 57, 710, (1940)
8. H. L. WELSH, P. E. PASHLER AND A. F. DUNN: J. Chem. Phys., 19, 340, (1951)
9. H. L. WELSH, P. J. SANDIFORD: J. Chem. Phys., 20, 1646, (1952)

*Using designations taken in monograph [3].

TOM VII, Vyp. 1
VOL. VII, No. 1

OPTIKA I SPEKTROSKOPIIA
OPTICS AND SPECTROSCOPY

Iiul', 19
July, 19

Optical Characteristics of Compounds of the Oxazole, Oxadiazole and Furan Series *

IU. N. PANOV, N. A. ADROVA, AND M. M. KOTON

Abstract: It has been established that in the oxazole and oxadiazole series, as the number of hetero - nitrogen atoms is decreased, there is a decrease of the quantum yield of luminescence and a shift of the lum nescence and absorption spectra to long wavelengths. Within the series, the shift of spectra to long wave- lengths and decrease of the quantum yield of luminescence occurs as one changes from phenyl to styryl radica

In order to establish the connection between the chemical structure of organic compounds and their scintillation characteristics we have undertaken an investigation of the optical properties in benzene solution of 2, 5-diaryl substituted oxazoles, oxadiazoles and furans. For this purpose the following compounds were synthesized [1-4] and investigated:

2, 5-diphenyl-1, 3-oxazole —PPO
2-α-naphthyl-5-phenyl-1, 3-oxazole —NPO
2-ω-styryl-5-phenyl-1, 3-oxazole —SPO
2-phenyl-5(4-biphenyl)-1, 3-oxazole —PBO
2-α-furyl-5-phenyl-1, 3-oxazole —FPO
1, 4-di-[2-(5-phenyloxazolyl] benzene —POPOP
2, 5-diphenyloxadiazole —PPD
2-ω-styryl-5-phenyl-1, 3, 4-oxadiazole —SPD
2-α-furyl-5-phenyl-1, 3, 4-oxadiazole —FPD
1, 4-di-[2-(5-phenyloxadiazolyl)]benzene —PDPDP
2, 5-diphenylfuran —PPF
3-acetyl-2, 5-diphenylfuran
n-terphenyl
anthracene

Data for anthracene and terphenyl are included for comparison.

EXPERIMENTAL RESULTS

We determined the absorption spectra, luminescence spectra, quantum yield of luminescence and light yield of scintillation of the compounds enumerated above.

Absorption spectra were taken on the SF-4 spectrophotometer. Luminescence spectra were taken on an apparatus where the SF-11 spectrophotometer was used as monochromator. A correction was introduced into the spectra for the spectral sensitivity of the instrument and for reabsorption according to a slightly altered formula of Levshin [5], taking into account the angle between the direction of the excitation beam and the luminescence beam. Determination of the quantum yields of luminescence were carried out by the method of complete absorption of the excitation energy and comparison of the energies of radiation of the material being investigated and anthracene (1 mg/cm3) in benzene. The quantum yields of the investigated materials were approximately equal to those of infinitely dilute solutions. The maximum amplitudes of scintillation, or the light yields of scintillation were determined by the method described earlier 6.

The results of the measurements of optical and scintillation characteristics for the oxazole series are presented in Table 1.

The values cited of light yield of scintillations were determined on plastic samples 30 mm in diameter and 17 mm in height. The luminescence spectra and absorption spectra of benzene solutions of the scintillators investegated are presented in Figure 1.

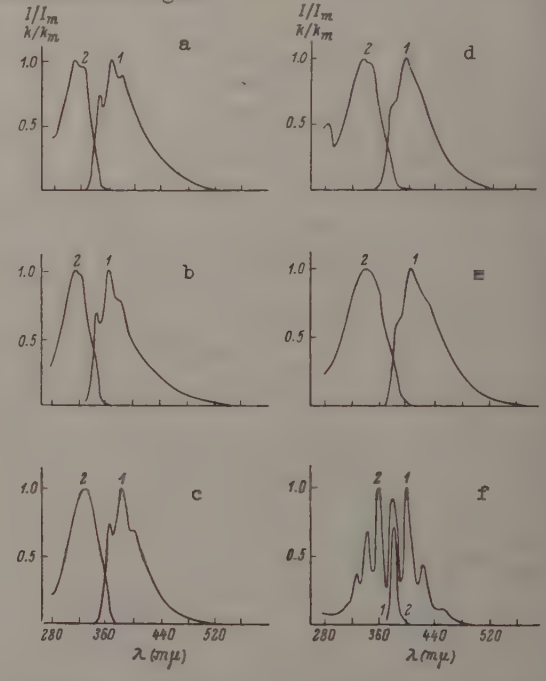

Figure 1. Spectra of luminescence (1) and absorption (2) of compounds of the oxazole series.
a — PPO, b — FPO, c — PBO, d — NPO, e — SPO, f — anthracene.

From examination of the spectra it is evident that on going from the phenyl radical to furyl, biphenyl, naphthyl, and styryl successively, a shift of the luminescence and absorption spectra is observed to the long wave region with simultaneous lowering of the quantum yield of luminescence. We should point out an anomaly in the relative position of FPO and PBO in Table 1. FPO has a somewhat smaller value for the relative quantum yield of luminescence and a materially lower value of scintillation light yield. The higher value of the quantum yield of luminescence in PBO is probably connected with the fact that the biphenyl radical which substitutes for the phenyl radical is found in position 5 and not in position 2 as in all othe cases.

If FPO is not taken into account, then the light yields of scintillation of PPO, PBO and NPO have approximately equal values. In the first approximation this could be explained from the value of the quantum yield of luminescence and the relative position of the luminescence spectra in relation to the curve of the distribution of spectral sensitivity of the photomultiplier (400-460mμ)

*Reported at the second meeting of the conference for the application and manufacture of scintillators in Kharkov, November, 1957

Table 1

Characteristics of Oxazoles

Compound	$\lambda_{max.}$ (in mμ)		Quantum Yield(%)	Light Yield(%)	Content in Polystyrene(%)	Structural Formula
	Luminescence	Absorption				
PPO	362	306	5.9	110	1	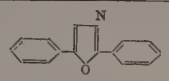
FPO	366	316	5.2	62	1	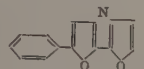
PBO	385	331	5.3	108	1	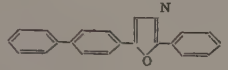
NPO	401	337	4.3	105	1	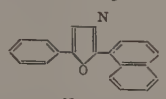
SPO	408	342	3.2	67	1	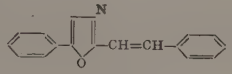
Terphenyl	342	283	6.5	100	2	
Anthracene	402	362	1	42	4	

Table 2

Characteristics of Oxadiazoles

Compound	$\lambda_{max.}$ (in mμ)		Quantum Yield(%)	Light Yield(%)	Content in Polystyrene(%)	Structural Formula
	Luminescence	Absorption				
PPD	334	287	~6.0	75	1.0	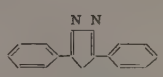
FPD	348	296	5.0	64	0.7	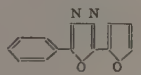
SPD	374	318	0.22	37	1.0	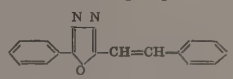

Gradual reduction of the quantum yield is compensated by the shift of the luminescence spectra toward the region of maximum spectral sensitivity of the photomultiplier. A quantitative connection between these phenomena has been established successfully at this time because of the fact that in γ-ray excitation the process of energy redistribution in vibrational levels differs from that process on irradiation by an ultraviolet source.

If now we turn to the class of oxadiazoles (Table 2, Fig. 2), then we can observe all the regularities which are found in the class of oxazoles.

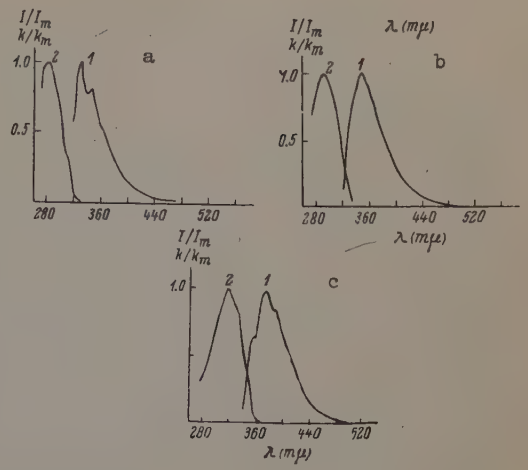

Figure 2. Luminescence (1) and absorption (2) spectra of compounds in the oxadiazole series.

a – PPD, b – FPD, c – SPD.

On going from the phenyl radical to furyl and styryl, there is found a reduction of the quantum yields of luminescence and the shift of the absorption and luminescence spectra toward the long wavelength region. There remains only the question of the comparatively high value of light yield of scintillation of SPD with a very small value of quantum yield of luminescence. The value of the quantum yield of PPD was shown to be of poor accuracy because the luminescence spectrum of PPD is distributed in the region of wavelength shorter than 313 mμ (the wave length of the irradiating light).

It was of interest to investigate the influence of the hetero-nitrogen atom on the optical and scintillation characteristics. For this purpose the series PPD, PPO and PPF (Table 3, Fig. 3) was examined. As the number of nitrogen atoms is increased to two (PPD), a gradual shift of the luminescence spectra toward the short wavelength region and a simultaneous increase of the quantum yield of luminescence are observed. The lower value of the light yield of scintillation of PPF can be explained by the significant reduction in the quantum yield for an insignificant shift of the luminescence toward long wavelengths (10 mμ) in the direction of the range of greatest spectral sensitivity of the photomultiplier.

It is interesting to observe that addition of a polar acetyl group to PPF in the 3 position causes cessation of scintillation and luminescence. The transition from POPOP to PDPDP can serve as another example of the influence of the heteratom of nitrogen on luminescence characteristics (Table 4, Fig. 4).

Introduction of a second hetero-nitrogen atom again leads to a shift of the spectra toward short wavelengths and to an increase in the quantum yield. The second

Table 3

Influence of the Hetero Nitrogen Atom

Compound	λ_{max} (in mμ) Lumi-nescence	λ_{max} (in mμ) Absorption	Quantum Yield(%)	Light Yield(%)	Content in Poly-styrene(%)	Structural Formula
PPD ...	334	287	~6.0	75	1	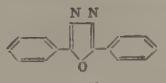
PPO ...	362	306	5.9	110	1	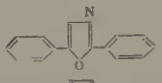
PPF ...	372	330	5.0	85	0.5	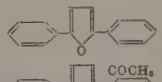
CH_3CO – PPF	Not luminescent, not a scintillator					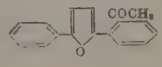

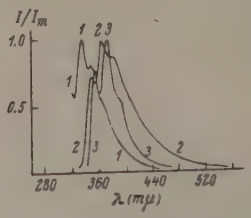

Figure 3. Luminescence spectra of PPD(1), PPO(2), and PPF(3).

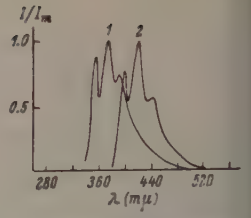

Figure 4. Luminescence spectra of POPOP and PDPDP (2).

Table 4

Influence of the Hetero Nitrogen Atom

Compound	λ_{max} (in mμ) Lumi-nescence	λ_{max} (in mμ) Absorption	Quantum Yield(%)	Light Yield(%)	Content in Poly-styrene(%)	Structural Formula
POPOP ...	417	368	4.5	95	0.5	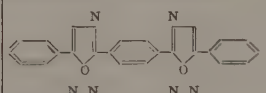
PDPDP ...	372	330	6.4	—	—	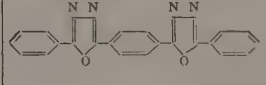

compound PDPDP has very little solubility in styrene and cannot be introduced as a basic scintillator.

On examining luminescence and absorption spectra of both series, mirror symmetry is not found. The structure is expressed more clearly in the luminescence spetra than in the absorption spectra.

We wish to thank E.V.Anufrieva for help in the work and valuable suggestions during discussions of the results.

August 2, 1958

REFERENCES

1. F. N. HAYES, B. S. ROGERS AND D. G. OTT: JACS, 77, 1850, (1955)
2. R. A. LUTZ, R. J. ROWLETT: JACS, 70, 1359, (1948)
3. N. A. ADROVA, M. M. KOTON, F. S. FLORINSKII IAN USSR, OKhN, chem. series, No. 3 385, (1957)
4. N. A. ADROVA, M. M. KOTON: IAN USSR, OKhN, (6) 759, (1957)
5. V. L. LEVSHIN: ZFKh, (2) 641, (1951)
6. N. A. ADROVA, M. M. KOTON, IU. N. PANOV, F. S. FLORINSKII: PiTE, (3) 43, (1957)

TOM VII, Vyp. 1 OPTIKA I SPEKTROSKOPIIA Iiul', 1959
VOL. VII, No. 1 OPTICS AND SPECTROSCOPY July, 1959

Luminescence of Stilbene Crystals at 20° K

A. F. PRIKHOT'KO, I. IA. FUGOL'

Abstract: The luminescence and absorption of stilbene crystals have been investigated at 20° K. The relation of the luminescence spectra to the weak lines near the intrinsic absorption region of the crystals has been established. It is shown that notable changes occur in the luminescence and weak line absorption spectra upon annealing the crystals, which confirms the hypothesis of a connection between the luminescence of organic crystals and the structural defects of the lattice.

The assumption has been expressed previously [1-3] that lattice defects, which are centers quenching the energy absorbed by the crystal, play an essential part in the luminescence of organic crystals. Violations of the translational symmetry of the lattice, which arise during the formation and growth of a crystal, lead to the appearance of a number of energy levels near the levels of a perfect lattice. Weak variable lines and bands in absorption spectra, appearing on the low frequency side of the intrinsic crystal absorption, correspond to transitions between such levels. Reversible resonance transitions in the normal state correspond to luminescence. As a rule, luminescence spectra consist of several series seemingly in succession, whose initial lines are also variable. Holding the crystals at a definite temperature for a long time or annealing them can lead to ordering of the molecule arrangement in the lattice, to a decrease in the number or type of structure defects and, as a consequence, to changes in the spectra, particularly in the luminescence spectra.

In order to explain the peculiarities of such phenomena, the present research was undertaken. Stilbene crystals were selected for this investigation. Their intense intrinsic absorption had been investigated earlier [4, 5]. As regards the luminescence of stilbene, little is known. There are just a few papers on the determination of the quantum yield at 293° K and on the measurement of the polarization of the spectral bands at 133° K [6,7]. Consequently, an investigation of the luminescence spectrum of stilbene is of considerable interest.

EXPERIMENTS

Stilbene crystals of various thicknesses (from 0.5 μ to 2mm) were used for the experiments. Thin single-crystal platelets were obtained by sublimation. Thicker slabs were obtained from large single crystals grown from a melt. Splitting them along the cleavage planes, it is easy to obtain plates of the thickness desired with smooth, pure slip surfaces. The axes of greatest (N_g) and least (N_p) refractive indices lie in the cleavage plane almost exactly coincident with the b and a axes (respectively) of the elementary cell. The ($N_g N_p$) face was also examined in the crystals obtained by sublimation. For investigations in polarized light, the crystal was mounted so that the oscillations of the light vector would be parallel to either the b or the a axis.

Luminescence was excited by a narrow spectral region near λ = 3100 Å, which was separated out of the spectrum of a SVDSh-1000 mercury lamp by a double monochromator. The intensity distribution curves in the luminescence spectra were obtained by the usual method of photographic photometry. The light source for the photography of the absorption spectra was a hydrogen lamp. Quartz spectrographs of high and medium dispersion, the Hillger E_1 and ISP-22, were used. The comparison spectrum was the spectrum of an arc between iron electrodes.

The crystals were annealed at liquid nitrogen temperature and near the sublimation temperature; they were held several days either in a cryostat filled with liquid nitrogen or in a special furnace at a temperature of around 70° C. After the annealing, the crystals were cooled rapidly to the temperature of liquid hydrogen. The spectra were always photographed at 20° K. Metal cryostats with quartz windows, described previously in [8], were used in the research.

We used chemically pure stilbene, recrystallized several times without further purification, as the initial material. The melting point of the material used was 129° C.

RESULTS

The stilbene crystals luminesce brilliantly upon exposure to ultraviolet light. The luminescence spectrum, which begins near 29200 cm^{-1} extends to the visible region. At 293° K it consists of several broad maxima separated by 1600 cm^{-1}. At 20° K each of these is divided into a series of narrow bands, almost lines; the whole spectrum is shifted approximately 200 cm^{-1} into the red. As is seen from figure 1, the intensity distribution varies noticeably. An analogous phenomenon also occurs in other crystals [1]. It is related partially to the overlapping of the beginning of the luminescence spectrum with the longwave part of the absorption spectrum, which recedes toward higher frequencies as the temperature is lowered.

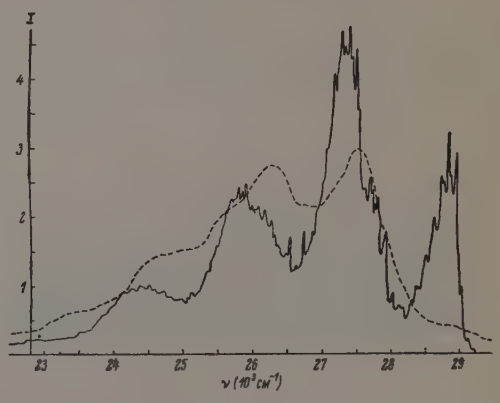

Figure 1. Intensity distribution in the luminescence spectrum of stilbene at T = 20° K (solid curve) and at T = 293° K (dashed line). Relative intensities plotted along the vertical axis.

The luminescence spectrum at 20° K is complex. It starts as a group of closely situated lines. The frequencies of the most intense lines are shown in figure 2. The variability of these lines (see fig. 3) involves a change in the whole spectrum.

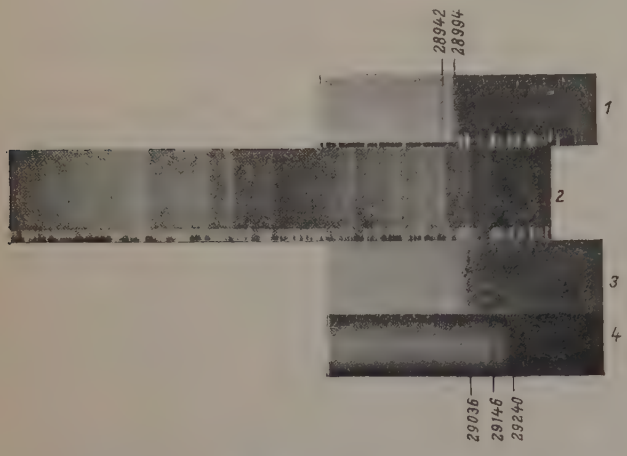

Figure 2. Comparison of luminescence and absorption spectra of stilbene. 1 — absorption spectrum (b-component) of a d = 30 μ thick crystal; 2 — luminescence spectrum; 3 — absorption spectrum of a d = 30 μ crystal (b-component); 4 — absorption spectrum of a d = 8 μ crystal (b-component).

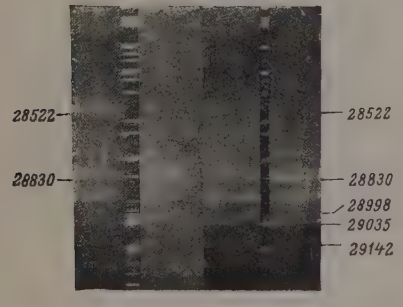

Figure 3. Variability of luminescence spectra in stilbene crystals of the same thickness (d ≈ 20 μ).

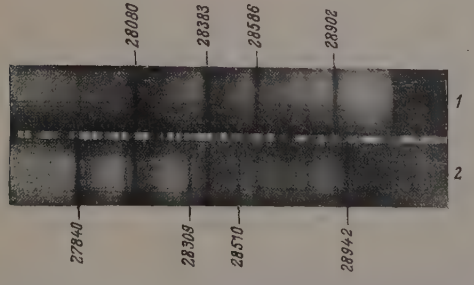

Figure 4. Line absorption spectra of stilbene (d = 150 μ).
1 — a-component; 2 — b-component.

The series of initial lines of the luminescence spectrum 29142, 29035, 28902 cm^{-1} and other weak lines coincide with the stilbene absorption lines. A whole series of sharp lines is manifest in stilbene crystals from 0.5 - 30 μ thick (intrinsic absorption is observed in thicknesses of the order of 0.1 μ [4]). These lines are also variable. They can have different intensities, widths and polarization in different crystals. Their frequencies also change slightly.

A group of new lines can be observed at large crystal thicknesses (d ~ 100-300 μ). The absorption spectrum of a 150 μ thick stilbene crystal is shown on figure 4. Several absorption lines from this region also coincide with the luminescence lines, for example, 28385, 28038, 27840 cm^{-1} and, possibly, a number of other very weak lines.

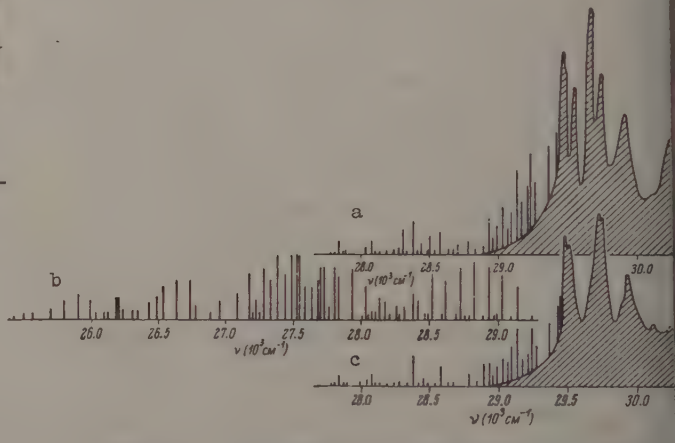

Figure 5. Diagram of the absorption and luminescence spectra of stilbene. a — absorption (a-component); b — luminescence; c — absorption (b-component).

Presented in table 1 are the frequencies of all the measured luminescence lines (second column). Two series with the initial lines 29142 and 29035 cm^{-1} are separated in the third and fourth columns. The frequencies in the last column refer to absorption lines which coincide with the corresponding lines of the luminescence spectrum. The intensities, estimated roughly by eye, are presented in the first column for the luminescence lines and in the last column in parentheses for the absorption lines (along the b and a axes, respectively).

A diagram of the absorption and luminescence spectrum is presented in figure 5. It was difficult to keep the same scale of intensities for different sections of the spectra. Actually, the intrinsic absorption, part of whose spectrum is presented in figure 5, is approximately 1000 times more intense than the red lines themselves and approximately 100 times stronger than the adjacent absorption lines shown by heavier strokes. The gap $\Delta\nu$ between the luminescence and intrinsic absorption spectra (about 200 cm^{-1}) is seen on the diagram.

The resonance lines in the luminescence and absorption spectra of the same crystal vary relative to other samples simultaneously. Thus, the lines in the series also vary. Using this fact, it was possible to choose a number of transitions with the frequencies 29236, 29142, 29035 cm^{-1} and weaker transitions with the

Table 1

Luminescence of stilbene crystals at 20° K

J	ν (in cm^{-1})	Interpretation		Frequency from the absorption spectrum (in cm^{-1})
0	29236			29240 (10,1)
5	29142	0_1		29146 (10,1)
0	29095			29095 (5,3)
8	29035		0_2	29036 (10,4)
2	28998			28994 (3,1)
1	28972			
8	28939	203		28942 (7,0)
0	28899			28902 (3,8)
10	28830		205	
0	28795			
0	28762			
8	28732	410 (2 × 205)		
0	28696			
7	28624		411 (2 × 205)	
0	28590			
6	28522	620 (3 × 205)		
0	28494			
0	28469			
3	28418		617 (3 × 205)	
4	28385			28383 (10,10)
2	28319			
1	28286	823 (4 × 205)		
2	28268	856		
1	28213		822 (4 × 205)	
3	28180		855	
4	28142	1000		
1	28112	1030 (5 × 205)		
1	28081	1061 (856 + 205)		28080 (7,6)
1	28066			
5	28038		997	28042 (5,1)
0	28008		1027 (5 × 205)	
8	27942	1200		
7	27840		1195	27840 (8,5)
8	27811			
7	27804	1338		
2	27765			
8	27735	1407 (1200 + 205)		
8	27705	1437		
6	27694		1341	
5	27639		1396 (1195 + 205)	
5	27596		1439	
10	27552			
9	27543	1599		
10	27498	1644		
8	27437		1598	
10	27393		1642	
5	27337	1805 (1599 + 205)		
7	27290	1852 (1644 + 205)		
0	27259			
2	27230		1805 (1598 + 205)	
1	27213			
7	27187		1848 (1642 + 205)	
3	27084	2058 (1644 + 410)		
2	26980		2055 (1642 + 410)	
1	26882	2260 (1644 + 620)		
2	26782		2253 (1642 + 620)	
5	26742	2400 (2 × 1200)		
5	26643	2499 (1644 + 855)	2392 (2 × 1195)	
4	26539	2603 (2 × 1200+205)	2496 (1642 + 855)	
3	26498	2644 (1644 + 100)		
2	26439		2596 (2 × 1195 + 205)	
6	26392		2643 (1642 + 997)	
1	26348	2794 (1599 + 1200)		
1	26302	2840 (1644 + 1200)		
1	26240		2795 (1598 + 1195)	
3	26207	2995 (1599 + 1338)		
3	26197		2838 (1642 + 1195)	
0	26131			
1	26100			
0	26035		3000 (1598 + 1341)	
2	25994			
3	25902	3240 (1644 + 1599)		
2	25794		3241 (1642 + 1599)	
1	25695	3447 (1644+1599+205)		
1	25541			
0	25487	3655 (1644+1599+410)		
0	25462			

frequencies 29095, 28998, 28899 cm^{-1}, with which a series of lines corresponding to the intermolecular vibrations of stilbene are related. All the measured luminescence lines and also the interpretation of the two most intense series of spectra are given in table 1.

Given in the first two columns of table 2 are the intensities of lines which are seen at a d ~ 150μ thickness (a visual estimate according to the 10 number scale for one of the characteristic crystal spectra).

Table 2

Line absorption in crystalline stilbene *

J_b	J_a	ν (in cm-1)	Remarks
0	0	27784	Probably "red" satellites of the 27840 cm^{-1} line, Δν=36 cm^{-1} and Δν=56 cm^{-1}
0	0	27808	
8	5	27840	Sharp, slightly polarized line
1	0	27872	Probably "violet" satellites of the 27840 cm^{-1} line, Δν=32 cm^{-1} and Δν=55 cm^{-1}
1	0	27895	
5	1	28042	Sharp line, predominantly polarized along the b-axis, somewhat weakened after annealing at high temperature
7	6	28080	Usually slightly polarized, sometimes more intense along the a-axis
1	1	28107	Probably, satellites of the 28080 cm^{-1} line, Δν=27 cm^{-1} and Δν=55 cm^{-1}
1	1	28135	
0	0	28191	
1	0	28246	
3	2	28282	
10	0	28309	Very sharp line, is observed only in the b-component, considerably weakened after annealing at high temperature
0	0	28342	
10	10	28383	Broad, very intense line, usually polarized slightly, intensified and broadened after annealing at 70° C
0	0	28419	
4	3	28442	
0	0	28491	
8	0	28510	Sharp line, seen only in the b-component, weakened after annealing at 70° C
0	0	28539	
9	8	28586	Broad line, intensified after annealing at 70°C
2	0	28642	
1	0	28677	
5	0	28712	Sharp line, seen only in the b-component, weakened after annealing at 70° C
4	4	28789	Broad line, intensified after annealing at 70° C
3	8	28902	Sharp line, usually polarized strongly along the a-axis
10	0	28942	Strongly polarized along the b-axis, seen for thicknesses of the order of 30 μ

* The intensities J_a and J_b of the far ultraviolet lines were not estimated since in the a and b components these lines are seen at different crystal thicknesses.

Table 2 (cont'd)

Line absorption in crystalline stilbene

J_b	J_a	ν (in cm^{-1})	Remarks
		28965	Sharp line, more intense in the b-component, observed at 50-150μ thicknesses
		28994	Seen in the b-component for $d \approx 30\mu$ and for $d \approx 100\mu$ in the a component
		29036	Intense line polarized primarily along the b-axis, seen in the b-component for $d \approx 20\mu$, in the a-component for $d \approx 150\mu$; extremely variable in intensity and polarization; usually intensified after annealing at 70° C
		29073	Seen in the b-component for $d \approx 30\mu$ and in the a-component for $d \approx 150\mu$
		29095	Seen in the b-component for $d \approx 20\mu$ and in the a-component for $d \approx 150\mu$
		29146	Very intense line polarized primarily along the b-axis; seen for $d \approx 5\mu$ in the b-component, for $d \approx 100\mu$ in the a-component; usually weakened after annealing at nitrogen temperatures.
		29176	Seen at 10-50μ thicknesses
		29224	" " 5-20μ "
		29240	" " 1-10μ "
		29276	" " 1- 5μ "
		29376	" " 0.5- 1μ "
		29436	" " 0.5μ "
		29443	" " 0.5μ "

The peculiarities of the lines and the crystal thicknesses at which the ultraviolet group of lines can be observed are mentioned in the remarks. Presented below are the frequencies of the intermolecular vibrations (in cm^{-1}) obtained from the luminescence spectra of stilbene crystals and crystalline solutions at 20° K. Also given for comparison are their values taken from the stilbene luminescence spectra in tolane and dibenzyl crystals [9, 10] and from the Raman spectra. The relative intensities are shown in the parentheses.

Stilbene	Stilbene-Tolane	Stilbene-Dibenzyl	Raman Frequencies
205(8)	204	210	226(1)
410(6)	409	422	402(0)
620(4)	616	638	620(2)
—	–	–	847(1)
1000(5)	–	998	1004(7)
1200(8)	1197	1187	1188(10)
1338(6)	1339	1337	1321(3)
1437(6)	1442	1447	1441(2)
—	–	1490	1486(2)
1599(9)	1594	1593	1590(10)
1644(10)	1636	1639	1632(10)

Annealing the crystals exerts a noticeable effect on the luminescence and absorption spectra. Thus, after annealing at high temperature, a number of absorption lines (28383, 28586, 28789 cm^{-1} etc.) is amplified at the same time as lines, strongly polarized along the b-axis (28309, 28510, 28712 cm^{-1} etc.) are weakened. A group of ultraviolet lines of the absorption spectra in the 29400-28900 cm^{-1} range changes independently of the lines in the 28900-27800 cm^{-1} range. At the same time all the resonance lines in both the absorption and luminescence spectra behave identically. Presented in figure 6 are spectra before and after annealing at nitrogen temperatures. The simultaneous attenuation of the resonance lines and the general poorness of the luminescence spectra is seen from figure 6. On the other hand, annealing at a high temperature often would lead to amplification of the intensities of many weak luminescence lines; for example, the intensity of the 28998, 29236 cm^{-1} etc. lines grew. Simultaneously, the lines in a series related to any one of them also varied with the initial lines (with the exception of the lines 28830 and 28522 cm^{-1} which appeared to be independent of the initial lines); this was used to check the correctness of the series assignment.

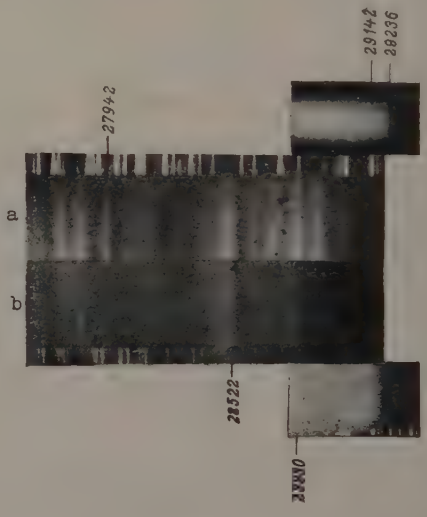

Figure 6. Influence of annealing at 77° K on the absorption and luminescence spectra of a stilbene crystal. a — crystal spectrum prior to annealing; b — after annealing.

The simple method of observation permits us to establish just the fact of change in the spectra by thermal treatment of the crystal. It would be impossible to obtain sufficiently stable reproducible results, attenuation and amplification of definite lines in a prescribed annealing region, with our experimental conditions. This is a problem for future research. However, the possibility of causing changes in the spectra (especially in the case of lines) by taking into account the effect of structural defects, is confirmed by the experiments conducted.

Making use of the data presented, the group of initial lines of the absorption spectra can positively be related to the lattice defects. The remaining weak lines of the spectrum are most probably dependent on impurities unknown to us. Judging by the difference in the character of these lines, by the coincidence of several of them with

lines of the absorption spectra (apparently, not always by chance), it could be thought that there is not just one but several similar impurities in the compound. It is still not possible to identify them. It can only be assumed that they are structurally similar to stilbene. It is possible that these are substituted or oxidized compounds. Annealing in an oxygen atmosphere can contribute to the oxidation of organic compounds and, consequently, certain lines can be intensified. The fact of a different change in the lines upon annealing, as well as the sharp polarization of certain lines, can aid identification of the impurities.

CONCLUSIONS

It follows from the abovementioned data that the luminescence of stilbene crystals, as well as of other organic compound crystals investigated earlier, is closely related to structural defects arising during the growth of the crystals. This is indicated by the variability of the luminescence spectrum caused by the variability of the resonance lines of the absorption spectrum, and the fact of the presence of many close resonance lines — the initial lines of the luminescence series. Each of such lines can be attributed to one or another structural defect which creates its own local energy level near the appropriate energy level of an ideal lattice. The influence of annealing on the behavior of such lines appears to be a convincing confirmation of our view point. A new opportunity is thereby disclosed to study crystal defects and their contribution to the structure of the energy bands in real crystals.

The results of experiments with annealed crystals show that the intensity and polarization of lines of the spectrum depend on the degree of thermal equilibrium in a crystal achieved before hardening. Judging by the spectra, many types of defects are possible. These can be unfilled vacancies, molecules in interstices , variously distorted molecules. As one of the possible models of a lattice defect, it is possible to propose a group of distorted molecules arranged around an unoccupied vacancy. Their variations lead to a number of possible energy levels.

Each of such defects, which always occur in crystals, is a separate absorption center and a center luminescing by the energy absorbed by the whole crystal. The mechanism of the phenomenon, closely related to the origin of excitons in crystals, is considered in [11].

September 15, 1958

References

1. A. F. PRIKHOT'KO, I. IA. FUGOL': OiS, 4, 335, (1958)
2. A. F. PRIKHOT'KO, I. IA. FUGOL': OiS, 5, 582, (1958)
3. I. IA. FUGOL', S. Z. SHUL'GA: OiS, 5, 34, (1958)
4. M. S. BRODIN: OiS, 1, 876, (1956)
5. M. S. BRODIN, O. S. PAKHOMOVA, A. F. PRIKHOT'KO: OiS, 5, 123, (1958)
6. G. T. WRIGHT: Proc.Phys.Soc., A68, 701, (1955)
7. P. PESTEIL: Ann. Phys., 10, 128, (1955)
8. V. P. BABENKO, V. L. BROUDE, V. S. MEDVEDEV: PiTE, 1, 99, (1956)
9. A.F. PRIKHOT'KO, M.T. SHPAK: OiS, 4 30, (1958)
10. A.F. PRIKHOT'KO, M.T. SHPAK: OiS, 4, 17, (1958)
11. V. L. BROUDE, A. F. PRIKHOT'KO, E. I. RASHBA: UFN, 67 99, (1959) (See:Sov. Phys.Progress of Sov. Phys.)

TOM VII, Vyp. 1 OPTIKA I SPEKTROSKOPIIA Iiul', 1959
VOL. VII, No. 1 OPTICS AND SPECTROSCOPY July, 1959

On the Question of the Interpretation of the Fluorescence Spectrum of Naphthalene

T. N. BOLOTNIKOVA

Abstract: The fluorescence spectra of solutions of naphthalene in normal saturated hydrocarbons from pentane to decane at 77° K were investigated. The sharpness of the fluorescence spectrum of the solution of naphthalene in pentane permitted the frequency intervals to be determined exactly and the difference of the first two intervals (495 and 927 cm^{-1}) to be established from the values of the completely symmetric frequencies 517 and 940 cm^{-1}. The hypothesis is advanced that the mechanism of the electronic-vibrational transition in fluorescence is the same as the mechanism of transition in absorption for naphthalene in durene.

INTRODUCTION

A large number of experimental and theoretical studies have been devoted to the investigation of the absorption and fluorescence spectra of naphthalene, but, up to the present time, the character of the first electronic transition of the naphthalene molecule has not been definitely established.

The naphthalene molecule belongs to the D_{2h} point group of symmetry. Combinations are allowed by the selection rules between the levels $A_{1g} \rightleftarrows B_{2u}$ (the transition must be polarized along the short molecular axis), $A_{1g} \rightleftarrows B_{3u}$ (the polarization must be parallel to the long axis of the molecule) and $A_{1g} \overrightarrow{\leftarrow} B_{1u}$ (for a transition polarized perpendicularly to the plane of the molecule).

Because the long wavelength absorption of naphthalene (2900-3200 Å) possesses a small molecular extinction coefficient (ϵ = 200-300) it was for a long time associated with the symmetry-forbidden electronic transition of the type $A_{1g} \rightleftarrows A_{1g}$ [1-4]. However, it was noted by Platt [5], that for simple aromatic hydrocarbons, the presence of positive and negative terms of the same order of magnitude in the integral of the transition moment can lead to a small value of the transition probability even if the transition is allowed by the selection rules. In addition, it turned out that the allowed character of the first electronic transition is confirmed by the presence of a clear 0-0 band in the spectra of solutions of naphthalene at room [6], and low [7] temperatures. On the other hand, it appeared that the relatively small intensity of the 0-0 band in all cases confirmed the forbidden character of the transition [2,3]. In such a case, the question can be resolved only by means of some sort of indirect measurements. In the case of allowed transitions, the interval between the (0-1) lines in absorption and (1-0) in fluorescence must be equal to the sum of the frequencies of vibrations of a single type, belonging to different electronic states; if the transition is forbidden by symmetry, but occurs as a result of perturbation of vibrations of the corresponding symmetry (for molecules of naphthalene -- β_{2u} or β_{3u}), the interval (0-1)–(1-0) must then include the sum of two frequencies of incompletely symmetric vibration in the upper and lower states. Measurements of this kind were performed for naphthalene under various conditions [1], but the sums of the frequencies, well known from the Raman and infrared spectra, fitted poorly within the limits of the measured intervals; and, in addition, the precision of the determinations of the frequencies in the spectra of solutions was not great even at low temperatures on account of the diffuseness of the bands (30-40 cm^{-1}). The latest studies of McClure devoted to the investigation of the absorption and fluorescence spectra of a solid solution of naphthalene in durene [8,9], are interesting. The sharpness of the spectra in this case permitted him to determine the frequencies of the bands with an uncertainty of only several cm^{-1}. In the absorption and fluorescence spectra of naphthalene in durene, McClure detected two systems of bands polarized parallel to the long (b-system) and short (c-system) axes of the molecule of naphthalene. McClure ascribed the first to an electronic transition of the type $A_{1g} - B_{3u}$ allowed by symmetry. The presence of intensive bands, polarized in a different manner, in the absorption and fluorescence spectra, McClure explains by the influence of a close-lying second electronic level of symmetry B_{2u}. This kind of interaction of various electronic states can be realized via the perturbation of frequencies of symmetry β_{1g}. In the absorption spectrum of naphthalene in durene, this interpretation does not lead to complications: the c-system begins with two lines at a distance of 430 and 905 cm^{-1} from the 0-0 band. These intervals are taken by McClure as the values of the frequencies of symmetry β_{1g}. However, analogs of these frequencies are absent in the fluorescence spectrum of naphthalene in durene; instead there appear the two Raman-active fully-symmetric frequencies of naphthalene, 509 and 938 cm^{-1}. A satisfactory explanation of this fact is not given in reference [9], and, consequently, the assumption is made that the mechanism of transition during fluorescence is different from the mechanism of transition during absorption.

The method of obtaining sharp quasi-line spectra of the fluorescence of frozen crystalline solutions of condensed aromatic hydrocarbons, worked out by Shpol'skii, Il'ina, and Klimova [10], permits one to determine accurately the frequencies of the bands in the spectra.

In the present work, results are presented for the fluorescence spectra of crystalline solutions of naphthalene in normal saturated hydrocarbons at liquid nitrogen temperature.

1. EXPERIMENTAL CONDITIONS AND CHOICE OF THE SOLVENT

We obtained the fluorescence spectra of solutions of naphthalene on a medium quartz "Bausch and Lomb" spectrograph (aperture ratio 1:15, linear dispersion 25 Å/mm in the 3100 Å region and 40 Å/mm in the 3600 Å region). The spectra were

otographed by the method described by Shpol'skii, Klimova, d Girdzhiiauskaite [11]. The fluorescence was excited by radiation with PRK-4 mercury lamps at an angle to the rface of the cell from the side of the slit of the spectro-aph. The lamps were water-cooled, which permitted them to e used at low pressure. Even after an exposure of several urs, the plate did not show any background spectra, charac-eristic of mercury lamps of this type. The absence of back-round and the small number of lines in this region permitted e fluorescence spectra of the solutions of naphthalene to e photographed without a filter.

All the aromatic hydrocarbons previously investigated 0, 11] had sharp spectra in frozen solutions of the normal turated hydrocarbons from hexane to nonane. An attempt to tain a sharp fluorescence spectrum of these same solutions naphthalene was not crowned with success — in all cases e spectrum proved to be more diffuse than the spectrum of ystalline naphthalene. In the published works of pol'skii and Klimova, for example in [12], a correspon-nce was noted between the sharpness of the spectra and the tios of the dimensions of the molecules of the fluorescing bstance and of the solvent.

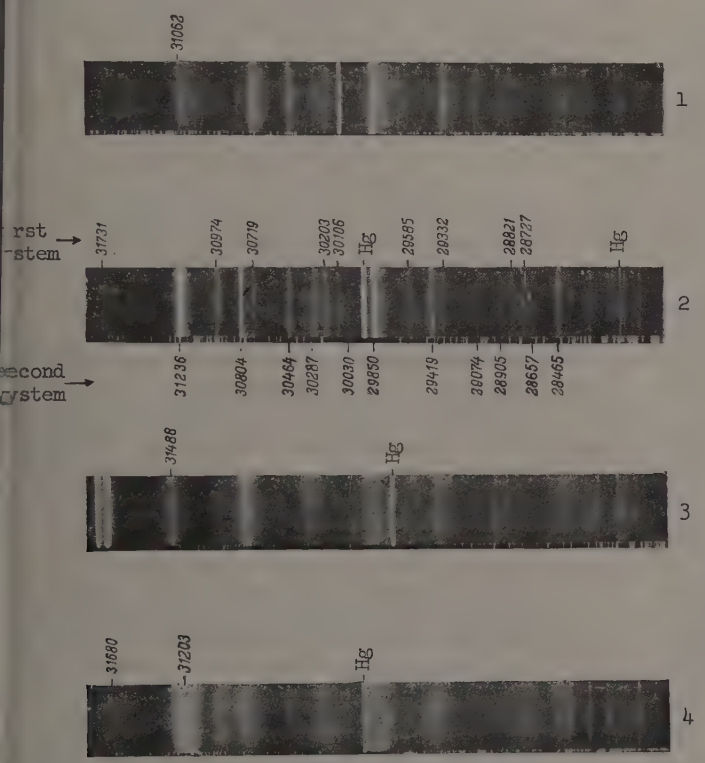

Fluorescence Spectra of Naphthalene

1 — Crystalline Naphthalene, 2 — Naphthalene in Pentane (77° K), 3 — In Hexane, 4 — In Heptane.

The molecule of naphthalene is considerably smaller than all the molecules previously investigated; it consequently seemed expedient to select a solvent molecule of correspondingly small dimensions. The only remaining solvent of this series which is found in the liquid state at room temperature is pentane, and this we used. Actually, the spectrum of the solution of naphthalene in pentane (see the figure) proved to be maximally sharp; the spectrum of the solution in heptane is perfectly analogous to the spectrum of the solution in ethyl alcohol or paraffin oil and consists of diffuse bands (100-120 cm^{-1}), the centers of which superpose well with the maximally intense lines of the spectrum in pentane. It is natural that the spectrum of a solution of naphthalene in pentane is more convenient for the detailed analysis and comparison with the spectra of naphthalene under other conditions.

2. RESULTS AND DISCUSSION

The fluorescence spectra of frozen solutions of naphthalene in n-pentane, n-heptane, n-octane, ethyl alcohol, and paraffin oil were studied. For comparison, the spectrum of crystalline naphthalene was photographed at the same temperature. Discrepancies from the data of Obreimov and Shabaldas [13] amount to 3-5 cm^{-1} for the intense lines and reach 10-15 cm^{-1} for the weak lines. The somewhat lesser precision in the determinations of frequencies due to the small dispersion of the apparatus in this region should be noted.

The spectrum of naphthalene in pentane begins with a weak sharp line $\nu_0 = 31{,}731$ cm^{-1}, an analog of which is not found in the fluorescence spectrum of crystalline naphthalene photographed under those same conditions (see the figure). The entire spectrum is displaced 170 cm^{-1} relative to the fluorescence spectrum of crystalline naphthalene in the direction of long wavelengths. Analogs of the lines which appear in the spectrum of naphthalene crystals as a result of the superposition of small vibrations of the crystal lattice are absent in the solution spectrum. All the frequencies we obtained for the fluorescence spectral bands of naphthalene in pentane and their interpretation are presented in Table 1.

A detailed analysis of the fluorescence spectrum of naphthalene in pentane shows the presence of two systems of bands. The first (Table 2) begins directly from the line $\nu_0 = 31{,}731$ cm^{-1}; it includes the least intense lines. The most intense line of the spectrum $\nu_3 = 31236$ cm^{-1} which is 495 cm^{-1} distant from ν_0, serves as the beginning of the second system (Table 3). The most intense and characteristic lines of the spectrum belong to this system. In both systems, the frequency of 1386 cm^{-1} is very clearly present: in the first system it forms one weak progression with a beginning at $\nu_0 = 31{,}731$ cm^{-1}, in the second, the two most intense lines (31,236 and 30,804 cm^{-1}) give rise to two strong progressions. In the first system, frequency differences of 660, 765, 1386, and 1625 cm^{-1} are present (Table 2). As has already been noted, all the lines are weak — the lines linked with the frequency of 765 cm^{-1}: 30,974; 30,203; 29,585; and 28,821 cm^{-1} being the only exceptions. By intensity they could be assigned to the second system, but the first

Table 1

Fluorescence Spectrum of Naphthalene in Pentane and in Durene

In Pentane			In Durene			
ν in cm^{-1}	$\nu_o - \nu$ in cm^{-1}	Intensity	ν in cm^{-1}	$\nu_o - \nu$ in cm^{-1}	Intensity in b-syst.	Intensity in c-syst.
31731	0	w	31554	0	vs	vw
31272	—	w	—	—	—	—
31236	495	int	31045	509	av	vw
31073	658	w	—	—	—	—
31014	723	w	—	—	—	—
30974	757	int	30793	761	vw	av
—	—	—	30771	783	av	w
30843	888	w	—	—	—	—
30804	927 = 927	int	30616	938	w	av
30719	1012 = 495 + 517	av	30530	1024	w	av
30635	1096 = 1102	w	30452	1102	vw	vw
—	—	—	30410	1144	0	vw
30575	1162 = 495 + 665	w	30392	1162	w	0
—	—	—	30378	1176	vw	w
30500	1231 (1240?)	w	30321	1233	vw	0
30464	1267 = 495 + 772	int	30284	1270 = 509 + 761	w	av
30405	1326 = 663 × 2	w	—	—	—	—
30350	1381	w	30174	1380	vs	av
—	—	—	30132	1422 = 1380 + 39	vs	0
30287	1444 = 927 + 517	int	30103	1451 = 509 + 938	vw	w
—	—	—	30075	1479 = 1380 + 98	vw	0
30203	1528 = 2 × 764	int	30036	1518 = 2 × 761	av	vw
—	—	—	30020	1534 = 509 + 1024	s	vw
—	—	—	30014	1540 = 761 + 783	w	0
30106	1625	av	29935	1619 } 1625	vw	w
—	—	—	29923	1631 }		
30030	1701 = 927 + 774	av	—	—	—	—
—	—	—	29769	1785 = 761 + 1024	vw	vvw
29850	1881 = 495 + 1386	int	29669	1885 = 509 + 1380	av	vs
—	—	—	29635	1919 = 509 + 1380 + 39	vw	w
29774	1957 = 495 + 1465	av	29600	1954 = 938 + 1024	0	w
29691	2040 = 1386 + 660	w	—	—	—	—
29639	2092	w	—	—	—	—
29585	2146 = 765 + 1386	av	29419	2135 = 761 + 1380	w	w
—	—	—	29395	2159 = 783 + 1380	w	vw
29483	2248	w	29275	2279 = 3 + 761	w	vw
—	—	—	29256	2298 = 2 × 761 + 783	w	—
29419	2312 = 927 + 1386	int	29240	2314 = 938 + 1380	w	av
29332	2399 = 495 + 1386 + 518	av	29156	2398 = 1024 + 1380	vw	vw
29264	2467 = 1102 + 1386	w	29074	2480 = 1102 + 1380	w	w
29175	2556 = 495 + 1386 + 666	w	29011	2543 = 2 × 761 + 1024	w	s
—	—	—	28990	2564 = 509 + 2 × 1024	vw	—
—	—	—	28943	2611 = 1233 + 1380	av	—
—	—	—	28908	2646 = 509 + 761 + 1380	vw	w
29074	2657 = 495 + 776 + 1386	av	28883	2671 = 509 + 783 + 1380	vw	—
—	—	—	28873	2681	vw	—
29009	2722 = 1386 + 2 × 665	w	—	—	—	—
28957	2774 = 2 × 1386	w	28798	2756 = 2 × 1380	av	vw
28905	2826 = 927 + 517 + 1386	av	28727	2827	w	—
—	—	—	28661	2893 = 2 × 761 + 1380	w	vw
28821	2910 = 2 × 764 + 1386	av	28642	2912 = 763 + 783 + 1380	w	—
28727	3004 = 1625 + 1386	av	28559	2995 = 1619 + 1380	av	—
—	—	—	28547	3007	—	—
—	—	—	28523	3031	vw	—
—	—	—	28501	3053	w	—
28657	3074 = 927 + 762 + 1386	av	28480	3074 = 761 + 938 + 1380	w	—
—	—	—	28394	3160 = 761 + 1124 + 1380	w	—
—	—	—	28370	3184	vw	—
28465	3266 = 495 + 2 × 1386	int	28294	3250 = 509 + 2 × 1380	vvw	—
—	—	—	28265	3289	vvw	av
—	—	—	28257	3297	w	—
28375	3346 = 495 + 1465 + 1386	av	28216	3338 = 938 + 1024 + 1380	vw	—
—	—	—	28189		w	—
—	—	—	28107	3447	vw	—
—	—	—	28096	3458	w	—
29264	3467	w	28045	3509 = 761 + 2 × 1380	vw	—
—	—	—	28021	3533 = 783 + 2 × 1380	w	0
—	—	—	27991	3563	vw	—
—	—	—	27906	3648	w	—
—	—	—	27888	3666	w	—
28034	3697 = 927 + 2 × 1386	av	27866	3688 = 938 + 2 × 1380	0	—
—	—	—	27784	3770 = 1024 + 2 × 1380	w	w
—	—	—	27742	3812	w	—
—	—	—	27641	3913	w	—
27794	3937 = 495 + 665 + 2 × 1386 (1162 + 2 × 1387) *	w	—	—	—	—
—	—	—	27540	4014	w	—
27703	4028 = 495 + 763 + 2 × 1386	w	27502	4052	w	—
27574	4157 = 3 × 1386	w	27428	4126 = 3 × 1380	w	—
27522	4209 = 925 + 513 + 2 × 1386	w	—	—	—	—
—	—	—	27294	4260	w	—
—	—	—	27272	4282	w	—
—	—	—	27236	4318	w	—
—	—	—	27127	4327	w	—
—	—	—	27112	442	w	—
27171	4560	w	—	—	—	—
27065	4666 = 3 × 1386 + 495	w	—	—	—	—

Note: Conventional designations: vvw(extraordinarily weak); vw(very weak; w(weak); av(average); int(intense); s(strong); vs(very strong).

* This line can be treated in more than one way.

Table 2

First System of the Fluorescence Spectrum of a frozen Solution of Naphthalene in Pentane

ν in cm^{-1}	$\Delta\nu$ in cm^{-1}	ν in cm^{-1}	$\Delta\nu$ in cm^{-1}	ν in cm^{-1}	$\Delta\nu$ in cm^{-1}
31731	0	30350	0	28957	—
31073	658	29691	659	—	—
30974	757	29585	765	28164	793
30635	1096	29264	1086	—	—
30405	663 × 2	29009	670 × 2	—	—
30350	1381	28957	1393	27574	1383
30203	764 × 2	28821	764 × 2	—	—
30106	1625	28727	1623	—	—

Table 3

Second System of the Fluorescence Spectrum of a Frozen Solution of Naphthalene in Penta

ν in cm^{-1}	$\Delta\nu$ in cm^{-1}	ν in cm^{-1}	$\Delta\nu$ in cm^{-1}	ν in cm^{-1}	$\Delta\nu$ in cm^{-1}
31236	0	29 50	0	28465	0
30804	432	29419	431	28034	431
30719	517	29332	518	—	—
30464	772	29074	776	27703	762
30287	947	28905	945	27522	943
30030	1003	28657	992	—	—
29850	1386	28465	1385	27065	1400
29774	1462	28385	1465		

of them is separated from the initial line of the second system by 260 cm^{-1}, while neither in the Raman nor in the infrared spectra is a frequency observed for the naphthalene molecule which is close to this. In addition, the corresponding lines in the spectrum of crystalline naphthalene are also associated with the frequency of totally symmetrical vibrations, 762 cm^{-1} [13]. The assignment of these lines to the first system consequently seems to be correct. It is evident from Table 2 that all the differences of frequencies are repeated almost strictly except 1380-1390 cm^{-1}; the small spread in their values was caused by the relatively small precision of the measurement ($\pm$ 10 cm^{-1}) of weak lines. The second system, as has already been noted, includes all the intense and most characteristic lines of the spectrum. Here the totally symmetric frequencies of the molecule of naphthalene are clearly manifest: 517, 772, 1033, 1386, 1465 cm^{-1} (Table 3).

A comparison of the fluorescence spectra of naphthalene in pentane with the fluorescence spectra of naphthalene in durene [9] (Table 1) shows the following:

1. The spectrum of the solution in pentane is shifted 170 cm^{-1} in the long wavelength direction.

2. One can bring the two systems of bands in the spectrum of naphthalene in durene [8, 9] into correspondence with the two systems of bands in the spectrum in pentane.

3. In pentane the 31,236 and 30,804 cm^{-1} bands, which are the beginnings of the progressions with a period of 1386 cm^{-1} in the second system, are 495 and 927 cm^{-1}, respectively, from the 0-0 band (31,731 cm^{-1}

n durene, as has already been noted, intervals of 09 and 938 cm^{-1} correspond to these values.

4. The interpretations of the corresponding ands are identical, if one takes into account the receding point (Table 1).

5. The first system in the fluorescence spectrum f naphthalene in pentane is considerably weaker n the whole than the corresponding b-system.

6. The frequency difference of 660 cm^{-1} is not resent in the spectrum of naphthalene.

The question of the values of the intervals etween the initial lines of the systems merits pecial attention in both cases. In durene 509 nd 938 cm^{-1} are the values of the frequencies of he totally symmetric vibrations, which are then ndependently repeated in the fluorescence spectra. t is absolutely impossible to understand in what anner the excitation of the totally symmetric ibrations can evoke the appearance of bands pola-ized in a different way than the bands allowed by ymmetry for the transition $A_{1g} - B_{3u}$. The state f the molecule with an excited quantum of totally ymmetric vibration should not be different in ymmetry from the vibrationless electronic state. t is natural that the polarization of the bands, hich appear during the combination of these and xcited levels with the ground electronic level, hould be identical.

In pentane the intervals 495 and 927 cm^{-1} re encountered only once each and were measured ery carefully by us. If they are taken as the alues of the frequencies of the vibrations which acilitate the appearance of bands of a different olarization, then they should be distinguished rom the values of the totally symmetric frequencies closest to them. Actually, in the spectrum of naphtha lene in pentane, a frequency interval of 517 cm^{-1} ppears. The interval of 938 cm^{-1} in the spectrum of naphthalene in durene appears only once at the eginning of the spectrum (Table 1). Besides, attri-uting this to the totally symmetric frequency is nreliable [14, 15]. It is of interest to examine he values of the first interval of frequencies or the fluorescence spectra of naphthalene under arious conditions (Table 4).

Table 4

Values of the first intervals of the fluorescence Spectra of Naphthalene under various conditions

Conditions under which the Spectra were obtained	Frequency in cm^{-1}	Author
Vitreous Solutions	482 ± 30	Kasha and Nauman [2]
	470 ± 50	Schnepp and McClure [1]
Mixed Crystals of Naphthalene and Anthracene	450 ± 30	Vol'f [13, 14]
Frozen solution in Heptane	477 ± 30	Bolotnikova
Frozen solution in Pentane	495 ± 5	Bolotnikova
Crystalline solution in Durene	509	McClure [9]

Note: The spectra were obtained at 77° K.

In spite of the low precision of the measurements it is evident from Table 4 that the average values of the first intervals of frequencies never exceed 500 cm^{-1} except in the case of naphthalene in durene. It is possible that the values of the frequencies which allow appearance of differently polarized bands for naphthalene in durene accidentally proved to be close to the values of the totally symmetric frequencies 512 and 938 cm^{-1}. Comparison of the fluorescence spectra with the absorption spectra permits one to assume that the frequencies 495 and 927 cm^{-1} in the ground state (fluorescence spectrum) belong to the same vibrational type as the frequency 433 and 905 cm^{-1} of the first excited state (absorption spectrum [8]). In this case, the mechanisms of the transitions in the processes of absorption and fluorescence are not different from each other in principle, and all the difficulties, associated with the fact that for naphthalene in durene the excitation of totally symmetric vibrations leads to the appearance of perpendicularly polarized bands, are eliminated.

The mechanism of the long wavelength transition of the molecule of naphthalene can now be represented in the following fashion: the symmetry of the first excited state is B_{3u} (polarization of the 0-0 band and the system of bands along the long molecular axis associated with it); the symmetry of the second excited level is B_{2u} (polarization of the second short wavelength region of absorption of naphthalene [8] along the short molecular axis); the first transition $A_{1g} - B_{3u}$ is allowed by symmetry; the proximity of the next electronic state exerts an influence on the character of the first transition and leads to the appearance of bands polarized parallel to the short molecular axis; the appearance of polarized bands in the spectrum in this fashion can only arise through excitation of vibrations of symmetry β_{1g}; the symmetry β_{1g} is therefore assigned to the frequencies 495 and 927 cm^{-1} in the ground state and 430 and 905 cm^{-1} in the excited state.

The analysis of the fluorescence spectrum of a solution of naphthalene in pentane which has been presented can serve as an example of the use of the method of frozen crystalline solutions for the study of molecular spectra of aromatic hydrocarbons.

In conclusion, the author avails herself of the opportunity to thank sincerely Professor E. V. Shpol'skii for his guidance and constant interest in the work.

August 27, 1958

REFERENCES

1. O. SCHNEPP, D.S. MC CLURE: J. Chem. Phys., 20, 1375-1383, (1952)
2. M. KASHA, R.V. NAUMAN: J. Chem. Phys., 17, 516-520, (1949)
3. L. A. BLUMENFEL'D: ZFKh, 24, 838-844, (1950)
4. H. SPONER, G. P. NORDHEIM: Discuss.Farad.Soc., 9, 19-26, (1950)
5. J. R. PLATT, H. B. KLEVENS: J. Chem. Phys., 17, 470-481, (1949)
6. H. G. de LASZLO: Z. f. Phys. Chem., 118, 369-414, (1925)
7. R. PASSERINI, I.G. ROSS: J. Chem. Phys., 22, 1012-1016, (1954)

8. D. S. MC CLURE: J. Chem. Phys., 22, 1668-1675, (1954)
9. D. S. MC CLURE: J. Chem. Phys., 24, 1-12, (1956)
10. E. V. SHPOL'SKII, A. A. IL'INA, L. A. KLIMOVA: DAN USSR, 87, 935-938, (1952)
11. E. V. SHPOL'SKII, L. A. KLIMOVA, E. A. GIRDZHIIAUSKAITE: Materialy X Vsesoiuznogo soveshchaniia po spektroskopii [Materials of the Tenth All-Union Congress on Spectroscopy], L'vov, 1957
12. E. V. SHPOL'SKII, L. A. KLIMOVA: IAN USSR, FS, 20, 471, (1956) (See CTT Bulletin)
13. I. V. OBREIMOV, K. G. SHABALDAS: J. Phys. USSR, 7, 168-178, (1943)
14. E. R. LIPPINCOTT, E. J. O'REILLY: J. Chem. Phys 23, 238-244, (1955)
15. A. L. MC CLELLAN, G. C. PIMENTEL: J. Chem. Phys 23, 245-248, (1955)

DM VII, Vyp. 1
OL. VII, No. 1

OPTIKA I SPEKTROSKOPIIA
OPTICS AND SPECTROSCOPY

Iiul', 1959
July, 1959

The Internal Field and the Position of the Electronic Absorption and Emission Bands of Polyatomic Organic Molecules in Solution

N. G. BAKHSHIEV

Abstract: The effect of solvents on the position of the electronic absorption and emission spectra of 36 derivatives of phthalimide was investigated, and the published experimental data on the shifts of the spectra of a series of organic compounds in solutions processed. Results obtained from a large body of experimental material — 14 aromatic compounds of various types — indicate that the position of the electronic transition frequency and the frequency corresponding to the symmetry axis of the spectrum in the case of a mirror-symmetrical absorption and fluorescence band, agree quantitatively with the theory relating the position of the spectra to the macroscopic characteristics of the solvents — the static dielectric constant ϵ and the index of refraction n.

On the basis of the results of these experiments, deductions are made concerning the change of certain characteristics of the molecules investigated during excitation, and conclusions are drawn concerning the nature of specific close-range interactions in solutions.

1. Following the well known work of Kundt, the effect of solvents on the electronic spectra of molecules became the subject of a large number of investigations. Nevertheless, this phenomenon, which depends on a number of properties of the dissolved substance and the solvent, was not successfully described in general form until recently.

The attempts undertaken by many authors [1-9] to classify the contradictory results of experiment and to explain them quantitatively by correlating changes in the spectra with the different characteristics of the medium have not produced any important results. Although many interesting correlations have been found experimentally between the position of the spectra and this or that physical property of the solvent, no unequivocal [10] or universal relationships have been deduced. Definite progress in this direction was achieved by Bayliss, Oshika, McRae, Mataga and others [11-14], who first suggested examination of the basic molecular characteristics of the solute and solvent (energy levels, oscillator strengths, dipole moments) and took account of the changes of these quantities during excitation. Assuming the existence of a dipole interaction between the molecules in solution, and making use of the Onsager model of the system "absorbing molecule-solvent", these authors [12-14] obtained general expressions relating the shift of the absorption and emission spectra to both the macroscopic characteristics of the solvent (index of refraction n, static dielectric constant ϵ), and the characteristics of the dissolved molecules.

Despite the fact that several years have passed since the publication of these theoretical investigations, their validity has not yet been subjected to comprehensive experimental verification. Consequently, since the theoretical analysis of the problem considered only the electronic states of the molecules, the expressions obtained, as the authors indicate, refer to the shift of the 0-0 frequency characterizing the electronic excitation energy. In the overwhelming majority of experimental studies as a consequence of the difficulty or impossibility of determining the 0-0 frequency directly, it is the effect of the solvent on the shift of absorption or emission maxima which is examined, even though it is well-known that in the case of broad electron-vibrational bands, the position of the maximum does not have much physical meaning and depends (see, for example, the model representations in [15]) on a number of different factors, whose roles may be changed considerably in going from solvent to solvent, complicating the phenomenon and masking the regularity studied.

By analyzing the results of references [11-14] and utilizing Mataga's [13] quantitative estimate of the relative importance of the various terms in the expression for the shifts of the spectra, it is easy to write down the following simplified relation for the displacement of the 0-0 frequency (we shall call it the electronic transition frequency ν_e) in solution relative to its value in vapor

(1)
$$\Delta\nu_e = \nu_{e\ soln} - \nu_{e\ vap} = \frac{1}{r^3}\left[C_1\frac{2\epsilon-2}{2\epsilon+1}+(C_2+fC_3)\frac{2n^2-2}{2n^2+1}\right],$$

r is the Onsager cavity radius [16], (practically equal to the radius of the molecules), f is the oscillator strength of the electronic-vibrational transition considered, and C_1, C_2, C_3, are constants which are determined by the properties of the molecules investigated and are usually different for the absorption and emission spectra. The first term of expression (1) is due to the interaction of the static dipoles of the solute molecules with the molecules of the solvent (the constant C_1 is proportional to the difference $\mu_g-\mu_e$ of the static dipole moments of the isolated molecules in the ground and excited respectively states). The second and third terms are determined by the interaction of the static and induced dipoles, and also by the dispersion interactions, where the constants C_1 and C_2 may acquire either positive or negative values, but the constant C_3 may have only negative values.

The following conclusions follow from an analysis of formula (1): 1) the dependence of the position of the spectra on the index of refraction n must take place in any case; 2) a dependence on the dielectric constant ϵ can appear only when the static dipole moment of the molecule is changed by excitation; for $\mu_e > \mu_g$ a blue shift takes place; 3) the specific effect of the solvent on the spectrum of this or that substance depends to a considerable degree on the relation between the constants C_1, C_2 and C_3, i. e., they are defined by the properties of the dissolved molecules.

Before turning to the results of the experiment it is particularly important to note that formula (1) can be no more accurate than the physical premises on which its derivation was based. The experimental verification of equation (1) may allow definite conclusions to be drawn about the applicability of the model utilized, and also about the nature of intermolecular effects in solutions.

2. It was shown in references [17, 18] for a series of polyatomic organic molecules that the changes in spectral intensities observed in going from vapor to solution are in good quantitative agreement with the deductions of the theory, considering the solvent as an external dielectric medium and utilizing, in particular, the Onsager model of the system "absorbing molecule-solvent". Assuming that this theory must be applied to the same or similar materials, we undertook an experimental verification of expression (1).

The full verification of formula (1), and also the intelligent selection of a sufficiently broad range of materials for investigation were substantially facilitated by the possibility of applying our previously developed methods of investigating the absorption and fluorescence spectra of vapors and solutions [19, 20] and our concepts of the spectra of complex molecules [15, 21-23]. Having in view the application of formula (1) to the electronic transition frequency, we restricted our selection to those substances possessing mirror-symmetric absorption and fluorescence spectra and belonging according to the classification of reference [21, 22] to the modulated class. The intersection point of these spectra ν_s, which in the vapor state represents the electronic transition frequency $\nu_{e\ vap}$, in solutions equals, to a sufficient degree of approximation, half the sum of the frequencies corresponding to the opposing transitions $\nu_s = \frac{\nu_{ea} + \nu_{ef}}{2}$ (ν_{ea} and ν_{ef} are the electronic transition frequencies for the absorption and emission spectra). It is not difficult to show that expression (1) is applicable to the shift of frequency ν_5 for appropriate values of the constants C_1, C_2, and C_3.

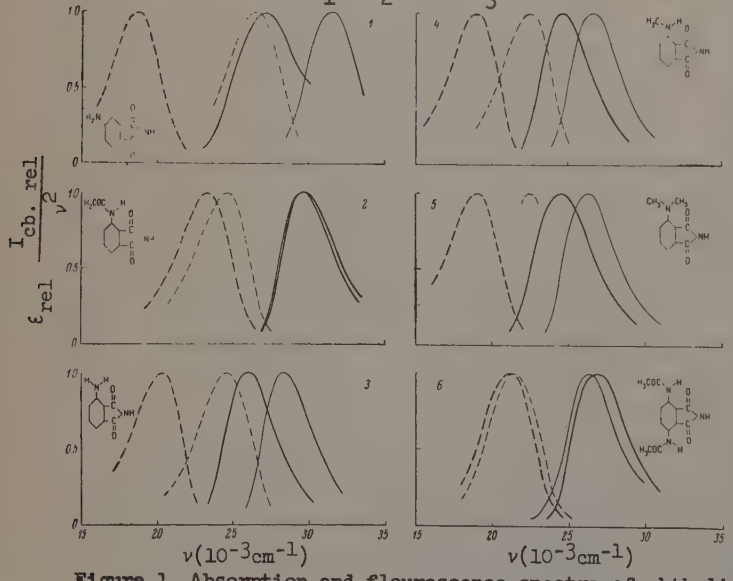

Figure 1. Absorption and flourescence spectra of phthalimide derivatives in the vapor state and of solutions in ethyl alcohol. 1) 4-Aminophthalimide; 2)3-Acetylaminophthalimide; 3)3-Aminophthalimide; 4)3-Monomethylaminophthalimide; 5)3-Dimethylaminophthalimide; 6)3,6-Diacetylaminophthalimide;

Solid lines: Absorption; Dotted: Fluorescence; Thin lines: Vapor; Thick lines: Solution.

As objects of investigation we chose six derivatives of phthalimide: 4-aminophthalimide, 3-acetylaminophthalimide, 3-aminophthalimide, 3-monomethylaminophthalimide, 3-dimethylaminophthalimide and 3, 6-diacetylaminophthalimide, which have continuous mirror-symmetrical absorption and emission spectra. Figure 1 shows absorption and fluorescence spectra of the compounds investigated in the vapor state for $T \approx 300^\circ$ and in solution for $T \approx 20^\circ$ and their structural formulas are also indicated. The measurement of the absorption spectra of the solutions was carried out with the aid of an SF-4 spectrophotometer, and the fluorescence spectra were measured with the aid of a set-up described in [20]. Data on the position of the vapor spectra were taken from [19].* The substances used as solvents had different chemical natures and widely different values of the parameters n and ϵ (see Table 1). Before going to the results of the experiment, let us transform formula (1) for use in the present case. The results of [17] showed that the oscillator strengths of the molecules of the substances investigated retain their values when dissolved in solvents of very different natures. Therefore, we may take $C_2 + fC_3 = C_4$, and rewrite (1) in the following more convenient form:

$$(2a) \quad \Delta\nu_s = \frac{C_1}{r^3}\left[\frac{2\epsilon - 2}{2\epsilon + 1} + p\,\frac{2n^2 - 2}{2n^2 + 1}\right]$$

or

$$(2b) \quad \Delta\nu_s = \frac{C_4}{r^3}\left[q\,\frac{2\epsilon - 2}{2\epsilon + 1} + \frac{2n^2 - 2}{2n^2 + 1}\right],$$

where

$$p = \frac{C_4}{C_1} \quad \text{and} \quad q = \frac{C_1}{C_4} = \frac{1}{p}.$$

Results of the measurements for all the substances investigated are depicted in figures 2 - 5. The linear dependence of the spectral shifts on the expressions included within the square brackets required by the expressions (2a) and (2b) is observed to be completely satisfied, including those points belonging to the vapors (origin of coordinates). In addition, the results obtained by processing the data from the literature are depicted in figures 6 - 12 for the following series of aromatic compounds: benzene (2000 and 2600 Å bands), toluene (2600 Å) and chlorobenzene (2600 Å) according to the results of [24, 25],

* The position of the spectra of the substances investigated is practically independent of temperature in the vapor state, which allows us to make use of data obtained at 200-300° in making comparisons with solutions.

α-naphthol, β-naphthol, β-methylnaphthalene, and β-naphthylmethylether according to the results of [13], and also anthracene according to the data of [26-28]. A calculation of the oscillator strength was made for the cases of benzene and its derivatives in accordance with the deductions of [17] using the Lorentz corrections for the internal field. Information on the position of spectra of anthracene in the vapor state was kindly communicated to us by V. P. Klochkov. The values of the constants $\frac{C_1}{r^3}$, $\frac{C_4}{r^3}$, q and p were calculated for all substances on the basis of the results cited and are presented in table 2. An accurate determination of the quantity for the derivatives of naphthalene (placed in brackets in table 2) is impossible in this case, since the positions of the spectra of these substances in the vapor state is unknown.

Table 1

No	Solvent	ε	n_D	No.	Solvent	ε	n_D
1	Vapor	1.0	1.0	11	Chloroform	5.2	1.445
2	n-Heptane	1.97	1.39	12	Ethyl Acetate	5.9	1.37
3	CCl_4	2.24	1.46	13	Pyridine	12.4	1.51
4	Benzene	2.25	1.50	14	Isoamyl Alcohol	15.3	1.41
5	Toluene	2.35	1.50	15	Isobutyl Alcohol	18.7	1.40
6	Xylene	2.57	1.50	16	Acetone	21.0	1.36
7	Dioxane	2.24	1.42	17	Ethyl Alcohol	26.3	1.36
8	Diethyl Ether	4.3	1.355	18	Methyl Alcohol	31.0	1.33
9	Anisole	4.3	1.51	19	Glycerine	44.0	1.47
10	Butyl Acetate	5.1	1.40	20	Water	81.0	1.33

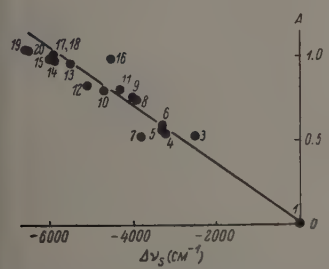

Figure 2. Dependence of displacement of the frequency ν_s of the spectra of 4-aminophthalimide on the dielectric constant ε and the refractive index n of the solvents.

For identification of the solvents, see Table 1.

$$A = \frac{2\epsilon-1}{2\epsilon+1} + p\,\frac{2n^2-2}{2n^2+1}.$$

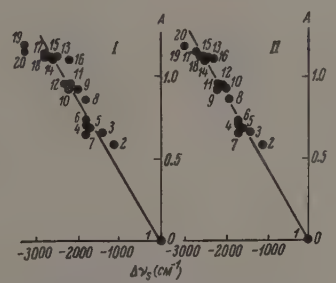

Figure 3. Dependence of displacement of the frequency ν_s in the spectra of 3-monomethylaminophthalimide (I) and 3-dimethylaminophthalimide (II) on the dielectric constant ε and the refractive index n of the solvent.

For identification of the solvents, see Table 1.

$$A = \frac{2\epsilon-2}{2\epsilon+1} + \frac{2n^2-2}{2n^2+1}.$$

The results quoted show that on the whole the changes of position of the spectra of various aromatic compounds in the transition from the vapor state to solutions in various solvents may be explained to a sufficiently good degree of approximation within the limits of the indicated theory. This allows us, in particular, to assume that in the cases considered the shifts of the spectra are determined on the whole by the presence of intermolecular interactions of the dipole-dipole type in the solution.

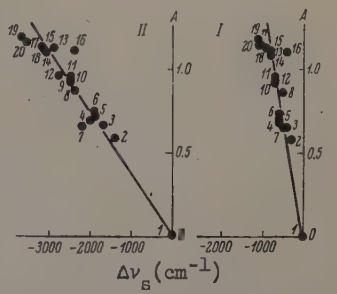

Fig. 4. Dependence of displacement of the frequency ν_s in the spectra of 3-acetylaminophthalimide (I) and 3-aminophthalimide (II) on the dielectric constant ε and on the index of refraction n of the solvent.

For identification of the solvents, see Table 1.

$$A = \frac{2\epsilon-1}{2\epsilon+1} + p\,\frac{2n^2-2}{2n^2-1}.$$

Figure 5. Dependence of displacement of the frequency ν_s in the spectra of 3,6-diacetylaminophthalimide on the dielectric constant ε and on the index of frefraction of the solvent, n.

For the identification of the solvents, see Table 1.

$$A = \frac{2\epsilon-2}{2\epsilon+1} + p\,\frac{2n^2-2}{2n^2+1}.$$

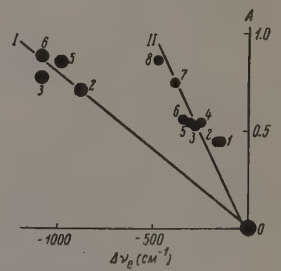

Figure 6. Dependence of displacement of the frequency of ν_{ea} in the spectra of benzene on the index of refraction of the solvent, n. Solvents: 1-water[25]; 2-water[24]; 3-ethyl alcohol[21]; 4-hexane[25]; 5-hexane [24]; 6-cyclohexane[24]; 7-chloroform[24]; 8-CCl_4[24]. Wavelengths (in Å): I-2000, II-2600.

$$A = \frac{2n^2-2}{2n^2+1}.$$

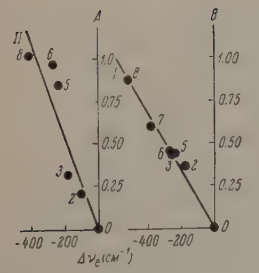

Figure 7. Dependence of displacement of the ν_{ea} in the spectra of toluene (I) and chlorobenzene (II) on the dielectric constant ϵ and on the refractive index n of the solvents [24].

For the identification of the solvents, see the caption of Figure 6.

$$A = -\frac{2\epsilon-2}{2\epsilon+1} + p\,\frac{2n^2-2}{2n^2+1};\quad B = \frac{2n^2-2}{2n^2+1}.$$

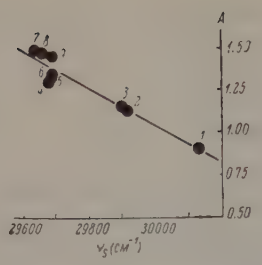

Figure 8. Dependence of the frequency ν_s in the spectra of β naphthol on the dielectric constant ϵ and on the index of refraction n of the solvents [13]. Solvents: 1-hexane; 2-benzene; 3-toluene; 4-butyl acetate; 5-ethyl acetate; 6-methyl acetate; 7-butyl alcohol; 8-ethyl alcohol; 9-methyl alcohol.

$$A = \frac{2\epsilon-2}{2\epsilon+1} + p\,\frac{2n^2-2}{2n^2+1}.$$

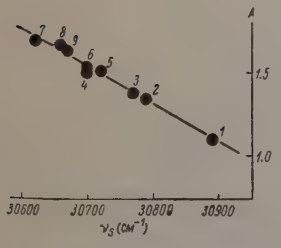

Figure 9. Dependence of the position of the frequency ν_s in the spectra of α-naphthol on the dielectric of constant ϵ and on the index of refraction n of the solvents [13]. For the identification of the solvents, see caption of Figure 8.

$$A = \frac{2\epsilon-2}{2\epsilon+1} + p\,\frac{2n^2-2}{2n^2+1}.$$

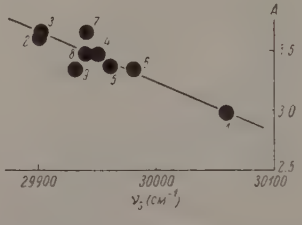

Figure 10. Dependence of the position of the frequency ν_s in the spectra of β-naphthylmethylether on the dielectric constant ϵ and on the index of refraction of the solvents, n [13]. For identification of the solvents, see caption of Figure 8.

$$A = \frac{2\epsilon-2}{2\epsilon+1} + p\,\frac{2n^2-2}{2n^2+1}.$$

At the same time there is not a sufficient quantity of data at our disposal for a definite judgment as to whether the model assumed as the basis of the theory is applicable to the phenomenon considered. One cannot exclude the possibility that certain other types of intermolecular forces may be described by expressions analogous to those used here. Thus, in the following section, which is devoted to the examination of different characteristics of the molecules investigated, it is shown that even in the case of the existence of specific close-range interactions between the molecules of the dissolved substance and the solvent, the theory satisfactorily describes the phenomenon. The applicability of the theory is possibly related to the fact that the intermolecular forces, in the last analysis, change the electrical characteristics of the solute molecules (dipole moment, polarizability etc.) The material presented in the next section of the paper shows the important role of these characteristics in the phenomenon considered.

3. Analysis of the results of the experiment permits a number of deductions about the properties of the molecules investigated. First of all, the strong dependence of the positions of the spectra of the majority of substances on the dielectric constant of the medium ϵ indicates a change of the static dipole moment of the molecules of these substances on excitation (in monosubstituted phthalimides and derivatives of naphthalene, $\mu_e > \mu_g$, and in di-substituted 3, 6-diacetylaminophthalimide and chlorobenzene, $\mu_e < \mu_g$). It is interesting to note the invariance of the constant p for all 3-amino derivatives of phthalimide investigated. This signifies, in particular, that the relative contribution to the magnitude of the frequency shift ν_s which is associated with changes of the static dipole moment and the existence of induced dipole moments, is identical for all substances investigated. Thus, the difference of the quantity p in 4-aminophthalimide indicates a larger relative (and, apparently, absolute) change of the magnitude of the static dipole moment on excitation in this compound than in 3-aminophthalimide. The similarity of the properties of the 3-amino derivaties of phthalimide also makes it possible to check up on the dependence of the magnitude of the shift of the spectra on the radius of the molecules which follows from formula (1). Indeed, if we assume that $C_1 \approx$ constant for all the indicated substances, then the substantial differences in the magnitudes of the shifts must be due to the difference in molecular dimensions (in terms of Onsager cavity radii). Table 2 presents data taken from [29] on the radii of the molecules investigated, determined according to the structural model (r); the adjoining column contains the radii of the same molecules (r') calculated according to the magnitude of the shift assuming $C_1 \approx$ constant, where the size of the 3-aminophthalimide molecule was taken as unity. It is easily seen that the relative dimensions of the molecules calculated according to the magnitude of the shifts agree well with the data obtained from the structural model. We may note here that the deductions about the high degree of dependence of the magnitude of the shift on the dimensions of the dissolved molecules corroborate the data of a number of investigations, and reflect a general rule to the effect that in a series of related compounds, the spectral shift is greater, the smaller the dimensions of the molecule (see, for example [10, 30]).

In the derivatives of naphthalene, a regular decrease was observed of the relative role of the term depending on ϵ in the series β-naphthol, α-naphthol, β-methylnaphthalene. This result is found in complete agreement with the data of Mataga [13], who investigated the change of the static

dipole moments of the substances indicated with changes of the relative positions of the absorption and emission spectra. A completely different picture of the dependence of the spectra on the solvents was observed for anthracene, benzene and its alkyl derivatives.

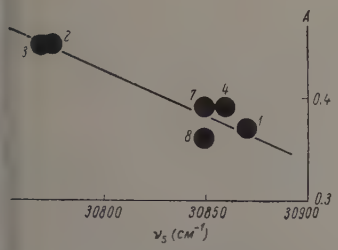

Figure 11. Dependence of the position of the frequency ν_s in the spectra of β-methylnaphthalene on the index of refraction of the solvents, n [13].

For identification of the solvents, see the caption to Figure 8.

$$A = \frac{2n^2-2}{2n^2+1}.$$

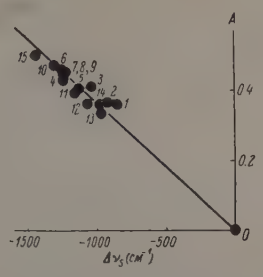

Figure 12. Dependence of the displacement of the frequency ν_s in the spectra of anthracene on the index of refraction of the solvents, n.

Solvents: 1-pentane[27]; 2-hexane[27]; 3-cyclohexane (110°) [27]; 4-CCl_4(110°) [27]; 5-dioxane[27]; 6-benzene[27]; 7-toluene[27]; 8-xylene[27];9-mesiethylene [27] 10-chlorobenzene[26]; 11-amyl alcohol[26]; 12- ethyl alcohol[26]; 13-methyl alcohol [26]; 14-ethyl alcohol[28]; 15-naphthalene (90°) [27].

Table 2

No.	Substance	C_1/r^3	$C_4\ r^3$	p	q	r (in Å)	r (in Å)
1	3-amino-phthalimide	-2800	-1400	0.50	2.0	3.8	3.8
2	3-monomethyl-aminophthalimide	-2250	-1150	0.51	1.95	3.9	4.1
3	3-dimethyl-aminophthalimide	-2250	-1150	0.51	1.95	3.9	4.1
4.	3-acetyl-aminophthalimide	-770	-390	0.51	1.95	5.0	5.3
5	4-amino-phthalimide*	-5600	-1000	0.18	5.55	–	–
6	3,6-diacetyl-aminophthalimide	1250	-2500	-2.0	-0.5	–	–
7	β-naphthol	- 900	(-1350)	(1.50)	(0.67)	–	–
8	α-naphthol	- 400	(- 800)	(2.0)	(0.50)	–	–
9	β-naphthyl-methylether	- 250	(-1750)	(7.00)	(0.14)	–	–
10	β-methyl-naphthalene	0	(-1150)	–	0	–	–
11	Benzene (2000 Å)	0	-1250	–	0	–	–
12	Benzene (2600 Å)	0	- 500	–	0	–	–
13	Toluene	0	- 550	–	0	–	–
14	Chlorobenzene	350	-1100	-3.1	-0.32	–	–
15	Anthracene	0	-2700	–	0	–	–

* Reworked values (compare with [33]).

As was to be expected, in this case C_1=0; i.e., only a dependence on the index of refraction of the medium showed up. The data quoted supply a basis on which to assert that the change in the magnitude of the static dipole moment on excitation which has been demonstrated for a number of substances – particularly for those whose substituent groups contain N or O atoms with unshared electrons – apparently takes place because of the inclusion of n-electrons of the substituent group in the conjugate π-electron system of the molecules. This agrees with the commonly accepted views on the spectra of substituted aromatic compounds and, in particular, with the abovementioned deductions of Mataga. We also point out the clearcut dependence of the magnitude of the displacement on the position of the substituent (3-amino- and 4-aminophthalimide, α- and β-naphthol). Here the magnitude of the spectral shift increases as the substitute approaches the long axis of the molecule. Interesting results were also obtained by comparing data on the displacements of the spectra of mono- and di-substituted compounds. (For example, 3-acetylamino- and 3, 6-diacetylaminophthalimide.) This makes it possible to draw definite conclusions about the redistribution of relative electron density in the molecules of the substances indicated on excitation. We regret that the size of our paper does not allow us pause to consider the details.

Besides the results enumerated, the experimental data also make it possible to make certain deductions with respect to the nature of the specific short-range interactions in solutions and, in particular, on the hydrogen bond.

The actual existence of a hydrogen bond in certain solutions of the substances investigated is indisputable; this bond exists because of the hydrogen atoms of the substituent amino groups*. The results obtained for the acetone solutions are characteristic in this sense. As is evident from figures 2-5, the points corresponding to solution in acetone deviate relatively more from the rule expressed by formulas (2a) and (2b), particularly in the case of 4-aminophthalimide. However, here the magnitude of the deviation decreases regularly in the series 4-aminophthalimide, 3-aminophthalimide, 3-monomethylaminophthalimide and, finally, practically vanishes in the case of 3-dimethylaminophthalimide, whole molecules cannot form a hydrogen bond.

On the whole the experimental data show that specific short range interactions, and in particular the hydrogen bond, are apparently described by the theory examined, though possibly formally.

Thus the large body of experimental material representing 14 aromatic compounds

* Apparently, the hydrogen atom of an imide nitrogen does not take part in hydrogen bonds, since its replacement by a methyl group does not lead to a change of the spectra [31].

of various types makes possible a series of deductions on the effect of solvents on the spectra of polyatomic organic molecules. First of all we note that when the experimental data* are correctly treated, the experimental results are in good agreement with all deductions of the theory relating the position of the spectra to the macroscopic parameters of the solvents ϵ and n. The model used for the investigated molecule-medium, as was shown, describes the phenomenon sufficiently well. This is explained to a considerable degree by the nature of the electron transitions (we have in mind allowed and relatively intense transitions), for which the entire generalized π-electron system of the molecule is responsible, and also by the structure of the molecules investigated, which present relatively compact formations, lending themselves well to approximation in terms of the spherical cavity. We note that a more extended object such as, for example, the stilbene molecule, would not lend itself nearly so well to such an approximation, as follows from the data of Lippert [32]. The rule expressed by formula (1) is satisfactorily obeyed not only by complex molecules possessing continuous spectra, but even by simpler objects whose absorption and emission spectra possess structure.

In conclusion I wish to express my deep appreciation to B. S. Neporent for his constant attention, interest and for a whole series of valuable remarks and advice.

July 25, 1958

References

1. T. HAVELOCK, M. ARMSTRONG: Proc. Roy. Soc., A86, 15 (1912)
2. G. SCHEIBE: Ang. Chem., 50, 212 (1937)
3. N. BAYLISS, A. REES: J. Chem. Phys., 8, 377 (1940)
4. S. SHEPPARD: Rev. Mod. Phys., 14, 303 (1942)
5. N. BAYLISS: J. Chem. Phys., 18, 292 (1952)
6. W. SIMPSON: J. Amer. Chem. Soc., 73, 5359 (1951)
7. S. NAGAKURA, H. BABA: J. Amer. Chem. Soc., 74, 5693 (1952)
8. N. BAYLISS: Ann. Rep. Phys. Chem., 3, 229 (1952)
9. S. VELJKOVIC: Trans. Farad. Soc., 53, 1181 (1957)
10. V. P. KLOCHKOV: OiS, 1, 546 (1956)
11. N. BAYLISS, E. McRAE: J. Phys. Chem., 58, 1002 (1954)
12. Y. OOSHIKA: J. Phys. Soc. Japan., 9, 594 (1954)
13. N. MATAGA, Y. KAIFU, M. KOIZUMI: Bull. Chem. Soc. Japan., 29, 115, 465 (1956)
14. E. McRAE: J. Phys. Chem., 61, 562 (1957)
15. B. S. NEPORENT: ZETF, 21, 172 (1951)
16. L. ONSAGER: J. Amer. Chem. Soc., 58, 1986 (1936)
17. B. S. NEPORENT, N. G. BAKHSHIEV: OiS, 5, 634 (1958)
18. N. G. BAKHSHIEV: OiS, 5, 646 (1958)
19. V. P. KLOCHKOV: ZFKh, 29, 1432 (1955)
20. B. S. NEPORENT, V. P. KLOCHKOV: IAN USSR, F.S., 20, 601 (1956) (See CTT Bulletin)
21. B. S. NEPORENT: Doctoral diss. GOI, Leningrad (1945)
22. B. S. NEPORENT: IAN USSR, F.S., 15, 533 (1951)
23. B. S. NEPORENT: ZFKh, 30, 1048 (1956)
24. N. BAYLISS, L. HULME: Austr. J. Chem., 6, 257 (1953)
25. V. M. CHULANOVSKII, T. G. MEISTER, E. N. STRUZHENSKAIA: Vestn. Leningrad Univ. No. 2 (1) 143 (1955)
26. S. SAMBURSKY, G. WOLFSOHN: Trans. Farad. Soc., 36, 427 (1940)
27. S. SAMBURSKY, G. WOLFSOHN: Phys. Rev., 62, 357 (1942)
28. A. S. CHERKASOV: ZFKh, 29, 2209 (1955)
29. N. A. BORISEVICH: Kand. diss. GOI, Leningrad (1954)
30. E. LIPPERT, F. MOLL: Zs. Elektrochem., 58, 718 (1954)
31. V. V. ZELINSKII, V. P. KOLOBKOV, L. G. PIKULIK: OiS, 2, 402 (1957)
32. E. LIPPERT: Zs. Naturforsch., 10a, 541 (1955)
33. N. G. BAKHSHIEV: IAN USSR, F.S., 22, 1387 (1958) (See CTT Bulletin)

* The position of the maxima of the emission and absorption bands of the derivatives of phthalimide investigated by us are included considerably more poorly in the regularity expressed by formula (1).

OM VII, Vyp. 1
OL. VII, No. 1

OPTIKA I SPEKTROSKOPIIA
OPTICS AND SPECTROSCOPY

Iiul', 1959
July, 1959

The Optical Properties of Concentrated Solutions and Melts. I.

V. A. KIZEL' AND V. M. RUBINOV

Abstract: Measurements have been made on the reflection and absorption spectra of bromine and of certain ye solutions in a wide range of concentrations. By comparing the experimental curves with those calculated n the basis of the classical theory of dispersion and the theory of Davydov, the advantage of the latter is emonstrated. The concentration dependences of the oscillator strengths of the dye solutions have been found. t is shown that the oscillator strengths decrease for large concentrations.

An investigation of the concentration dependences of the optical parameters of solutions makes it possible to follow the origin and growth of the interactions of the solute molecules with each other. In particular, much information may be extracted from the data on absorption and dispersion. For small concentrations there is an enormous number of such investigations, but for large concentrations the number is very small. To a considerable degree this may be explained by the difficulty of theoretical interpretation of the results obtained, due to the variety and complexity of the interactions.

An interpretation of the experimental data on absorption and dispersion of solutions using the classical formulas (so called "gas formulas", which suppose the molecules to be completely free of interactions) does not give good agreement with experiment, even for single oscillator transitions. A quantum theory of absorption and dispersion of light by solutions has been given by Davydov [1]. This theory takes into account the interaction between the vibrations of the solute molecules and the vibrations of the solvent molecules (the so-called "molecule-solvent" interactions) and shows that the "gas formulas" are applicable to solutions in the case of extremely weak interactions; if the interaction is strong, different formulas apply which are given in [1].

Thus the determination of the applicability of the Davydov theory for various concentrations will allow a more precise characterization of the "molecule-solvent" interaction as a function of concentration.

In studying the optical properties of solutions it is usual to use as a rough approximation the idea that the "molecule-solvent" interaction in dilute solutions is independent of increases in concentration, and that this interaction will change only at a very high concentration when the number of adjacent solvent molecules surrounding a solute molecule has decreased considerably.

In this scheme, the changes in optical properties as the concentration is increased by 10-20% (depending on the liquid) are attributed to the occurrence of specific interactions of the solute molecules with each other ("molecule-molecule" interactions). Hence one may make certain deductions concerning the character of these interactions (not taken account of in the Davydov theory). These deductions might concern, for example, the occurrence of association, "inductive resonance", etc.

These studies may also give a verification of the theory for large concentrations.

For highly dilute solutions the comparison of theory with experiment shows good agreement [2, 3], whereas for large concentrations comparison can be made only for one dye [3]. In the present work, proceeding on the scheme outlined above, a wider comparison with experiment is undertaken for solutions of high concentration, for melts, and for liquids. We chose as our samples solutions of dyes in transparent liquids.

For very high concentrations it is necessary to take account of another factor, viz. the possibility that surface phenomena will arise. The width of the layers in which absorption occurs extends in from the surface from less than 2000 to 5000 Å; meanwhile in individual cases, the orientational and concentrational surface effects may reach to a depth of from 200 to 2000 Å. This certainly complicates the picture. For these concentrations and those values of the absorption coefficient under consideration here, surface effects should not play an important role.

In order to obtain the complete picture of the concentration dependence and in order to have data obtained under uniform conditions of measurement for a given sample and solvent, we carried out measurements for small concentrations as well.

EXPERIMENTAL TECHNIQUE

The measurements of the optical constants [the index of refraction $n(\nu)$, and the absorption coefficient $\kappa(\nu)$] were made using the method of selective reflection of light by the dye solution; the coefficient of reflection $R(\nu)$ was measured. Direct measurements of the absorption for large values of κ present considerable difficulty. There are methods for obtaining films of thickness down to $d \sim 0.2\ \mu$, but it is hard to extend them further; for $d < 2\ \mu$, measurements of the thickness become unreliable. We used a cell with $d = 5\ \mu$, and we measured only the reflection curves.

The shapes of the reflection and absorption bands were measured with the aid of a ZMR-2 monochromator with automatic recorder. The light source was an incandescent lamp, and the receivers used were TsV and STsV photocells. The accuracy of measurement may be estimated to be as follows: 3% for the measurements of the absorption spectra for small concentrations, and 10% for large concentrations; for the reflection measurements the corresponding figures are 15% and 10%, respectively.

The cell design used in measuring the reflection spectra is shown in figure 1. The front wall 1 of the cell is of chemically inert K-8 glass (cf. also below), and the angle of the wedge is 8°. The angle of incidence of the light on the wedge is 40°, and at the solution-glass interface about 14°. The light passing through the solution leaves the cell via a mirror (2). The absence of any appreciable amount of scattered light was checked when the apparatus was assembled.

It is necessary that there be contact between the solution and the glass at the reflecting surface, since at a free surface the "normal" Fresnel reflection would be too large and the small relative changes in $R(\nu)$ could not be measured. The glass

of the wedge prism was selected from a series of inactive glasses to have its index of refraction n' nearly the same as n_{sol}; this favored high contrast for the reflection spectra. A shortcoming of such a reflecting surface is the possibility of the formation of an adsorbed film of the dye in the pores of the glass. To check on the possible presence of such a film, reflection spectra were made using both freshly cleaned glass in contact with the solution and also glass which had been long immersed in the solution. In addition, a comparison was made between the reflection spectra at the glass-solvent interface for both freshly cleaned glass and glass long immersed in the solution; in all cases no difference was observed. The presence of the contact with the glass might increase the complications mentioned in the introduction related to surface effects in the liquid. However, for the concentrations used, and to the accuracy of our measurements, we may neglect them in first approximation.

Analine was chosen as the solvent in view of the fact that it does not promote association. It is well known that the tendency of a dye to associate is significantly decreased with the decrease of the dielectric constant of the solvent [4-6].

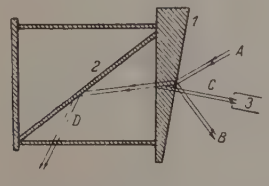

Figure 1. Diagram of the cell to obtain reflection spectra from solutions.

A- incident rays; B- reflection from the front surface of the wedge; C- reflection from the solutions in the monochromator; D- ray passed through the solution; 1- glass wedge; 2- mirror; 3- monochromator.

In water, for our concentrations, association is nearly 100% [7], and in methyl alcohol ($\epsilon \sim 35$) it is considerably less [8], etc. For aniline, $\epsilon = 7.2$ In fact, association plays no role in practice even for the highest concentrations (cf. discussion below). Following the considerations outlined above, in order to distinguish the various aspects of the "molecule-molecule" interaction it was all the more desirable that the association phenomenon connected with the appearance of a diameter spectrum be studied more closely [7, 9, 10] than the other aspects of the interaction at high concentrations. On the other hand, the comparisons which we carried out on solvents (on acetone, chloroform, benzyl, isoamyl alcohols, and acetic acid) showed that aniline is a good solvent for our dyes and many others.

The following dyes were investigated: nitrosodimethylaniline, fuchsin, crystal violet, rhodamine, 6G , and methylene blue. No special cleaning operations were carried out, since at this stage of study the particular characteristics of the dyes were not especially important.

METHOD OF CALCULATION

The experimental curves $R(\nu)$ were approximated by calculated curves which may be obtained from Davydov's equations for the strong interaction case.

$$(1)\quad \begin{cases} n(\omega) = 1 + \dfrac{2\pi N_l \left|D_l\right|^2 \kappa}{3\hbar B} \cdot \dfrac{\Omega_n - \omega}{2B} \exp\left\{-\left(\dfrac{\Omega_n - \omega}{2B}\right)^2\right\} \\ \kappa(\omega) = \dfrac{\pi N_l \left|D_l\right|^2 \kappa}{3\hbar B} \exp\left\{-\left(\dfrac{\Omega_n - \omega}{2B}\right)^2\right\} . \end{cases}$$

Here N_l is the number of molecules of the sol per cc., B is a quantity proportional to the half width of the absorption band, $\Omega_n = \Omega_l + A$, where Ω_l is the frequency of the electronic transition, and A is the displacement of the band in the solu tion; κ is a factor taking into account the diffe ence between the effective field and the field in vacuum; the remaining notation is conventional.

Approximations were then made for the case of extremely weak interactions (the classical formulas

Combining the Fresnel formulas with the above equations, and after simple but laborious transfor mations, one may obtain (to terms of second order)

$$(2)\quad \begin{cases} R(\nu) = \dfrac{\left(\sqrt{\dfrac{\sqrt{L^2 + M^2} + L}{2}} - \eta'\right)^2 + \kappa^2}{\left(\sqrt{\dfrac{\sqrt{L^2 + M^2} + L}{2}} + n'\right)^2 + \kappa^2} , \\ L = L_o \dfrac{a + bx\beta + c\beta^2 + dx^2\beta^2}{a_1 + b_1 x\beta + c_1\beta^2 + d_1 x^2\beta^2} , \\ M = M_o \dfrac{\beta + 2x\beta^2}{a_1 + b_1 x\beta + c_1\beta^2 + d_1 x^2\beta^2} . \end{cases}$$

Here we have

$$(3)\qquad \beta = \frac{gf}{B} \cdot \frac{1}{1 + x^2} ; \quad x = \frac{2\pi}{\nu B}(\nu^2 - \nu_o^2)$$

for the case of an extremely weak interaction, and we have

$$(3')\qquad \beta = \frac{gf}{B} \exp\left[-x^{-2}\right] ; \quad x = \frac{\pi(\nu - \nu_o)}{B}$$

for the case of an extremely strong interaction.

$2\pi\nu_o = \Omega_n$; $g = \dfrac{\pi N_l e^2}{6m\Omega_n}$; a, b, c, d, M_o, and L_o are constants dependent on the index of refraction of the solvent. The latter is introduced via the Lorentz-Lorenz formula, assuming refraction to be additive.

The process of approximating the experimental curves using (2), (3), and (2), (3') was carried out by choosing the parameters B, f, ν_o so that the experimental curve and both theoretical curves coincided in the neighborhood of the value ν_o. This choice seemed the most natural; both theoretic

treatments give the same results in this region; and as one moves further from the point ν_0, the divergence between them increases. The value of ν_0 was determined both from the absorption curve at low concentrations (as will be shown later, ν_0 coincides with ν_{max}), and also by a method of successive approximations; the results were practically identical. Hence for the cases (2), (3), and (2,), (3'), the values of ν_0 turned out to be practically the same; B and f, naturally, were different. The parameters B, f, and ν_0 depend more or less on the choice of the point for superposition of the curves; however, in practice, their choice is almost unique. In figure 2 we show the two calculated curves, giving f = 0.86 and 0.96 and ν_0 equal to 5.18 and $5.17 \cdot 10^{-14}$ sec.$^{-1}$, respectively.

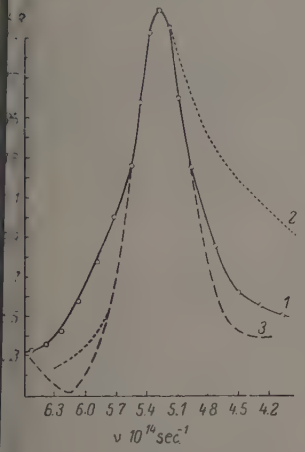

Fig. 2. Reflection coefficient of a crystal violet solution, C = 0.05 g/ml 1- experimental curve, 2- computed for weak interaction, 3- computed for strong interaction.

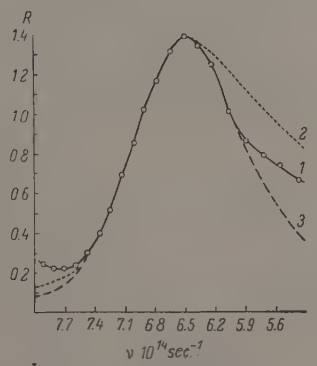

Fig. 3. Reflection coefficient for nitrosodimethyl aniline, solution, C = 0.10 g/ml 1- experimental curve, 2- computed for weak interaction, 3- computed for strong interaction.

In a few cases it was possible to carry out direct measurements of absorption as well as of selective reflection to be followed by calculation of $x(\nu)$ from values found for B, f, and ν_0. From the tables and graphs it is clear that the results agree within the accuracy of the measurements.

The best method for verifying equations (2), (3), and (3') would be to make separate measurements of $n(\nu)$ and $\kappa(\nu)$ by selective reflection. The procedure for such methods is standard, for instance, by measuring $R(\nu)$ for two angles of incidence or two azimuthal angles of polarization, or by the method of T. P. Kravets [11, 12]. However, our values of $\kappa(\nu)$ are too small for the application of these methods, and the accuracy would be extremely low ($\Delta n \approx \Delta\kappa \approx 10\Delta R$).

Nevertheless measurements were made by the two methods outlined,* the resulting values of n, and κ corresponded to ours within the low accuracy mentioned.

*We are grateful to S.O.Mirumiants and N. N. Pribytkova for providing the glass samples.

RESULTS AND DISCUSSION

In figures 2-7 we give the results of the measurements (curves 1) and of the calculations (curves 2 for the weak interaction, curves 3 for the strong interaction).

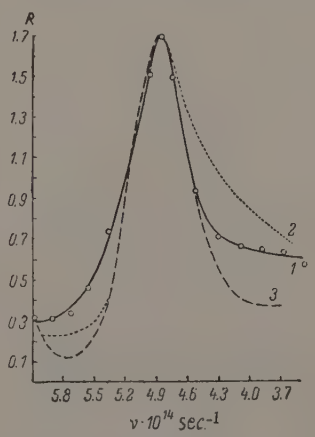

Fig. 4. Reflection coefficient of fuchsine, C = 0.12 g/ml. 1- experimental curve; 2- computed for weak interaction; 3- computed for strong interaction.

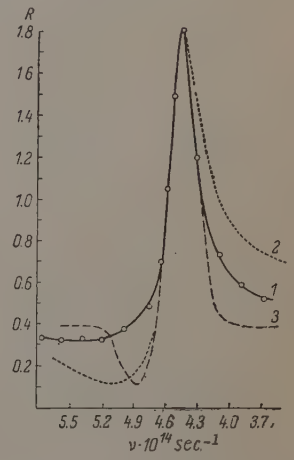

Fig. 5. Reflection coefficient for methylene blue, C = 0.03 g/ml. 1- experimental curve; 2- computed for weak interaction; 3- computed for strong interaction.

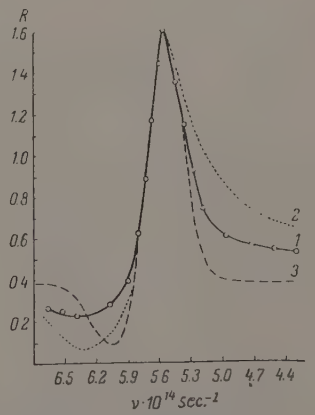

Fig. 6. Reflection coefficient for rhodamine 6G, C = 0.06 g/ml. 1-experimental curve; 2- computed for weak interaction; 3- computed for strong interaction.

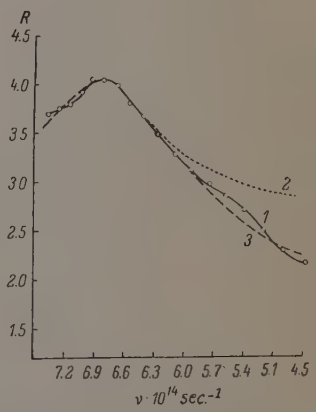

Fig. 7. Reflection coefficient for bromine 1-experimental curve; 2- computed for weak interaction; 3- computed for strong interaction.

Consider first the low frequencies side. Here it is quite clear that, as should have been expected, the curve corresponding to the strong interaction gives the better representation of the experimental data, despite the fact that the curve is for the extreme case; the actual interactions are somewhat

weaker than is supposed in equations (3'); the agreement deteriorates, as mentioned earlier, with increasing separation from the point ν_0. In the examples studied, the agreement is complete only for bromine.

For the high frequencies it is difficult to give the advantage to either of the theoretical models, even though they differ significantly from each other. A similar situation was noted in [13]. It is likely that this situation is due to the proximity of the next absorption bands. We must recall, moreover, as has been shown [14] for the cases of crystal violet and fuchsine, that the long wavelength absorption band considered here is not a single oscillator band (the same may be supposed to hold for the cases of rhodamine and methylene blue). Clearly the consequences of this will not be to improve the agreement for any choice of the parameters, since any negligible improvement in the wings will lead to significant worsening of the agreement at the maximum. This is natural since the theory [1] is similar to the classical theory only for the single oscillator transition.

No important qualitative changes occur in the picture outlined as the concentration is increased.

In Tables 1 and 2 we give the values of f and ν_0 obtained using the equations of the Davydov theory (2), (3'). The values of ν_0 obtained from relations of the form (2), (3) as well as (2), (3') agree well with the values for ν_{max} obtained from our absorption measurements. There is no data in the literature on the absorption curves for aniline; the agreement with the data for the other solutions is as good as one should expect. From what has been said it is clear that the parameter ν_0 of the theory does not coincide with the frequency of the pure electron transition; but is separated from it by a distance of the same order of magnitude for all our dyes. A more precise measurement of this separation i.e. the quantity A in formula (2) would be very interesting, but would require additional investigation to determine α_{elect}.

One may note also the more or less clearly developed tendency for f to decrease with concentration in the region $c > 10^{-3}$ gm/mol, i.e. in the region of intermolecular separations of from ~50 to 10 Å. This point is illustrated in figures 8 and 9.

For a more thoroughgoing determination and explanation of the concentration dependence of f it would be necessary to have more information; in

Table 1

Oscillator Strength f of Dyes in Aniline Solutions

Dye	By reflection						By absorption					
	By formulas (2), (3')						By literature data	By formulas (2), (3')				By literature data
Methylene blue	0.65 (0.03)	0.68 (0.015)						0.71 (0.005)	0.79 (10^{-3})	0.88 (10^{-4})	1.01 (10^{-5})	1.05 (10^{-6})	0.60;0.86[6]
Nitrosodimethyl aniline	0.33 (0.10)	0.33 (0.06)	0.27 (0.03)					0.44 (0.01)	0.44 (10^{-3})	0.44 (10^{-4})	0.44 (10^{-5})	0.44 (10^{-6})	
Crystal violet	0.90 (0.05)	0.89 (0.025)							1.00 (0.01)	1.00 (10^{-3})			
Rhodamine 6G	0.54 (0.06)	0.50 (0.03)	0.80 (0.015)	1.03 (0.005)				0.68 (0.01)	1.13 (10^{-3})	1.38 (10^{-6})			0.72[6]
Fuchsine	0.41 (0.12)	0.40 (0.08)	0.42 (0.06)	0.52 (0.04)	0.84 (0.02)	0.74 (0.01)	0.48[6] (film)	0.75 (0.01)	0.79 (10-3)	0.82 (10^{-4})	0.90 (10^{-5})	0.89 (10^{-6})	1.16[6] 1.09[11]

Remark: Lower numbers in parentheses denote concentration in g/ml.

Table 2

Frequency ν_0 10^{-14} sec^{-1} of Dyes in Aniline Solutions

Dye	By reflection					By absorption				
Methylene blue		0.48 (0.03)		0.59 (0.015)		4.56 (0.005)	4.56 (10^{-3})	4.56 (10^{-4})	4.56 (10^{-5})	4.56 (10^{-6})
Nitrosodimethyl aniline	7.05 (0.10)		7.07 (0.06)		7.04 (0.03)	6.92 (0.01)	6.92 (10^{-3})	6.92 (10^{-4})	6.92 (10^{-5})	6.92 (10^{-6})
Crystal violet		5.18 (0.05)		5.18 (0.025)				5.13 (0.01)	5.13 (10^{-3})	
Rhodamine 6G	5.75 (0.06)	5.73 (0.03)	5.77 (0.015)	5.80 (0.005)		5.68 (0.01)	5.68 (10^{-3})	5.68 (10^{-4})	5.68 (10^{-5})	5.68 (10^{-6})
Fuchsine	5.60 (0.12)	5.48 (0.08)	5.48 (0.06)	5.62 (0.04)	5.70 (0.02)	5.60 (0.01)	5.60 (10^{-3})	5.60 (10^{-4})	5.60 (10^{-5})	5.60 (10^{-6})

Remark: Lower numbers in parentheses denote concentration in g/ml.

particular it seems to us that one may seek a preliminary and approximate explanation by taking account of the fact that, for these intermolecular separations, interactions must occur of the "inductive resonance" type. As is well known, it is precisely in this concentration region that the above mentioned interaction appears in emission; it should be expected to occur also in the absorption of light by coupled oscillators. It was in this fashion that the analogous situation was explained for mercury vapor at high pressures [13].

Fig. 8. Oscillator strength of fuchsine as a function of the intramolecular spacing. 1- from reflection spectra; 2- from absorption spectra.

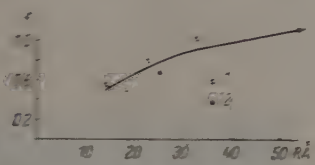

Fig. 9. Oscillator strength of rhodamine 6G as a function of the intramolecular spacing. 1- from reflection spectra; 2- from absorption spectra.

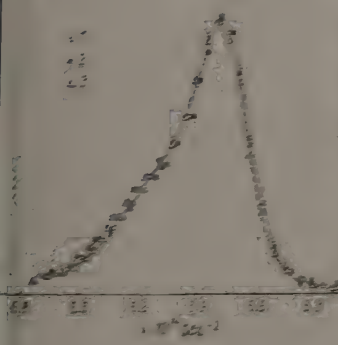

Fig. 10. Absorption of an aqueous solution of rhodamine 6G for $C = 10^{-5}$ g/ml. 1- for 15°; 2- for 50°; for 90°.

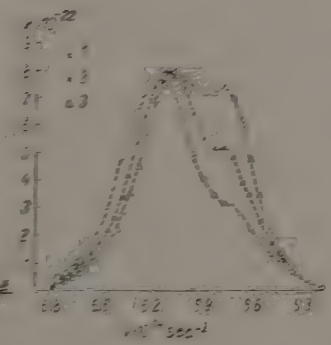

Fig. 11. Absorption of an aqueous solution of rhodamine for $C = 10^{-2}$ g/ml. 1- for 15°; 2- for 50°; for 90°.

It seems improbable that association is of importance in the case considered. In figures 10 and 11 are shown the temperature and concentration dependence of absorption in aqueous solutions of our rhodamine compound; in figure 12 is given the same information for aniline solutions. In the second case there are absolutely no indications of the appearance of the typical second maximum attributable to a dimer. There is a slight displacement of the maxima of curves 7, 8, 9, obtained by reflection, which may be attributed to the involved process of obtaining them from the approximations discussed previously. This is naturally a conclusive demonstration of the absence of association, which would have to be included, but which cannot be treated in the same fashion.

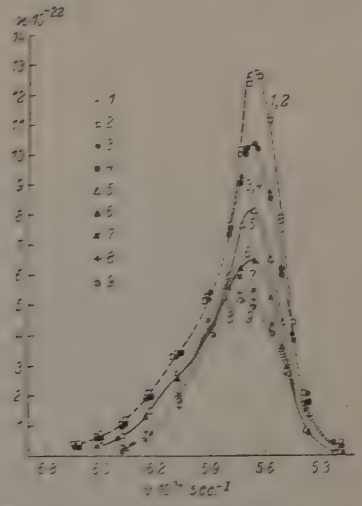

Fig. 12. Absorption of a solution of rhodamine 6G in aniline. 1- $C = 10^{-6}$ g/ml; t – 15°; 2- $C = 10^{-3}$ g/ml, t = 15°; 3- $C = 10^{-6}$ g/ml, t = 90°; 4- $C = 10^{-3}$ g/ml, t = 90°; 5- $C = 10^{-2}$ g/ml, t = 15°; 6- $C = 10^{-2}$ g/ml, t = 90°; 7- $C = 6 \cdot 10^{-2}$ g/ml, t = 15; 8- $C = 10^{-2}$ g/ml, t = 15°; 9- $C = 6.10^{-2}$ g/ml, t = 90.

It is also difficult to explain the reduction of f by means of surface effects; the dye would have to be the surface-active component [15, 16]. If, however, N_1 in the surface layer were to be greater than was assumed in the calculation, the correction introduced would further lower f.

Of our dyes, luminescence occurs in rhodamine; concentration quenching ensues for somewhat lower concentrations than in methyl alcohol and the other solvents [10]. On the other hand, it seems possible that for oscillators in excited and unexcited states, the quenching might become important for somewhat different separations (between the states).

In the transition from vapors or dilute solutions of the dyes to their (probably molecular) solid films, f decreases strongly, as a rule [6]. It is possible that the same effects are operative here as in our cases, but that their development is less pronounced. Incidentally the value of f for solid films of fuchsine practically coincides with our value of f for high concentrations.

In Davydov's theory the quantity B is proportional to the halfwidth of the absorption band. This is indeed found to be the case if we compare the values of B for small concentration calculated from Davydov's formulae with those obtained directly from the absorption measurements. For example, for nitrosodimethylaniline in concentration 10^{-5} we have respectively 1.77 and $0.9 \cdot 10^{-14}$ sec.$^{-1}$ and for rhodamine 0.93 and $0.45 \cdot 10^{-14}$ sec.$^{-1}$. However, for large concentrations, while B remains practically unchanged (for example in rhodamine) the half-width of the curve increases considerably (for $c = 6\ 10^{-2}$, $B = 1.00 \cdot 10^{-14}$ sec.$^{-1}$). This requires a more accurate physical interpretation of the parameter B.

The discussion given here of considerations

relative to the change in f requires many additional confirmations; the discussion is doubtless preliminary and in need of theoretical foundation and further experimental refinement. However, the very fact that f changes is itself of interest.

CONCLUSIONS

1. It has been shown possible to determine the optical constants of solutions of dyes at high concentrations in the region of an absorption band by the method of selective reflection.

2. The curves of absorption and reflection (and hence also dispersion) for a series of dyes of various classes in concentrated solutions and also for bromine, are described better by the formulae of Davydov for the case of strong interaction between the vibrations of the molecules of the solute and the solvent, than by the classical formulae for dispersion, corresponding to the case of an extremely weak interaction.

3. By applying the theory of Davydov values have been found for the oscillator strengths and electronic transition frequencies of a series of dyes. The values of the oscillator strengths are in general close to the corresponding quantities determined by other methods for different solvents. Thus one may assert that the theory is very firmly in agreement with experiment.

4. It has been shown that the oscillator strength decreases with increasing concentration in the region of intermolecular separation of 50-10 Å. It is proposed that this is due to coupling between the absorbing oscillators.

July 14, 1958

References

1. A. S. DAVYDOV: ZETF, 24, (2) 197, (1953)
2. I. S. GORBAN, A. A. SHISHLOVSKII: DAN USSR, 108, 210, (1956)
3. I. S. GORBAN: Dissertation, Kiev, 1955
4. L. D. DERKACHEVA: IAN USSR, FS, 20, 410, (1956) (See CTT Bulletin)
5. KH L. ARVAN: IAN USSR, FS, 20, 441, (1956) (See CTT Bulletin)
6. A. N. TERENIN: Fotokhimiia krasitelei (Photochemistry of dyes), Akad. Nauk Press, Len., Mos., 1947
7. Ch. FORSTER, KONIG: Zs. f. Elektrochem., 61, 344, (1957)
8. L. V. LEVSHIN, V. S. SUVOROV: OiS, 4, 678, (1958)
9. E. RABINOVITSCH, EPSTEIN: JACS, 63, 69, (1941); 77, 4197, (1956)
10. V. L.LEVSHIN: Fotoliuminestsenstiia tverdykh i zhidkikh veshchestv (Photoluminescence of solids and liquids) GTTL, Mos., 1951
11. T. P. KRAVETS: Absorbtsiia sveta v rastvorakh okrashennykh veshchestv (Light absorption in solution of colored substances) St. Petersburg, 1912
12. (Was omitted in Optika i Spektroskopiia)
13. J. A. GALT, M. L. WELSH: Can.,J. Phys., 35, 98 and 114, (1957)
14. P. P. FEOFILOV, I. G. FAERMAN: DAN USSR, 87, 931, (1952)
15. GIBBY, ADDISON: J. Chem. Soc., 119, (1936)
16. BLUE, SHTARK: Adsorbtsiia (Adsorption) GTTL, Mos., 1928

TOM VII, Vyp. 1 OPTIKA I SPEKTROSKOPIIA Iiul', 1959
VOL . VII, No. 1 OPTICS AND SPECTROSCOPY July, 1959

On the Kinetics of Photo- and Gamma- Luminescence in Certain Thallium Activated Alkali-Halide Crystals*

I. K. PLIAVIN'

The luminescence of activated alkali-halide crystals has long been studied and it has attracted particularly great attention recently because these crystals are being used in scintillation counters. Nevertheless, the kinetics of the short-time luminescence of these crystals has been investigated only slightly up to now. Only in recent years have several works [1, 2] appeared in which the duration of the short-time luminescence under the effect of high-energy particles or quanta has been studied.

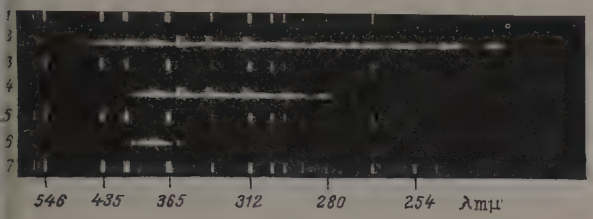

Figure 1. Spark spectrum (platinum electrodes). 1, 3, 5, 7 – spectrum of the PRK-2 mercury lamp; 2 – spark spectrum; 4 – spark spectrum through the UFS-1 filter; 6 – spark spectrum through an UFS-1 and WG-1 filter.

In order to clarify the kinetics of gamma-luminescence, it is very essential to study also the kinetics of photo-luminescence during excitation in activated absorption bands. In the case of photo-excitation in the band corresponding to the $^1S_0 - {}^3P_1$ transition in the Tl ion, the absorbed energy does not leave the luminescence center [4] and the kinetics of photo-excitation should be distinguished from the kinetics of gamma-excitation luminescence, when the energy arrives at the luminescence center by a complex path, by way of the host material. It was expected that certain hypotheses on the structure of the luminescence center and on the mechanism of energy transport from the host material to the activator could be made on the basis of data on the kinetics of photo-luminescence if the data on photo- and gamma-luminescence were compared.

METHOD

Co^{60} was used as the source of gamma-excitation and a short-time spark with a duration of 10^{-8} sec was the source of photo-excitation. The spark operated at a voltage of about 3500 V. A 10 megohm resistor was connected in series with the spark gap. Platinum wires were the spark electrodes. The spark spectrum (Fig. 1) is sufficiently intense in the 240-300 Mμ range where are the long-wavelength absorption bands of activated alkali-halide crystals. In order to estimate the duration of the exciting spark impulse, it was compared with gamma-scintillations in organic tolane and naphthalene crystals ($\tau = 1 \cdot 10^{-8}$ and $8 \cdot 10^{-8}$ sec, respectively, figure 2).

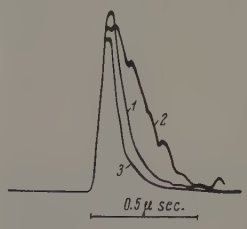

Figure 2. Oscillograms. 1 – spark impulse; 2 – gamma scintillation in naphthalene; 3 – gamma scintillation in tolane.

Both in the case of photo- and in the case of gamma-excitation, the luminescent pulses were investigated which occur in a given crystal upon the scattering of separate gamma quanta (i.e., separate Compton or photo electrons) or upon light absorption from separate spark impulses. In the majority of cases, the duration of the photo- and gamma-luminescence in alkali-halide crystals is in a region intermediate between the "fluorometric" ($10^{-8} - 10^{-9}$ sec) and the "τ-metric" ($10^{-5} - 10^{-1}$ sec). The apparatus (Fig. 3), consisting of an excitation source, a temperature chamber to cool or heat the crystals under investigation, a photo-multiplier (FEU-S or FEU-29), a pre-amplifier and amplifier (in the gamma-excitation case), a delay line which was a 700 M long RK-3 coaxial cable and a high-frequency OK-17M oscilloscope, was used herein to measure these durations.

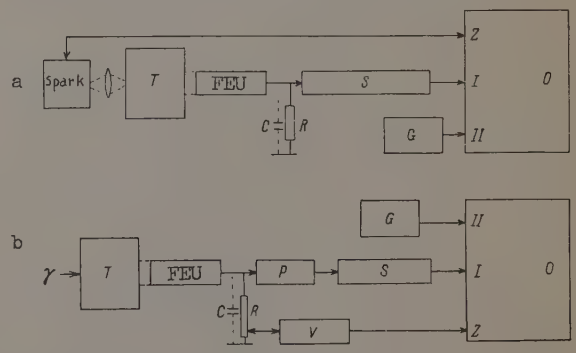

Figure 3. Block diagram: a – for photo excitation; b – for hard excitation.
T – temperature chamber; S – delay line; G – sine voltage generator; O – OK-17M oscilloscope; P – pre-amplifier; V – amplifier; R – load resistance; C – parasitic capacitance; I and II – inputs of the first and second beams; Z – sweep start input.

The resolving time of the apparatus was about $2 \cdot 10^{-8}$ sec. The photo-multiplier load resistance R was selected as large as possible but so that there would still be compliance with the inequality $RC \ll \tau$, where C is the parasitic capacitance, τ the time for the luminescence impulse to damp.

*Presented to the VII Conference on Luminescence in Moscow, June 1958.

The scintillations were photographed from the oscilloscope screen. The photo-scintillations obtained in KI-Tl at different temperatures are presented on figure 4 as an example.

Figure 4. Photo scintillations in KI-Tl for a – 30° C; b – 80° C; c – 120° C.

RESULTS OF THE MEASUREMENTS AND DISCUSSION

Using the above-mentioned method, the time-to-damp of the photo- and gamma-scintillations were investigated as a function of the crystal temperature (within +100 to -160° C limits) for NaI-Tl, KI-Tl, CsI-Tl during gamma-excitation. The decay law of the photo- and gamma-scintillations appeared to be exponential or could be represented (in the gamma excitation case) as the sum of exponentials within the limits of experimental error.

Photo excitation. It has been detected that the decay time of photo-scintillations for light excitation of the crystals being studied depends on the temperature in the long-wavelength absorption band of the activator (Tl) (figure 5, dashed curve). The decay time of the photo scintillations depends exponentially on the reciprocal of the temperature and $\ln \tau$ versus $\frac{1}{T}$, correspondingly is linear (figure 6, dashed lines).

The temperature change in decay time, observed in the experiment, cannot be explained by temperature quenching in the luminescence center since the luminescence quantum yield is constant for the majority of crystals under investigation in the temperature range in which the observations were made [5]. In order to explain the temperature dependence of the decay time which is observed, the assumption is made that there are two close-lying levels (levels 2 and 3) in the activator ion in the excited state between which the activator ions have an opportunity to be thermally redistributed during the lifetime of the excited state. The time change in the number of ions in these levels is given by the system:

$$(1)\quad \frac{dn_2}{dt} = n_3 p_3 \exp\left[-\frac{W}{kT}\right] - n_2 p_2 \exp\left[-\frac{W+\epsilon}{kT}\right] - n_2 f_{21},$$

$$\frac{dn_3}{dt} = n_2 p_2 \exp\left[-\frac{W+\epsilon}{kT}\right] - n_3 p_3 \exp\left[-\frac{W}{kT}\right] - n_3 f_{31},$$

where n_2, n_3 are the number of excited ions in the second and third levels; W is the activation energy of the radiationless transition $3 \rightarrow 2$; ϵ the energy spacing between the minimums of levels 2 and 3; p_2, p_3 the frequency factors of the thermal $2 \rightarrow 3$ and $3 \rightarrow 2$ transitions, respectively; f_{21}, f_{31} the probabilities of a radiative transition from levels 2 and 3 to the ground level 1.

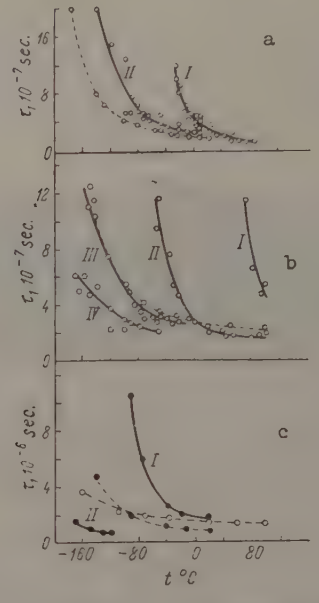

Figure 5. Decay time of photo and gamma scintillations as a function of temperature.

a – in NaI=Tl; b – in KI=Tl; c – in CsI=Tl; and KCl=Tl (circles for the visible radiation band). Solid curves–gamma excitation; dashed curves–photo excitation. I, II, III, IV - different decay components.

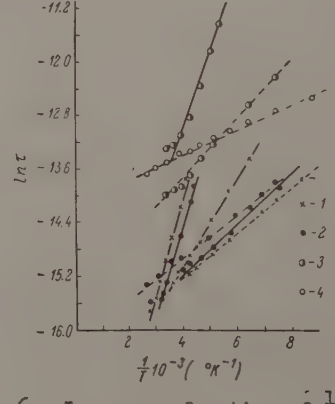

Figure 6. $\ln \tau$ as a function of $\frac{1}{T}$ for photo- and gamma- scintillations. The I and II decay components were used for gamma excitation in NaI=Tl (Fig. 5a); the II and III components in KI=Tl (Fig. 5b) and component I in CsI=Tl (Fig. 5c).

1 – NaI=Tl; 2 – KI=Tl; 3 – CsI=Tl; 4 – KCl=Tl; Solid curves – gamma excitation; dashed curves – photo excitation.

For the two extreme cases: 1) When the probability of the radiative transition f_{31} is so much larger than the probability of the thermal transitions between both excited levels (f_{31} is assumed to equal zero) under the initial conditions $n_3(0) = 0$, $n_2(0) = n_o$ (see [6]) and 2) when the probability of the radiative transition f_{31} is so much less than the probability of the thermal transitions (f_{21} is also assumed to be zero) under the initial conditions

$$\frac{n_2(0)}{n_3(0)} = \exp\left[-\frac{\epsilon}{kT}\right], \quad n_2(0) + n_3(0) = n_o \quad \text{or}$$

$$n_2(0) = n_o \quad \text{and} \quad n_3(0) = 0;$$

expressions describing the temporal behavior of the photo-scintillation intensity were obtained for the solution of the system (1). In the first case the photo-scintillation equals

$$(2) \qquad I(t) = n_3(t) f_{31} = \frac{n_o p_2 \exp\left[-\frac{W+\epsilon}{kT}\right]}{f_{31} - p_2 \exp\left[-\frac{W+\epsilon}{kT}\right]} \times$$

$$\times \left(\exp\left\{ [-p_2] \exp\left[-\frac{W+\epsilon}{kT}\right] \cdot t \right\} - \exp\left[-f_{31} \cdot t\right] \right);$$

and in the second case

$$(3) \qquad I(t) \approx n(t) = n_2(t) + n_3(t) = n_o \exp\left[-\frac{t}{\tau}\right],$$

where

$$\tau = \frac{1}{f_{31}} \left(\exp\left[\frac{\epsilon}{kT}\right] + 1 \right).$$

In the first case (formula 2), the photo-scintillation kinetics is a two-stage one: There is growth in the photo-scintillation which characterizes the lifetime of the excited level 3 and a decay characterizing the probability of the thermal transition $p_2 \exp\left[-\frac{W+\epsilon}{kT}\right]$.

Both the cases considered yield an exponential photo-scintillation decay law. In the first case the dependence of $\ln \tau$ on $\frac{1}{T}$ is linear and in the second case, nonlinear, but which can be considered linear when $\exp[\frac{\epsilon}{kT}]$ is large compared with unity. The experimental results obtained showed a linear dependence of $\ln \tau$ on $\frac{1}{T}$, but on this basis it is impossible to give the preference to the first or second case, since the experiments were made for such temperatures as when the $\ln \tau$ versus $\frac{1}{T}$ dependence is practically linear in both cases. In order to clarify which of the cases actually holds, it is necessary to investigate photo-scintillation at higher temperatures. On the basis of existing temperatures, it can only be said that real fluorescence (i. e., the spontaneous transition from the excited to the ground level) is not observed in the excitation of the crystals investigated in the long-wavelength absorption band of the activator. Apparently, thermal transitions between both close-lying excited levels occur prior to the act of radiation. It has not been excluded that both the excited levels hypothesized are two low levels of the triplet $^3P_0$, $^3P_1$, $^3P_2$, which are observed, for example, in the absorption spectra of mercury-like ions [7] in the lattices of alkali-halide crystals.

Gamma excitation. The growth and temperature-dependent decay (Fig. 5 and 6, solid curves) of gamma-scintillations are observed, which indicates that the kinetics of gamma luminescence, at least, is two stage. The expression (2) can be used to describe the temporal behavior of the gamma-scintillation intensity, under the conditions that the time of migration and localization of electrons and holes, which are formed in the crystal upon the scattering of gamma quanta, is negligibly small as compared with the duration of those processes which can be observed in experiment.

The expression (2) describes the experimentally observed gamma impulses well if $p_2 \exp[-\frac{W+\epsilon}{kT}] \gg f_{31}$. Then the time $\tau_1 = \frac{1}{p_2 \exp[-\frac{W+\epsilon}{kT}]}$, characterizing the temperature dependent process, will be manifest in conformance with experiment as the decay of gamma-scintillations.

According to (2), the time $\tau = \frac{1}{f_{31}}$, which is manifest in the growth of the pulse, should characterize the time of a radiative transition. This time could be estimated during gamma excitation in certain crystals in which the decay time of the radiative transition of the activator is larger than the resolving time of our apparatus. As should have been expected, the rise time of gamma scintillations agreed, within the limits of experimental error, with the life-time of the excited state of the activator as determined from the absorption coefficient by means of the Kravetz formula [8]:

$$(4) \qquad \frac{1}{\tau} = \left(\frac{3n}{n^2+2}\right)^2 \frac{g_1}{g_2} \frac{8\pi c}{\lambda^4} \frac{1}{N} \int_{\lambda_1}^{\lambda_2} \alpha(\lambda) d\lambda,$$

where n is the refractive coefficient of the host material; g_1, g_2 the statistical weights of the ground and excited levels (for a free ion); α the activator absorption coefficient in the host material; λ_m the maximum absorption wavelength; N the number of activator ions per cm^3.

For example, the rise time of gamma scintillation for NaI-Tl is $6 \cdot 10^{-8}$ sec, which agrees with the results obtained by a more high-frequency apparatus and the lifetime of the excited $^3P_1$ state of the Tl ion, determined from (4), is $4.5 \cdot 10^{-8}$ sec. Not observed in KI-Tl is a rise time of the gamma scintillations distinct from the rise time due to the apparatus, which is conceivable since the lifetime of the excited Tl^+ state in KI-Tl, calculated from (4), equals $2 \cdot 10^{-8}$ sec, which is also the resolving time of the installation.

The growth of gamma scintillations in a CsI-Tl crystal depends on temperature (Fig. 7). The growth time of gamma scintillations increases when the temperature is reduced below room temperature. Such an increase in the growth time with the reduction in temperature in these crystals apparently does not contradict the assumption that this time can characterize the lifetime of the excited state of the activator since it is known that the temperature quenching for a given transition in CsI-Tl crystals starts around room temperature [5].

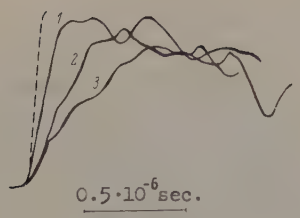

Figure 7. Oscillograms of the growth of gamma scintillations in CsI=Tl.
1 – 20° C; 2 – 10° C; 3 – 40° C (dashed curved marks the growth due to the apparatus).

The decay time of gamma scintillations in Tl-activated crystals depends strongly on the crystal temperature. The decay time increases as the temperature is reduced (Fig. 5, continuous curves), where the logarithm of the decay time depends linearly on the reciprocal of the temperature (Fig. 6, continuous lines). This indicates that the decay of gamma-scintillations characterizes some kind of thermal process which is manifest in the radiative transition of an activator ion. In the gamma excitation case, energy is absorbed in the host material and the temperature-dependent decay can be determined by the longest of the following processes: exciton migration, exciton lifetime in the localized state (if the exciton mechanism of energy transfer occurs in the crystals under consideration), electron and hole migration, thermal liberation of electrons and holes from trapping levels or thermal transitions of excited activator ions from shallow metastable levels (if an electron-hole mechanism of energy transfer occurs).

The decay of gamma scintillations apparently is not determined by the rate of electron and hole migration since the electron and hole lifetimes in the free state are several orders of magnitude less than the decay time of the gamma scintillation. It is also impossible to explain it by thermal liberation of electrons or holes from capture levels of the host material since, for example, no general capture level for short-time luminescence has been detected in investigations of gamma scintillations in NaI-Tl and NaI-In crystals. There is a similarity between photo and gamma scintillations. Thus, for example, the decay time of photo-scintillations is $2.4\cdot10^{-6}$ sec and the decay time of gamma scintillations is $2.4\cdot10^{-6}$ sec in NaI-In, $2.2\cdot10^{-7}$ and $3.3\cdot10^{-7}$ sec., respectively, in NaI-Tl, $2.8\cdot10^{-7}$ and $2.3\cdot10^{-7}$ sec in KI-Tl and $0.8\cdot10^{-6}$ and $1.6\cdot10^{-6}$ sec in CsI-Tl. As is seen, the decay times of photo and gamma scintillations have the same order of magnitude in each of these crystals.

Taking all the above into account as well as the experimentally established fact that the activator generates deep trapping levels for electrons [4, 9], the following mechanism is proposed for the kinetics of short-time gamma luminescence. Free electrons, arising in the scattering of a gamma quantum in a crystal, are captured by activator ions at the beginning. After the electrons have been trapped, the holes are trapped (Van Sciver [3] has expressed a similar viewpoint on energy transfer by a luminescent center on the basis of data on the radiation spectra during photo and gamma excitation), where excited ions are formed which are in a metastable state similar to the state detected during photo excitation in the activator absorption bands. Later the excited ions are thermally liberated from the metastable state and yield radiation whose duration is determined by the lifetime of the excited ions in the metastable levels.

Lushchik and his colleagues [10] expressed the assumption that the energy is transmitted to the luminescence center by using excitons in activated alkali-halide crystals during absorption in the host material. The kinetics of luminescence excited by light in exciton absorption bands was not investigated successfully in the present work and, consequently, there is still not sufficient data to verify this energy transfer mechanism.

It can only be said that the results obtained do not contradict the exciton mechanism of energy transport proposed in [10] for a singly-valent activator. According to our hypothesis, the luminescent center is excited during absorption in the host material by the successive trapping of an electron and hole (in the same center), where the time interval separating the trappings could not be detected experimentally. Consequently, all the deductions remain valid even if it is assumed that the energy is transmitted to the luminescent center not by the trapping of an electron and hole but by the production of energy, corresponding say to the energy of a localized exciton.

In conclusion, I am very grateful to M.D.Galanin, who supervised the present research. I am grateful too to A. M. Leontovich, I. K. Vitol for discussions and to N. V. Kostin for assistance with the measurements.

October 11, 1958

References

1. F. S. EBY, W. K. JENTSCHKE: Phys. Rev., 96, 911 (1954)
2. J. BONANOMI, J. ROSSEL: Helv. Phys. Acta, 25, 725 (1951) H. KNOEPFEL, L. LOEPFE, P. STOLL: Zs. f. Naturf., 12a, 348, (1957)
3. W. VAN SCIVER: IRE Trans. Nucl. Sci., NS-3, 39 (1956), Nucleonics, No. 4, 50, (1956)
4. CH. B. LUSHCHIK: Tr. IFAAN ESSR, (3), 3 (1955)
5. K. K. SHVARTS: Tr. IFA AN ESSR, (7), 153 (1958)
6. C. KLICK, D. DEXTER, G. RUSSELL: Phys. Rev., 100, 603, (1955)
7. N. E. LUSHCHIK, CH. B. LUSHCHIK: Tr. IFA AN ESSR, (6), 5, (1957)
8. M. D. GALANIN, E. D. CHIZHIKOVA: IAN USSR FS, 22, 1043 (1958) (See CTT Bulletin) B. S. NEPORENT, N. G. BAKHSHIEV: OiS, 5, 634, (1958)
9. V. L. LEVSHIN: IAN USSR FS, 9, 355 (1945) V. V. ANTONOV-ROMANOVSKII: IAN USSR, FS, 15, 637 (1951) L. M. SHAMOVSKII, L. M. RADIONOVA: DAN USSR, 92, 989, (1953) L. M. SHAMOVSKII, IU. N. ZHVANKO: OiS, 3, 267 (1957)
10. CH. B. LUSHCHIK, N. E. LUSHCHIK, G. G. LIID'IA, L. A. TEISS: Tr. IFAAN ESSR, No. 6, 63 (1957)

VII, Vyp 1
. VII, No.1

OPTIKA I SPEKTROSKOPIIA
OPTICS AND SPECTROSCOPY

Iiul', 1959
July, 1959

A Quantum Mechanical Calculation of the Luminescent Center in KCl-Tl

N. N. KRISTOFEL'

Abstract: With the help of a quantum mechanical method proposed earlier [1], adiabatic potentials and ectral characteristics have been calculated for the luminescent center in KCl-Tl. It is shown that the sults of the calculation are in good agreement with the experimental results.

In reference [1] a quantum mechanical method s proposed for the calculation of adiabatic poten- als for luminescent centers in alkali halide rstal-phosphors. Using this theory we analyzed - $^1S_0$ and $^3P_1$ states of the luminescent center KCl-Tl. Results of calculations for the $^1S_0$ ate were presented in [2]. In the present paper give the results for an excited state and the ctral characteristics of the center.

As a model for the center, we assume an activa- r ion to have replaced a cation of the host terial at a lattice site. The electrons on the tivator interact with local vibrations. The ber of ions which make up the center is defined the number of ions which take part in these local brations.

We use the so-called single-oscillator approxi- tions, which takes account only of the interactions the activator with totally symmetric local vibra- ons *. If it is not important to take into account e electronic symmetry of the activator, then from e requirement that the adiabatic potential be variant under all transformations of the symmetry oup of the center, it follows that changes in the uilibrium positions of the ions are due only to teractions of the activator with the totally sym- tric local vibrations. In the case of an excited ate, interactions with non-totally symmetric brations may also make contributions to changes the equilibrium positions of the ions (the analog the Jahn-Teller effect in molecules [3]). The gnitude of this contribution depends on the degree which the electron, because of the degeneracy of e excited state, takes part in the bonds forming quasi-molecule of the center. In alkali-halide rystal-phosphors, the change in the equilibrium sitions of the ions caused by the interaction of e activator with the non-totally symmetric local brations is, it seems, considerably less than the fect due to the totally symmetric vibration, and the first approximation it is permissible to use e single-oscillator approximation.

In the totally symmetric local vibrations are aken into account displacements of the activator's earest neighbors (q) and the next-nearest cations f the host lattice [$q^+ = \alpha_m \left(\frac{M}{M_+}\right)^{\frac{1}{2}} q$, where the damping factor" α_m is determined from the require- ent of an absolute minimum in the adiabatic poten- al for the case of fixed nuclei].

For the wave-function of the 6p-electron of Tl^+ the excited state we chose

$$\psi_{6p}(\vec{r}) = \frac{f_{6p}(r)}{r} \cdot \frac{1}{\sqrt{3}} \left(K_{\Gamma_4 1}^{-1} + K_{\Gamma_4 1}^{0} + K_{\Gamma_4 1}^{+1} \right),$$

where K are the appropriate cubic harmonics [4]. A table of the functions $f_{6p}(r)$, computed taking account of the deformation effect of the field of a point crystal, were kindly provided by T. L. Gutman [5].

A calculation shows that when the activator is excited there is a rapid growth in those contributions to its interaction energy with the rest of the lattice (W_1) which correspond in sign to forces of attraction; the primary contribution is an increase in the exchange energy of the electrons on Tl^+ and Cl^-.

Table 1

State	W_M	$\frac{1}{6} W_{e.p.}$	$\frac{1}{6} W_{ex}$	$\frac{1}{6} W_S$	W_V	W_1
$^1S_0$	−0.2940	−0.0079	−0.0322	0.0548	−0.0317	−0.2375
$^3P_1$	−0.2940	−0.0130	−0.0413	0.0577	−0.0486	−0.3222

In table 1 are listed the contributions to the interaction energy of Tl^+ with the rest of the lattice for q=0 for the $^1S_0$ and $^3P_1$ states (in atomic units).

W_M is the Madelung energy; $W_{e.p.}$ is the energy of the electrostatic correction for the lack of complete directionality of the ions; W_S is the so-called S-energy which comes from the orthogonalization of the one-electron wave functions of the various ions in the crystal; W_{ex} is the exchange energy and W_V is the Van der Waal's energy.

In table 2 we give the calculated values of the quantities which determine the adiabatic potential for the $^3P_1$ state. For an excited Tl^+ the local vibration falls off rather more slowly; however the increase in α_m is so negligible that the effective mass M of the vibrating system remains practically unchanged.

Excitation of the Tl^+ leads primarily to an increase in the forces of attraction and the equilibrium separation between Tl^+ and Cl^- turns out to be 0.065Å smaller than in pure KCl. At the same time the K^+ move closer to the Tl^+ ions. Their displacement is considerably smaller. From this it follows that at a separation of the order of 4a-5a from Tl^+ (a is the separation between

* The symmetry of the center is determined by e symmetries of the basis of the phosphor and the ptical electrons of the activator.

neighboring atoms of different type), the ions of the host lattice may be considered not to take part in the local vibrations. For the ground state $q_0 = +0.093$Å and the new equilibrium separation between Tl^+ and Cl^- is equal to 3.24Å, which is very near to the magnitude of the separation (3.22Å) between the same ions in TlCl (considered to have a structure of the NaCl type).

Table 2

α_m	q_0	q_0^+	ω_0	M	$\frac{1}{2}M\omega_0^2 q_0^2$	W
0.434	−0.065Å	−0.027Å	$2.93\cdot10^{13}$ sec^{-1}	$6M_- \cdot 1.73$	0.071 eV	−53.20 eV

The frequency of the totally symmetric vibration ω_0 depends on the electronic state of the activator, and for the $^3P_1$ state it is considerably smaller.

The quantity $-\frac{1}{2}M\omega_0^2 q_0^2$ (cf. Table 2) determines the "Stokeslosses during activation", and W is the total internal energy of the Tl^+, W_0 and W_1.

If we neglect the change in the internal energies of the ions in the crystal, the substitution energy to replace a K^+ at a KCl lattice site by Tl^+ in the ground state is equal to

$$E = W_1(Tl^+) - W_1(K^+) - \tfrac{1}{2}M\omega_0^2 q_0^2 = 0.43\,(eV).$$

In order to test the quality of the calculation of the interaction between the ions K^+ and Cl^-, we calculated the bond energies and equilibrium separation between nearest neighbors in KCl. The values obtained were $U = -164.6 \frac{Kcal}{mole}$, $a = 3.25$Å; these values are close to the experimental values of $-167.8 \frac{kcal}{mole}$ and 3.145Å. The separation between the minima of the adiabatic potentials of the $^1S_0$ and $^3P_1$ states includes the difference between the appropriate internal energies of the ions. This difference, calculated with the help of wave functions for Tl^+ which take account of the effect of the crystalline field, turns out to be 0.05 eV larger than for the free ion (6.49 eV). The internal energy of the cation itself is, in the crystal, lowered when account is taken of the deformation effect of the point lattice on the wave function of this ion.

For the adiabatic potentials of the $^1S_0$ and $^3P_1$ state of the luminescent center in KCl-Tl we have *

$$^1S_0\, I(q) = 26.4(q-0.093)^2$$

$$^3P_1\, I^*(q) = 4.39 + 16.7(q+0.065)^2$$

* The zero of energy is chosen so that $I_0 = 0$.

The form of $I(q)$ and $I^*(q)$ is shown in figure 1.

The transition energy equals

$$E(q) = 4.23 + 7.08q - 9.7q^2.$$

The absorption and emission spectra in the semi-classical approximation are determined from the for (kT $\gg \hbar\omega_0$)** [6]

$$P_K(E) = A(7.08 - 19.4q)^{-1} \exp\left[-\frac{26.4}{kT}(q-0.093)^2\right]_{q=q(E)},$$

$$P_I(E) = A'(7.08 - 19.4q)^{-1} \exp\left[-\frac{16.7}{kT}(q+0.065)^2\right]_{q=q(E)}$$

where A and A' are normalization constants $\left(\int P(E)dE = 1\right)$.

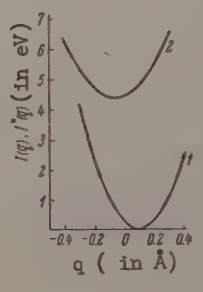

Figure 1. Form of the adiabatic potentials I(q) for the luminescent center in KCl-Tl. Curve 1 is for I(q) ($^1S_0$ state); curve 2 is I*(q) ($^3P_1$ state).

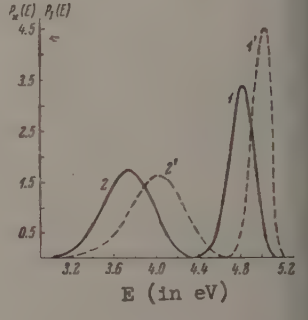

Figure 2. The experimental (dotted line) and the calculated (solid line) spectra of the luminescent center in KCl-Tl. 1 and 1' are the $^1S_0 \rightarrow {}^3P_1$ transition; 2 and 2' are the $^3P_1 \rightarrow {}^1S_0$ transition.

The solid curve in figure 2 shows the calculated spectra for the center, and the dotted line the experimental results from [8]. For $P_K(E)$ the vertical axis is laid off in units of $\kappa(\nu)/\nu$ and for $P_I(E)$ in units of $I(\nu)\,\nu^3$).

The theoretical spectrum agrees well with the experimental results. Both the emission and the absorption spectra fall off somewhat more slowly on the long wavelength side than do the experimental spectra (this is due to the fact that $\omega_0 > \omega_0^*$), which corresponds to experiment. In Table 3 we give the calculated spectral characteristics of the luminescent center in KCl-Tl which we have calculated, along with the experimental data [7].

For all of the characteristics listed the agreement between theory and experiment is good.

The quantity ρ (cf. Table 3) is the so-called "coefficient of compression" [7]. Having $\rho > 1$ is due to the overwhelming increase in the energy corresponding to the forces of attraction in W_1 duri

** T = 298° K.

e excitation of Tl^+, i.e. to "static" inter-
tion. $E_m^K - E_m^I$ gives the Stokes losses and
$- I_0$ the energy of the so-called pure electron
ansition. *

Table 3

	E_m^K (eV)	E_m^I (eV)	ρ	$E_m^K - E_m^I$	δ^K (eV)	δ^I (eV)	δ^I / δ^K	$\gamma = (\omega_0^*/\omega_0)^2$	$I_0^* - I_0$(eV)
eory:	4.80	3.74	1.35	1.06	0.27	0.55	2.04	1.59	4.39
periment:	5.02	4.06	1.29	0.96	0.23	0.51	2.22	1.70	4.58

The half-widths of the absorption and emission ectra (δ^K, δ^I) which we obtained are somewhat o large. This points to the possibility of the erestimation of ω_o and ω_o^* by a certain amount in our calculation.

Theory gives $q_0^* - q_0 < 0$, which is supported experiments under multilateral compression [10,11].

In the homologous series of thallous phosphors th hosts like KCl → KBr → KI one must expect always increasing relative role for the attractive rces during activator excitation. This should ad to a displacement of the spectral bands in the ng wavelength direction, as is also observed in periment [12].

We believe that the results of this quantum chanical calculation firmly support the model we ve taken for the luminescent center in KCl-Tl e general agreement of theory and experiment is od, although the numerical values we obtained ould not be taken as absolute. The value of the uantum mechanical theory lies in the possibility of more detailed orientation for the theory of lumi-escent centers. The conclusions of the semi-mpirical method of Williams [13] are in general upported by our results.

The results of [13] lead to smaller values of ω_o and ω_o^* than were obtained in the present work.

The displacement of the equilibrium positions of the ions in the excited state obtained by Williams seem to us unjustifiably large. It would seem that this is indicated also by the results in [11] where it was shown that the calculation of the displacement of the absorption spectrum with pressure (calculated with the value of $(q_o^* - q_o)$ from [13]) turns out to be about two times larger than the experimental displacement. It is impossible to explain this divergence in terms of an inequality of the effective surface areas of the center in the $^1S_0$ and $^3P_1$ states, since according to our estimates the effective area in the excited state is only slightly larger [14].

A more detailed article will be published in the Trudy IFA AN, ESSR.

The author is deeply grateful to M. I. Petrashen' for guidance with the work and constant interest in it, and also to K. K. Rebane and Ch. B. Lushchik for a number of useful suggestions and observations.

Jan. 10, 1959

REFERENCES

1. N. N. KRISTOFEL': Tr. IFA AN, ESSR, N 7,85 (1958)
2. N. N. KRISTOFEL': Mat. of the VIIth Conference on Luminescence, 1958
3. H. JAHN, E. TELLER: Proc. Roy. Soc., A161, 220, (1937); U. OPIX, M. PRYCE: Proc. Roy. Soc., A238, 425, (1957)
4. F. van der LAGE, H. BETHE: Phys. Rev., 71, 612, (1947)
5. M. I. PETRASHEN', T. L. GUTMAN: IAN USSR, FS 22, 668, (1958) (See CTT Bulletin)
6. M. LAX: J. Chem. Phys., 20, 1753, (1952)
7. N. E. LUSHCHIK, CH. B. LUSHCHIK: Tr. IFA AN, ESSR No. 6, 5, (1957)
8. CH. B. LUSHCHIK, N. E. LUSHCHIK, K. K. SHVARTS: Tr. IFA AN, ESSR No. 8, 3, (1958)
9. K. K. SHVARTS: Tr. IFA AN, ESSR, No. 7, 153, (1958)
10. P. JOHNSON, F. WILLIAMS: Phys. Rev., 95, 69, (1954)
11. R. EPPLER, H. DRICKAMER: J. Phys. Chem. Solids, 6, 180, (1958)
12. F. D. KLEMENT: Tr. IFA AN, ESSR, No. 1, 3, (1955)
13. F. WILLIAMS: J. Chem. Phys., 19, 457, (1951)
14. N. N. KRISTOFEL': Tr. IFA AN, ESSR, No. 10, (1959)

* Extrapolating our potential curves to their intersection one may roughly estimate the activation energy for thermal quenching to be $E_T = 1.8$ eV. Experiment gives $E_T = 1.3$ eV [9].

TOM VII, Vyp. 1 OPTIKA I SPEKTROSKOPIIA Iiul', 1959
VOL. VII, No. 1 OPTICS AND SPECTROSCOPY July, 1959

The Influence of Temperature on Electromagnetic Wave Propagation in Crystals in which Excitons Occur

M. S. BRODIN AND A. F. LUBCHENKO

Abstract: An investigation has been made of the equations which determine the indices of refraction (n) and absorption (κ) of light for crystals in which excitons may occur, for the case of weak coupling between the exciton and the lattice vibrations [1-3]. It is shown that with an increase in temperature there is a tendency for these equations to go over into the well-known equations for n and κ of classical crystal-optics [4]. An increase in the effective mass of the exciton and also an increase in exciton-phonon coupling reinforce this tendency. Hence one may expect that with an increase in temperature, effective mass, and strength of the exciton-phonon interaction, the divergence between the experimental curves of dispersion and the curves as calculated according to classical optics would be reduced.

Dispersion curves for several crystals have been calculated from the Kramers-Kronig relations [5] and comparison has been made with experimental curves. It is shown that for the crystals investigated, the agreement improves as the temperature is raised. It is also shown that for a fixed temperature the agreement improves as one moves from the "pure" electron absorption band to the nearest electron-vibration bands.

1. EQUATIONS DEFINING THE INDICES OF REFRACTION AND ABSORPTION

In the works of Davydov and Pekar [6,7] it was shown that the formulae determining the dispersion (n) and absorption (κ) curves in the excitation of exciton states differ from the corresponding formulae of classical crystal-optics. However in reference [6], a calculation of n and κ was made for linear chains in the region of exciton absorption, and in reference [7] the calculation was made for the region far from exciton absorption ($\kappa = 0$) and for $T = 0$. In the same connection, references [1-3] developed a method of calculating the indices of refraction and absorption and the optical activity for crystals of arbitrary symmetry at $T \neq 0$ and for an arbitrary value of κ, but for the case of a weak exciton-phonon coupling. An analysis carried out on the equations obtained shows that under certain conditions [2] the solutions of these equations correspond with the solutions of classical crystal-optics (the number of waves propagating in the crystal is the same as in the classical theory), and in reference [1] it was shown that for negative effective mass of the exciton, generally speaking, even for very low temperatures the equations determining n and κ correspond with the classical equations.

In the present paper, we investigate the behavior of the equations derived in [1-3] for changes in the magnitude of the exciton effective mass, the strength of the exciton-phonon interaction, and the temperature of the crystal. Comparison is also made between the dispersion curves calculated from the Kramers-Kronig relations and the experimental curves.

The equations determining the absorption coefficients and the indices of refraction of an electromagnetic wave in a crystal in the region of exciton absorption have the form *

$$(1) \qquad (n-i\kappa)^2\{\vec{E}_0-\vec{s}(\vec{s}\vec{E}_0)\} = \epsilon\vec{E}_0 + \frac{d\chi\vec{E}_0(n^2-\kappa^2-g+\theta+i\rho)}{(n^2-\kappa^2-g+\theta)^2+\rho^2},$$

where $\vec{E}_0$ is the amplitude of the electromagnetic field intensity in the crystal; $\vec{s}$ is a unit vector along the wave normal; ϵ is the tensor dielectric susceptibility, due to virtual transitions to all other states except the exciton state under consideration; χ is a tensor quantity which takes account of the difference between the transverse field acting on the molecule and the average macroscopic field; d is a quantity proportional to the dyad formed from the dipole moments of the cell $g = \frac{2M_s c^2}{\hbar\omega}\left(1-\frac{U}{\hbar\omega}\right)$, M_s is the effective mass of the exciton in the direction $\vec{s}$, c and ω are, respectively the velocity of light in a vacuum and the frequency, U is the energy difference between the ground and excited (exciton) states of the crystal when the reduced wave vector $\vec{k}$ is equal to zero. The dimensionless quantity ρ is proportional to γ_1. This latter quantity is the sum of two terms; one of these (γ_1') comes from the effect of the interaction of the exciton with the lattice vibrations (according to [1] this term is 0 beyond the region of exciton light absorption), the second term (γ_1'') comes from the finite radiation lifetime of the excited state of the molecule and is always different from zero. In the region of exciton absorption $\gamma_1' \gg \gamma_1''$, hence the character of the curves of n and κ is completely determined by the quantity γ_1', which, as has been shown in [1], increases with increasing temperature T, magnitude of the effective mass $M_{\vec{s}}$ and strength of the exciton-phonon interaction.

Let us consider the solution of (1) far from the region of exciton absorption where $g \gg n^2$ and one may put $\rho = 0$. Under these conditions, equations (1) go over into the well-known equations of classical crystal optics

$$n^2\{\vec{E}_0-\vec{s}(\vec{s}\vec{E}_0)\} = \epsilon\vec{E}_0 + \frac{d\chi\vec{E}_0}{g},$$

determining the changes in the index of refraction far from the region of absorption [7]. As one approaches the absorption region the quantities n^2 and g become comparable (or even $n^2 > g$); in this case, for small values of ρ, it is already impossible to neglect the square of the index of refraction in the denominator of (1). However, the equation then derived from (1) for the determination of n^2 will be of higher degree than the second, and hence for a given direction of propagation of

* We are using the notation of ref. [2].

e light wave $\vec{s}$ there may be in general more than
p solutions $n^2 > 0$, to which there correspond more
an two plane waves propagating simultaneously in
e crystal. Of course the dependence of the index
refraction on the frequency of the incident light
ll not be determined by the classical dispersion
rmula, but instead by a more complicated expression
].

In the region of exciton absorption for small
lues of ρ (whose magnitude, as was already pointed
t, grows with increases in the temperature, effec-
ve mass, and strength of the exciton-phonon inter-
tion) we may also not neglect n^2 in comparison
g and ρ, and also in this region the equation
r n^2 will be higher than the second degree.

At high temperatures when the quantity ρ
comes important, the square of the index of refrac-
on may be neglected in equations (1); in this case
) goes over into the equations of classical crystal-
tics for the determination of $n(\omega)$ and $\kappa(\omega)$. In
neral it is impossible to state the temperatures at
ich this changeover will have taken place. They
ll be different for different crystals; however for
ry weak exciton-phonon interactions these tempera-
res may lie above the melting point of the crystal.
us in general one may speak only of a tendency
r the system (1) to go over into the equations of
assical optics at high temperatures.

Furthermore if one realizes that γ_1' (and hence
also) increases with increasing exciton effective
ss, then it becomes understandable that for other
uilibrium conditions the changeover of the system
) to the classical equations takes place first of
l for those exciton absorption bands to which cor-
spond the excitons with a high effective mass.
nce in this case, if the excitons with large effec-
ve mass correspond to electron-vibrational excita-
ons rather than to purely electronic excitations,
en the transition of (1) into the classical equa-
ons must take place, generally speaking, at lower
mperatures for the frequencies which correspond
o electron-vibrational bands.

Thus one may expect that with an increase in
e temperature, effective mass M_s and the strength
f the exciton-phonon coupling, the disparity between
e experimental dispersion curves and the curves
alculated from classical formulae will decrease.

COMPARISON OF THE CALCULATIONS AND EXPERIMENT.

It is very difficult to obtain direct experi-
ental verification of the qualitative deductions of
e above calculation, and hence in the present
rticle we will take as an indication of the agree-
ent of our calculations with experiment the corres-
ondence or lack of correspondence between the dis-
ersion curves obtained from the Kramers-Kronig rela-
ions and from experiment. The Kramers-Kronig dis-
ersion relations follow from very general considera-
ions of electrodynamics and are quite universally
alid within the limits of classical electrodynamics.
ritten for the case of a relation between optical
uantities the Kramers-Kronig relation has the fol-
owing form

$$n^2(\omega)-\kappa^2(\omega)-1=\frac{4}{\pi}\int_0^\infty \frac{xn(x)\kappa(x)}{x^2-\omega^2}\,dx, \qquad (2)$$

where n is the index of refraction, and κ is the coefficient of absorption. If the curves for $n(\omega)$, and $\kappa(\omega)$ may be written as sums of Gaussian functions $A_i \exp\left\{-\frac{(\nu-\nu_i)}{\delta^2}\right\}$, then as has been shown earlier [8, 9] formula (2) may be written in a more convenient form for comparison with experiment

$$n^2(\nu)-\kappa^2(\nu)-1=-\frac{4}{\sqrt{\pi}}\sum_i A_i W\left(\frac{\nu-\nu_i}{\delta_i}\right), \qquad (3)$$

where

$$W(z)=\exp(-z^2)\int_0^z \exp(x^2)\,dx.$$

When the results calculated from this formula agree with experiment one may conclude that in this region of the spectrum the classical conception of the index of refraction and its relationship to absorption are valid for the crystal. Disagreement indicates a more complicated optical picture.

Equation (2) has already been verified experimentally for a series of molecular crystals [8, 9]. In comparing the calculations with experiment [8], important deviations were revealed [9]. In reference [9] this deviation and its temperature dependence were illustrated for the case of the 1, 2-benzanthracene crystal (in the region of its lowest electronic transition bands), and also for other crystals in the region of their lowest "pure" electron bands. In the present work anthracene and stilbene, which were studied earlier, have been chosen as illustrations. The experimental material necessary for comparison with the Kramers-Kronig relations, i. e. the dispersion and absorption curves, were obtained earlier for room temperature and some lower temperatures by one of the authors [8, 10]. We have added to the material on anthracene the results of measurements at 360° K. Thus for the case of anthracene it is possible to make calculations with (2) at four temperatures: 20, 80, 290, and 360° K.

The method of measuring the absorption and dispersion curves was the same as in the previous papers [8, 9] i. e. the dispersion curves were measured by an interferometric method, and the absorption curves by the method of photoelectric photometry. For measurements at elevated temperatures the crystal section, pressed between two plane parallel quartz slabs, was placed in a circular oven which was heated by means of an electric current. The oven containing the crystal was placed between the mirrors of the interferometer or else put in the system for measuring the absorption curves. The temperature of the crystal was measured with a thermocouple. As has already been mentioned the crystal of anthracene was heated to 360° K. in our experiments. At this temperature and with the arrangement described, the crystal was undamaged during the experiment, which lasted 30-40 minutes on the average. It was dangerous to take measurements at higher temperatures since during the experiment the crystal began to deteriorate noticeably and at the same time the accuracy of the measurements fell sharply. Measurements were made with polarized light. An analysis of the

errors in the determination of $n(\nu)$ and $\kappa(\nu)$ is given in [9].

We now turn to a comparison of the experimental dispersion curves with those calculated from the Kramers-Kronig formula.

Anthracene. We will consider only the b-component of the spectrum of the anthracene crystal, whose b-axis is monoclinic, since from considerations of symmetry it is only to this component that one may meaningfully apply the Kramers-Kronig relation. The absorption curves at 290 and 20°K. and also the dispersion curves at 20°K. are given in [10]. The dispersion curves for 290 and 360°K. are taken from [11]. The curve for $n^2(\nu)$ in the interval 24000-28000 cm^{-1}, obtained during the present work, is given in figure 1 (curve 1). In the same figure we also present the curve for $n^2(\nu)$ calculated from formula (3) (curve 2). This latter curve includes a contribution to n^2 which is made by the bands of the first electron-vibrational transition being analyzed due to the swing of the dispersion curves within these bands. More remote transitions have practically no influence on the magnitude of the swing (range of variation) of the dispersion curves but rather lead to a parallel displacement of the whole curve. We have not taken account of this displacement here, and hence the scales of the experimental and calculated curves in figure 1 are displaced correspondingly.

If, as was done in [9], we take as a measure of the disparity between formula (2) and the experimental data for a given band the ratio of the square of the range of n^2 as measured and as calculated from (2), i.e. $\frac{\Delta n^2_{exp.}(\nu)}{\Delta n^2_{theory}(\nu)}$, then for the three principal bands we obtain the following values for k.

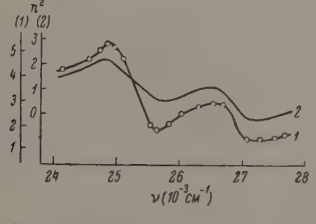

Figure 1. Temperature dependence in $n^2(\nu)$ for anthracene in the 24000–28000 cm^{-1} range at 360° K. —— 1 - experimental curve. 2 - curve calculated from formula (3). (1) - the scale for curve 1. (2) - the scale for curve 2.

T (in °K)	Band		
	I	II	III
20	6.0±1.2	4.7±0.94	2.0±0.4
80	3.40±0.68	1.80±0.36	1.20±0.24
290	2.50±0.50	1.40±0.28	~1.0
363	1.97±0.39	1.40±0.28	~1.0

The numbers I, II, and III, for the bands designate respectively, the first purely electronic transition and the following two principal electron-vibrational transitions (for T = 20°K, ν_I = 25 420 cm^{-1}, ν_{II} = 26 800 cm^{-1}, ν_{III} = 28 175 cm^{-1}).

The temperature dependence of k is easily seen from the above data. It is easy to note that k decreases as the transition is made to the electron-vibrational bands. The result obtained at T = 360° confirms the tendency noted in reference [9] for k to decrease with increasing temperature. For the bands labeled I, k decrease from 6 to 2 in the temperature interval considered. If we extrapolate the data obtained for the bands I to the value k = 1, then the corresponding temperature will be close to the melting point (of the order of 200° C.). Only at such a high temperature does the Kramers-Kronig relation correspond to experiment for the spectral interval under consideration. The disparity decreases significantly for II and even more so for the principal vibrational bands III. Thus for bands III, k is close to 1 even at liquid nitrogen temperature.

Stilbene. We investigated the N_p-component of the spectrum of crystalline stilbene; the corresponding experimental material is given in [8]. Comparison with formula (3) was made over the whole region of the first electronic transition (the frequency ν equals 29000 – 35000 cm^{-1}), for temperatures of 20, 80, and 290°K. As illustration, in figure 2, we give the experimental (1) and calculated (2) curves of $n^2(\nu)$ for 20° K. (the scales, as in figure 1, are displaced relative to one another).*

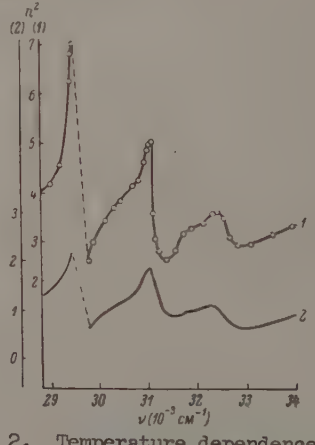

Figure 2. Temperature dependence in $n^2(\nu)$ for stilbene in the 29000 – 34000 cm^{-1} range at 20°K. 1-experimental curve. 2-curve calculated from formula (3). (1)-the scale for curve 1. (2)-the scale for curve 2.

* In order not to complicate the figure, the fine structure of the $n^2(\nu)$ curves is omitted – this fine structure is due to the corresponding fine structure of the first strong absorption band (ν = 29660 cm^{-1}) – and hence the curves in figure 2 are dotted for this band in the region of the extrema of n^2.

The difference in the range of the two curves obvious from the figure. For the three fundamental bands at the three temperatures used we tained the following values of k:

T (n °K)	Band I	Band II	Band III
20	3.60±0.70	2.50±0.50	2.0±0.4
80	2.70±0.54	1.70± 0.34	~1.0
290	~1.0	~1.0	~1.0

At 20°K the maxima of the bands I – III cur at the following frequencies respectively: 660, 31300, and 32700 cm^{-1}.

It is clear that the tendency for k to change th temperature and frequency is the same here as the case of anthracene. The distinctive characristic of stilbene lies in the agreement between e experimental and theoretical dispersion curves room temperature.

The experimental results here obtained are in greement with the results of our calculations. As increases, ρ increases, and in the limiting se equations (1) go over into the equations of lassical optics. In this case the Kramers-Kronig elations should agree with experiment. The magnide of the corresponding temperature depends on e characteristics of the material and in part, as s pointed out above, on the strength of the xciton coupling with the phonons. The stronger is coupling, the lower the limiting temperature. was shown in Table 2, for the case of stilbene is temperature coincides with room temperature. r anthracene, it is near the melting point. dging from the temperature dependence of the absorption bands, particularly the band corresponding to urely electronic transitions, the exciton-phonon upling must be particularly strong, as was shown n [8]. The nature of the temperature change in the hape of the absorption band for anthracene leads e to assume that in this case the coupling is onsiderably weaker.

With regard to the change in k with the frequency of the band there is also qualitative agreement with the results obtained in section 1, if one assumes that the effective mass of the exciton for the purely electronic bands is smaller than for the electron-vibrational bands and that for the latter the effective mass increases with increasing order of the vibrational band.

It is necessary to point out that for the case of 1, 2-benzanthracene [7], in the region of the first few principal bands of its ultraviolet absorption spectrum (25000 – 30000 cm^{-1}) at low temperatures, k differs from 1 and is the same for all of these bands. It is possible that this is related to an overlap in the indicated region of two different electronic transitions [12, 13], whose effective exciton masses are different.

The above example indicates that the peculiarities examined in this work are complicated and depend on the specific characteristics of each particular material; this must be kept in mind when comparing theory with experiment.

In conclusion we express our thanks to A. F. Prikhot'ko and A. S. Davydov for valuable discussions.

July 23, 1958

References

1. A. S. DAVYDOV, A. F. LUBCHENKO: ZETF 35, 1492, (1958) (See Sov. Physics JETP)
2. A. F. LUBCHENKO: UFZ 3, 575, (1958)
3. A. F. LUBCHENKO: OiS 5, 404, (1958)
4. M. BORN: Optics, DNTVU, Khar'kov 1937
5. L. D. LANDAU, E. M. LIFSHITZ: Elektrodinamika sploshnykh sred, GITTL, 1957
6. A. S. DAVYDOV: Tr. IF AN UKR SSR No.3, 100, (1952)
7. S. I. PEKAR: ZETF 33, 1022, (1957) (See: JETP)
8. M. S. BRODIN, A. F. PRIKHOT'KO: UFZ 3, 79, (1958)
9. M. S. BRODIN, A. F. PRIKHOT'KO, M. S. SOSKIN: OiS (in Press)
10. M. S. BRODIN, A. F. PRIKHOT'KO: OiS 2, 448, (1957)
11. L. IU. EICHIS: THESIS. Kiev 1950.
12. C. SANDORYA, R. N. JONES: Canad. J. Chem., 34, 888, (1956)
13. M. S. BRODIN, M. S. SOSKIN: OiS (in Press)

TOM VII, Vyp. 1 OPTIKA I SPEKTROSKOPIIA Iiul', 1959
VOL. VII, No. 1 OPTICS AND SPECTROSCOPY July, 1959

Determination of the Luminescent Energy Yield of Plastic Scintillators under the Action of γ-Rays

I. IA. BREIDO, IU. A. TSIRLIN AND L. N. SHISHOVA

The fundamental characteristic of a scintillator is its luminescent energy yield, i.e. its efficiency in transforming incident radiation into light energy. In practice, however, it is the "technical efficiency" which is usually measured; this is lower than the true ("physical") efficiency due to absorption of light by the scintillator itself and by the reflectors which are used to increase the amount of light absorbed in the phosphor. Very few papers have been concerned with a direct determination of the luminescent energy yield of a scintillator. Usually what is investigated is the energy yield of a given scintillator relative to that of a certain "selected" scintillator which is taken as the unit of measurement [usually anthracene; sometimes stilbene or NaI (Tl)].

The disparity between the data of various authors investigating a given scintillator may be explained by the differences in the properties of the "selected" scintillators which they have chosen. There is considerable interest in the direct determination of the luminescent energy yield of a given scintillator.

In the present paper the energy yield of γ-luminescence is measured for a scintillator composed of a 2% solution of terphenyl and 0.15% POPOP in polystyrene,* which will be referred to henceforth as polystyrene. The energy yield was studied for scintillation due to electrons from γ-rays of Cs^{137}. To determine the energy yield we analyzed the pulse heights from a scintillation counter consisting of a FEU-29 photomultiplier to whose photocathode a polished cylindrical scintillator (d=30 mm., h = 40 mm.) was affixed with Vaseline jelly (for optical contact). The following formula was used for the magnitude of the pulse at the output of the counter**:

$$V_{out} = \frac{E_k \eta \alpha \bar{C}_\Phi M e k}{\epsilon c}, \quad (1)$$

E_k is the energy of the primary radiation (in this case Compton electrons), ϵ is the photon energy (of the scintillation light), α is the light gathering coefficient, C_Φ is the average photo-efficiency of the photocathode of the FEU for the conditions of the experiment, e is the electronic charge, c is the input capacitance of the preamplifer (or of the anode of the FEU), k is the electronic amplification factor of the amplifier.

1. DETERMINATION OF ε

The value of ϵ was determined by averaging the emission spectrum of the scintillator. We found $\lambda = 430$ mμ, $\epsilon = 2.88$ eV.

2. DETERMINATION OF $\bar{C}_\Phi$

To determine $\bar{C}_\Phi$, use was made of the sensitivity curves of the FEU photo-cathode $C_{\Phi\lambda}$, obtained (in relative units) by illuminating the photo-cathode with light from a monochromator. Independently, the efficiency of the photo-cathode C_Φ^δ was determined with light from a small incandescent lamp with a color temperature of 2850° K and a spectral energy distribution l_λ. The value of C_Φ^δ determined in this manner allows one to introduce a normalized sensitivity for the photo-cathode $C_{\Phi\lambda}$ (cf., e.g.[1] p.37).

The efficiency of the photo-cathode $\bar{C}_\Phi$ for the spectrum of the scintillation was found from the formula

$$\bar{C}_\Phi = \frac{\int C_{\Phi\lambda} r_\lambda d\lambda}{\int r_\lambda d\lambda},$$

where r_λ is the emission spectrum of the scintillator.

In this manner we found a value of

$$\bar{C}_\Phi = (12.5 \pm 0.5) \cdot 10^{-2}.$$

3. DETERMINATION OF M

The amplification factor M of the photomultiplier was determined in the following way. The current in the first stage was measured for a given illumination; then after diminishing the incident light flux by a known factor (by reflection off white scattering surfaces) the current was measured at the out put of the photomultiplier. For the conditions of the experiment, $M = (7.9 \pm 0.5) \cdot 10^{-6}$

4. DETERMINATION OF k AND c.

These parameters were determined by standard electronic methods. The values obtained were $k = 400 \pm 10$ and $c = (30 \pm 0.5)$ cm.

5. DETERMINATION OF V_{out}.

The output pulse V_{out} was determined under the following conditions. A beam of γ-rays defined by a horizontal slit in a lead collimator was allowed to fall on the scintillator from a known height (30 mm) and a spectrum of the pulses was recorded at the output of the counter, giving the distribution of the Compton electrons.

The limiting energy of Compton electrons is given by the wellknown relation:

$$E_k = E_\gamma \frac{2\frac{E_\gamma}{mc^2}}{1 + 2\frac{E_\gamma}{mc^2}},$$

* The authors extend sincere thanks to A. P. Klimova for preparing the samples for investigation and for data on their optical properties.

** Assuming that the time constant of the anode circuit of the photomultiplier is longer than the emission time of the phosphor (which is clearly the case in the present instance).

ere mc^2 is the rest mass of the electron and E_γ the photon energy. The theoretical electron stribution is perturbed due to statistical atter introduced by the photomultiplier. The gnitude of V_{out} corresponding to the limiting ergy E_k is determined from the experimental distribution of the pulses (Fig. 1) with the help of a nograph given in reference [2].

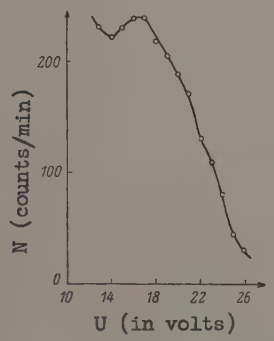

Figure 1. Spectrum of the Compton Electrons rom Cs^{137} obtained by irradiating the scintillator rom a height of 30 mm.

N – count rate (counts/min); U – discrimination level (in volts).

6. DETERMINATION OF α

In order to determine α, the ratio of the technical (actual) light yield to the physical (true) yield we studied the absorption of light in the plastic scintillator. For this purpose the scintillator was replaced by a model of the same dimensions — an empty cylinder of polystyrene with walls, bottom and top of about 3 mm thickness. As a light source we used a miniature incandescent lamp. The model was filled with a liquid whose index of refraction was close to that of the polystyrene, whereas the absorption of the light from the little lamp by the liquid model corresponded to the self-absorption of the luminescence by the polystyrene. The model was placed in the photomultiplier and the current I was measured at the photomultiplier output as a function of the height z of the lamp above the photo-cathode and as a function of its distance r from the axis of the model. The curves obtained were normalized in units of the total light flux I_o from the miniature lamp, which was measured for the indicated geometry by means of the same photomultiplier. The curves obtained in this way give the dependence of $\alpha = \frac{I}{I_o}$ on z and r (Fig. 2).

We note that the curve α(z) has a minimum for z = 30 mm. Since the dependence of α on z is very weak near this value, the measurements of V_{out} were made with light from a height of 30 mm.

The value of α used was obtained by averaging the α(z,r) curve over r for z = 30 mm.

Since we did not have available a suitable liquid with an index of refraction equal to that of polystyrene, we used glycerine — water mixtures as the liquid in our model. In figure 2 we show the dependence of the coefficient of absorption $\alpha = \frac{I}{I_o}$ for pure glycerine (n = 1.47). Experiments with mixtures having indices of refraction n up to 1.4 gave a small displacement to the curve α (z,r). The value of α for solid polystyrene was obtained by extrapolating α (z) to the corresponding index of refraction.

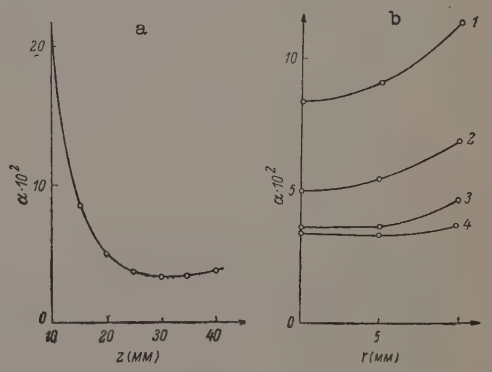

Figure 2. Dependence of the coefficient of light gathering on z and r.

a. Dependence of α(z) for r = 0;
b. Dependence of α(r) for z:

1- 10 mm, 2- 15 mm, 3- 20 mm, 4- 30 mm.

RESULTS

From formula (1) we obtained the quantity η. It was found to be $(1.7 \pm 0.3) \cdot 10^{-2}$. The indicated error is due primarily to the error in the amplification factor of the photomultiplier (~4-5%). All the electronic measurements together contribute an error of the same order. The error in measuring the light gathering efficiency (due to the light not being a point source and errors in alignment) is smaller.

As has already been pointed out, the data in the literature on the luminescent energy yield are quite contradictory. This is clear from the following table, which lists the most recent data known

$П/П_o$	$П_o/C_m$	$П_o/A$	$П/C_m$	$П/A$	C_m/A	C_m/NaI	A/NaI	η_A	η_{NaI}
170[3]	50[4]	38[4]	85[3]	50[4]	46[8]	42[8]	91[8]	4.2[12]	6–10[15]
132-134[4]	18–30[6]	26[7]	85[4]	—	62[9]	29[10]	48[10]	3.7[13]	—
135-140[5]	50[3]	—	—	—	60[10]	47[11]	58[11]	10[14]	—
	—	—	—	—	81[11]	44[5]	—	—	—

to us on the absolute and relative values of the luminescent energy yield of various substances.

П is the energy yield for the plastic studied. $П_0$ is the yield for the most widely used plastic, composed of polystyrene plus 2% p-terphenyl*, C_m is the yield for stilbene, A for anthracene, and NaI the yield for monocrystals of NaI(Tl).

Combining the quantities in the table to get an absolute energy yield for plastic of the sort considered, one may get values from $0.6 \cdot 10^{-2}$ to $6 \cdot 10^{-2}$. If one excludes the data for anthracene as the most contradictory, (cf. e.g. references [7 and 9, 12 and 13]), then for the plastic under consideration one obtains values of $(1.6 - 2.7) \cdot 10^{-2}$, which are not in conflict with our value.

In turn, our value of η makes it possible to find corresponding values of the scintillation energy yield for particular samples and for other scintillators, for which the data in the literature are conflicting.

August 30, 1958

*Certain variations in the concentrations of additives used by different authors will have little influence on the magnitude of the luminescent energy yield.

References

1. N. O. CHECHIK, S. M. FAINSHTEIN, T. M. LIFSHITS: Electronic Multipliers, GITTL, Moscow, (1957)
2. D. MAEDER, R. MULLER, V. WINTERSTEIGER: Helv. Phys. Acta, 27, 3, (1954)
3. M. N. MEDVEDEV, E. N. MATVEEVA, L. IA. ZHIL'TSOVA PiTE, No. 1, 55, (1957)
4. M. M. KOTON': IAN USSR, FS, 22, 1000, (1958) (See CTT Bulletin)
5. Report of the Khar'kov Branch of the All-Union Scientific Research Inst. for Chem. Reagents 1957
6. M. G. SCHORR, E. C. FARMER: Phys. Rev., 81, 891, (1951)
7. R. K. SWANK, W. S. BUCK: Phys. Rev., 91, 927, (1953)
8. R. C. SANGSTER, J. W. IRVINE: J.Chem.Phys., 24, 670, (1956)
9. W. S. KOSKI, C. O. THOMAS: J. Chem. Phys., 19, 1286, (1951)
10. R. K. SWANK: Nucleonics, 12, 3, 14, (1954)
11. S. DHAR: Indian. J.Theor. Phys., 7, 329, (1955)
12. R. K. SWANK: Ann.Rev.Nucl.Sci., 4, 111, (1954) UFN, 58, 519, (1956)
13. J. B. BIRKS, M. E. SZENDREI: Phys. Rev., 91, 197, (1953)
14. M. FURST, H. KALLMAN, B. KRAMER: Phys. Rev., 89, 416, (1953)
15. G. A. MORTON: Reports of the Foreign Delegates to the Intern. Conf. on the Peaceful Uses of Atomic Energy (Geneva, 1955) GITTL, Moscow, 1956

VII, Vyp. 1 OPTIKA I SPEKTROSKOPIIA Iiul , 1959
VII, No. 1 OPTICS AND SPECTROSCOPY July, 1959

Absorption and Dispersion by Thin Gold Layers

A. N. TEKUCHEV

Abstract: On the basis of an analysis of the ellipticity of light reflected from metallic gold ms 500, 115, and 50 Å thick, deposited on a glass base by cathode sputtering, curves of dispersion and corption showing two anomalous regions in the visible portion of the spectrum were obtained.
Experimental data on the microstructure of the surface of these thin layers is presented.

The study of the physical properties of thin tallic and semiconducting layers has practical terest, particularly in view of applications the manufacture of optical devices and the gnetic recording of sound. Moreover, it is also teresting from a theoretical point of view.

The difference between the properties of In metallic layers and the properties of massive als is analysed in detail in Konozenko's review ticle [1].

Schulz [2] presented values of the absorption efficient K and the index of refraction n for nsparent layers of Ag, Au, Cu, Al, in the region om 0.45 to 0.95 μ but without stating their icknesses. Since the thickness of the metallic yers must influence the optical constants to me extent, we performed experiments on gold layers different thicknesses (50, 115, 500 Å), transrent in the visible region of the spectrum, which not oxidize under normal conditions.

The optical properties of metallic films pend on the history of their formation, and on e nature and temperature of the substrate. In der to exclude these influences, thin layers were ways obtained by cathode sputtering on a glass se under the very same conditions.

Figures 1 and 2 are microphotographs (multiication factor of 1300) of the surface of separate gions of thin layers of gold, which were obtained th an MII-4 interference microscope. In these crophotographs it is apparent that the formation the thinnest layers by cathode sputtering occurs a rather complicated manner. More than half of e surface is covered by a fine grained structure ig. 1a and 2a). Also observed were undeveloped ystals in the form of dendritic-skeletons and parate crystalline aggregates (Fig. 1b and 2b) the shape of twigs, wreaths, and chains. The rmation of these aggregates is connected, apparntly, with the rapid growth of the crystalline edium near the comparatively coarse grained rticles of the metal, which was initially deposited n the glass substrate.

The index of refraction n and the absorpion coefficient K of the films were determined n the basis of an analysis of elliptically eflected monochromatic light. The incident light as plane polarized at an azimuth of 45°. A UM-2 onochromator with a special polarizing attachment nd an FEU-19 photomultiplier were used. The rincipal angle of incidence of the light φ_0 and he principal azimuth ρ_0 between the planes of ncidence and polarization were determined. As s well known, the angles φ_0 and ρ_0, the index efraction n and the absorption coefficient K of etallic surfaces are connected by the relations

$$\left.\begin{aligned} n &= \sin\varphi_0 \cdot \tan\varphi_0 \cdot \cos 2\rho_0 \\ K &= \tan 2\rho_0 \cdot \end{aligned}\right\} \qquad (1)$$

For the determination of ρ, a compensator is usually used to establish the direction of the reduced linear polarization, for which the relation

$$\operatorname{tg}\rho = \frac{|R_p|}{|R_s|} \qquad (2)$$

holds, where R_p and R_s are the amplitude components of the reflected light, parallel and perpendicular to the plane of incidence.

However, it is possible to determine ρ without resorting to a compensator. If the ellipse of reflected light is arranged symmetrically relative to the axes, then the ratio $\frac{|R_p|}{|R_s|}$ may be written $\sqrt{\frac{I_{min}}{I_{max}}}$, where I_{min} and I_{max} -are reflected light intensities corresponding to the minor and major semiaxes of the ellipse. These intensities are measured by photomultipliers, where a symmetric arrangement of the reflected light ellipse corresponds to the largest value of the ratio I_{min}/I_{max} which is found by selecting the angle of light incidence.

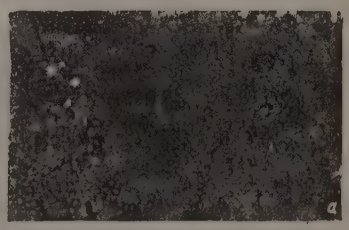

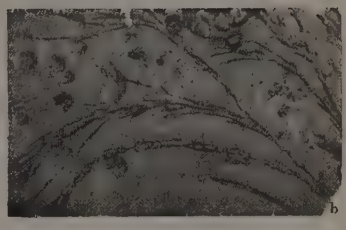

Figure 1, a.b. Microstructure of thin layers of gold Thickness of the layers is 500 A° magnification x 1300

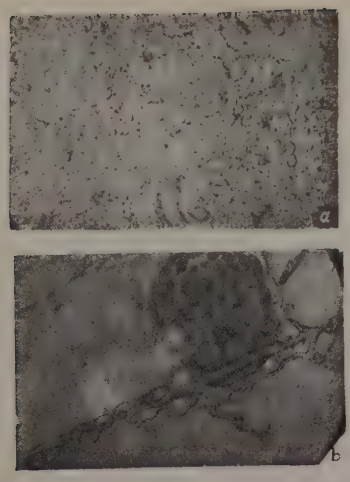

Figure 2, a.b. Microstructure of the surface layers of gold. Thickness of the layers is 115 Å. magnification x 1300

The data on the measurements of φ_o and ρ_o for gold films are presented in the table.

From the table it is obvious that the angles φ_o and ρ_o depend on the wavelength and on the thickness of the metallic layer. The value of ρ_o decreases sharply as the thickness of the layer is reduced; the changes in φ_o are approximately within the limits of the values found for other metals, silver, copper, and sodium.

Presented below is a comparison of our data for φ_o and ρ_o obtained for 500 Å thick gold samples with data presented by Drude [3] (λ=5895 Å)

φ_o	ρ_o
72° 18′	41° 39′
70°	41° 11′ .

Knowing φ_o and ρ_o, it is not difficult to calculate the optical constants n and κ for metallic gold films.

The dispersion of three metallic gold films of different thicknesses is shown in Figure 3. The largest value of the refractive index corresponds to the thinnest metallic gold layer. The same results were obtained by Lisitsa and Tsvelykh [4], who investigated the optical properties of tellurium. All three dispersion curves are characterized by two sharply pronounced minima occurring in the same spectral regions for each sample, and located in the longwave and shortwave visible regions of the spectrum. In these regions of anomalous dispersion, maxima in the values of the absorption coefficient are also observed (Fig. 4). In the spectral region of the anomalous dispersion, a reversal of the major and minor axes of the reflected light ellipse was observed.

These experimental data confirm the well-known fact that regions of anomalous dispersion coincide with the absorption region. However, the resonance absorption maxima were obtained only for the 500 and 115 Å layers, while for the 50 Å films (Fig. 5) the dependence of the absorption coefficient κ in

λ (in Å)	Film Sample: 500 Å φ_o	500 Å $\sqrt{I_{min}/I_{max}}$	500 Å ρ_o	150 Å φ_o	150 Å $\sqrt{I_{min}/I_{max}}$	150 Å ρ_o	50 Å φ_o	50 Å $\sqrt{I_{min}/I_{max}}$	50 Å ρ
6150	68°	0.63	30°19′	73°	0.42	23°12′			
5895	70	0.87	41 11	75	0.53	27 54	70°	0.29	1
5650	70	0.89	41 40				68	0.18	1
5550	69	0.90	42 36	70	0.50	26 54			
5400	70	0.92	42 37	71	0.96	43 48	70	0.22	1
5300	69	0.63	32 18	67	0.40	21 48	72	0.20	1
5100	71	0.56	29 31	66	0.39	24 47	72	0.19	1
5000	71	0.61	31 06	64	0.37	20 23	70	0.18	1
4800	64	0.59	30 25	64	0.33	18 12	64	0.17	9
4600	63	0.52	27 36	67	0.32	17 51	70	0.10	5
4400	63	0.97	44 12	65	0.59	30 41	68	0.09	5
4200	62	0.43	23 24	60	0.38	20 54	72	0.11	6
4150	62	0.43	23 24	70	0.37	20 42	73	0.10	5

the visible region of the spectrum resembles the dependence of the atomic and mass absorption coefficient of X-rays in platinum for the spectral interval from 3.7×10^{18} - 1.5×10^{19} sec^{-1} [5].

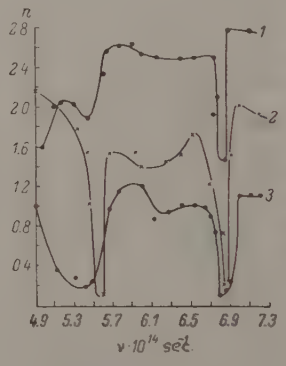

Figure 3, Dispersion curves for thin gold layers. Thickness (in Å): 1-50, 2 -115, 3 -500

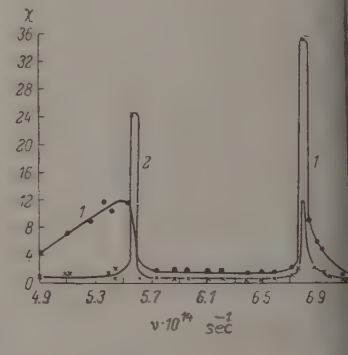

Figure 4, Absorption curves for thin gold layers. Thickness (in Å): 1-500, 2 -115

It is well known that absorption of X-rays in a substance is caused by two factors - true absorption, when the photon energy is enough to ionize the atom, and coherent and incoherent scattering, when the photon collides with either strongly bound electrons or with the outer weakly bound electrons. Comparing the curve of the atomic and mass absorption coefficient of platinum, which represents a true absorption, with the dependence of the absorption coefficient of 50 Å gold films one is forced to assume that the absorption mechanism in the thinnest gold films is connected with its ionization of the atoms; whereas in thicker layers, having a surface structure of granules and patterns of significant linear dimensions which exceed the wavelength of visible light by several hundred times, the light absorption mechanism was caused, apparently, by the interaction of radiation with the crystal lattice of the substance.

The appearance of two resonance absorption regions (Fig. 4) in the 115 and 500 Å gold films obviously are accounted for by these mechanisms.

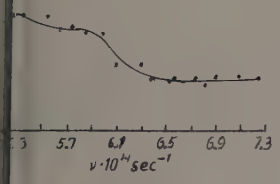

Figure 5,
sorption curve for
thin layer of gold.
hickness is 50 Å

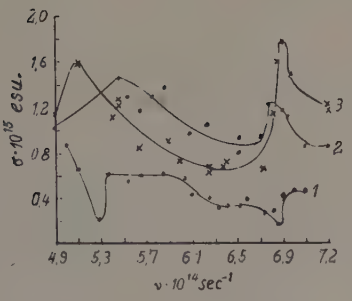

Figure 6,
Conductivity curves
of thin gold layers.
Thickness (in Å)
1-50, 2-500, 3-115

In conclusion we will examine the conduc-
ity of the thin gold samples described above by
king advantage of the relation between the con-
ctivity, the refractive index, the absorption
efficient and the frequency of the incident light.

In Figure 6 curves of the dependence of the conductivity of thin gold samples of various thicknesses on the frequency of incident light are presented. The curves were calculated from the experimental data using the formula

$$\sigma = nK\nu \tag{3}$$

Notice that the conductivity increases with increasing thickness of the metallic layers, reaching maximum values for the 115 and 500 Å films in the resonance absorption regions; a deviation from the described rule is observed, in the 50 Å film which is caused, in all probability, by a special conduction mechanism in the very thin layers.

July 14, 1958

REFERENCES

1. I. D. KONOZENKO: UFN, 52, 561, (1954)
2. L. SCHULZ: J. Opt. Soc. Amer., 44, 5, 357, (1954)
3. P. DRUDE: Wied. Ann., 35, 885, (1889); 39, 481, (1890)
4. M. P. LISITSA, N. G. TSVELYKH: OiS, 4, 373, (1958)
5. M. A. BLOKHIN: The Physics of X-Rays, (GITTL, Moscow, 1953)

TOM VII, Vyp. 1 OPTIKA I SPEKTROSKOPIIA Iiul', 19
VOL. VII, No. 1 OPTICS AND SPECTROSCOPY July, 19

Development of a Method of Determining the Relaxation Time of the Vibratory State of Molecules Using a Spectrophone

I. Establishment of a More Accurate Dependence Between the Measured Phase Shift and Relaxation Time

P. V. SLOBODSKAIA AND E. S. GASILEVICH

It is established that the relationship between relaxation time τ and the corresponding phase shift ψ, is expressed by the equation* $\operatorname{tg}\psi = \omega\tau$, and a basis is given for the fact that the phase shift caused by the relaxation time can be separated from the shift caused by thermal inertia. The results are listed of checking the validity of the given equation by determining τ at various frequencies of chopping the radiation.

INTRODUCTION

A number of methods exist for determining the relaxation time of excited vibrational states of molecules. The majority are non-selective, i.e., the relaxation time cannot be found for each mode of oscillation independently of others. However, to obtain conception of the process of the build-up of equilibrium between vibratory and progressive degrees of freedom, a differentiated determination of relaxation times corresponding to various vibratory degrees of freedom of a molecule is highly essential.

A selective phasometric method of determining the relaxation time of molecules (duration of excited vibratory state) using Veingerov's [2] spectrophone was described in Ref. [1]. The method is based on measuring the phase shift of a pressure pulsation in an optic-acoustic receiver with respect to entering radiation. This article gives the results of further development of this method.

A MORE PRECISE THEORY OF THE METHOD

In the initial version of the method [1, 3, 4] it was supposed that there is a linear dependence between the phase shift measured by a phase shifter** and referred to instrument shift, and the relaxation time in the region of low values of these quantities. When the values approached the period of modulation, a correction was introduced computed according to theory by Stepanov and Girin [5]***. It will be shown below that the relaxation time is related by tangent function to the measured phase shift over the entire range of its values.

The theory of a spectrophone as a device for measuring the relaxation time of the excited vibrational state of molecules is analogous, to a certain degree, to the theory of the fluorometer [6], where it was also initially assumed that there is a linear dependence of the phase shift on the duration of excited state corresponding to electron transitions. The theory of the spectrophone and the theory of the fluorometer differ in that in the case of the former the relaxation process is studie with another inertial process, the change in the gas temperature in the chamber, as background.

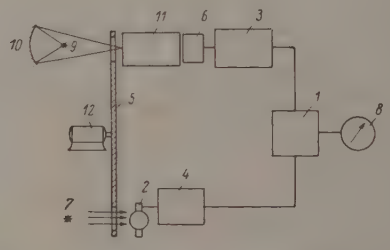

Figure 1. Diagram of the setup.

1—synchronous detector, 2—photocell, 3—4—amplifiers, 5—modulating disc, 6—optic-acoustic receiver, 7—lamp, 8—galvanometer, 9—radiation source, 10—mirror, 11—monochromator, 12—motor.

The diagram of the apparatus is shown in figure 1. It was used in the phasometric method of gas analysis [7] and differs from the scheme described in [1] by the use of an electrical phase-sensitive device, the synchronous detector-1, instead of a mechanical chopper. One input of the synchronous detector gets a signal developed by the microphone and the reference voltage, the signal developed by the photocell 2, is applied to the other input. Both inputs are pre-amplified by amplifiers 3 and 4. These signals are synchronous since the photocell is illuminated by the light modulated by the same disc 5, as is the radiation entering the detector. The photocell with the lamp 7 illuminating it can be moved in a direction perpendicular to the plane of the drawing, but tangent to the circumference of the disc+, by means of a micrometer screw not shown in the figure; displacement is measured on a drum provided with the screw. This setup also serves as a phase shifter. When the photocell is placed in such a position that the phase shift between the signals applied to the synchronous detector is 90°, the galvanometer read zero; as this condition is changed there is a reading.

---

* ω is the angular frequency of chopping the radiation flux.

** The phase shifter used there was such that the disc could be placed in different positions with respect to the prism of the mechanical chopper.

***Calculations of relaxation times, needing corrections, are approximate and cannot be done for large phase shifts.

+The error due to displacement along the tangent instead of the arc is 0.5% at the end of the scale of the screw.

The determination of the relaxation time is
e by measuring the phase shift it causes in the
ic-acoustic receiver with respect to the refer-
e voltage by introducing a compensating phase
ft. A similar setup was used independently by
ox and Bauer [8] in the work devoted to applica-
n of the spectrophone for investigating proces-
of energy exchange between colliding molecules*.
ir scheme differs from the one described here in
t they used an electrical phase shifter in the
lifying channel of the photocell.

The phase shifter of the setup described
sures the phase shift φ between the first
rmonic components of the Fourier series of the
nals applied to the synchronous detector from the
eiver and photocell. This phase shift consists
the several shifts due to apparatus and the
se shift caused by relaxation time.

Let us examine the case of radiation entering
chamber in the form of Π-shaped impulses. As
result of radiation absorption by gas molecules
the chamber (when radiation enters it), fluctu-
ons of temperature and pressure occur within its
ume. The shape of the curve describing these
ctuations depends on the time constant of thermal
rtia and on relaxation time of the vibratory
te corresponding to given absorption band. The
ger these values the greater the phase shift
bsequently denoted by φ_1) of the first harmonic
the pressure fluctuation relative to the first
rmonic of radiation entering the chamber, i.e.,
th respect to the instant of beginning of illu-
nation. The microphone membrane vibrates with
e additional phase shift, and as a result the
st harmonic of the microphone emf is shifted an
le $\varphi_{acoust.}$ with respect to the pressure
ctuation curve. In addition, several phase
ifts must be taken into account, due to the inertia
the photocell and the difference in the ampli-
ing channels of the receiver and photocell. Let
denote the sum of these shifts by $\varphi_{el.}$. This
ift will add to the first two.

Thus, the total phase shift between the first
rmonics applied to the synchronous detector
ong the two channels and measured by the phase
ifter is equal to

$$\varphi = \varphi_1 + \varphi_{acoust.} + \varphi_{el.}.$$

As shown by Stepanov and Girin [5], the build-
of temperature, and, consequently of pressure
ring illumination, and their decay during dim-out
described by exponential laws for a negligibly
all value of relaxation time. When the relaxa-
on time is finite, the shape of the curves change,
mely: now they are described by the difference
tween two exponential functions, one of which is
termined by thermal inertia and the other by
laxation time. This follows from the equations
tained by the authors mentioned:

(2)
$$\bar{T}_{ill.} = \mu_1\left(\frac{p\exp[-\beta_1 t]}{1+\exp[-\beta_1\theta]} - \frac{\beta_1\exp[-pt]}{1+\exp[-p\theta]}\right)\frac{\mu_1}{p-\beta_1};$$

$$\bar{T}_{d.i.} = \frac{\mu_1}{p-\beta_1}\left(\frac{p\exp[\beta_1 t]}{1+\exp[-\beta_1\theta]} - \frac{\beta_1\exp[-pt]}{1+\exp[-p\theta]}\right),$$

where $\bar{T}_{ill.}$ is the change in temperature during illumination averaged over the chamber volume; $\bar{T}_{d.i.}$ —the same during the dark interval, p is the sum of the probabilities of the transformation from vibrational to progressive energy and of spontaneous radiation, $\frac{1}{p} = \tau$ is the relaxation time, β_1 is the reciprocal of the time constant determining the thermal inertia of the gas in the receiver, θ is half-period of modulation, μ_1 is a quantity independent of time.

Fourier analysis of the periodic function, described by Eq. (2), and singling out the first harmonic component enables one to establish the relationship between the relaxation time and the phase shift φ_1.

As is known, the ratio between the Fourier coefficients

$$a_1 = \theta\int_0^{2\theta} f(t)\cos\omega t dt \text{ and } b_1 = \theta\int_0^{2\theta} f(t)\sin\omega t dt$$

equals the tangent of the angle of the first harmonic phase shift with respect to the time taken as a reference**. Taking as this instant of time when the radiation starts to enter the chamber, we get the following expressions for coefficients of expanding Eq. (2) into a series:

$$a_1 = \frac{2\mu_1}{\theta}\cdot\frac{\beta_1 p}{(p-\beta_1)}\left[\frac{1}{p^2+\omega^2} - \frac{1}{\beta_1^2+\omega^2}\right];$$

$$b_1 = \frac{2\mu_1}{\theta}\left[\frac{1}{\omega} - \frac{\omega p}{(\beta_1^2+\omega^2)(p-\beta_1)} + \frac{\omega\beta_1}{(p^2+\omega^2)(p-\beta_1)}\right].$$

After performing transformations we get

(3)
$$\operatorname{tg}\varphi_1 = \frac{\frac{\omega}{\beta_1}+\frac{\omega}{p}}{1-\frac{\omega^2}{p\beta_1}}.$$

It is obvious, that $\operatorname{tg}\varphi_1$ is the tangent of the sum of two angles, one depending on relaxation time, and the other on the thermal inertia of the gas in the chamber, i.e.

*The authors of this work conducted a theoretical examination, as a result of which they obtained a linear relationship between the phase shift and relaxation time.

** Since temperature lag with respect to entering radiation is considered, $\operatorname{tg}\varphi_1 = -\frac{a_1}{b_1}$.

(4) $$\operatorname{tg}\varphi_1 = \operatorname{tg}(\psi + \varphi_{\text{therm.}})$$

where $\psi = \operatorname{arctg}\frac{\omega}{p}$, and $\varphi_{\text{therm.}} = \operatorname{arctg}\frac{\omega}{\beta_1}$.

Hence, it follows that the phase shift corresponding to relaxation time, and the phase shift caused by thermal inertia, are additive at any value of β_1

$$\varphi_1 = \psi + \varphi_{\text{therm.}}$$

If thermal inertia is large (small β_1), $\varphi_{\text{therm.}}$ is close to 90°, i.e., it is the case examined by Jacox and Bauer [8].

It can be seen from eq. (4) that whatever the value of β_1, as τ varies from zero to infinity, φ_1 varies between the limits of $\operatorname{arctg}\frac{\omega}{\beta_1}$ and $\operatorname{arctg}(-\frac{\beta_1}{\omega})$, i.e., the maximum possible change of the angle ψ is 90°.

Substituting the obtained value of angle φ_1 in equation (1) we find that the phase shift measured by the described setup,

$$\varphi = \psi + \varphi_0$$

where $\varphi_0 = \varphi_{\text{therm.}} + \varphi_{\text{acoust.}} + \varphi_{\text{el.}}$ is the total phase shift due to the apparatus. In this work the phase shift due to apparatus is assumed to be independent of mixture density and of the absorption band. Both of these assumptions (especially the first) are correct only approximately. Details about this will be given in another publication.

Thus, the examination conducted shows that the values ψ_λ measured using the described setup at a given chopping frequency for various absorption bands λ, must be measured from the shift due to apparatus φ_0, which includes thermal inertia of the gas in the chamber. Relaxation time will then be determined from the relation:

(5) $$\tau_\lambda = \frac{1}{\omega}\operatorname{tg}\psi_\lambda.$$

As follows from the work by Sall'[9], a similar dependence is obtained for radiation entering the chamber according to any law.

If instead of Eq. (5), a linear approximation is used $\tau = \frac{\psi_\lambda}{\omega}$ as was done previously, the resulting values τ_λ are lowered. The larger the ψ_λ, the larger is the reduction, i. e., the larger τ_λ and ω (with $\psi_\lambda = 40^\circ$ the error of the approximation is 17%, and with $\psi_\lambda = 60^\circ$, it is 40%).

EXPERIMENTAL RESULTS

Experimental verification of Eq. (5) was carried out using the described setup. For this purpose, phase shifts were measured in mixtures of carbon dioxide and nitrogen of various concentrations at the following radiation chopping frequencies: 250, 600, 2000, and 1100 cps.* At the first three frequencies the measurements were made for the absorption bands of 2.7 and 4.3 microns and at 1100 cps for the 4.3 micron band only.

The gases were taken from the cylinders and were dried by calcium chloride and phosphorous pentoxide. The spectrum region corresponding to the absorption bands was separated by a monochromator. The modulating disc was revolved by a synchronous motor at 3000 rpm. the chopping frequency was varied by changing discs with various numbers of openings.

The displacement of the photocell l, measured with a micrometer, is related to the phase shift φ by $l = \frac{L}{\pi}\varphi$, where L is the arc of the modulating disc equal to the width of a tooth. Therefore, the micrometer readings represent phase shifts, scaled differently for different chopping frequencies. The displacement of the photocell is directly proportional to time $t = \frac{\varphi}{\omega}$, where the coefficient of proportionality remains the same for various chopping frequencies (provided the motor speed stays constant).

The results of measurements of the phase shift versus concentration of the mixture, corresponding to the 2.7 and 4.3 microns absorption bands of the carbon dioxide and nitrogen mixture are given in Figure 2. The concentration of carbon dioxide in the mixture is plotted along the abscissa, with the phase shift in degrees and time t along the ordinate axis. Besides, the micrometer readings l are given in Figure 2b and 2c.

In order to obtain the data on relaxation times from the graphs of Figure 2, one has first to determine the phase shift of the apparatus in each case. The method for excluding the phase shift due to the apparatus, by examining the shape of the curve in the region of high concentrations, where the difference between the ordinates for various bands becomes less than the measurement errors, was given in Ref. [1]. Assuming that the values of φ measured in this case are equal to the phase shift of the apparatus φ_0, and that the phase shift due to apparatus stays constant at all concentrations, this phase shift can be eliminated by measuring the values of ψ from the line 00', which the curves 1 and 2 approach asymptotically at high concentrations.

Comparison of the curves given in Figure 2 shows that the values of t measured for the 4.3 micron band at different frequencies from the line 00', depend substantially on frequency. The higher the frequency the lower they become compared to the values at the lowest frequency, 250 cps. They become lower as the concentration decreases.

If the results of measurements for the 4.3μ band are interpreted on the assumption that there is a linear dependence between the relaxation time and phase shift, i.e., considering, as was done previously, that the relaxation time is $\tau = \frac{\varphi}{\omega} = t$, then the values of $\tau_{4,3}$, found at different chopping

*The measurements at 250 cps. were made using the mechanical chopper described in Ref. [1].

quencies do not coincide. If the relaxation times $\varphi_{4.3}$ evaluated from the values $t = \frac{\psi}{\omega}$, given in Figure 2 for fferent frequencies, and using Eq. (5), the computed values ncide within the limits of error. The good agreement bet-n the results of determining the relaxation time for the μ band on the basis of measuring the delay time t at dif-rent frequencies is shown by Figures 3 and 4. The solid rve 1 in Figure 3 is the result of calculations of the axation time made by substituting the values ψ measured 250 cps in Eq. (5). Curve 2 is plotted by means of the ues of t corresponding to these values ψ. Curves 3, 4, were computed from curve 1, and the relationship $= \frac{1}{\omega}$ arctg ωτ. The agreement between the results of measure-nts, shown dotted, and calculated curves is to be consi-red satisfactory.

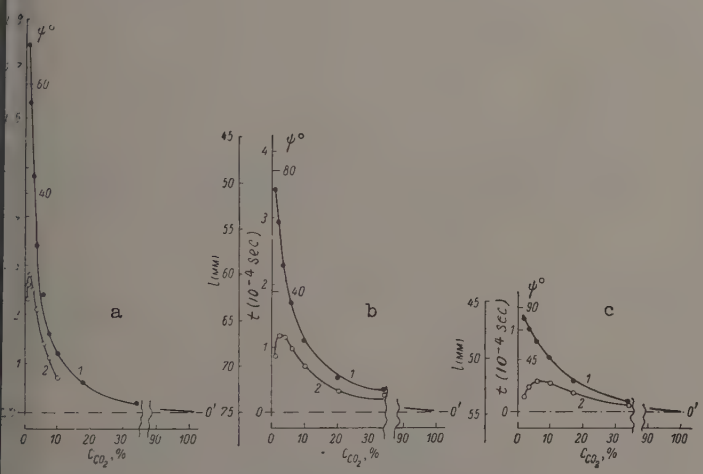

Figure 2. Phase shift curves, corresponding to 4.3μ urve 1) and 2.7μ (curve 2) absorption bands of carbon dio-de mixed with nitrogen, versus mixture concentration. The asurements were made at: a—250, b—600, c—2000 (cps).

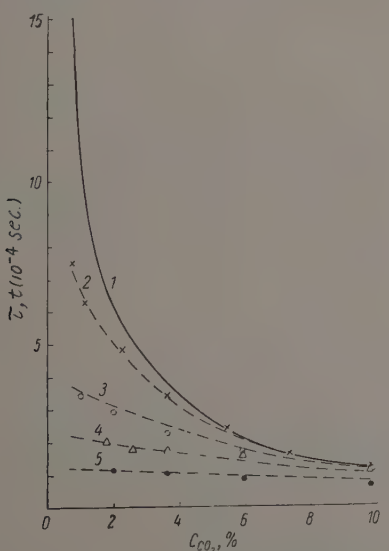

Figure 3. Relaxation time τ(curve 1) and lag time(curves ,3,4,5) curves versus concentration of the carbon dioxide and itrogen mixture. Frequency(in cps): 2-250, 3-600, 4-1100, d 5-2000. The values of t obtained experimentally are arked with dots.

In Figure 4 the graph of the following function is given:

$$\frac{t}{\tau} = \frac{\text{arctg } \omega\tau}{\omega\tau}.$$

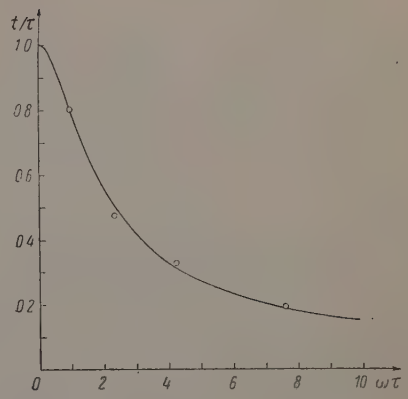

Figure 4. Graph of the function $\frac{t}{\tau} = \frac{\text{arctg } \omega\tau}{\omega\tau}$.

This curve describes a law according to which the quantity t decreases with increasing modulation frequency. It is apparent that the function decreases most rapidly near such values of the argument where ω equals approximately $\frac{1}{\tau}$. At higher frequencies, for a given value of τ, the ordinates of the curve asymptotically approach zero*. The points in Figure 4 correspond to $C_{CO_2} = 2\%$.

As was pointed out earlier [11], measurement of the relaxation time corresponding to a 2.7 μ absorption band is difficult since, in spite of thorough drying of the mixture under investigation, it still retains small amounts of water vapor which also has an absorption band in the 2.7 μ region. This is the reason for the big difference in the results of measurements of the phase shift, represented by the curves of t versus concentration of Figure 2, for the 2.7μ and the 4.3μ absorption bands. The difference consists in that curves corresponding to the 2.7μ band have a maximum, and that upon transition from lower to higher chopping frequencies, the ordinates of these curves off maximum are more undersized than is to be expected from Eq. (5). (The maxima are located at higher concentrations, as the chopping frequency is increased). The reason for maxima is the following. The signal developed by the receiver in the 2.7μ region is a sum of signals caused by carbon dioxide and water vapor, therefore, the phase shift of each component of the signal. The phase shift γ of the resultant signal can be found from the parallelogram in Figure 5 which represents a sum of two vectors:

*Gorelik [10] pointed out the possibility of determining relaxation time in a spectraphone by observing the effect of modulation frequency on the amplitude and phase of fluctuations.

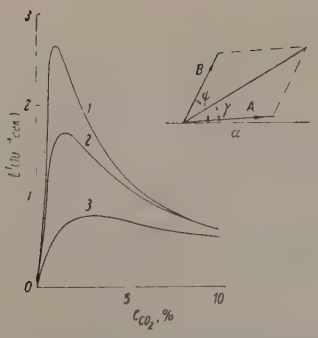

Figure 5. The curve t' versus concentration of the carbon dioxide and nitrogen mixture. Frequency (in cps): 1-250, 2-600, 3-2000.

$\vec{A}$ - corresponding to water vapor, and $\vec{B}$ - the carbon dioxide. The moduli $\vec{A}$ and $\vec{B}$ of these vectors are proportional to the amplitudes of the signals under examination. Since all "2" curves in Figure 2 pass through the origin on extrapolation to low concentrations, one can assume that the relaxation time of water vapor is very small and, therefore, the phase shift $\alpha = 0$. The phase shift ψ of vector $\vec{B}$ is found from Eq. (5). At low concentrations of carbon dioxide in the mixture with nitrogen, the modulus of this vector is related to CO_2 concentration through an almost linear relationship, i.e., $B=kC_{CO_2}$, where k is a constant of proportionality, and C_{CO_2} — the CO_2 concentration. The time $t' = \frac{\gamma}{\omega}$ corresponds to the resultant phase shift γ. Assuming that $\frac{1}{\tau_{2.7}} = \frac{1}{b} C_{CO_2}$ (where b is a constant of proportionality), we get

$$(6) \qquad t' = \frac{1}{\omega} \operatorname{arctg} \frac{\frac{k}{A} C_{CO_2} \sin \operatorname{arctg} \frac{\omega b}{C_{CO_2}}}{1 + \frac{k}{A} C_{CO_2} \cos \operatorname{arctg} \frac{\omega b}{C_{CO_2}}}.$$

Assuming that at a CO_2 concentration of 1%, the amplitudes of the signals, caused by CO_2 and H_2O, are equal, and that the relaxation time $\tau_{2.7}$ at a concentration of 10% equals 0.6 τ, then $b = 0.7 \cdot 10^{-5}$ and $\frac{k}{A} = 100$. A graph of Eq. (6) is given in Figure 5 for frequencies 250, 600, and 2000 cps and the given values of the parameters. Comparison of the curves of Figure 5 with the curves 2 of Figure 2 shows that they are analogous. This indicates that the character of dependences observed for the 2.7 μ band can be explained by the effect of an admixture of water vapor.

August 2, 1958

REFERENCES

1. P. V. SLOBODSKAIA: IAN USSR FS, 12, 656, (1948)
2. M. L. VEINGEROV: DAN SSSR, 19, 687, (1938) DAN USSR, 46, 200, (1945), ZL, 13, 426, (1947)
3. P. V. SLOBODSKAIA AND B. I. STEPANOV: Tr. GOI, 23, 133, (1951)
4. P. V. SLOBODSKAIA: Kand. diss. GOI, Leningrad, (1951)
5. B. I. STEPANOV AND O. P. GIRIN: ZETF, 20, 947 (1950)
6. L. A. TUMERMAN: ZETF, 11, 515, (1941)
7. P. V. SLOBODSKAIA, IA. I. GERLOVIN, M.L. VEINGEROV Tr. komissii po analiticheskoi khimii, 8, (11), M., Izd. AN SSSR, 1958 [tezisy doklada na soveshchanii po spectrografotometricheskim i kolorimetricheskim metodam analiza. Moskva, 1955] (Abstracts of reports at the Conference on Spectrographic and Photometric Methods of Analysis)
8. M. JACOX, S. H. BAUER: J. Phys. Chem., 61, 833, (1957)
9. A. O. SALL': ZETF, 24, 1, 157, (1956) [See Sov. Phys. JETP]
10. G. S. GORELIK: DAN USSR, 54, 783 (1946)
11. P. V. SLOBODSKAIA: DAN USSR, 120, 1238 (1958) [See Sov. Phys. Doklady]

VII, Vyp. 1 OPTIKA I SPEKTROSKOPIIA Iiul', 1959
VII, No. 1 OPTICS AND SPECTROSCOPY July, 1959

Enhancement of the Sensitivity of the Optic-Acoustic Method of Gas Analysis by Using Cells with Multiple Passage of Radiation

IA. I. GERLOVICH AND P. V. SLOBODSKAIA

Abstract: A method is described of enhancing the sensitivity of an optic-acoustic gas analyzer, based on ng cells with multiple passage of radiation. Dependence of the signal developed by the receiver on the ective thickness of the absorbing layer of gas in the cells is examined. It is shown that increase in sen- ivity of the gas analyzer depends on the reflection coefficient of the mirror and astigmatism of the pencils radiation. Relations are obtained which enable one to determine the optimum number of passages. The depen- ce of the sensitivity of a gas analyzer on the amount of gas being determined in the comparison cell is ablished.

Lately, in investigating infrared absorption spectra of es and vapors, multipass cells have been widely used, by ch means one can increase the effective thickness of the er of absorbing substance without changing the size of the trument [1, 2]. Therefore it seemed rational to employ tiple passage of radiation in the cell of a gas analyzer determine the gain in sensitivity of the intrument ained by doing so.

An optic-acoustic gas analyzer employing a single pas- e of radiation is described in [3] and [4]. The opera- n of the multipass gas analyzer we have developed *, is cribed by the diagram given in Figure 1.

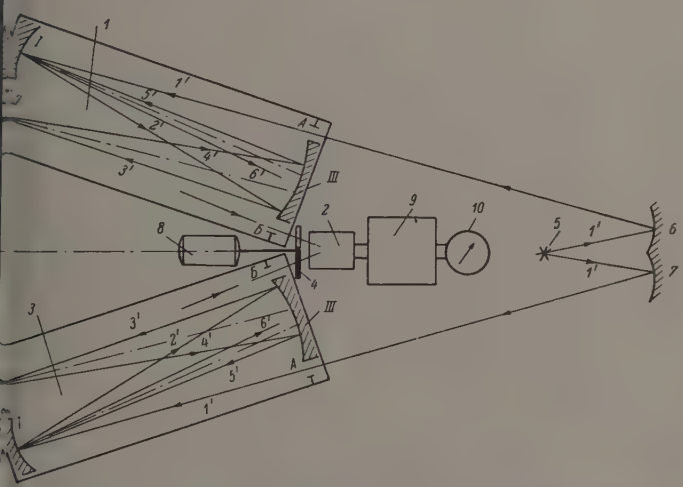

Figure 1. Diagram of operation of a multipass gas analyzer.

1—Operating cell, 2—optic-acoustic receiver, 3—compa- son cell, 4—disc, 5—source, 6 and 7—spherical mirrors source, 8—motor, 9—amplifier, 10—output meter; A- and B- slits I, II, III — mirrors. Numbered arrows indicate the path of the main beam in e cells.

e operating cell 1 is filled with the mixture of gas being vestigated. Part of the gas absorbs light and the rest es not, it being desired to find the content of the former the mixture. The cell of optic-acoustic receiver 2 con- ins the same absorbing gas. The comparison cell 3 con- ins non-absorbing gas either without any or with some admix- re of absorbing gas. The radiation is modulated by disc 4 such a way that there is a phase shift of 180° between diation fluxes passing through the operating and comparison lls, i. e. the output of the receiver will be zero for ual concentrations of the absorbing component and equal fluxes of radiation directed into the cells.

Cells 1 and 3 are built according to White's diagram. Multiple passage of radiation occurs in them. Radiation enters each of the cells through slit A and leaves through slit B. A series of intermediate images of the slit is formed on the surface of mirror III. The number of passages of radiation through the cell depends on the angle between mirror I and II, and can vary from 4 to 52. The relative aperture of the cells is 1:6; the radii of curvature of mirrors I, and II, and III, are identical at 500 mm. The source of radiation is a Nernst glower, 5; it is magnified three times by spherical mirrors 6 and 7 and projected on the input slits of the cells. The width of the slits of the cells is 5 mm, while their height is 25 mm. The cells are placed one above the other; in Figure 1, for simplicity, they are shown in one plane.

DEPENDENCE OF THE SIGNAL GENERATED BY THE OUTPUT METER OF THE GAS ANALYZER ON EFFECTIVE THICKNESS OF THE LAYER OF GAS

Let us establish the dependence of the output signal developed by the gas analyzer on the number of passages of radiation through the cells. Let us assume for generality that the gas of interest is in both cells and the difference between its concentrations in the two is to be found. Under the effect of infrared radiation passing through the cells and into the detector, the microphone develops a signal ΔS equal to the difference of signals S_1 and S_2, which are developed by the receiver when one of the radiation fluxes is blocked and radiation passes through one of the cells only:

$$(1)\ \Delta S = S_1 - S_2 = \int_0^\infty RJ_0 \exp[-k_\nu C_1 lN]\,(1-\exp[-k_\nu w])\,d\nu -$$

$$\int_0^\infty RJ_0 \exp[-k_\nu C_2 lN]\,(1-\exp[-k_\nu w])\,d\nu =$$

$$-\int_0^\infty RJ_0 \exp[-k_\nu (C_1 lN+w)]\,d\nu + \int_0^\infty RJ_0 \exp[-k_\nu C_1 lN]\,d\nu$$

$$+\int_0^\infty RJ_0 \exp[-k_\nu (C_2 lN+w)]\,d\nu - \int_0^\infty RJ_0 \exp[-k_\nu C_2 lN]\,d\nu$$

where R is a proportionality constant**; J_0

* Built by A. F. Dobretsov and V. N. Nikiforov.

** Meaning linear relationship between J_0 and S.

is the spectral intensity of radiation entering the cells; k_ν is the absorption coefficient for radiation of frequency ν; w is the product of the thickness of the gas layer and concentration in the optic-acoustic chamber of the receiver; C_1 is the concentration of absorbing gas in the operating cell; l is the length of the cell; N is the number of passages of radiation inside the cells (same in both cells).

Since k_ν is a complex function of frequency, the integrals in (1) cannot be solved in closed form. Elsasser [5] found a solution for such integrals by assuming that the vibration-rotation band in absorption consists of equally spaced rotation lines of equal intensity; the transmittance T can be expressed as follows:

$$T = \frac{\int I d\nu}{J_0 \Delta\nu} = 1 - \varphi(x),$$

where, according to Elsasser, $\varphi(x)$ is the error integral of argument $x = \sqrt{\beta u}$; β is a constant dependent on molecular parameters; u is the effective thickness of the layer; I is the spectral intensity of the transmitted radiation. The value of β can be found experimentally.

It is shown in Ref. [6] that, in spite of several assumptions made in the derivation of Elsasser's formula, it can be used, with sufficient accuracy, in a certain thickness range of the absorbing layer, for extrapolating values of transmission for various thicknesses from the values obtained for one thickness. Therefore, it can be assumed that each of the integrals in (1) can be replaced by an expression $\varphi(\sqrt{\beta u})\Delta\nu$, where $\Delta\nu$ is the effective width of the band: i.e., the spectral interval within which the radiation is actually being absorbed in the given band. Outside of this interval absorption is small and varies little with varying thickness of the absorbing layer.

Thus, we have

$$\Delta S = RJ_0\Delta\nu\{[\varphi\sqrt{\beta(w)+C_1 l N}) - \varphi\sqrt{\beta C_1 l N}] - [\varphi\sqrt{\beta(w + C_2 l N}) - \varphi\sqrt{\beta C_2 l N}]\}.$$

We have verified this equation by measuring the value of transmission T_c, using an optic-acoustic receiver*

$$T_c = \frac{\varphi\sqrt{\beta(w + C_2 l N}) - \varphi\sqrt{\beta C_2 l N}}{\varphi\sqrt{\beta w}}. \quad (3)$$

The measurements were made on atmospheric air, containing approximately 0.03% of carbon dioxide. Radiation was passed through one of the cells only, the other being completely blocked. The effective thickness of the layer was varied between 0.06 to 0.6 cm by turning the mirrors which changed the number of passages. The effective thickness of the layer of carbon dioxide in the receiver was approximately 1 cm.

The circles in figure 2 indicate experimental values of T_c. The validity of Eq. (3) is confirmed by the fact that the curve to which it corresponds, assuming $\beta = 1.2$ cm^{-1}, passes through the experimental points.

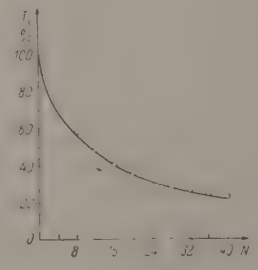

Figure 2. Curve of transmission vs. number of passages of radiation inside the cell.

Equation (2) indicates that the signal developed by the receiver in the gas analyzer, with absorbing gas present in both cells, will first increase with an increase in the number of passages of radiation in the cells, and then will start decreasing toward zero, since each term in Eq. (2) approaches unity. The probability integral for low values of the argument can be replaced by the first term of its series, i. e., $\varphi(x) \approx x$. As the argument, i.e., the effective thickness of the layer, increases, the error of the approximation increases. For values of x less than 0.6 the error does not exceed 10%.

Since it is expedient to use the multipass gas analyzer to indicate low concentrations of gas, the quantities $C_1 l N$ and $C_2 l N$ are considerably smaller than w, and the first and third terms in Eq. (2) cancel. Therefore, this expression can be approximately replaced by the following:

$$\Delta S = RJ_0\Delta\nu\,(\sqrt{\beta C_2 l N} - \sqrt{\beta C_1 l N}), \quad (4)$$

i. e. at low effective thicknesses the signal is governed by a square-root absorption law, and does not depend on the effective thickness of the gas layer in the receiver.

In practice, the case when there is no absorbing gas in the comparison cell is of greater interest. Then

$$\Delta S = RJ_0\Delta\nu\sqrt{\beta C_2 l N}. \quad (5)$$

From Eq. (1) it can be seen that when $k_\nu C_2 l N \ll 1$ and $C_1 = 0$, we have

$$\Delta S = RJ_0 C_2 l N \int_0^\infty k_\nu d\nu = RJ_0 C_2 l N \sigma, \quad (6)$$

where σ stands for Krafts' integral $\int_0^\infty k_\nu d\nu$.

It will be shown later that linear absorption takes place at even lower effective thicknesses than the square-root absorption given above.

* The transmission T_c measured with an optic-acoustic detector differs from the value of transmission measured with a non-selective receiver, and agrees with it for $\varphi(\sqrt{\beta w}) = 1$.

SENSITIVITY OF THE GAS ANALYZER

The sensitivity of a gas analyzer is defined as smallest detectable concentration of gas under stigation. Let us call a concentration the eshold concentration" when the signal ΔS_{th} corponding to it is twice the size of the noise. a square-root dependence of the signal on the ctive thickness of the layer, the threshold conration, according to (5), is

$$C'_t = \frac{\Delta S_{th}^2}{R^2 J_o^2 \Delta\nu^2 \beta l N}$$

for a linear dependence it is:

$$C'_t = \frac{\Delta S_{th}}{R J_o \sigma l N}.$$

In both cases the sensitivity of a gas analyzer, a constant intensity of radiation, depends arly on the number of passages. An increase in intensity of radiation has a greater effect on eshold sensitivity of the square-root case than of linear one.

The effective thicknesses for which Eq. (6) ls have been determined. For this purpose, a gle-pass cell was placed in front of the optic-astic receiver filled with carbon dioxide (w=1cm). pressure in the cell could be varied from 1 to atm.* A mixture of carbon dioxide and argon was roduced. The effective thickness was varied by nging the pressure. It follows from the graph n in figure 3 that linear absorption takes place he effective thickness is varied from 0.001 to 06 cm.

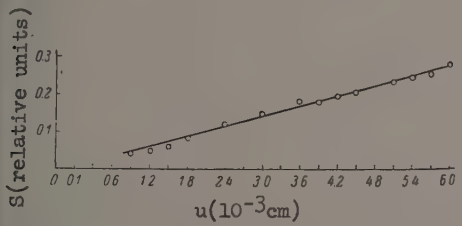

Figure 3. Curve of signal vs. effective thickss of the layer.

In the pressure range investigated (3–20 atm.), otal pressure dependence of the signal caused by adening of lines was not observed for the same ective thickness. Therefore, if the sensitivity the receiver is such that it can detect reduced cknesses of carbon dioxide, less than 6.10^{-3} cm, should use Eq. (8) in order to estimate the sitivity.

Sometimes the comparison cell may contain a ture of non-absorbing gas and the gas under inveation. We need to estimate how great the difence between the gas concentrations in the rating and comparison cells must be for detection.

The concentration of gas in the comparison cell will henceforth be called the initial concentration. (For instance, with air in the comparison cell containing 0.03% CO_2, it is necessary to estimate the sensitivity of the gas analyzer indicating CO_2 under these conditions). If the initial concentration is so small that a linear absorption law remains valid in the total range of variation of the number of radiation passages, then the smallest detectable difference in concentrations $\Delta C'_t = C_2 - C_1$ does not depend on initial concentration C_1 and equals the threshold concentration C_t. At initial concentrations where a square-root law prevails and concentrations in the two cells differ but little, i.e. $\frac{C_2-C_1}{C_1} \ll 1$, the threshold signal is, to a sufficient degree of accuracy, expressed by the relation

$$\Delta S'_t = \frac{1}{2} R J_o \Delta\nu \sqrt{\frac{\beta l N}{C_1}}\, \Delta C'_t, \qquad (9)$$

i.e., $\Delta C'_t$ is inversely proportional to the square-root of the number of passages and depends on initial concentration.

Thus, if the absorbing gas present in the comparison cell is of such concentration that the square-root law holds the sensitivity of the gas analyzer drops as compared with the case where the absorption is linear.

We have determined the threshold concentration for two cases. In the first, the comparison cell contained argon, and the operating cell contained a mixture of argon and carbon dioxide. The threshold concentration of carbon dioxide was 2.10^{-5}%. In the second case, the comparison cell had air containing 0.03% carbon dioxide, while the operating cell contained air with a somewhat larger carbon dioxide content. Under these conditions the smallest difference in concentrations which could be detected was 2.10^{-4}%.

Using Eqs. (8) and (9) one can determine the effective width $\Delta\nu$ of the 4.3μ band of CO_2 where the absorption we have observed, mainly, took place. It follows from Eqs. (8) and (9) that

$$\Delta\nu = 2\sigma \frac{C_t}{\Delta C'_t} \sqrt{\frac{C_1 l N}{\beta}}.$$

Assuming that $\sigma = 2700\ \text{cm}^{-2}$ [7], we have on the basis of the last equation, $\Delta\nu \approx 250\ \text{cm}^{-1}$.

OPTIMUM NUMBER OF PASSAGES

In Eqs. (5) and (6) the signal is proportional to the number of passages, assuming that the intensity of radiation remains constant. However, one must keep in mind that with an increase in the number of passages the radiation flux decreases due to losses in reflection from the mirrors and due to astigmatism** which increases as the number of passages of radiation in the cells increases.

*Experiments on investigation of the relationween the signal developed by an optic-acoustic eiver and pressure of the mixture in the cell e carried out together with V. V. Stolypin.

** Weakening of the flux due to astigmatism occurs because of spreading of the image of the input slit on the plane of output slit.

Let us assume that astigmatism can be neglected. If κ is the reflection coefficient of the mirrors, the intensity of radiation after N passages will be equal to $J_o\kappa^{N-1}$. Finding a maximum of Eqs. (5) and (6), while taking into account the dependence of intensity on the number of radiation passages, leads to the optimum number of passages; for the case of the square-root law,

$$N_{opt} = -\frac{1}{2\ln\kappa} \tag{10a}$$

and for the linear case

$$N_{opt} = -\frac{1}{\ln\kappa}. \tag{10b}$$

Thus, the largest number of passages which it is expedient to use in a multipath gas analyzer is different for the two cases; the largest number of passages can be realized with the linear law. Experimental determination of the weakening of the radiation flux, due to losses in reflections from aluminum coatings of the mirrors in one of the cells, has shown that the reflection coefficient in the 4.3μ region is 0.97. This verification was carried out by measuring the signal with different numbers of passages in the cell filled with argon. On the basis of Eqs.(10a) and (10b) the optimum number of passages for the cases considered is 16 and 32 respectively. If the aluminum coating is replaced with a gold one (coefficient of reflection 0.98) it can be expected that optimum number of passages will increase in the square-root case to 24, and in the linear case to 48.

Let us now examine the effect of astigmatism. It was shown in Ref. [8] that the weakening of the radiation flux F, proportional to the spectral intensity J_o, due to astigmatism in the cell, may be represented by the relation

$$F = F_o\left(1 - \frac{A\Delta x'}{2b}\right), \tag{11}$$

where F is the flux weakened by astigmatism, F_o is the unweakened flux; 2A is the relative cell aperture, b is the slit height, $\Delta x'$ is the magnitude of longitudinal astigmatism which in turn is represented by [9]

$$\Delta x' = \frac{8d^2}{\ell N^2}\left[\left(\sum_{i=1}^{i=\frac{N}{2}} i^2\right) - \frac{N}{8} - \frac{1}{2}\right],$$

where d is the distance between the centers of the input and output slits of the cell and i is a positive integer.

Usually d is chosen such that all of the surface of mirror III is covered with the image of the slit, i. e., $d = \frac{aN}{2}$, where a is the width of the cell slit. Substituting this relation into the expression for $\Delta x'$, and the latter into (11) and letting $\eta = \frac{Aa^2}{b\ell}$ and $\theta = \sum_{i=1}^{i=\frac{N}{2}} i^2 - \frac{N}{8} - \frac{1}{2}$, we find that the weakening of the flux is determined by the product of η (which is independent of the number of passages), and θ, (which is a function of the number of passages).

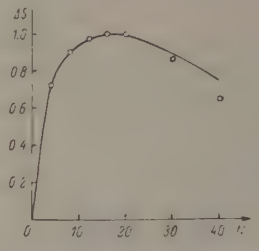

Figure 4. Curve of signal developed by a multipass gas analyzer vs. number of passages of radiation inside a cell.

The relation between the signal developed by the multipass gas analyzer and the number of passages (accounting for losses due to astigmatism and reflections from the mirrors for the two cases — square-root and linear) with no absorbing gas in comparison cell is

$$\Delta S = RF\Delta\nu\sqrt{\beta C_2 \ell N}[(1-\eta\theta)\kappa^{N-1}], \tag{12a}$$

$$\Delta S = RF\sigma C_2 \ell N[(1-\eta\theta)\kappa^{N-1}]. \tag{12b}$$

Since θ is not a monotonic function of N, the determination of the optimum number of passages in closed form is impossible. However, it can be found (for an instrument with known design parameters which determine the value of η) by choosing N such that the expressions in the square brackets of Eqs. (12a) and (12b) are maximum. Since η depends on the design parameters A, b, ℓ, and a, the latter must be selected in designing instruments such that losses due to astigmatism do not exceed a certain prescribed value. In the gas analyzer described losses due to astigmatism were approximately 3% at N=16, 10% at N=24, and 48% at N=40. Therefore, the optimum number of passages, considering losses from astigmatism, is not greater than 24, even for a comparatively small relative aperture of the cells (1:6).

For determination of the optimum number of passages, the operating cell was filled with atmospheric air, containing approximately 0.03% carbon dioxide and the comparison cell with pure nitrogen. A curve corresponding to Eq. (12a) for negligibly small astigmatism and κ=0.97, and also experimental values of the signal with a different number of passages (circles), are given in figure 4. The curve is normalized with respect to the signal corresponding to 16 passages, where a maximum occurs. The largest signal is observed approximately for the same number of passages. As is seen from the graph, in the range of N from 0 to 30 ($C\ell N$=0.45 cm) the points lie on the curve; as the number of passages is increased further, the signals computed from the formula are larger than the measured ones. This is due to the fact that at effective thicknesses greater than 0.45cm one can not use the square-root approximation but must use Eq. (2), and astigmatism cannot be neglected.

On the basis of the equations derived here, one can estimate how many times greater the sensitivity of a multipass gas analyzer is than the sensitivity

one with a single pass of the beam. Sensitivity selective optic-acoustic receivers nowadays is n that in many cases they can be used to detect in the cells at such low concentrations that re is a linear relationship between the signal and thickness of the layer. In this case, with ciple passage and no absorbing gas in the compa-on cell, the gain in sensitivity is given by

$$\alpha = N\kappa^{N-1}(1-\eta\theta),$$

re α is the ratio of the threshold concentration n single passage of radiation, to the threshold centration with multiple passage. Substitution he values of the parameters of the instrument ribed in (13) shows that approximately 10 times ller concentrations can be detected with it, as pared to a single-pass instrument of equivalent rture ratio. When a small difference in concen-tions is to be detected in the background of an tial concentration in the comparison cell, and n absorption in this cell following the square-t law, the gain α' will be smaller. It is given

$$\alpha' = \sqrt{N}[\kappa^{N-1}(1-\eta\theta)].$$

On the basis of this study one can conclude t a multipass gas analyzer can most rationally used to indicate small concentrations of gas, n absorption in the cells follows a linear law.

The data on threshold sensitivity of a gas analyzer ($C_t = 2.10^{-5}\%$) corresponds to a bandwidth Δf=50 cps. the sensitivity of a gas analyzer would be $6.10^{-7}\%$. Using an output meter with greater inertia, for instance, when Δf = .0.05 cps, the sensitivity of a gas analyzer would be 6:10-7%

If a gas mixture, to be analyzed in a multi-pass gas analyzer, were compressed, the sensitivity threshold should correspondingly increase approxi-mately in proportion to the degree of compression.

August 2, 1958.

REFERENCES

1. J. U. WHITE: JOSA, 32, 285, (1942).
2. H. J. BERNSTEIN, G. HERZBERG: J.Chem.Phys., 16, 30, (1948)
3. M. L. VEINGEROV: DAN USSR, 19, 687, (1938)
4. M. L. VEINGEROV: ZL, 13, 426, (1947)
5. W. M. ELSASSER: Heat transfer by infrared radia-tion in the atmosphere. Harvard, 1942.
6. J. N. HOWARD, R. M. CHAPMAN: JOSA, 42, 856, (1952)
7. D. WEBER, R. J. HOLM, S. S. PENNER: J.Chem.Phys. 20, 1820, (1952)
8. N. N. GÜBEL': Zhurn. opt.-mekh. prom., (2), 33, (1956)
9. T. P. REESOR: JOSA, 41, 1059, (1951)

TOM VII, Vyp. 1
VOL. VII, No. 1

OPTIKA I SPEKTROSKOPIIA
OPTICS AND SPECTROSCOPY

Iiul', [illegible]
July, [illegible]

BRIEF REPORTS

On One Characteristic of Image Curvature in Short Focal-Length Lenses in Electron Optics

O. I. SEMAN

Electron optic images, like light images, have a curved image surface. From field aberrations vanishing in the center of the image, curvature and astigmatism lead to great lack of sharpness, especially noticeable at the edges when the image is of a large surface area. The curvature of the image is different for pencils of unequal spatial orientation, meridian, sagittal and intermediate. Of the general characteristics of electron-optic curvature of short focal-length lenses it is known that (1) the Petzval curvature is positive $\frac{G_{00}}{m} > 0$, and (2) the mean curvature of magnetic lenses is positive $\frac{\beta_n}{m} > 0$. Although these conditions have already been described [1, 2] in somewhat more general form, however, as shown in [3] their actual significance is limited to the statements cited. The conditions in (1) and (2) are insufficient for any kind of conclusion concerning the sign of the meridian or sagittal curvature. In [4] are given the bounds of the coefficients from which the positivity of the sagittal curvature of magnetic lenses and the corresponding numerical inequalities follow. Certain sufficient conditions for positive curvature coefficients have been cited in the literature [5]. They are complicated differential expressions, which require checking along the whole optical path.

Further information regarding the general characteristics of curvature, and especially conditions for their correction, is highly desirable. If it is established that $\frac{G_{22}}{m} > 0$, then, in view of condition (1), it follows that all the rest of the coefficients of curvature are positive. This follows (see [6]) from the relation.

$$\frac{\beta_e}{m} = e\frac{G_{00}}{m} + (3-e)\frac{G_{22}}{m}, \tag{1}$$

where β_e is the coefficient of curvature and the subscript $e = 0, 1, 2, 3$ refers, respectively, to the meridian, mean, sagittal, and Petzval curvature.

Let us examine the normal coefficient of meridian curvature G_{22}, which can be stated:

$$32\left(r_\alpha^B \frac{G_{22}}{m} + \frac{1}{6\rho}\right) = \int_{Z_a}^{Z_b} \left\{[2h' r_\alpha r_\gamma + h(r_\alpha r_\gamma)']^2 + \right.$$

$$\left. + \frac{1}{2}[2h^2 r_\alpha r_\gamma + r'_\alpha r'_\gamma]^2 + \frac{13}{6} r'^2_\alpha r'^2_\gamma \right\} dr + \frac{20}{3}\left|\frac{r'_\gamma}{r_\gamma}\right|_{Z_a}^{Z_b}.$$

In the field-free regions $h \equiv 0$, the constant integrable member $(\frac{1}{2} + \frac{13}{6})\, r'^2_\alpha r'^2_\gamma$ remains. In the short section of the lens with non-zero field, essentially positive members are added. The final sum of integrated members is not larger than the coefficient of curvature. Setting up the formula for the coefficient $\frac{G_{22}}{m}$ for electric lenses is more complicated The bounds obtained by this means for the coefficient $\frac{G_{22}}{m}$ are given in the one inequality*.

$$\left(r_\alpha^B \frac{G_{22}}{m} + \frac{1}{6\rho}\right) > \frac{1}{3} k_1 \left|\sqrt{\frac{V_a}{V}}\, \frac{r'_\gamma}{r_\gamma}\right|_{Z_a}^{Z_b} + \tag{2}$$

$$+ \frac{1}{3} k_2 \left(l_a r'^2_{\gamma a} + l_b \frac{1}{m^2} \sqrt{\frac{V_a}{V_b}}\, r'^2_b\right),$$

where m is the magnification, l_a, l_b are the lengths of field-free sections adjoining the obj and image, and k_1, k_2 are numerical multiplier We clearly distinguish the position of the diaphr

$$r_\gamma = r_\beta - k r_\alpha,$$

where $k = \left(\frac{r_\beta}{r_\alpha}\right)_B$, we introduce the notations:

$$A = k_2\left[l_a + \frac{l_b}{m^4}\left(\frac{V_a}{V_b}\right)^{3/2}\right] > 0; \tag{3}$$

$$C = \left(k_1 + k_2 l_b \frac{r'_{\beta b}}{m}\right)\frac{r'_{\beta b}}{m}\sqrt{\frac{V_a}{V_b}} > 0;$$

$$B = k_1\left(1 - \frac{V_a}{V_b}\cdot\frac{1}{m^2}\right) - 2k_2 l_b \frac{V_a}{V_b}\cdot\frac{r'_{\beta b}}{m^3}.$$

The right part of inequality (2) is a quadra function of the quantity k, which characterizes the position of the diaphragm. From (2), (3), we obtain the following condition of positivity and the inseparability of the meridian curvature inde pendently of the position of the diaphragm

$$B^2 - 4AC < 0. \tag{4}$$

If (4) is not fulfilled, then when k lies within the limits $\frac{1}{A}(-B \pm \sqrt{B^2-4AC})$, the right part of (2) is negative, but for other values of k, this part is, as before, positive as is $\frac{G_{22}}{m}$. In order to illustrate in more detail the clusion arrived at, let us consider single vanish thin lenses, for which there holds

$$V_a = V_b;\ l_a = \frac{l}{1-m};\ l_b = \frac{l}{1-\frac{1}{m}}; \tag{5}$$

$$-\frac{1}{r'_{\beta b}} = f_2 = \frac{-l}{m\left(1-\frac{1}{m^3}\right)^2},$$

* In future we will take a flat object $\frac{1}{\rho} =$ [illegible]

...e $l = Z_b - Z_a$, is the overall length of the ...em. Defining $x = -\frac{1}{m}$, we obtain

$$B^2 - 4AC = k_1^2(1+x)^2\left\{x^2 - 2\left[1 + 2\frac{k_2}{k_1} + 2\left(\frac{k_2}{k_1}\right)^2\right]x + 1\right\}.$$

For electric lenses $k_1 = 3 \cdot 0.1305$; $\frac{5}{64} \cdot 3 \cdot 2.9130$. Substituting these values in ... it is possible to find the sufficient condition ...he defectiveness of G_{22}, i.e.

$$0.05 < -m < 22.$$

In every region of practical importance for ...le-stage reflection from 20-power reduction to ...power magnification in very short electric lenses meridian curvature is uncorrected.

For magnetic lenses $k_1 = \frac{5}{8}$, $k_2 = \frac{1}{4}$. Accord-...ly, the sufficient condition of the positivity ...$\frac{G_{22}}{m}$ is written

$$\frac{1}{4} < -m < 4.$$

In view of the fact that in inequality (2) part ...he positive terms were omitted, the meridian ...vature of short focal-length lenses is positive ...a considerably wider region of magnification. ...s region decreases, becomes dependent on the ...ition of the diaphragm, or vanishes, when trans-...ring to long and immersion lenses.

The sufficient conditions obtained here are ...remely simple. The exact conditions of the ...itivity of $\frac{G_{22}}{m}$ or of the correction of G_{22} ...low from considering G_{22} as functions of the ...fficients of spherical aberration, coma and ...vature with focal localization of the diaphragm, ...ressed through R_α R_β of the solution

$$G_{22}(\gamma) = G_{22}(\beta) + 2kG_{21}(\beta) + k^2G_{20}.$$

If the coefficients $G_{22}(\beta)$, $G_{21}(\beta)$, G_{20} ... known, then from the right side of the equality ... considered as a function of k, the character-...ics of the lens may also be determined; the ...rrection corresponds to the real roots, if they ...st, but when

$$G_{21}^2(\beta) - G_{22}(\beta)\cdot G_{20} < 0$$

... image curvature is uncorrected.

From formulas (2), (3) qualitative conclusions ...o follow for long focal-length lenses. Indepen-...t of multiplicity, as follows from (2), we have the relation

$$r_\alpha^B \frac{G_{22}}{m} > \frac{1}{3}k_1\left|\sqrt{\frac{V_a}{V}}\cdot\frac{r'_\gamma}{r_\gamma}\right|_{Z_a}^{Z_b}.$$

When the position of the diaphragm corresponds to k is determined from the inequality

$$k\left(1 - \frac{V_a}{V_b}\cdot\frac{1}{m^2}\right) + \frac{r'_{\beta b}}{m}\sqrt{\frac{V_a}{V_b}} > 0, \tag{11}$$

the coefficient of meridian curvature is positive, $\frac{G_{22}}{m} > 0$. If, here, there is no magnetic field at the object and image points, then the meridian surface curvature is positive and the corresponding surface of meridian foci is inverted concave to the object.

We distinguish two regions of magnification: I) $-m > \sqrt{\frac{V_a}{V_b}}$, II) $-m < \sqrt{\frac{V_a}{V_b}}$. Considering that $r'_{\beta b} = -\frac{1}{f_2} < 0$, it is easy to find, as a sufficient condition of the positivity of $\frac{G_{22}}{m}$, the following bound for the position of the diaphragm

$$k > -\frac{r'_{\beta b}}{m}\sqrt{\frac{V_a}{V_b}}\;\frac{1}{1 - \frac{V_a}{V_b}\cdot\frac{1}{m^2}}, \tag{12}$$

in which the inequality sign relates to region I and the minus sign to region II.

As a particular result of (12) we find: when magnification is greater than $\sqrt{\frac{V_a}{V_b}}$ (region I) and the diaphram is between the second focus and the object $(k>0)$, or when the magnification is less than $\sqrt{\frac{V_a}{V_b}}$ (region II) and the diaphram is between the second focus and the image, the coefficient of meridian curvature $\frac{G_{22}}{m}$ is uncorrected, and the meridian curvature is also uncorrected.*

May 9, 1958

REFERENCES

1. H. VOIT: Zs. f. Instrumentenkunde, 59, 71, (1939)
2. V. K. ZWORYKIN, G. A. MORTON, E. G. RAMBERG, I. HILLIER, A. W. VANCE: Electron Optics and the Electron Microscope, John Wiley and Sons, New York, 1945
3. O. I. SEMAN: Radiotekhnika i Elektronika, 3, No. 2, 283 (1958) (See Radio Engineering & Electronics)
4. O. I. SEMAN: DAN USSR 93, 443 (1953)
5. P. P. KAS'IANKOV: ZTF 20, 1426 (1950)
6. O. I. SEMAN: Tr. IFAAN ESSR, No. 2, 3 (1955)

* In the absence of magnetic immersion.

TOM VII, Vyp. 1 OPTIKA I SPEKTROSKOPIIA Iiul', 195
VOL. VII, No. 1 OPTICS AND SPECTROSCOPY July, 195

The Valence Angle of Oxygen in the HOCl Molecule

L. V. GURVICH AND M. M. NOVIKOV

In molecules of the type X_2O the valence angle of oxygen ranges from 102 degrees (F_2O) to 110 degrees (Cl_2O). Some increase in the angle of the Cl_2O molecule in comparison with its value in other molecules of this type is perhaps explained by both the steric factors and the change of the valence state of the oxygen atom. At the same time, these two causes apparently cannot effect any substantial increase in the valence angle of oxygen in such a molecule as HOCl. The value $\angle$ HOCl = 113 degrees as calculated by Hedberg and Badger is therefore questionable.

Hedberg and Badger investigated the infrared spectrum of gaseous HOCl and measured five intervals in the fine-structure of the $2\nu_2$ band. Using these data, the authors determined the quantities $A'' - \frac{1}{2}(B'' + C'') = 19.97$ cm^{-1} and $\frac{1}{2}(B'+C') = 0.48$ cm^{-1}. They compared their results with calculations based on the values $r_{OH} = 0.957$ Å (as in H_2O) and $r_{OCl} = 1.70$ Å (as in Cl_2O) for various values of the angle HOCl; they came to the conclusion that the best agreement was obtained for $\angle$ HOCl = 113 degrees.

Since one may assume that the valence angle of oxygen in the HOCl molecule cannot exceed 110 degrees, we again calculated $A - \frac{1}{2}(B + C)$ and $\frac{1}{2}(B + C)$ for various values of HOCl and various O-H and O-Cl distances as well. (These distances in the HOCl molecule can differ as much as 0.01 – 0.05 Å from their values in H_2O and Cl_2O). The results of these calculations are presented in the table.

The Values $a = A - \frac{1}{2}(B + C)$ and $b = \frac{1}{2}(B + C)$ for various values of r_{OH}, r_{OCl}, and $\angle$HOCl (in cm^{-1})

Experimental values: $a = 19.97$ cm^{-1} and $b = 0.48$ cm^{-1}.

r_{OCl}(in Å)		r_{OH}(in Å)									
		0.940			0.957			0.970			
		$\angle$ HOCl (in degrees)									
		94	96	98	98	101	104	113	102	104	106
1.65	a	19.81	19.99	20.21	19.48	19.88	20.52	22.96	19.56	19.92	20.34
	b	0.53	0.53	0.53	0.52	0.52	0.52	0.52	0.52	0.52	0.52
1.70	a	19.85	20.02	20.23	19.52	19.95	20.54	23.03	19.60	19.96	20.39
	b	0.49	0.50	0.50	0.49	0.49	0.49	0.48	0.48	0.48	0.48
1.75	a	19.86	20.00	20.22	19.53	19.96	20.55	23.13	19.61	19.97	20.39
	b	0.47	0.47	0.47	0.47	0.47	0.47	0.46	0.47	0.47	0.47

Comparing the values $A - \frac{1}{2}(B + C)$ and $\frac{1}{2}(B + C)$ calculated for various geometrical parameters of HOCl, one may draw the following conclusions:

1. The quantity $A - \frac{1}{2}(B + C)$ is practica (within the limits of the accuracy of the determi tion) independent of the length of the O-Cl bon from 1.65 to 1.75 Å but is greatly dependent the length of the O-H bond and on the angle HO

2. The quantity $\frac{1}{2}(B + C)$ remains constant for 0.94 Å $\angle r \angle 0.97$ Å and $94^\circ \angle$ angle HOCl $\angle 113^\circ$, but the discrepancy between the val $\frac{1}{2}(B + C)$ which were calculated for r_{OCl} values 1.70 and 1.75 Å are within the limits of the e of determination of this quantity.

Thus, the value of the valence angle of oxyg in the HOCL molecule may be determined by the pre method only by comparing the calculated and the observed values of $A - \frac{1}{2}(B + C)$. At the same time it is seen from the table for the geometrical parameters assumed in reference [1] ($r_{OH} = 0.95$ $r_{OCl} = 1.70$ Å and HOCl = 113 degrees), the valu calculated for $A - \frac{1}{2}(B + C)$ differs from the experimentally determined value by more than 2 c This indicates an erroneous choice of the values of the geometrical parameters for HOCl in [1] despite the coincidence of the values for $\frac{1}{2}(B+C$

Comparing the values of $A - \frac{1}{2}(B + C)$ whic were calculated for various values of $\angle$ HOCl and r_{OH} with the value $A - \frac{1}{2}(B + C) = 19.97$ cm^{-1}, and taking into account that the error of the lat cannot exceed 0.5 cm^{-1}, we conclude that $\angle$ HOCl 104 ± 3 degrees. We may eliminate any lower values which lead to agreement between calculated and observed values of $A - \frac{1}{2}(B + C)$ for $r_{OH} = 0.$ since the valence angle of oxygen in all molecule exceeds 100° degrees. This permits us to take $r_{OH} = 0.96 \pm 0.01$ Å. The data obtained from [1] do not permit of an accurate definition of the length of the Cl-O bond in the HOCl molecule, although it is seen from the table that

$$1.68 \text{ Å} \leqslant r_{OCl} \leqslant 1.75 \text{ Å}.$$

Thus we conclude that the estimation of the angle between the bonds of HOCl in reference [1] was in error and that the correct value of the angle is 104 ± 3 degrees.

November 5, 19

Reference

1. K. HEDBERG, M. BADGER: Journal of Chemical Physics, 19, 508,(1951)

VII, Vyp. 1
VII, No. 1

OPTIKA I SPEKTROSKOPIIA
OPTICS AND SPECTROSCOPY

Iiul', 1959
July, 1959

On the Nature of the Intermediate Product in the Photoreduction of Eosin

N. N. BUBNOV, L. A. KIBALKO, V. F. TSEPALOV, AND V. IA. SHLIAPINTOKH

The photoreduction of eosin consists in the con-ion of the dye into the leuco-compound. The anism of this reaction has been studied [1, 2] otentiometric and spectral methods. It has been blished that the reaction proceeds in stages the formation of an intermediate product.

The detailed study of the kinetics of the reac- which was conducted in these investigations led he assumption that the relatively stable inter-ate product is a free radical – a semiquinone of dye. The kinetics of the reaction are best des-ed by the scheme:

$$E^* \xrightarrow{k_1} E{\cdot}H \xrightarrow{k_3} EH_2$$

$$\downarrow k_2$$

$$E$$

re E^* and E are eosin in the excited and ground es, respectively; $E{\cdot}H$ is the semiquinone of n, and EH_2 is the leuco compound.

The lifetime of the intermediate product depends ely on the temperature and varies from several nds at room temperature to 1-2 minutes at −35 −40° C. When the experiments were conducted at temperature, the concentration of the inter-ate product amounted to 10–15%, while at −35 -40° C., the concentration amounted to approxi-ly 50% of the initial concentration of the dye. bsolute units, for an eosin concentration of moles/liter this would amount to $5 \cdot 10^{15}$ ticles per cm^3 (at room temperature).

If the intermediate product is actually a free ical, then it would be natural to expect that it ld be detected by the electron paramagnetic nance (EPR) method.

The present work was carried out with the object elucidating the nature of the intermediate luct.

The photoreduction reaction was conducted in the nator of an EPR-spectrometer with high-frequency ulation of the magnetic field [3]. An SVDSh-250 p was used as light source. The light of the p was filtered through a 4 cm layer of a 10% ution of $CuSO_4$. With the aid of an optical tem, an image of the arc was projected into the ction ampoule, located in the resonator of the -spectrometer.

The concentration of eosin in the pyridine solu-ns amounted to 10^{-4} moles/liter. Ascorbic acid $^{-3}$ moles/liter) was used as reducing agent. In er to remove oxygen, the ampoule with the mixture reagents was twice frozen under vacuum and sealed er vacuum.

When the light is turned on, an EPR signal ses. In the presence of uninterrupted illumina-n, the intensity of the signal gradually increases, ches a maximum, and then falls to zero. Thus, the etics of the variation of the signal intensity ee qualitatively with the kinetics of variation of concentration of the intermediate product. Appropriate checking experiments showed that when binary dye-solvent and reducing agent-solvent systems are illuminated, the EPR signal is absent. The lifetimes of the intermediate product and of the radical registered by the EPR method proved to be identical. These facts indicate that the EPR method detects the same intermediate product which was detected earlier by the spectral and potentiometric methods [1, 2].

The EPR spectrum obtained is presented in the figure, from which it is evident that the spectrum consists of a triplet with a hyperfine splitting of $\Delta H = = 4.6 \pm 0.2$ Oersteds. The ratio of the intensity of the components of the hyperfine structure is 1 : 2 : 1.

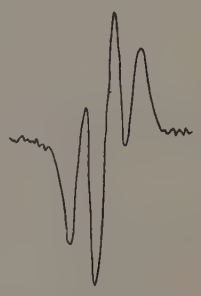

10 Oersteds

EPR spectrum of the semiquinone of eosin.

To elucidate the EPR spectrum obtained, let us consider the mechanism of the photochemical reactions of eosin and the properties of its excited molecules. The photochemically active state of eosin appears to be a metastable biradical state [4-7]. In this state eosin can enter into both oxidation and reduction reactions [2, 8, 9]. In particular, the biradical of eosin can take on either an atom of hydrogen or a molecule of oxygen, depending on experimental conditions.

To explain the double reaction capacity of the biradical of eosin, Schenck [10] advanced the hypothesis that the biradical is formed via the opening of a double bond of the quinoid oxygen. Under these conditions, the free valencies are localized on the atom of oxygen and on the 9 carbon atom, which explains the capacity of the biradical to add hydrogen and to add oxygen. According to the scheme of Schenck, the semiquinone of eosin has structure III.

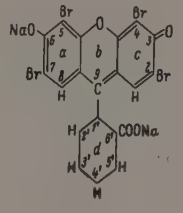

I – Eosin

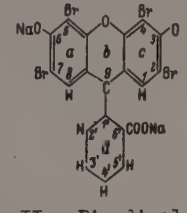

II – Biradical of Eosin

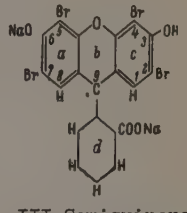

III-Semiquinone of Eosin

The free valence was localized on the 9 carbon atom. From an analysis of the EPR spectrum, one can deduce an interaction of the free valence in the semiquinone with the two hydrogen atoms which are in an equivalent position in relation to the site of the free valence. Two such hydrogen atoms are actually in radical III; they are found in positions 8 and 1. In general, no other two hydrogen atoms in rings a, b, and c, are equivalent. The interaction of the unpaired electron with the hydrogen atom in position 2' is not manifested in the EPR spectrum. This interaction should apparently be very weak, inasmuch as the plane of the benzene ring d is oriented at an angle to the plane of the molecule.

The transition from the eosin molecule (I) to the free radical (III) is associated with the disappearance of the quinoid structure of the ring. Such a change in structure always leads to a displacement of the optical absorption band of the corresponding compound toward shorter wavelengths. The existence of a similar shift of the absorption band was noted in [2]; the shift in this case amounted to 115 mμ (pyridine solution).

Thus, the present theories concerning the structure of the biradical and the semiquinone of eosin permit one to explain their chemical properties, the change of the optical spectra, and the hyperfine structure of the EPR spectrum.

CONCLUSIONS

1. The EPR [electron paramagnetic resonance] spectrum of the half-reduced form of eosin has bee obtained. The spectrum consists of a triplet; the magnitude of the hyperfine splitting is $\Delta H = 4.6 \pm 0.2$ Oersteds. The ratio of the intensity of the components is 1: 2: 1, which indicate an interaction of the unpaired electron with two equivalent protons.

Analysis of the EPR spectrum permits one to co clude that the free valence of the half-reduced fo of eosin is localized on the carbon atom in positi 9.

November 25, 195

REFERENCES

1. V. F. TSEPALOV, V. IA. SHLIAPINTOKH: DAN USSR, 116, 641-644, (1957)(See Sov. Phys. Dokla
2. V. F. TSEPALOV, V. IA. SHLIAPINTOKH: IAN USSR, OKhN, (4), 637-643, (1959)
3. A. G. SEMENOV, N. N. BUBNOV: PiTE, (1), 92, (1959) (See Translation)
4. S. BOUDIN: J. Chim. Phys., 27, 285-290, (1930)
5. E. V. GRISHKUN, E. V. SHPOL'SKII: ZFKH, 19, 97-106, (1945)
6. G. N. LEWIS, D. LIPKIN, T. T. MAGEL: J. Amer. Chem. Soc., 63, 3005-3018, (1941)
7. A. H. ADELMAN, G. OSTER: J. Amer. Chem. Soc., 78, 3977-3980, (1956)
8. H. KAUTSKY, A. HIRSCH, W. FLESCH: Ber., 68, 152-162 [156], (1935)
9. K. BURGHERR: Zeitschrift f. Wiss. Phot., 24, 393-408, (1927)
10. G. O. SCHENCK: Zeitschrift f. Elektrochem., 56, 855-868, (1952)

TOM VII, Vyp. 1 OPTIKA I SPEKTROSKOPIIA Iiul', 195
VOL. VII, No. 1 OPTICS AND SPECTROSCOPY July, 195

Investigation of the Temperature Dependence of the Intensity and Width of Raman Lines

N. I. REZAEV AND A. S. ANDREEV

A number of investigations [1-11] have shown an anomalous temperature variation of the intensity of the Stokes lines in the Raman effect of substances in the liquid state. As the temperature increased, the integrated intensity of the lines decreased or remained constant, and did not show the increase expected from the well-known theoretical relation

$$I \sim \frac{1}{1-\exp[-\frac{h\nu}{kT}]} . \quad (1)$$

The reasons for this deviation from the theory have not been definitely established. It should be noted that in many investigations no account was taken of the temperature broadening of the lines, which can have an effect on the measured intensities.

The method followed in the present investigation permitted accurate measurement of the integrated intensities of the lines and, at the same time, observation of the temperature variation of their widths. The spectrum of liquid m – xylene was investigated in the temperature range −30° to 160°C on a photoelectric spectrometer with narrow slits. The values of the intensity were not corrected for the variation of the density d and the refractive index n of the substance with temperatu These corrections can be taken in account [12-14] by multiplying the experimental values of the inte sity by the ratio n^2/d; however, calculations show that the ratio changes very little in the temperature range used.

A study of the line-widths is in itself of scientific interest. It has already been establis that the width of depolarized lines depends in a definite way on the temperature and on the dimensions of the molecule [11, 15, 16]; this can be explained as an effect of relaxation processes in liquid [17]. The present investigation is a conti nuation of these studies.

The results of the investigation of the tempe ture dependence of the integrated intensities of t lines of m – xylene are given in Table 1. Data ar also given in the table for the intensities of the lines of p – xylene, which was studied previously one of the authors [11]. Inasmuch as the molecule of these substances have very similar structures i is of interest to compare the temperature behaviou of their line intensities. The table gives the ra

Experimental and Theoretical Dependence of the Line Intensities I on the Temperature

Frequency (cm^{-1})	279	517	538	726	1000	1036	1095	1171	1251	1267	1379	1592	1613
Primary vibrational form	β_{CCC}	γ	γ	Q	γ	β_{CH_3}	β	β	q_{C-C}	β	β_{CH_3}	β	β
$I^{+160°C}/I^{-30°C}$ (expt)	0.27	0.57	0.63	0.84	0.61	0.30	0.22	0.25	0.57	0.57	0.38	0.65	0.52
$I^{+160°C}/I^{-30°C}$ (theor)	1.33	1.16	1.14	1.08	1.03	1.03	1.025	1.02	1.01	1.01	1.00	1.00	1.00
Departure from theory (%)	80	51	45	22	41	71	78	76	43	43	62	35	48
Frequency (cm^{-1})	313	645	459	829	—	—	—	—	1205	—	1379	—	1618
Primary vibrational form	β_{CCC}	γ	γ	Q	—	—	—	—	q_{C-C}	—	β_{CH_3}	—	β
$I^{+90°C}/I^{+4°C}$ (expt)	0.77	0.86	0.85	0.86	—	—	—	—	0.78	—	0.69	—	0.81
$I^{+90°C}/I^{+4°C}$ (theor)	1.14	1.09	1.05	1.02	—	—	—	—	1.01	—	1.00	—	1.00
Departure from theory (%)	33	21	19	16	—	—	—	—	23	—	31	—	19

the intensities of the lines for the two extreme mperatures, as determined experimentally and as lculated by the theoretical formula given in Eq.). The assignment of the lines to the various des of vibration was made by a comparison of the brations of m – xylene [18] and p – xylene [19] th those of benzene for which theoretical calcula- ons of the vibrational modes are available [20].

It is seen from the table that the integrated tensities of the lines of both substances studied crease with rising temperature and do not increase would be expected on the basis of the theoretical rmula. The results which show the greatest viation from the theory are underlined in the ble. As a rule the greatest anomaly is observed r the lines which originate in deformation vibra- ons involving the outer angles of the ring and e CH_3 groups, that is, vibrations of the form β.

e intensity of the line due to the valence vibra- on Q of the skeleton of the ring departs least of l from theory. The deformation vibrations of the rm γ, which are related to changes in the inner gles of the ring, and the valence vibrations of rm q have the same temperature dependence for eir line intensities. It is conceivable that ese deviations from the theory are caused by ntermolecular interactions. If this is the case, e deformation vibrations of the outer angles uld experience the greatest effect from the neigh- oring molecules. The influence of the form of the ibration on the dependence of the intensities of aman lines on temperature [6, 10] and concentra- ion [21] has been noted previously. Our results nfirm the investigations [6, 21] in which a marked eparture of the intensities from the expected rend was observed for the line of deformation ibrations involving HCC angles (form β).

There is no close correlation between line roadening and the anomalous temperature variation f line intensities. For example, the polarized ine at 1036 cm^{-1} is broadened relatively little ith temperature, whereas the departure of its inten- ity from the theoretical trend is very great. The absence of any correlation between the temperature variation of the width and anomalies of the line intensity has been noted previously [11]. Apparently a marked temperature broadening of the lines and the deviation of their intensities from theory are related to different physical causes.

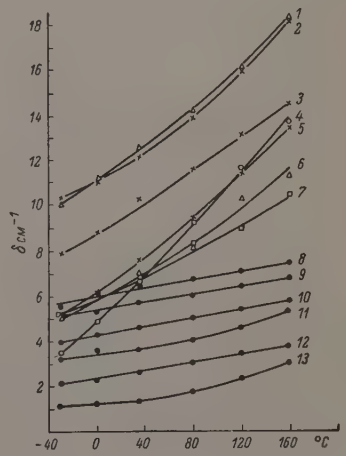

Figure 1. Variation of the line-widths, δ, of m-xylene with temperature:

Curve 1- ν=1613 cm^{-1}, ρ=0.68; 2- ν=279 cm^{-1}, ρ=0.65; 3- ν=517 cm^{-1}, ρ=0.60; 4- ν=1171 cm^{-1}, ρ=1.00; 5- ν=1592 cm^{-1}, ρ=0.68; 6- ν=1379 cm^{-1}, ρ=0.59; 7- ν=1095 cm^{-1}, ρ=0.50; 8- ν=1036 cm^{-1}, ρ=0.20; 9- ν=1267 cm^{-1}, ρ=0.10; 10- ν=1251 cm^{-1}, ρ=0.15; 11- ν=538 cm^{-1}, ρ=0.25; 12- ν=1000 cm^{-1}, ρ=0.12; 13- ν=726 cm^{-1}, ρ=0.16.

ν — frequency, ρ — depolarization factor of the line.

The temperature broadening of lines depends on their degree of depolarization, as shown in figure 1. The lines with the largest degree depolarization show the most rapid change of line-width with temperature. The shape of the line contour at different temperatures approximates the dispersion line form. These facts agree with the theoretical conception of the effect of random orientational transitions of the molecules in a liquid on the width of Raman lines [17].

The temperature broadening of completely depolarized lines due to orientational transitions of molecules is determined by the quantity $1/\tau$, where τ is the mean time between the random reorientation transitions of the molecules (relaxation time). The results of various investigations [11, 15, 16], and also of the present one, show that a part δ_o of the line width is not connected with temperature broadening brought about by reorientation transitions but is due to other causes. This is seen for example, from the fact that lines with the same depolarization factor have different widths at the same temperature (see Figure).

With this fact as a basis and also recalling that the observed and the theoretical profiles due to relaxation effects have the dispersion form, it is possible by using the well-known expression for the relaxation time τ to express the width of a line having an arbitrary polarization by means of the formula

$$\delta = \delta_o + \gamma \frac{1}{\tau_o} \exp\left[-\frac{U}{kT}\right], \qquad (2)$$

In this expression γ is a function of the depolarization factor, ρ, of the line with the following limits: $0 \leqslant \gamma \leqslant 1$, when $0 \leqslant \rho \leqslant \frac{6}{7}$; τ_o is a constant having the significance of a period of vibration of the molecule about a relatively stable position of equilibrium; U is the activation energy necessary for the transition of the molecule from one relatively stable equilibrium position to another; k is Boltzmann's constant and T is the absolute temperature.

From a comparison of the experimental temperature variation of the line-width with formula (2), values of δ_o, γ, τ and U were determined for the lines with $\rho \geqslant 0.5$. In the calculations τ_o was assumed to be 0.38×10^{-12} sec, as determined from the temperature variation of the width of the line at 1171 cm^{-1} for which $\rho = 1.00$ and $\gamma = 1.00$. The relaxation time τ was determined for 20° C. The quantities $\tau_{20^\circ C}$ and U have almost the same values for all the lines investigated; the mean values were $\tau_{20^\circ C} = 5.8 \times 10^{-12}$ sec and $U = 1600$ cal per mole. The lines differed from one another in the width δ_o; this is apparently related to some individual characteristic of each vibration of the molecule.

The values obtained for τ, τ_o and U agree very well with the results of determinations by other methods. For example, $\tau_{20^\circ C}$ for m – xylene determined from the depolarized background in the neighborhood of the Rayleigh line [22] is equal to 5.4×10^{-12} sec, by the resonance filter method, and 6.6×10^{-12} sec by the line-width method. The activation energy, U obtained from the temperature variation of the viscosity of m – xylene is equal to 1800 cal per mole.

Thus the temperature broadening of the lines of m – xylene can be explained in the main as a result of relaxation processes in the liquid. This, of course, does not exclude the possibility that intermolecular forces influence the temperature broadening of the lines to some extent. It is possible that the observed increase in width with temperature in the case of strongly polarized lines is connected with an effect of this kind.

In conclusion we express deep gratitude to P. A. Bazhulin for his great assistance in bringing this work to completion.

December 24, 1958.

REFERENCES

1. K. VENKATESWARLU: Nature, 159, 96 (1947)
2. K. VENKATESWARLU: Curr. Sci., 16, 15 (1947)
3. L. M. FISHKOVA: DAN USSR, 75, 523 (1950)
4. IA. S. BOBOVICH, D. K. ARKHIPENKO: DAN USSR, 86, 247 (1952)
5. IA. S. BOBOVICH, V. M. PIVOVAROV: DAN USSR, 97, 801 (1954)
6. IA. S. BOBOVICH: DAN USSR, 98, 39 (1954)
7. IA. S. BOBOVICH: IAN USSR, Phys. Ser., 19, 219 (1955) (See CTT Bulletin)
8. A. I. STEKHANOV, E. V. CHISLER: ZTF, 25, 2209 (1955)
9. IA. S. BOBOVICH, V. M. PIVOVAROV: Mat. of the X All-Union Conference on Spectroscopy, 1, 223 (1957)
10. A. I. SOKOLOVSKAIA, P. A. BAZHULIN: Mat. of the X All-Union Conference on Spectroscopy, 1, 225 (1957)
11. N. I. REZAEV: Vestn. MGU, No. 2, 145 (1957)
12. L. A. WOODWARD, J. H. B. GEORGE: Nature, 167, 193 (1951)
13. H. J. BERNSTEIN, G. ALLEN: J. Opt. Soc. Amer., 45, 237 (1955)
14. A. I. SOKOLOVSKAIA, S. G. RAUTIAN: OiS, 6, 51 (1959) (See 6, p. 29)
15. N. I. REZAEV: Mat. of the X All-Union Conference on Spectroscopy, 1, 230 (1957)
16. N. I. REZAEV: OiS, 5, 561 (1958)
17. I. I. SOBEL'MAN: IAN USSR, Phys. Ser., 17, 554 (1953)
18. M. A. KOVNER, A. M. BOGOMOLOV: OiS, 4, 301 (1958)
19. M. A. KOVNER: DAN USSR, 97, 229 (1954)
20. M. A. KOVNER: ZETF, 26, 598 (1954)
21. IA. S. BOBOVICH, T. P. TULUB: ZETF, 30, 189 (1956) (See Sov.Physics JETP)
22. A. K. ATAKHODZHAEV, M. F. VUKS, V. L. LITVINOV: Mat. of the X All-Union Conference on Spectroscopy, 1, 118 (1957)

VII, Vyp. 1
VII, No. 1

OPTIKA I SPEKTROSKOPIIA
OPTICS AND SPECTROSCOPY

Iiul', 1959
July, 1959

On The Problem of the Chemiluminescence Of Lucigenin and Its Derivatives

A. V. KARIAKIN

Research on the kinetics of the chemi-inescence of lucigenin made it possible B. Ia. Sveshnikov to conclude that an ited molecule occurs as a result of suc-sive transformation of the molecule of starting material, and that the main p is the formation of a peroxide compound lucigenin under the action of hydrogen oxide [1]. The hypothesis of Drew, Gleu Petsch was confirmed by this research

It was further shown that a peroxide pound is produced as a result of the ion of the OOH^- ion formed by the elec-lytic dissociation of hydrogen peroxide, that the emission process occurs during interaction of this same ion with the oxide compound [3].

When catalysts are introduced into the ction mixture the luminosity is intensi-d, which the investigators connect with acceleration of the decomposition of the sultant peroxide compound [4], but not of hydrogen peroxide [1].

In order to identify more precisely the arate stages of the kinetics of the chemi-inescence of lucigenin, A.M.Grigorovskii ained various derivatives of lucigenin showed that the pseudo-base of lucigenin not responsible for emission; while -dimethyl biacridine oxide, obtained from pseudo-base of lucigenin by the action alkali, is already capable of emitting k light during the heating of a solution n without the addition of hydrogen oxide. A solution of NN'-dimethyl biacri-e oxide in pyridine combined with hydrogen oxide produces a bright yellow-green miluminescence [5]; NN'-dimethyl biacri-e emits analogously [5,6].

Spectral investigations of lucigenin miluminescence at room and higher tem-ratures could not clarify the mechanism the phenomenon in question, but did show at the fluorescence and chemiluminescence ectra are identical only at room tempera-re and in the absence of a catalyst [7]. high temperature or in the presence of introducible catalyst the chemiluminescent ectrum shifts toward the shortwave region the spectrum.

The present work is devoted to a more tailed study of the photoluminescent and emiluminescent spectra of aqueous solu-ons of lucigenin and of pyridine solutions NN'-dimethyl biacridine oxide and -dimethyl biacridine.

Fluorescent and chemiluminescent spectra the above indicated substances were asured with a photoelectric instrument [8], d their phosphorescence spectra were asured at the temperature of liquid air th the aid of a phosphoroscope by photo-aphic [9] and photoelectric [10] methods.

The following concentrations of solutions were used: lucigenin bromide-0.5%, alkali-2%, and hydrogen peroxide-1%; NN' dimethyl biacridine-1.2%, and hydrogen peroxide 1-2%; NN' dimethyl biacridine-0.2% and hydrogen peroxide 1-2%.

Position of the Main Maxima of the Photo and Chemiluminescence Spectra of Lucigenin and its Derivatives

Designation of Compound	Principal Maxima of Emission (in mμ)		
	Fluo-rescence	Chemi-luminescence	Phospho-rescence
Lucigenin Bromide	480,515	480,515	480,515*
NN'- Dimethyl-biacridine Oxide	505	550	548 **
NN'- Dimethyl-biacridine	515	525	523 **

* From the measurements of B. Ia. Sveshnikov.
** From data of V. L. Ermolaev.

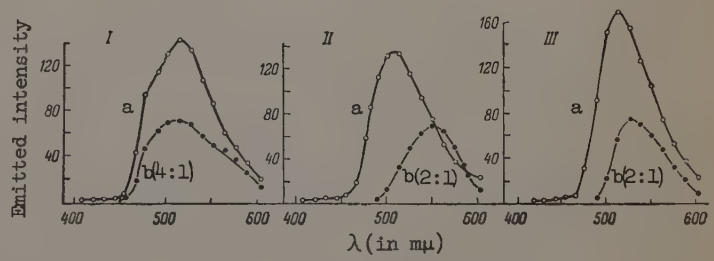

Luminescence spectra of an aqueous solution of lucigenin (I) and of pyridine solutions of NN'-dimethyl biacridine oxide (II) and NN'-dimethyl biacridine (III).

a. Fluorescence. b. Chemiluminescence.

The fluorescence and chemiluminescence spectra of lucigenin (the bromide), NN'-dimethyl biacridine oxide, and NN'-dimethyl biacridine are represented in the figure, and their main emission maxima are shown in the table, where the phosphorescence maxima are also shown.

From the photoluminescence and chemiluminescence spectra it follows that the spectra of NN'-dimethyl biacridine oxide and dimethyl biacridine represent monotonic curves with a single, clearly expressed maximum. In the spectra of lucigenin, two basic maxima are visible. (Some authors note three [7]). Furthermore, for lucigenin bromide, the basic maxima of the fluorescence, phosphorescence and chemiluminescence spectra are the same within the limits of experimental error. In NN'-dimethyl biacridine oxide and NN'-dimethyl acridine, a good correspondence was observed only for the chemiluminescence and phosphorescence spectra. Consequently, it is possible to conclude that the phosphorescent, i. e., metastable, triplet level and not the excited singlet level, is responsible for chemiluminescence.

This supports the hypothesis about the chemiluminescence mechanism in complex organic compounds, which postulates the initial formation of transannular peroxides which later decompose into oxygen and a biradical under the influence of thermal

energy. An organic biradical having two unpaired electrons (triplet state) emits a quantum of light corresponding to chemiluminescence [11] during conversion to the singlet ground state.

As a consequence of the fact that the spectra of the chemiluminescence of lucigenin and of NN'-dimethyl biacridine oxide do not coincide with each other (see figure and data of table), their chemiluminescent reactions must be considered as being independent, but related, processes. This is supported by supplementary data on the poor solubility of NN'-dimethyl biacridine oxide in water [5]. Therefore the chemiluminescent mechanism of aqueous solutions of lucigenin should be somewhat clarified, since it follows from the above that NN'-dimethyl biacridine oxide is not an intermediate in the reaction of lucigenin. It is possible that during the reaction there is formed a similar, short-lived, intermediate compound which is easily soluble in water.

As the concentration of hydrogen peroxide in pyridine solutions of NN'-dimethyl biacridine oxide and NN'-dimethyl biacridine is increased, a steady shift of the chemiluminescence spectrum toward the short wave part of the spectrum is observed. By a chemical method, A. M. Grigorovskii discovered N-methylacridone in such a reaction mixture [5]. In all probability, in the present case, the transannular peroxide of the corresponding compound breaks down and two excited molecules of N'-methylacridone, having maximum fluorescence at 415 millimicrons, are formed.

On the basis of published data and this spectral study of the chemiluminescence of lucigenin, NN'-dimethyl biacridine oxide and NN'-dimethyl biacridine, it is possible to conclude that the hydrogen peroxide or, more rapidly, the product of its electrolytic dissociation, forms with the original substance a corresponding transannular peroxide which is responsible for emission. By the action of thermal energy the peroxide is decomposed with the displacement of oxygen and the formation of the corresponding biradical, emitting a quantum of ligh during the transition to the ground state.

The author expresses deep thanks to B. IA. Sveshnikov for allowing the use of his data, and to V. L. Ermolaev for supplying the measurements of the phosphorescence spectra.

December 29, 195

REFERENCES

1. B. IA. SVESHNIKOV: DAN USSR, 35, 311 (1942); Izv. AN USSR, ser.fiz., 9, 341 (1945); B. IA. SVESHNIKOV: P.P. DIKUN: ZFKh, 19, 289 (1945)
2. K. GLEU, W.PETSCH: Zs.Ang.Chem., 48, 57, (1935); H.DREW: Trans.Farad.Soc., 35, 207 (1939)
3. L. ERDEY: Acta. Chim., Acad. Sci. Hung., 3, 81, 103, (1953)
4. H. DECKER, W. PETSCH: J. prep. Chem. (2), 143 230, (1935); K. WEBER: Zs. Phys. Chem., B50, 100, (1941); B. TAMAMUSHI: Sci. Papers Inst. Phys. Chem. Research (Tokyo) 41, 166 (1943); J. KROH: Wiadowasci Chem 7, 23, (1953); 9, 580 (1955)
5. A. M. GRIGOROVSKII, A. A. SIMEONOV: Zh. FKh., 21, 589, (1951)
6. K. GLEU, R. SCHAARSCHMIDT: Ber., 73, 909 (1940)
7. K. KAUTSKY, K. H. KAISER: Naturwiss., 31, 505 (1943); A. SPRUIT van der BURG: Rec. Trav. Chim., 69, 1525 (1950); J. KROH: J. Roczn. Chem., 28, 70, (1954); V. D. RYZHIKOV: Izv. AN USSR, Ser. Fiz., 20, 533, (1956); (See CTT Bulletin) J.KROH, Z.CZERUIK: J.Koczn.Chem., 31, 915(1
8. A. KARIAKIN: Zh. F. Kh., 23, 1332 (1949)
9. B. IA. SVESHNIKOV: ZETF, 19, 1000 (1949)
10. V. L. ERMOLAEV: OiS, 1, 523, (1956)
11. R. B. KURTZ: Trans. N. Y. Acad. Sci., 16, No.8, 399, (1954)

TOM VII, Vyp. 1 OPTIKA I SPEKTROSKOPIIA Iiul', 1959
VOL. VII, No. 1 OPTICS AND SPECTROSCOPY July, 1959

On the Positions of the Extrema of the Light Scattering Function for Spherical Particles

IU. V. MAL'TSEV

The ratio of the radiant flux scattered in all directions by a spherical particle to the flux incident on an area equal to its cross section in a collimated beam, is well know to be described by the function $K(\alpha, m)$, in which $\alpha = \frac{2\pi r}{\lambda}$ is a parameter characterizing the size of the particle, r is its radius, λ is the radiation wavelength in the medium surrounding the particle; $m = n(1 - ix)$ is the complex refractive index in which n is the index of refraction of the particle relative to the external medium, and x is an absorption index.

The scattering functions have primary maxima and minima on which are superposed secondary oscillations in the absence of absorption.

For the calculation of the position of the principal extrema of the curves $K(\alpha, m)$ the following empirical formula is proposed:

$$\alpha_k = 1 + \frac{4k}{mm^* - 1}, \quad (1)$$

where k is a positive whole number, and m^* is the complex conjugate of m.

If $k = 1, 2, \ldots, \nu$, is substituted into (1), the corresponding values of the parameter $\alpha_1, \alpha_2, \ldots, \alpha_\nu$ gives the location of the first, second, . . . , ν-th extrema. Odd k correspond to maxima and even k to minima.

We shall compare results computed by formula (1) with data for transparent and absorbing particle available in the literature.

Transparent particles do not absorb light, and for them $x = 0$ and $mm^* = n^2$. Their scattering function is the function $K(\alpha, n)$. In the lower part of figure 1 appears the simplified function $K(\alpha, n)$ of particles with a refractive index n=1.33 computed by Penndorff [1]. The function has primary and secondary maxima and minima.

The solid lines in figure 1 show the position the maxima of the function $K(\alpha, n)$ for particles different n and the broken lines the position minima. The curves were computed by formula (1). separate points mark the location of the primary rema of the curves $K(\alpha, n)$ computed by ndorff [1, 2], La Mer and Barnes [3], Van de Hulst , and Johnson and Terrell [5]. These points fall the curves satisfactorily with the exception of computations of Penndorff [2] for $n = 2$. It to be noted that the two primary extrema taken n the curve $K(\alpha, n)$ computed by Penndorff agree quately in this region with the curves of figure ut the subsequent extrema diverge from these ves. Penndorff's method of calculation of the rema is not reported.

Figure 1 shows the characteristic properties the light scattering function of transparent icles. The distance between the extrema of n function $K(\alpha, n)$ is constant and equal to ; for functions with different n it decreases

n increasing refractive index. The parameter α, responding to the first maximum also decreases n increasing n; in all curves this parameter is ger the greater the distance between extrema.

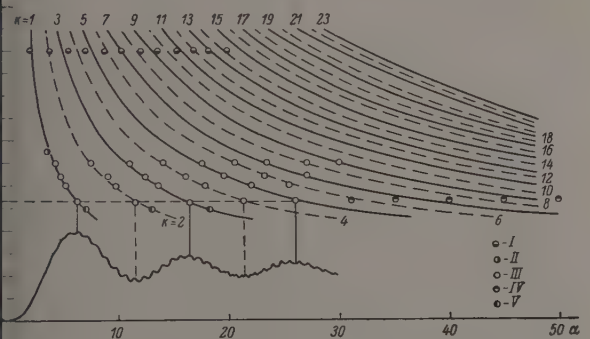

Figure 1. Location of the extrema of the light ttering function for transparent particles with fferent refractive indices.
I. According to Penndorff [2];
II. According to La Mer and Barnes [3];
III. According to Penndorff [1];
IV. According to Van de Hulst [4];
V. According to Johnson and Terrell [5].

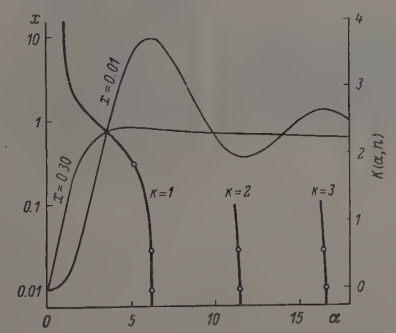

Figure 2. Scattering function for particles $n = 1.33$, and absorption index $x = 0.01$ and $= 0.30$ (light lines). Location of extrema of e light scattering function in relation to the sorption index x (heavy lines).

Absorbing particles both scatter and absorb light; for them $mm^* = n^2(1 + x^2)$. In figure 2 are shown two light scattering functions $K(\alpha, n)$ of spherical particles with $n = 1.33$ and with absorption coefficients $x = 0.01$ and $x = 0.30$. The curves are taken from reference [5]. As x increases, the scattering functions all have less pronounced maxima and finally become curves with one maximum.

In addition, figure 2 shows curves giving the relation between positions of the first three extrema ($k = 1, 2, 3$) computed by formula (1) for particles with $n = 1.33$ and absorption index x. The separate points show the location of the extrema according to Johnson and Terrell. The points lie satisfactorily on the calculated curves. Formula (1) similarly indicates the presence of maxima of the function $K(\alpha, m)$ for large values of x, but such is not the case: formula (1) is correct only for scattering functions with small x and is suitable for the computation of the position only of the first maximum for all x. In the table are shown results of the location of the first maximum calculated by use of the formula (1).

Location of the First Maximum of the Function $K(\alpha,m)$ for Particles $n = 1.29$ and Different x

Absorption Coefficient - x -	The Parameter α_1, corresponding to a Maximum	
	According to Johnson and Terrell [5]	Calculated by Formula (1)
0	7.0	7.0
0.05	6.6	7.0
0.10	6.8*	6.9
0.25	6.6	6.2
0.50	4.0	4.7
1.00	1.5	2.7
1.73	0.8	1.7
2.00	1.2*	1.5
2.25	1.2*	1.46
4.00	1.2*	1.15
100	1.2*	1
∞	1.5*	1

*Maximums are recorded according to the tabular data of [5].

For weakly absorbing particles the first maximum computed by formula (1) agrees satisfactorily with the data of reference [5]. For large x, the values diverge. For a definite judgement concerning the applicability of formula (1) for large x, it is necessary to have supplementary information about the function $K(\alpha, m)$.

We note the following characteristic of the location of the extrema of the scattering function of absorbing particles. If $x \ll 1$, then the location of the extrema of the curves remains the same as for transparent particle curves. However, the magnitudes of the maxima decrease and for further increase of x only the first maximum remains, and its parameter α_1 tends to unity.

The computation of the location of the extrema of the scattering function by formula (1) is very simple and gives sufficiently accurate results for practical purposes.

December 30, 1958

REFERENCES

1. R. B. PENNDORFF: JOSA, 47, 1010, (1957)
2. R. B. PENNDORFF: JOSA, 46, 1001, (1956).
3. V. K. LA MER, M. D. BARNES: J. Colloid Sci., 1, 79, (1946) (cited in D.Sinclair, JOSA, 37, 475, (1947)
4. H. C. VAN de HULST: Recherches Astronomiques de l'Observatorie d'Utrecht 9, part 1, 1946. (cited in Houghton, H.C., and Chalker, W.R., JOSA, 39, 955, (1949)).
5. J. C. JOHNSON, J. R. TERRELL: JOSA, 45, 451, (1955).

TOM VII, Vyp. 1 OPTIKA I SPEKTROSKOPIIA Iiul', 1959
VOL. VII, No. 1 OPTICS AND SPECTROSCOPY July, 1959

Luminescence of Alkali Halides Containing Uranyl Salts

I. P. SHAPIRO

It is well known that uranium is capable of yielding a series of ions ranging from U^{3+} to U^{6+}. The investigations of Feofilov [1] showed that monocrystals of CaF_2+U luminesce brilliantly only after being heated in air. From this it may be inferred that this phenomenon is linked with the formation of hexavalent U^{6+} ions in the crystal. It follows from the principle of local compensation [1] that when CaF_2+U crystals are heated in air, oxygen ions diffuse into the crystals.

An investigation of powders of KBr, KCl, KF, and NaCl containing small amounts of ammonium-uranyl sulphate [$(NH_4)_2UO_2(SO_4)_2.2H_2O$], disclosed that these salts fluoresce intensely at room temperature under the action of near ultra-violet. (These powders were precipitated from aqueous solution.) The intensity of luminescence increases in the direction KBr → KF.

The melt obtained from the above mentioned compounds at a temperature on the order of 1,000° C is also characterized by a strong luminescence, the intensity of which becomes greater, the longer the sample is kept (from 15 to 30 minutes) in the smelting furnace. If these compounds are fused in a nitrogen atmosphere, they will not luminesce; however, if the fusion is repeated in air, their ability to luminesce is restored. Repeated fusion of the same samples in a nitrogen atmosphere and in air indicated that the availability of oxygen during fusion plays an important role in the ability of these salts to luminesce. Apparently, during the fusion the formation of the hexavalent ion U^{6+} also occurs owing to the diffusion of the oxygen ions, which isomorphically replace the positively charged ions in the previously mentioned alkali-halide compounds.

In view of the fact that the luminescence of these compounds differs from the luminescence of pure uranyl compounds in intensity and coloration, an investigation was made of the fluorescence spectrum of NaCl for various uranyl salt [$(NH_4)_2UO_2(SO_4)_2 \cdot RH_2O$] contents. The spectra were obtained with an MS-3 glass spectrograph, using three-hour exposure periods. (10 minutes for pure ammonium-uranyl-sulfate). The spectra are shown in figure 1a. The phosphor NaCl + U... is characterized by a continuous spectrum, the appearance of which one may interpret as the emission of the uranium ions transformed by the crystalline lattice. The spectrum of the same phosphor at liquid air temperature (figure 1b) is characterized by the presence of bands superimposed on the continuous spectrum. This is connected with the weakening of the oscillations of the crystalline lattice.

The duration of the luminescence was measured with a phosphoroscope and proved to be of the order of 10^{-4} sec.

No photo-conductivity was detectable by the capacitor method in the wave-length region of 230-800 mμ.

The results of investigations of the dependence of the intensity of the luminescence of the phosphor KCl + U... on the concentration of uranyl salts are given in figure 1c. Figure 2 shows micro-photometer tracings of the spectra. The most intense spectrum was that obtained at a concentration of 10^{-3} g/g. The luminescence is no longer observed for a concentration of 10^{-4} g/g.

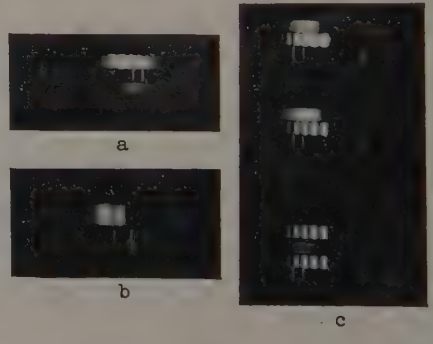

Figure 1. Emission spectra of compounds of the type NaCl+U.

a -- NaCl+U... and pure ammonium-uranyl-sulfate at room temperature; b -- NaCl+U... at liquid air temperature; c -- KCl+U... as a function of the concentration of ammonium-uranyl-sulfate in KCl. Top-- 10^{-2} g/g; middle -- 10^{-3} g/g; bottom -- 10^{-1} g/g.

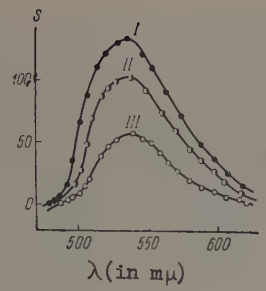

Figure 2. Microphotometer (in mμ) tracings he spectra of the radiation of KCl+U... as a tion of the concentration of ammonium-uranyl- fate in KCl. Concentrations (in g/g): I-- ; II-- 10^{-2}; III-- 10^{-1}.

In conclusion, I express my thanks to L. V. Volod'ko who participated in the discussion of the results of this work.

January 15, 1959

References

1. P. P. FEOFILOV : IAN USSR FS, 21, (5), 779, (1957) (See CTT Bulletin 776)
2. S. M. RYVKIN : ZTF, 18, 1521, (1948)

M VII, Vyp. 1 O P T I K A I S P E K T R O S K O P I I A Iiul', 1959
L. VII, No. 1 O P T I C S A N D S P E C T R O S C O P Y July, 1959

Optical and Scintillation Characteristics of Oxadiazoles

N. A. ADROVA, V. N. ANDREEV, M. M. KOTON,
IU. N. PANOV, AND N. S. MUSALEV

In order to obtain more effective plastic scin- lators, compounds of the oxadiazole series were estigated: 2-α-naphthyl-5-(n-biphenyl)-1, 3, 4- diazole (α-NBD) (I) and 2-phenyl-5-(n-biphenyl)- 3, 4-oxadiazole (PBD), (II).

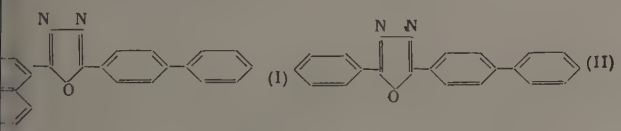

For comparison, the characteristics of the viously investigated [1] 2, 5-diphenyl-oxadiazole I) and n-terphenyl (IV) are cited.

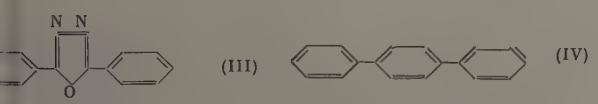

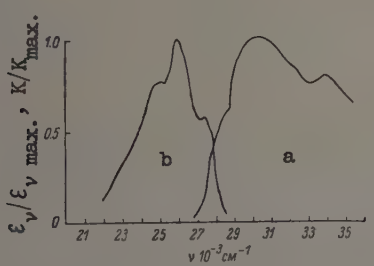

Figure 1. Spectra of absorption (a) and lumi- cence (b) of α-NBD.

Syntheses of these compounds were carried out cyclization of the corresponding diaroylhydrazines Plastic scintillators were obtained by the low perature polymerization method [3]. Scintillation ivity, or light yield of scintillation, was deter- ed on an apparatus described earlier [4].

The standard taken for 100% activity is the sample which contained 2% by weight of terphenyl in polystyrene. The scintillator was irradiated by γ-rays from a Co^{60} source. The absorption spectra of the materials were determined on a SF-4 spectrophotometer in benzene solution. The luminescence spectra were determined with a quartz monochromator and FEU-19 photoelectric multiplier while irradiating with an ultraviolet source of λ=313 mμ. A correction was introduced into the spectra for the spectral sensitivity of the apparatus and the self-absorption. The quantum yields of luminescence were measured in relation to a solution of anthracene in benzene (1 mg/cm3 in concentration). The values of the quantum yields cited are approximately those of an infinitely dilute solution. The results of the investigations are presented in the table.

From the data in the table, we see that α-NBD and PBD have significantly greater scintillation activity than n-terphenyl (by about 25%).

Compound Name	Optimal Concentration in Polystyrene (%)	Scintillation Light Yield (%)	Quantum Yield of Luminescence	λ_{max} Absorption (mμ)	λ_{max} Luminescence (mμ)
Terphenyl	2	100	6.5	287	342
α-NBD ..	1	125	5.5	328	384
PBD	1.5	123	5.1	310	360
PPD	1.5	83	6.0	300	334

The improvement in scintillation activity might be explained by the data in the table and the optical characteristics in figures 1, 2, and 3. The first representative of the series studied, PPD, has a comparatively high quantum yield, however, the luminescence spectrum of this compound lies in the spectral

region where the sensitivity of the photoelectric multiplier is very low. This leads to a low value of scintillation activity.

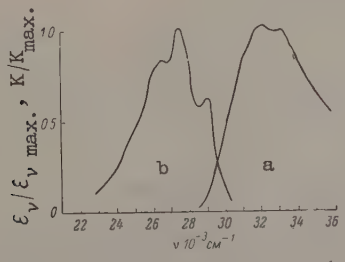

Figure 2. Spectra of absorption (a) and luminescence (b) of PBD.

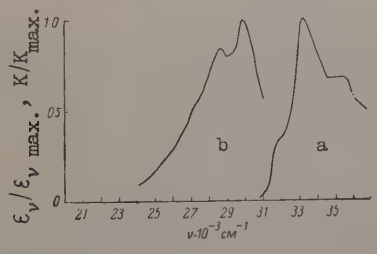

Figure 3. Spectra of absorption (a) and luminescence (b) of PPD.

In the compounds α-NBD and PBD the quantu yield remains comparatively high, while at the sam time the luminescence spectrum is shifted to the region of maximum sensitivity of the photoelectric multiplier (400-500 mμ).

Earlier, in a large number of compounds it wa established that an increase in the number of rin in a scintillator molecule causes an increase in scintillation activity due to a displacement of th luminescence spectrum to longer wave-length.

In examining the absorption and luminescence spectra of the compounds studied, we must observe that in PPD (Fig. 3) the distance between the maxi of the curves is approximately equal to 3000 cm^{-1} while this distance in α-NBD (Fig. 1) and PBD (Fig is 5000 cm^{-1}. This might cause additional self-absorption and, consequently, a lowering of the scintillation activity.

In conclusion, we must note that the compound studied of the oxadiazole series might be used as effective scintillation admixtures for registering radioactive radiations.

January 30, 195

REFERENCES

1. IU. N. PANOV, N. A. ADROVA, M. M. KOTON: OiS, 29, (1959) (See this issue)
2. F. N. HAYES, B. S. ROGERS AND D. G. OTT: JACS, 77, 1850, (1955)
3. N. A. ADROVA, M. M. KOTON, F. S. FLORINSKII: IAN USSR, OKhN, No. 3, 385, (1957)
4. N. A. ADROVA, M. M. KOTON, IU. N. PANOV, F. S. FLORINSKII: IAN USSR FS, 22, 41, (1958) (See CTT Bulletin)

TOM VII, Vyp. 1 OPTIKA I SPEKTROSKOPIIA Iiul', 195
VOL. VII, No. 1 OPTICS AND SPECTROSCOPY July, 195

Influence of Current Strength on the Intensity of the Spectrum of Hydrogen in the Region 2500-1200 Å

I. I. GROMOVA AND S. A. KULIKOV

Hydrogen lamps, operated on either low or high voltage, are widely used at the present time as light sources for the vacuum region of the spectrum. The hydrogen discharge shows a continuous spectrum in the region 4000-1700 Å, but beginning at 1670Å and extending to shorter wave-lengths the many-line spectrum of the hydrogen molecule is observed.

An increase in the current strength in the lamp leads to an increase in the intensity of the emission. As has been shown in the investigations of Chalonge [1], the emission intensity of the hydrogen discharge is proportional to the current at low current strengths. The dependence on current strength of the intensity of the line L_α= 1216 Å of atomic hydrogen can also be represented as a linear function of the current, as has been shown by experiments with phosphors [2]. Only in the investigation of Ivanova and Iakovleva [3], who worked with a low-voltage hydrogen lamp in the region 1700-2500 Å, was the dependence of the intensity on the current strength found to be non-linear. However, no special studies of such dependence appear to have been carried out for the vacuum region of the spectrum.

In the present study the intensity measurement were made with the SP-68 vacuum monochromator. The radiation detector in this instrument is a FEU-19 photomultiplier with a sodium salicylate screen. The photocurrent of the multiplier passes through a DC amplifier and is measured by a microammeter.

Measurements were first carried out for high-voltage hydrogen lamps with a lithium fluoride win and without any window. This type of water cooled lamp is an extended source with power of 350-400 watts. In the present work the lamp capillaries were 4 mm in diameter and 100 mm long, and wer filled with hydrogen to a pressure of 3-4 mm Hg. The pressure of the stream of hydrogen through the lamp without a window was 2-2.5 mm Hg. The hydro gen used in filling the lamps was obtained from an electrolyzer and then dried over phosphorus pentoxide. The current strength of the lamp was varied from 0.02 to 0.4 amp. For the lamp without a window the intensity was measured at the wave-lengths 1216, 1350, 1610, 1900, 2250 and 2558 Å. The results of the measurements are shown in figure 1, in which the current strength in

eres is plotted along the abscissa, and along the inate axis the ratio, $I_i/I_{0.04}$, of the intenty at a given current i to the intensity at the est current intensity. As may be seen from the ph, the variation of the emission intensity with current strength is linear only for the line, of atomic hydrogen.

Similar measurements were made for a lamp with ithium fluoride window; the results are given figure 2.

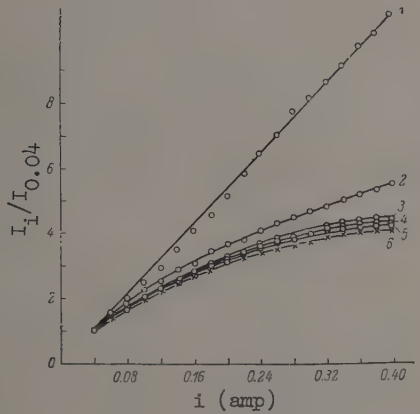

Figure 1. Curve 1) 1216 Å; 2) 1350 Å; 1610 Å; 4) 1900 Å; 5) 2250 Å; 6) 2558 Å.

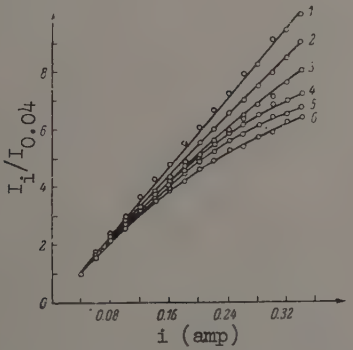

Figure 2. Curve 1) 1216 Å; 2) 1250 Å; 1610 and 1350 Å; 4) 2250 Å; 5) 1975 Å; 2558 Å.

In addition, intensity measurements were made for e low-voltage GOI hydrogen lamp. This gives a int source of light; it has an oxide-coated cathode d operates without water cooling at a power level about 300 watts. The current was varied from 6 to 5 amp. The results of the measurements e given in figure 3.

In further experiments with the high-voltage mp with the lithium fluoride window, the variaon of the emission intensity was measured as a nction of the pressure of hydrogen in the lamp; e pressure was varied from 0 to 50 mm Hg. A eady discharge appeared in the lamp at a pressure about 1.5 mm Hg, but at a pressure of about mm Hg the lamp went out. The graph given in gure 4 shows that the intensity of the hydrogen ntinuum depends only slightly on the hydrogen essure.

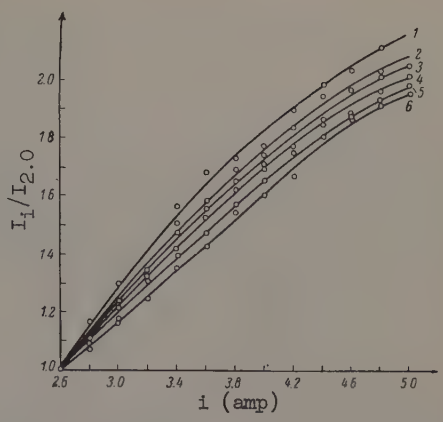

Figure 3. Curve 1) 1250 Å; 2) 1350 Å; 3) 1600 Å; 4) 1825 Å; 5) 1900 Å; 6) 2558 Å.

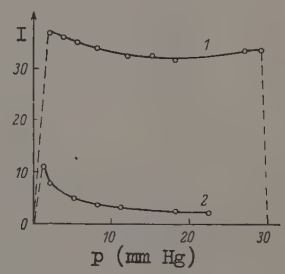

Figure 4. Curve 1) region of the continuous spectra around 1900 Å; 2) the line at 1216 Å.

An examination of the graphs in figures 1, 2, and 3, shows that the dependence of the emission intensity on the current strength has the same form for all the lamps, and that the curves show only slightly different slopes for the various lamps. In all three cases the curves which refer to the continuous spectrum of hydrogen show the greatest departure from linearity. The curves which refer to the many-lined spectrum of hydrogen have markedly smaller curvatures, especially for the high-voltage lamp with the window. For the atomic line, L_α, the dependence of the intensity on the current strength is linear in all cases. From this one can conclude that an increase in the current strength affects the excitation of the triplet state and of the singlet state of the hydrogen molecule in different ways; the difference is even greater for the excitation of the atomic spectrum.

The discrepancy between the results of the present investigation and the results of Ivanova and Iakovleva [3] can be ascribed to the lower reliability, especially in the vacuum region, of the method of photographic spectrophotometry used in their work. One must also remember that the measurements in the two investigations were not carried out on the same lamp.

February 5, 1959.

REFERENCES

1. D. CHALONGE: Ann. de Phys., 1, 123 (1934)
2. K. WATANABE: Phys. Rev., 83, 785, 792 (1951)
3. M. K. IVANOVA, A. V. IAKOVLEVA: IAN USSR, Ser. Fiz., 14, 561 (1950)

TOM VII, Vyp. 1 OPTIKA I SPEKTROSKOPIIA Iiul', 195
VOL. VII, No. 1 OPTICS AND SPECTROSCOPY July, 195

Influence of the Thickness of Anthracene Crystals on Their Absorption Curves at 20° K

M. S. BRODIN AND A. F. PRIKHOT'KO

Among the numerous investigations of the spectral and optical properties of anthracene crystals there are several [1-4] in which absorption curves were measured, some at low temperatures [1, 2, 4]. These investigations show that anthracene crystals are dichroic in the region of the first electronic transition, and strongly absorb light. Thus, according to our investigation [2], the oscillator strengths of this transition for the a-, b-, and c-components of the spectrum are respectively equal to 0.04, 0.12, and 0.1 *. In the work cited, crystals of approximately equal thickness (~25μ) were employed. The limits of crystal thickness useful for the measurement of κ at the band peaks may range from 0.1 to 0.4μ. The absorption curves of crystals placed in optical contact with a quartz plate, measured at 20° K, showed considerable dependence of κ upon d, indicating significant departures from the Lambert-Buger Law. The results of these measurements form the subject of our report.

Plane-parallel monocrystalline films of anthracene, grown by sublimation from the pure compound, were selected for the work. These films were in good optical contact with the quartz. The optical density curves were measured photoelectrically, with the aid of a photomultiplier. The absorption coefficient was calculated from the usual formula

$$(1) \qquad \kappa(\nu) = \frac{\lg \frac{I_0}{I}(\nu)}{4\pi d \cdot \nu \cdot 0.434},$$

where $\lg \frac{I_0}{I}$ — is the measured optical density, corrected for reflection, and d is the thickness of the crystal. For a calculation of the reflected light, we made a special measurement of the reflection curves of crystals of different thicknesses (0.15 - 0.4μ) with polarized light at 290 and 20° K. It turned out that the correction for reflection obtained by means of direct measurement of R and that calculated with the aid of the Fresnel formula led to approximately the same result.

It should be recalled that the thicknesses of the crystals employed are comparable with the wavelength in the region of the spectrum under investigation. In this case, in order to calculate $\kappa(\nu)$ it is usually necessary to employ the more complete formula, taking into account the phenomenon of interference connected with the small thickness. In our case, however, thanks to the strength of the absorption, it is possible to neglect multiple reflections in even the thinnest crystals and to carry out the calculation of $\kappa(\nu)$ by formula (1). Moreover, assuming that the error in κ is not large, it may be estimated (cf. [5]) by means of the formula

$$(2) \qquad \Delta\kappa = \frac{\lambda}{4\pi d} \ln\left(1 - \frac{(1-\mu^2)(\mu-\mu_q^2)\cos 4\pi\mu d}{8\mu_q \cdot \mu^2\lambda \cdot \frac{I_0}{I}}\right),$$

where μ is the refractive index of the crystal, μ_q is the refractive index of the substrate, and λ is the wavelength. For the first maximum (~25,400 cm^{-1}) of the b-component of the spectrum $\Delta\kappa$ does not exceed 5% of κ in the most unfavorable case. Including a calculation of the other errors connected with the measurement of optical density and thickness, the overall accuracy of determination of κ is estimated to be 12%.

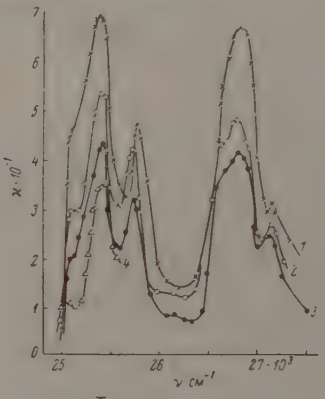

Curves of $\lg \frac{I_0}{I}(\nu)$ were measured at a temperature of 20° K for about 20 crystals with thicknesses in the range 0.15 – 0.40μ. The corresponding curves of absorption coefficient show a substantial dependence on thickness. To illustrate this dependence, the figure shows absorption curves for the b-component spectrum, measured for four crystals: 0.16, 0.21, 0.29, and 0.4μ (curves 1, 2, 3, 4 respectively). Curves 1-3 pertain to the interval 25,000 – 27,500 cm^{-1} and include bands of pure electronic and electron-vibrational (1400 cm^{-1}) transitions; curve 4 represents an electronic transition band only (25,000 – 25,600 cm^{-1}). The dependence of the curves of $\kappa(\nu)$ on thickness is evident, in that κ changes in the same way at the maxima as in other parts of the curves; i.e. the area under the curves changes. Upon decreasing the crystal thickness from 0.40 to 0.16μ, the magnitude of κ at the first maximum increases by almost a factor of two. κ also changes in approximately the same way at the other maxima. Thus the ratio of the maxima at 25,400 and 25,100 cm^{-1} (a band sharply polarized along the b-axis) is essentially constant within the observed range of thickness, increasing somewhat only for the very thickest samples. This indicates a gross violation of the Lambert-Buger Law for the whole region of the first transition.

Everything mentioned above pertains to the b-component of the crystal spectrum. As regards the a-component, the changes occurring in its spectrum

*The oscillator strength of the c-component of the crystal spectrum was estimated by comparison with the absorption of vapors.

h change of crystal thickness have exactly the e character. Roughly speaking, the ratio

is approximately constant, and increases only

ghtly upon thickening the crystal. Along with t abovementioned changes in intensity at T=20°K, re are also some shifts in the absorption ima with change of crystal thickness. Thus upon reasing d from 0.40 to 0.16μ, the maximum 25,400 cm^{-1} shifts in the direction of longer elength by approximately 60 cm^{-1}. The peak responding to the vibrational transition 26,820 cm^{-1} undergoes a shift, which is less tinct, apparently because of the diffuseness of band. The tendency of shift of the maximum at 800 cm^{-1} is opposite: upon decreasing the ckness it shifts in the direction of shorter elengths.

The described changes were observed at a perature of 20° K. Absorption curves measured room temperature in the same range of thick- ses proved to be independent of thickness.

A deviation from Lambert-Buger's Law at the e of the b-component absorption spectrum of an hracene crystal at low temperatures was men- ned in a recently published work of Ferguson Schneider [4]. In their investigation, how- r, no attention was paid to reflection, which quite important in this spectral range. Certain bts are thus raised as to the magnitude of the iation as a function of thickness.

An unequivocal explanation of the observed endence of $\kappa(\nu)$ on d is difficult to make at sent. Therefore in this connection it is only sible to make certain hypotheses. Cooling the stal, which is rigidly attached to the quartz strate, produces large strains in the crystal. This may lead to substantial changes in the spectrum. These usually produce a change in the location and form of the bands [6]. It does not appear very probable that any significant change takes place in the area under the absorption curve as a result of lattice deformation.

It is possible to postulate that in the case of electronic absorption at low temperatures the usual formulas for calculation of the absorption curves are inadequate. There is some basis for this, (however, see [5, 7]) but further experimental and theoretical examination are required for a complete solution of this question.

February 21, 1959

REFERENCES

1. D. P. CRAIG, P. C. HOBBINS: J. Chem. Soc. 539, 2302, 2309 (1955)
2. M. S. BRODIN, A. F. PRIKHOT'KO: OiS, 2, 448, (1957)
3. A. BREE, L. E. LYONS: J. Chem. Soc., 2662, (1956)
4. J. FERGUSON, W. G. SCHNEIDER: J. Chem. Phys., 28, 761, (1958)
5. M. S. BRODIN, A. F. PRIKHOT'KO, M. S. SOSKIN: OiS, 6, 28, (1959) (See 6, 14)
6. V. L. BROUDE, V. V. EREMENKO, V. S. MEDVEDEV, O. S. PAKHOMOVA, A. F. PRIKHOT'KO: OiS, 3, 232, (1958)
7. S. I. PEKAR: ZETF, 34, 1176, (1958) (See Sov. Phys. JETP)

Anniversaries and Dates

VLADIMIR PAVLOVICH LINNIK

(On His 70th Birthday)

In July 1959, Academician Vladimir Pavlovich Linnik, a most outstanding specialist in the field of applied optics, will celebrate his 70th birthday.

V. P. Linnik was born in the town of Khar'kov into the family of a laborer. In 1909, he completed high school in the town of Belaia Tserkov', receiving a gold medal, and in 1914 he graduated from the mathematical physics department of the University of Kiev with a diploma of the 1st class. During World War I, at the University of Kiev, V. P. Linnik organized the production of military optical instruments. After the end of the war, Vladimir Pavlovich taught physics, first at the Belaia Tserkov' technical school and later at the Kiev Polytechnic Institute, where he was in charge of the workshop for precision tools and where he was active in research.

In 1926, at the invitation of Academician D. S. Rozhdestvenskii, V. P. Linnik transferred to the Government Optical Institute. After 1948, Vladimir Pavlovich also worked at the Main Astronomical Observatory of the Academy of Sciences of the USSR at Pulkova. He is a member of the Astrosoviet [Council for Astronomy] at the Academy of Sciences of the USSR and heads a committee for the development of the large six meter telescope.

In 1939, V. P. Linnik was elected a full member of the Academy of Sciences of the USSR.

V. P. Linnik's work is extremely diversified: X-ray optics and the alignment of lenses; optical methods for the study of deformation and microscopy; a variety of applications of the interference of light and the construction of range finders; methods of control of shape and purity in the finishing of metal surfaces and astronomy; the combining of optical methods of measurement with photoelectronics; and many, many other subjects. Vladimir Pavlovich' broad knowledge helps him to recognize important problems in the national economy and to find origina frequently completely unexpected solutions to the problems which arise.

In 1926, V. P. Linnik developed a method of measuring the index of refraction of X-rays which, compared with previously used methods, possessed a significantly greater degree of accuracy. In 1930, he built an apparatus for obtaining Lloyd interference of X-rays, which for the first time made it possible to calculate their wave-length directly. A method of study of the structure of crystals developed by V. P. Linnik is very original. This method, known in the literature as the Linnik metho or the rotating crystal method, makes it possible t obtain a picture of diffraction lines on a photogra plate, the interpretation of these lines being simp than that of Laue photographs.

In the thirties, Vladimir Pavlovich started a round of studies devoted to the development of optic methods of measurement and control used in the machi construction industry. For the first time, he pose and solved the extremely important problem of contac less control of purity in the finishing of metal surfaces. For this purpose he proposed and develope in 1930-1932, two instruments: a double microscope designed to measure the depths of relatively coarse surface marks, and a microinterferometer which permi the control of surfaces to a high degree of purity. The utilization of V. P. Linnik's instruments precludes the danger of scratching the surface being controlled. Additionally, with the help of the microinterferometer it is possible to achieve a high degree of accuracy in measuring the height of irregularities (to the order of 0.01 λ), unattainable with other means of control used in industry. Currently, the microinterferometer and the double micro scope are manufactured here as well as abroad.

In 1945, V. P. Linnik developed another interference instrument for the control of purity of surfaces — a "microprofilometer" which permits, as distinguished from a microinterferometer, the measurement of the depth not only of marks parallel to each other, but also marks caused by finishing which run in all directions. This possibility is achieved as a result of a clever utilization of a cylindrical lens, magnifying in one and only one direction two coherent images of a reflecting flaw. For his work in the control of purity of surfaces V. P. Linnik was awarded the Stalin Prize, 1st Class, in 1946.

Vladimir Pavlovich also did a large amount of work in the development of optical methods of shape or "macroprofile" control of surfaces. He constructed the original interferometer for the control of the rectilinearity of profiles of large flat and cylindrical surfaces (up to 5 m in length) as well as an applied interferometer for the control of metal surfaces up to 200 mm in length. The interference instruments developed on the basis of V. P. Linnik's ideas and under his supervision received the highest award, the "Grand Prix" at the Brussels International Exhibition in 1958. For introducing these interference instruments,

P. Linnik, as well as a group of plant workers, ceived another Stalin Prize in 1950.

Through his work with optical methods of control the machine construction field, V. P. Linnik ve applied optics an increased impetus.

A great service was also rendered by V. P. Linnik the development of the optical-mechanical indus- y. He developed a series of rather original thods of investigation of optical systems, of ich the most interesting one is an "interfero- ter with a translucent disk." In this, as dis- nguished from existing interferometers, an tremely simple method is utilized instead of the nsiderably complicated apparatus for obtaining eal wave patterns: the distorted image of the ght source, produced by the system under examina- on coincides with a small aperture in the trans- cent disk, which is applied to a glass plate. is aperture appears to be the center of an ideal ffractional wave which interferes with the dis- rted wave being studied and which passes through e translucent disk.

Of great practical significance is a method of sembling microscope objectives developed by P. Linnik jointly with P. D. Radchenko. The new thod simplifies considerably the complicated pro- ss of centering the lenses and permits average aftsmen to accomplish an assembly of great curacy. It should also be mentioned that under e supervision of V. P. Linnik there were developed series of instruments for the checking of photo- aphic lenses during their assembly.

V. P. Linnik devoted considerable attention to e problems of microscopy. He was the first to int out the possibility of interference study of orly contrasting biological objects under a icroscope and developed one of the first micro- opes for this purpose.

Even in his early years V. P. Linnik was nterested in astronomy, but he became especially tive in this field later on. Above all he was nterested in broadening the capabilities of the nstruments of astronomy and, particularly, of such n excellent instrument as the Michelson stellar nterferometer. Vladimir Pavlovich showed that the tellar interferometer could serve as a viewfinder for remote luminous object of small angular dimensions. ased on this property was the development, under he supervision of V. P. Linnik, of four new stronomical instruments: an interference transit, stellar interferometer for the measurement of idely-spaced double stars, an interference helio- eter and an interference angle-measuring instru- ent. The last instrument also found application n heavy industry for especially accurate measure- ents of great lengths.

Vladimir Pavlovich proposed a method of making atum marks on spectrum photographs, obtained with he help of a slitless stellar spectrograph. The resence of these datum marks and the method of tudying spectrograms with the help of a stereo- omparator, as developed by V. P. Linnik, consider- bly simplified the measurements of the Doppler hift of spectral lines and increased the accuracy f such measurement.

V. P. Linnik was one of the first to point out he necessity for the uttermost development of pplied optics in conjunction with photoelectronics hich permits replacement of subjective methods f optical measurement and control with accurate bjective methods and makes it possible to realize utomation of control. Currently, in connection with the resolutions of the 21st Congress of the Industrial Cooperatives of the Soviet Union on the automation of industry, this problem assumes a particularly important significance. A series of studies on photoelectronics was completed under the direct supervision of Vladimir Pavlovich. In this manner a photoelectric method for fixing the location of the zero-th interferential fringe was developed, making it possible to automate especially accurate measurements, realized with the help of interferometers operating in white light. There was developed a photoelectric method for the study of aberrations of photographic lenses and a method of control of large flat optical surfaces, permitting the immediate obtaining of a profile of the surface on the chart of an automatic recorder, as well as a method of registration of the moment of passing of interference fringes of the image of a star in a stellar interferometer.

To reduce the influence of the nonuniformity of the atmosphere on the image of a star produced by large telescopes, V. P. Linnik proposed and developed an extremely bold idea regarding the manufacture of an auxiliary telescope mirror composed of sections and the automatic direction of these sections with the help of a tracking system containing an interferometer and a series of photocells. The realization of this idea will make it possible to utilize fully the optimum resolving power of telescopes and will open abundant new possibilities for the study of the universe.

Constant search for the new, latitude and daring in stating and solving new problems connected with various sections of physics, unexpected solutions of specific problems, great mastery in conducting delicate experiments, great intuition, permitting him to forecast results of his work without the execution of complex mathematical calculations, — these are the special characteristics of the style of V. P. Linnik's work. Possessing the craft of an expert mechanic and optician, Vladimir Pavlovich frequently takes pleasure in making various components for his instruments and equipment himself.

During the many years of his fruitful work, V. P. Linnik has gathered around him a group of scientific collaborators, many of whom have independently developed the trends begun by him, but who accept, as before, his help and assistance not only as from a highly learned, but also as from a considerate older comrade.

For his outstanding services to the nation, Academician V. P. Linnik has been decorated with the Order of Lenin, with the Order of Red Workers and the Order of the Red Star.

V. P. Linnik holds a position as member of the editorial staff of the journal "Optics and Spectroscopy".

Currently, V. P. Linnik is occupied with fruitful projects and is full of energy. The editorial staff of "Optics and Spectroscopy", in the name of all Soviet opticians, heartily congratulates Vladimir Pavlovich Linnik on this occasion and wishes him many years of health, good spirit and new successes in his work.

ABBREVIATIONS OFTEN ENCOUNTERED AND USED HEREIN

DAN USSR	Doklady Akademii Nauk	(Reports of the Academy of Sciences of the USSR)
DAN UkrSSR	Dopovidi Akademii Nauk UkrSSR	(Reports of the Academy of Sciences of the Ukraine SSR)
DAN ArmSSR	Doklady Akademii Nauk ArmSSR	(Reports of the Academy of Sciences of the Armenia SSR)
IAN USSR	Izvestiia Akademii Nauk USSR	(Bulletin of the Academy of Sciences of the USSR)
	SF Seriia fizika	(Physics series)
	SM Seriia matematika	(Mathematics series)
	OKhN Otdelenie khimicheskikh	(Section of Chemical sciences)
OiS	Optika i Spektroskopiia	(Optics and Spectroscopy)
PiTE	Pribory i Tekhnika Eksperimenta	(Instruments and Techniques of Experiment)
AE	Atomnaia Energiia	(Atomic Energy)
AZ	Astronomicheskii Zhurnal	(Astronomy Journal)
FMM	Fizika Metallov i Metallovedenie	(Physics of Metals and Metallography)
Radiotekh.	Radiotekhnika	(Radio Engineering)
RiE	Radiotekhnika i Elektronika	(Radio Engineering and Electronics)
UK	Uspekhi Khimii	(Progress in Chemistry)
UFN	Uspekhi Fizicheskikh Nauk	(Progress in Physical Sciences)
UFZ	Ikraninskii Fizichni Zhurnal	(Ukraine Physical Journal)
ZETF	Zhurnal Eksperimental'noi Teoreticheskoi Fiziki	(Journal of Experimental Theoretical Physics - JETP)
ZTF	Zhurnal Tekhnicheskoi Fiziki	(Journal of Technical Physics)
FTT	Fizika Tverkogo Tel	(Solid State Physics)
ZFKh	Zhurnal Fizicheskoi Khimii	(Journal of Physical Chemistry)
ZOKh	Zhurnal Obshchee Khimii	(Journal of General Chemistry)
ZNKh	Zhurnal Neorganicheskoi Khimii	(Journal of Inorganic Chemistry)
ZPKh	Zhurnal Prikladnoi Khimii	(Journal of Applied Chemistry)
Tr.	Trudy	(Transactions, as for instance, Tr. FIAN)
FIAN	Fizicheskii Institut Akademii Nauk USSR	(P.N.Lebedev Physical Institute of the Academy of Sciences USSR)
Sb.	Sbornik	(Collection, as for instance, Fizich. sb. L'vovskogo Universitet) Fizich. sb. Fizicheskaia sbornik (Physics Collection)
Uch. Zap.	Uchenye Zapiskii	(Scientific Records)
Vestn.	Vestnik	(Herald or Messenger)
FTIAN	Fiziko-Tekhnicheskii Institut A Akademii Nauk	(Physical-Technical Institute of the Academy of Science
GOI	Gosudarstvennyi Opticheskii Institut	(State Optical Institute)
VEI	Vsesoiuznyi Elektrotechnicheskii Institut	(All-Union Electrotechnical Journal)
MFTI	Moskovskaia Fiziko-Tekhnicheskii Institut	(Moscow Institute of Physics and Technology)
NIZMIR	Nauchno-Issledovatel'skii Institut Zemnogo Magnetizma, Ionosfery i Rasprostraneniia	(Research Institute of Terrestrial Magnetism and Ionospheric Propagation)
GIFTI	Gor'kovskii Issledovatel'skii Fiziko-Tekhnicheskii Institut	(Gor'kii Research Institute of Physics and Technology)
NIFI	Nauchno-Issledovatel'skii Fizicheskii Institut	(Scientific Research Institute of Physics, Leningrad Univ.)
NIRFI	Nauchno-Issledovatel'skii Radio-fizicheskii Institut	(Scientific Research Institute of Radiophysics, Gor'kii Univ.)
GITTL	Gostekhizdat-Gosudarstvennoe Izdatel'stvo Tekhniko-Teoreticheskoi Literatury	(State Publishers of Technical-Theoretical Literature)
GIFML	Fizmatgizdat-Gosudarstvennoe Izdatel'stvo Fiziko-Matematicheskoi Literatury	(State Publishers of Physical-Mathematical Literature) formerly Gostekhizdat)
IL or IIL	Izdatel'stvo Inostrannoi Literature	(Publishers of Foreign Literature)
Izd. AN USSR	Izdatel'stvo Akademiia Nauk USSR	(Academy of Sciences Press)
ZL	Zavodskaia Laboratoriia	(Factory Laboratory)
GOST	Gosudarstvennyi Obshchesoiuznyi Standart	(All-Union State Standard)
LIPAN USSR	Laboratoriia izmeritel'nykh priborov AN USSR	(Laboratory of Measuring Instruments)
IFAN UkrSSR	Institut Fiziki AN UkrSSR, Kiev	(Physics Institute AN UkrSSR)
SFTI	Sibirskii Fiziko-Tekhnicheskii Institut, Tomsk	(Siberia Physical-Technical Institute)
IFAAN ESSR	Institut Fiziki i Astronomii AN ESSR, Tartu	(Institute of Physics and Astronomy)
IFA AN USSR	Institut Fiziki atmosfery AN USSR	(Institute of the Physics of the Atmosphere)

VII, Vyp. 1
.. VII, No. 1

OPTIKA I SPEKTROSKOPIIA
OPTICS AND SPECTROSCOPY

Iiul', 1959
July, 1959

INFORMATION FOR AUTHORS (Russian)

The following rules apply to manuscripts being submitted to the Editors.

1. Papers which are the results of research conducted in institutions must certainly have the direction of the appropriate institution.

2. The paper should be explained as briefly as possible, compatible with clarity of explanation, and in final form. Repetition of tabular or graphical data in the text should be avoided, as should the representation of numerical results in the form of tables and graphs simultaneoulsy. Each paper should not exceed 12 pages of typewritten text, including figures. Two copies of both text and graphical material should certainly be provided.

3. The paper should start with a brief annotation mentioning the purpose and results of the research. The annotation and the section CONCLUSIONS (if such there be in the paper) must not, however, duplicate each other.

4. The paper should be typewritten on one side of the page, handwritten inserts are not permitted. Formulas should be written legibly in ink. All the manuscript pages should be numbered. The tables and references should be written on separate sheets.

The papers must certainly be signed by the author and when there are several authors, by all of them.

5. In order to avoid confusion and errors, explicit distinction should be made between capital and small letters in the formulas. When the upper and lower case letters are identical in outline but differ only by their size (C and c, I and i, K and k, O and o, P and p, S and s, U and u, V and v, W and w), the upper case letters should be double-underlined (for example, -S) and the lower case letters should receive a double-overline (for example, $\bar{\bar{s}}$). It is necessary to differentiate between the letter O (capital), o (small) and) (zero), where the letters O and o are differentiated by the double underlining and overlining while the zero remains unmarked. The letters I and J should also be differentiated; in order to write the letter I in the manuscript as the Roman one underlined doubly. Greek letters are emphasized by red crayon, vectors by blue or black pencil.

6. Footnotes should be enumerated in order over the whole paper. The references are placed in one list at the end od the paper with the text mention indicated by ordered numbers enclosed in square brackets (for example [1]). The list of references should be composed as follows: a) For journal articles, the initials and surname of the author (or authors), the journal designation (only usually accepted abbreviations to be used), the volume number (underlined by a wavy line), the starting page and the year should be indicated; b) for books it is necessary to indicate the initials and surname of the author (authors), the complete title of the book, the place and year of publication (for foreign books, indicate the data on the Russian translation if such there be).

7. The editors request the authors to use the least number of figures possible.

Figures and photographs should be presented separately from the manuscript and must in no case be glued to the original. It is desirable to provide the figures with clarifying captions which should be collected on a separate sheet. On the back of each figure (and photograph) there should be mentioned: Surname of the author (authors), title of the paper, figure number. Inscriptions on the figures should, if possible, be replaced by numbers (or letter notations) explained in the caption to the figure (or in the text).

8. The editors request the authors to indicate the places in the manuscript which can be in smaller type.

9. There should be indicated at the end of the paper: The exact address, surname, given name and patronymic of the author as well as the home or office telephone number.

10. In case the paper is returned to the author for revision, the date of receipt should be considered the date the Editors receive the final text.

11. The Editors will provide the author with 50 unbound reprints, free.

The journal is published monthly in two volumes per year (6 issues per volume).

SYMBOLS FOR SOURCES OF TRANSLATIONS

AIP
American Institute of Physics
335 East 45th Street
New York 17, New York

ATS
Associated Technical Services Inc.
P. O. Box 271
East Orange, New Jersey

CB
Consultants Bureau, Inc.
227 West 17th Street
New York 11, New York

CCT
Consultants Custom Translations, Inc.
227 West 17th Street
New York 11, New York

CTT
Columbia Technical Translations
5 Vermont Avenue
White Plains, New York

HB
Henry Brutcher
P. O. Box 157
Altadena, California

LC
Photoduplication Service
Publication Board Project
Library of Congress
Washington 25, D. C.

MDF
Morris D. Friedman, Inc.
P. O. Box 35
West Newton 65, Mass.

NRCC
National Research Council Library
Ottawa 2, Canada

OTS
Office of Technical Services
Department of Commerce
Washington 25, D. C.

PS
Primary Sources
11 Bleecker Street
New York 12, New York

RIS
Research Information Service
40 East 23rd Street
New York 10, New York

SLA
SLA Translation Center
The John Crerar Library
86 East Randolph Street
Chicago 1, Illinois

V. GURVICH, M. M. NOVIKOV
O valentnom ugle kisloroda v molekul HOCl 116
The Valence Angle of Oxygen in the HoCl Molecule 70

N. BUBNOV, L. A. KIBALKO, V. F. TSEPALOV, V. IA SHLIAPINTOKH
O prirode promezhutochnogo produkta v reaktsii fotovosstanovleniia eozina
On the Nature of the Intermediate Product in the Photoreduction of Eosin 71

I. REZAEV, N. S. ANDREEV
Issledovanie temperaturnoi zavisimosti intensivnosti i shiriny linii kombinatsionnogo rasseianiia 119
Investigation of the Temperature Dependence of the Intensity and Width of Raman Lines 72

V. KARIAKIN
K voprosu o khemiliuminestsentsii liutsigenina i ego proizvodnykh 122
On The Problem of the Chemiluminescence of Lucigenin and Its Derivatives 75

U. V. MAL'TSEV
O polozhenii ekstremumov funktsii rasseianiia sveta sfericheskimi chastitsami 124
On the Positions of the Extrema of the Light Scattering Function for Spherical Particles 76

P. SHAPIRO
Liuminestsentsiia shchelochno-galoidnykh soedinenii s primes'iu uranilovykh solei 126
Luminescence of Alkali Halides Containing Uranyl Salts 78

A. ADROVA, V. N. ANDREEV, M. M. KOTON, IU. N. PANOV, N. S. MUSALEV
Opticheskie is tsintilliatsionnye kharakteristiki soedinenii riada oksidiazola 128
Optical and Scintillation Characteristics of Oxadiazoles 79

I. GROMOVA, S. A. KULIKOV
Vliianie sily toka na intendivnost' vodorodnogo spektra v oblasti 2500-1200 Å 130
Influence of Current Strength on the Intensity of the Spectrum of Hydrogen in the Region 2500-1200 Å 80

S. BRODIN, A. F. PRIKHOT'KO
Vliianie tolshchiny kristallov antratsena na ikh krivye pogloshcheniia pri temperature 200 K 132
Influence of the Thickness of Anthracene Crystals on Their Absorption Curves at 20° K 82

IUBILEI I DATY
JUBILEES AND DATES

P. LINNIK (K 70-letiiu so dnia rozhdeniia) 134
VLADIMIR PAVLOVICH LINNIK (On His 70th Birthday) 84

Abbreviations Often Encountered and Used Herein 86

Information for Authors (Russian) 87

Symbols for Sources of Translation 88

Alfred J. Klapperich 10-19-59
131 Walker Ave
Clarendon Hills Ill.

TOM VII, Vyp. 1 OPTIKA I SPEKTROSKOPIIA Iiul', 1959
VOL. VII, No. 1 OPTICS AND SPECTROSCOPY July, 1959

SODERZHANIE

L. A. VAINSHTEIN, G. G. DOLGOV
Effektivnye secheniia vozbuzhdeniia n^1P-urovnei He medlennymi elektronami 3

IU. I. TURKIN
Anomali v intensivnostiakh komponent sverkhtonkoi struktury rezonansnykh linii talliia 10

V. K. PROKOF'EV, D. B. GUREVICH, I. M. BELOUSOVA, IU. A. SNIGIREV
K voprosu o vremeni ustanovleniia termodinamicheskogo ravnovesiia v plazme dugovogo razriada 14

L. M. SVERDLOV
Teoriia intensivnostei infrakrasnykh spektrov metana, etana i geksadeiteroetana 21

IU. N. PANOV, N. A. ADROVA, M. M. KOTON
Opticheskie kharakteristiki soedinenii riadov oksazola, oksidiazola i furana 29

A. F. PRIKHOT'KO, I. IA. FUGOL'
Liuminestsentisiia kristallov stil'bena pri 20° K 35

T. N. BOLOTNIKOVA
K voprosu ob interpretatsii spektra fluorestsentsii naftalina 44

N. G. BAKHSHIEV
Vnutrennee pole i polozhenie elektronnykh polos pogloshcheniia i ispuskaniia mnogoatomnykh organicheskikh molekul v rastvorakh 52

V. A. KIZEL', V. M. RUBINOV
Opticheskie svoistva kontsentrirovannykh rastvorov i rasplavov. I 62

I. K. PLIAVIN'
O kinetike foto- i gamma- liuminestsentsii v nekotorykh shchelochnogaloidnykh kristallakh, aktivirovannykh Tl 71

N. N. KRISTOFEL'
Kvantovomekhanicheskii raschet tsentra liuminestsentsii v KCl-Tl 78

M. S. BRODIN, A. F. LUBCHENKO
Vliianie temperatury na rasprostranenie elektromagnitnykh voln v kristallakh, v kotorykh voznikaiut eksitony 83

I. IA. BREIDO, IU. A. TSIRLIN, L. N. SHISHOVA
Opredelenie energeticheskogo vykhoda liuminestsentsii plastmassovykh stsintilliatrorov pod deistviem gamma-luchei 89

A. N. TEKUCHEV:
O pogloshchenii i dispersii tonkikh sloev zolota 93

P. V. SLOBODSKAIA, E. S. GASILEVICH
Razvitie metoda opredeleniia vremeni relaksatsii kolebatel'nogo sostioianiia molekul s pomoshch'iu spektrofona. I. Utochnenie zavisimosti mezhdu ismeriaemym sdvigom fazy i vremenem relaksatsii 97

IA. I. GERLOVIN, P. V. SLOBODSKAIA
Povyshenie chuvstvitel' nosti optiko-akusticheskogo metoda gasovogo analiza putem primeneiia kiuvet s mnogokratnym prokhozhdeniem radiatsii 105

KRATKIE SOOBSHCHENIIA

O. I. SEMAN
Ob adnom svoistve krivizny izobrazheniia v korotkikh linzakh elektronnoi optiki 103

CONTENTS

Effective Excitation Cross-Sections of n^1P Levels of He by Slow Electrons

Anomalies in the Intensities of the Components of the Hyperfine Structure of Resonance Lines in Thallium

On the Question of the Build-Up Time for Thermodynamic Equilibrium in the Plasma of an Arc Discharge

Theory of the Intensities of the Infrared Spectra of Methane, Ethane and Hexadeuteroethane

Optical Characteristics of Compounds of the Oxazole, Oxadizole and Furan Series

Luminescence of Stilbene Crystals at 20° K

On the Question of the Interpretation of the Fluorescence Spectrum of Naphthalene

The Internal Field and the Position of the Electronic Absorption and Emission Bands of Polyatomic Organic Molecules in Solution

The Optical Properties of Concentrated Solutions and Melts. I.

On the Kinetics of Photo- and Gamma- Luminescence in Certain Thallium Activated Alkali-Halide Crystals

A Quantum Mechanical Calculation of the Luminescent Center in KCl-Tl

The Influence of Temperature on Electromagnetic Wave Propagation in Crystals in which Excitons Occur

Determination of the Luminescent Energy Yield of Plastic Scintillators under the Action of γ-rays

Absorption and Dispersion by Thin Gold Layers

Development of a Method of Determining the Relaxation Time of the Vibratory State of Molecules Using a Spectrophone. I. Establishment of a more Accurate Dependence Between the Measured Phase Shift and Relaxation Time

Enhancement of the Sensitivity of the Optic-Acoustic Method of Gas Analysis by Using Cells with Multiple Passage of Radiation

BRIEF REPORTS

On One Characteristic of Image Curvature in Short Focal-Length Lenses in Electron Optics